ARIZONA DEPARTMENT OF WATER RESOURCES

REGIONAL GROUNDWATER FLOW MODEL OF THE TUCSON ACTIVE MANAGEMENT AREA TUCSON, ARIZONA: SIMULATION AND APPLICATION

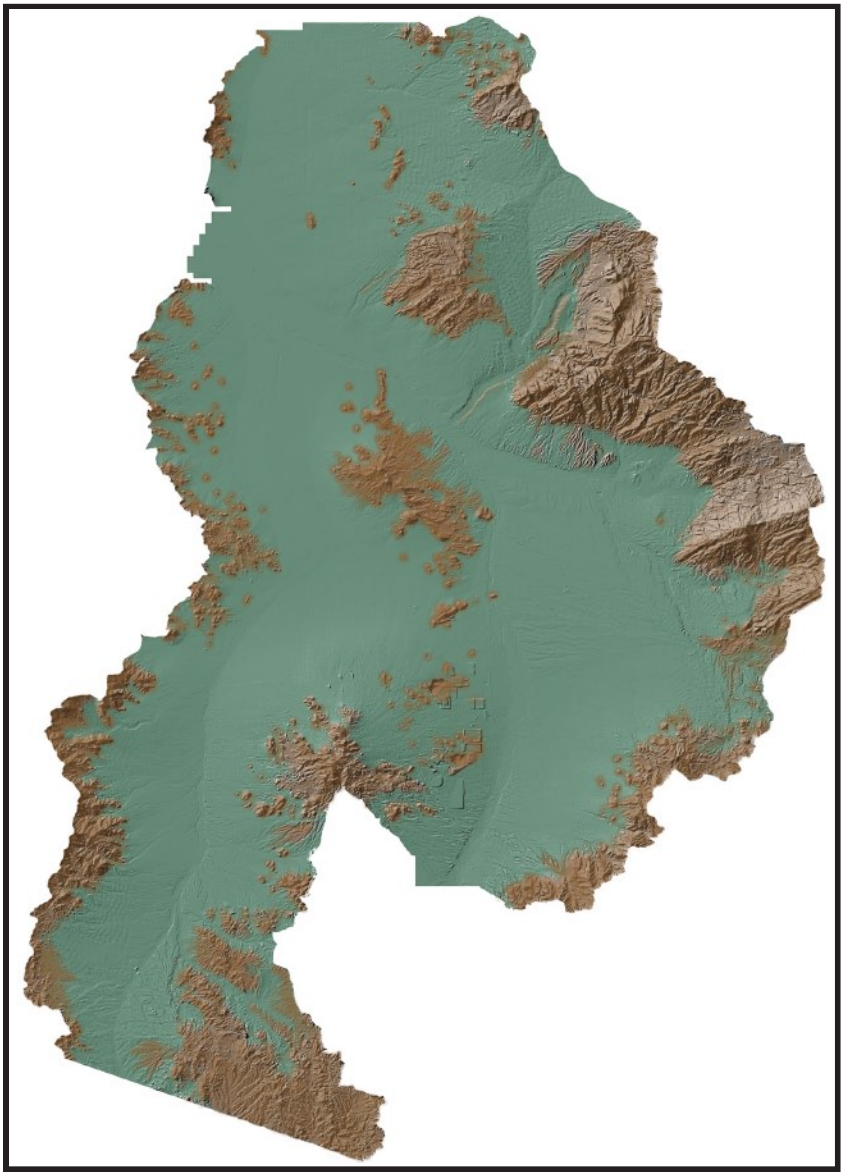

MODELING REPORT NO. 13

BY

DALE A. MASON AND **LICINIU BOTA**

HYDROLOGY DIVISION

PHOENIX, ARIZONA

2006

Table of Contents

ABSTRACT .... **VI**

ACKNOWLEDGEMENTS .... **VII**

CHAPTER 1 INTRODUCTION **1**

Groundwater Management Act 1
Tucson Active Management Area 1
Purpose and Objectives 1
General Description of Model Area 4
Upper Santa Cruz Sub-basin 4
Avra Valley Sub-basin 4
Previous Investigations 5
Sources of Data 5

CHAPTER 2 REGIONAL HYDROGEOLOGIC SETTING **7**

General Overview of Regional Hydrogeology 7
Structural Geology and Tectonic History 7
Hydrogeology 10
Upper basin-fill 10
Lower Basin-fill 13

CHAPTER 3 REGIONAL GROUNDWATER FLOW SYSTEM **14**

Conceptual Model of the Regional Aquifer System 14
Aquifer System 15
Fort Lowell Formation 16
Upper Tinaja beds 17
Middle and lower Tinaja beds 17
Pantano Formation 17
Predevelopment Groundwater System 17
Inflows 18
Outflows 23
Groundwater in Storage 24
Groundwater Development Period: 1941 – 1999 25
Inflows 27
Outflows 31
Transient Water Level Conditions 34
Change in Storage 34

CHAPTER 4 NUMERICAL MODEL **35**

Modeling Approach 35
Model Code 35
Model Development 35
Model Grid and Cell Definitions 35
Model Layer Definitions 37
MODFLOW Packages 39
Boundary Conditions 40
Model Data Development 40
Water Levels 40
Aquifer Parameters 41
Pumpage Data 49
Evapotranspiration 52
Natural Recharge 52
Incidental Recharge 53

CHAPTER 5 SIMULATION OF GROUNDWATER FLOW 55

Model Calibration Process 55
Calibration Criteria and Model Error 55
Calibration Targets 56
Steady-State Calibration 57
Steady-State Calibration Criteria 58
Steady-State Model Results 58
Transient Calibration 67
Transient Calibration Criteria 67
Transient Calibration Process 67
Transient Calibration Results 68

CHAPTER 6 SENSITIVITY ANALYSIS 83

Model Sensitivity 83
Sensitivity Procedures 83
Steady-State Sensitivity Analysis 83
Transient State 84

CHAPTER 7 BASE CASE FUTURE SIMULATION 87

Introduction 87
Base Case Water Demands 87
Well Pumpage Distribution 87
Municipal Water Demand 88
Agricultural Water Demand 88
Industrial Water Demand 89
Miscellaneous Water Demands 90
Base Case Water Supplies 90
CAP Surface-water 90
Effluent 92
Base Case Future Scenario Predictions 93
Water Budget 93
Water Level Changes 96
Summary 104

CHAPTER 8 SUMMARY 106

Summary 106
Model Limitations 106
Recommendations 107

SELECTED REFERENCES 109

APPENDIX A. MODEL WATER BUDGETS
Steady-state Water Budget……………………………………………………………………A-1
Transient Water Budget……………………………………………………………...…….A-2

APPENDIX B. MODEL RESIDUALS
Head Observation Weights……………………………………………………………………B-1
Table B-1. Weighting factors for observed water levels as determined from site altitude accuracy values in the GWSI database…………………………………………………………………B-2
Table B-2. 1940 Steady-state Weighted Residuals……..………………………………….….B-3
Table B-3. 1960 Weighted Residuals…………………………………………………....…B-5
Table B-4. 1983 Weighted Residuals…………………………………………………....…B-9
Table B-5. 1999 Weighted Residuals…………………………………………………….B-15

APPENDIX C. SELECTED HYDROGRAPHS
Map of Hydrograph Locations……………………………………………………………..C-1

List of Figures

Figure 1. Map showing location of study area, Tucson AMA, Arizona. 2
Figure 2. Map showing water level declines 1940 to 1995, in the Tucson AMA, Arizona. 3
Figure 3. Generalized geologic cross-section of the Upper Santa Cruz sub-basin. 8
Figure 4. Generalized geologic cross-section of the Avra Valley sub-basin. 9
Figure 5. Map showing the location of known or suspected faults and areas of perched water, Tucson AMA, Arizona. 11
Figure 6. Average monthly rainfall 1896-2000, Tucson, Arizona. 16
Figure 7. Estimated pumpage in the Tucson area, 1915 to 1940. 19
Figure 8. Map showing 1940 water level elevations, location of 1940 water level data, and location of groundwater inflow and outflow, Tucson AMA, Arizona. 20
Figure 9. Estimated and reported pumpage in the Tucson AMA: 1940 – 1999. 25
Figure 10. Map showing 1999 water level elevations, Tucson AMA, Arizona. 26
Figure 11. Maximum potential agricultural recharge in Tucson AMA, 1940 - 1999. 28
Figure 12. Annual CAP water use in Tucson AMA, 1993 - 1999. 29
Figure 13. Estimated and reported effluent releases into the Santa Cruz River 1950 – 2000 30
Figure 14. Estimated and reported pumpage in the Avra Valley sub-basin of the Tucson AMA, Arizona, 1941 - 1999 32
Figure 15. Estimated and reported pumpage in Upper Santa Cruz sub-basin, Tucson AMA, Arizona, 1941 - 1999. 33
Figure 16. Map showing location of the cell grid and the maximum extent of the three model layers, Tucson AMA, Arizona. 38
Figure 17. Map showing the distribution of hydraulic conductivity and transmissivity values (a) layer 1, (b) layer 2, (c) layer 3, and (d) total composite model transmissivity: Tucson groundwater flow model, Tucson AMA, Arizona 42
Figure 18. Map showing specific yield distribution: Tucson groundwater flow model, Tucson AMA, Arizona. (a) Layer 1, (b) Layer 2, (c) Layer 3 46
Figure 19. Map showing the distribution of (a) layer 1 vertical leakance (Vcont) and (b) layer 2 vertical leakance (Vcont), Tucson AMA, Arizona. 50
Figure 20. Map showing measured and simulated 1940 water levels and the distribution of the steady-state model weighted residuals, Tucson AMA, Arizona. 60
Figure 21. Steady-state weighted residual histogram Tucson AMA, Arizona. 61
Figure 22. Scatter plots of steady-state a) weighted observed heads vs. weighted simulated heads and b) weighted residuals vs. unweighted observed heads. 62
Figure 23. Map showing steady-state boundary conditions (a) natural recharge cells and inflow/outflow boundaries, (b) boundary conditions and discharge cells, Tucson AMA, Arizona. 65
Figure 24. Map showing 1999 observed vs. simulated water level contours Tucson AMA, Arizona. 69
Figure 25. Histogram of 1999 weighted residuals Tucson AMA, Arizona. 71

Figure 26. Scatter plots of transient a) weighted observed heads vs. weighted simulated heads and b) weighted residuals vs. unweighted observed heads. 72
Figure 27. Map showing distribution of simulated 1999 head residuals, Tucson AMA, Arizona....73
Figure 28. Map showing transient boundary conditions and distribution of recharge cells, Tucson AMA, Arizona – 1999....76
Figure 29. Graph showing total effluent released and simulated effluent infiltrated into the Santa Cruz River – 1951 to 1999. 78
Figure 30. Map showing transient model boundary conditions and distribution of cells with pumpage cells, Tucson AMA, Arizona – 1999....80
Figure 31. Graph showing simulated annual change-in-storage for Avra Valley sub-basin 1941 - 1999, Tucson AMA, Arizona. 81
Figure 32. Graph showing simulated annual change-in-storage for USC sub-basin 1941-1999, Tucson AMA, Arizona. 81
Figure 33. Projected population for Tucson AMA model area, 2000 – 2025....89
Figure 34. Projected future agricultural water use and supply sources, 2000 – 2025....90
Figure 35. Annual CAP surface-water recharge allocations (recharge and In Lieu use) by stress period for the Base Case projection....93
Figure 36. Annual projected change in storage 2000 - 2025, Avra Valley sub-basin, Tucson AMA, Arizona...94
Figure 37. Annual projected change in storage 2000 - 2025, USC sub-basin, Tucson AMA, Arizona....94
Figure 38. Projected water level changes for the Tucson AMA Tucson, Arizona: 2000 – 2025, a) change 2000 – 2005, b) change 2000 – 2010, c) change 2000 – 2015, d) change 2000 – 2020, and e) change 2000-2025.97
Figure 39. Projected depth to water in the Tucson AMA, Arizona: 2025 102
Figure 40. Estimated annual pumpage in the central well field area for the Base Case projection. 103
Figure 41. Hydrograph of measured, simulated, and projected water levels for well D-14-14 16ccc in the central well field area....103
Figure 42. Hydrograph of measured, simulated, and projected water levels for well D-11-10 08ddd in the northern Avra Valley. 104

List of Tables

Table 1. Correlation of stratigraphic units and Tucson AMA model units to orogenic events....12
Table 2. Average monthly precipitation totals for Tucson, Arizona 1894-2000. 15
Table 3. Summary of previously published groundwater budget components 1940 to 1984. 21
Table 4. Conceptual steady-state groundwater budget for study area. 24
Table 5. Tucson model components. 36
Table 6. Vertical conductance values used in the Tucson AMA, Arizona. 49
Table 7. Statistical summary of steady-state model weighted residual, Tucson AMA, Arizona....59
Table 8. Frequency distribution of the absolute value of the steady-state weighted residuals, Tucson AMA, Arizona. 59
Table 9. Comparison between 1940 conceptual water budget and steady-state simulated water budget, Tucson AMA, Arizona. 64
Table 10. Statistical summary of transient model weighted head residuals 70
Table 11. Frequency distribution of the absolute value of the 1999 weighted residuals. 71
Table 12. Weighted head residuals for the transient period 1941- 1999, Tucson AMA. Arizona....74
Table 13. Annual simulated model water budget, 1941 - 1999 77
Table 14. Sensitivity analysis of the steady-state and transient models: a) head changes, and b) water budget changes, Tucson AMA, Arizona....85
Table 15. Water providers in the Tucson AMA participating in developing the Base Case projection data....88
Table 16. Permitted recharge projects in the Tucson AMA. 91
Table 17. Base Case water budget 200-2025 Tucson AMA, Arizona....95

Abstract

A numerical groundwater flow model of the Tucson Active Management Area (AMA) in Pinal, Pima and Santa Cruz Counties, Arizona, was developed to simulate the regional hydrologic system during a pre-development (steady-state) period of 1940, a developed (transient) period from 1941 to 1999, and for a projection period from 2000 to 2025. The upper and lower basin-fill alluvium in the Tucson AMA forms a complex regional aquifer system that is divided into 3 model layers.

The steady-state groundwater conditions indicate inflows into Tucson AMA include 34,425 acre-feet of mountain-front recharge, 39,445 acre-feet of stream infiltration, and 24,155 acre-feet of groundwater underflow. Steady-state outflows consisted of 59,695 acre-feet of pumpage, 17,170 acre-feet of evapotranspiration, and 21,191 acre-feet of groundwater outflow. Groundwater underflow within the Tucson AMA from the Upper Santa Cruz (USC) sub-basin to the Avra Valley sub-basin was about 14,580 acre-feet. Transient model results indicate a cumulative loss of 6.9 million acre-feet of water from the regional aquifer between 1941 and 1999. Transient outflows were simulated as 15.9 million acre-feet of groundwater pumpage and natural outflows of about 1.5 million acre-feet; simulated inflows included about 4.0 million acre-feet of incidental recharge from agricultural and industrial sources and about 6.5 million acre-feet of natural inflows. Simulated irrigation recharge ranged from 33 percent of total irrigation pumpage in the 1940s and 1950s, to 25 percent of pumpage in the 1980s and 1990s.

The transient model simulated both the widespread, long-term water level declines in agricultural areas of the northern Avra Valley sub-basin and recoveries in the area since the mid-1970s. The model also simulated the historic overdrafting of large areas of the regional aquifer in the USC sub-basin, which has resulted in long-term water level declines throughout much of the sub-basin during the transient period. Observed and simulated water level recoveries in the USC sub-basin are generally limited to areas along the Santa Cruz River and its tributaries where flood flows provided sufficient recharge to offset local pumpage.

The results of a Base Case projection simulation from 2000 to 2025 that maximized the utilization of renewable water supplies indicates that the Tucson AMA will not achieve its goal of reaching “Safe Yield” by 2025. However, the AMA-wide annual overdraft is projected to be between 14,000 and 20,000 acre-feet. The Avra Valley sub-basin will have a net increase in storage during the Base Case projection of about 453,000 acre-feet and water levels are projected to continue to recover due to extensive artificial recharge of renewable water and projected declines in agricultural pumpage. The Upper Santa Cruz sub-basin will experience a net loss of storage of 1,000,000 acre-feet; however, water levels are projected to rise in the City of Tucson’s central wellfield area, T 14 S, R 14 E, for the period 2000 to 2020. The projected recovery is due to dramatically reduced withdrawals as pumpage is shifted to recovery of renewable supplies from recharge projects. After 2020, the water level recovery in the central wellfield is projected to slow as increasing municipal demand is satisfied by increased pumpage. Water levels in the southern areas of the basin near the Santa Cruz River are projected to rise due to recharge projects. However, water levels are projected to decline by between 50 to 225 feet in the eastern and southeastern areas of the Tucson AMA where demand is expected to be satisfied by non-renewable groundwater.

Acknowledgements

The Department would like to thank those individuals and organizations that have provided information, guidance, and suggestions during the development and review of this modeling project. Special recognition goes to the City of Tucson and the U. S. Geological Survey who provided large amounts of hydrologic data from their files used to update and improve the numerical model. Many water providers in the Tucson AMA furnished estimates of future water use that were incorporated into the future projection model simulation. Without their assistance and input the Base Case future projection would have been impossible to develop.

Numerous individuals have provides information, suggestions and comments, and assistance during the development of the model. Special thanks go to the following: Stan Leake, John Hoffman, and Don Pool of the U. S. Geological Survey; Ralph Marra and Wally Wilson of the City of Tucson; Mike Block of the Metropolitan Water District, and Brad Prudhom of the Bureau of Reclamation for their help during model development and comments on the model report; Ken Seasholes, Cindy Shimakosu, Ann Philips, Laura Grignano, Jeff Tannler, Matt Weber, and those Tucson AMA staff members who worked with the various Tucson AMA water providers on the future water use data that allowed the Department develop the Base Case future projection data sets; and to Susan Smith and Carlos Renteria for their assistance and patience in preparing the maps and figures for this report.

Chapter 1

Introduction

Groundwater Management Act

In 1980, the Arizona legislature passed the Groundwater Management Act (GMA), which created the Arizona Department of Water Resources (ADWR) and established four Active Management Areas (AMAs) within the state; a fifth AMA was added in 1994. The AMAs are designated for special, intensive management of groundwater resources due to the impacts of historic groundwater withdrawals. By 1980, overdrafting of regional aquifers within the AMAs had created water level declines of as much as 500 ft in some areas. The goal for most AMAs is the elimination of groundwater overdrafting by achieving "safe-yield". Safe-yield is defined as," *a groundwater management goal which attempts to achieve, and thereafter maintain, a long-term balance between the amount of groundwater withdrawn in an active management area and the annual amount of natural and artificial recharge in the active management area*." To accomplish this goal, each AMA provides a water rights-system for allocating existing water resources, requires new urban development to have long-term, dependable water supplies, and is responsible for developing and setting water management goals so that future water needs may be met.

Tucson Active Management Area

The Tucson Active Management Area (AMA) is one of the original management areas designated in 1980. In 1994, the southern portion of the Tucson AMA located in Santa Cruz County was split off to form the Santa Cruz AMA. The current extent of the Tucson AMA is shown in Figure 1. The management goal of the Tucson AMA is to achieve "safe-yield", as defined by the GMA, by 2025. To achieve this goal the Tucson AMA has implemented mandatory conservation requirements for agricultural, industrial, and municipal water users, and encouraged the use of renewable surface water supplies from the Central Arizona Project (CAP) and reuse of effluent.

By 1995, groundwater overdrafting in the Tucson AMA had lowered water levels by as much as 200 ft in Upper Santa Cruz (USC) sub-basin and by at least 150 ft in the agricultural areas of the Avra Valley sub-basin (Figure 2). The loss of saturated aquifer thickness in central Tucson and in the northern part of Avra Valley has resulted in land subsidence and loss of well productivity. To help Tucson AMA staff evaluate the effectiveness of various water management alternatives in reversing these declines and achieving safe-yield, the ADWR has developed a regional groundwater flow model of the AMA. The study began in 1996 with the assembling of reference literature, review of past modeling efforts by the ADWR and the United States Geological Survey (USGS), and collection of various types of hydrologic data. The model study area was selected to coincide with several previous regional modeling studies completed in the Tucson area by the ADWR and the USGS. A common model grid was utilized so that the information developed during previous modeling studies could be utilized in development of the new ADWR model, and so that the results of the ADWR model could be more easily compared to the results of previous models.

Purpose and Objectives

The purpose of this modeling effort is to produce an updated regional groundwater flow model for the Tucson AMA by combining existing regional models developed by the USGS and the ADWR with updated modeling capabilities and new data. The updated model used existing data from modeling studies by Anderson (1972), Mooseburner (1972), Travers and Mock (1984), Hanson and others (1990), and Hanson and Benedict (1994). The existing models were either one-layer or two-layer models that used older groundwater flow model software codes. The updated model has three layers and uses the latest MODFLOW software code, well

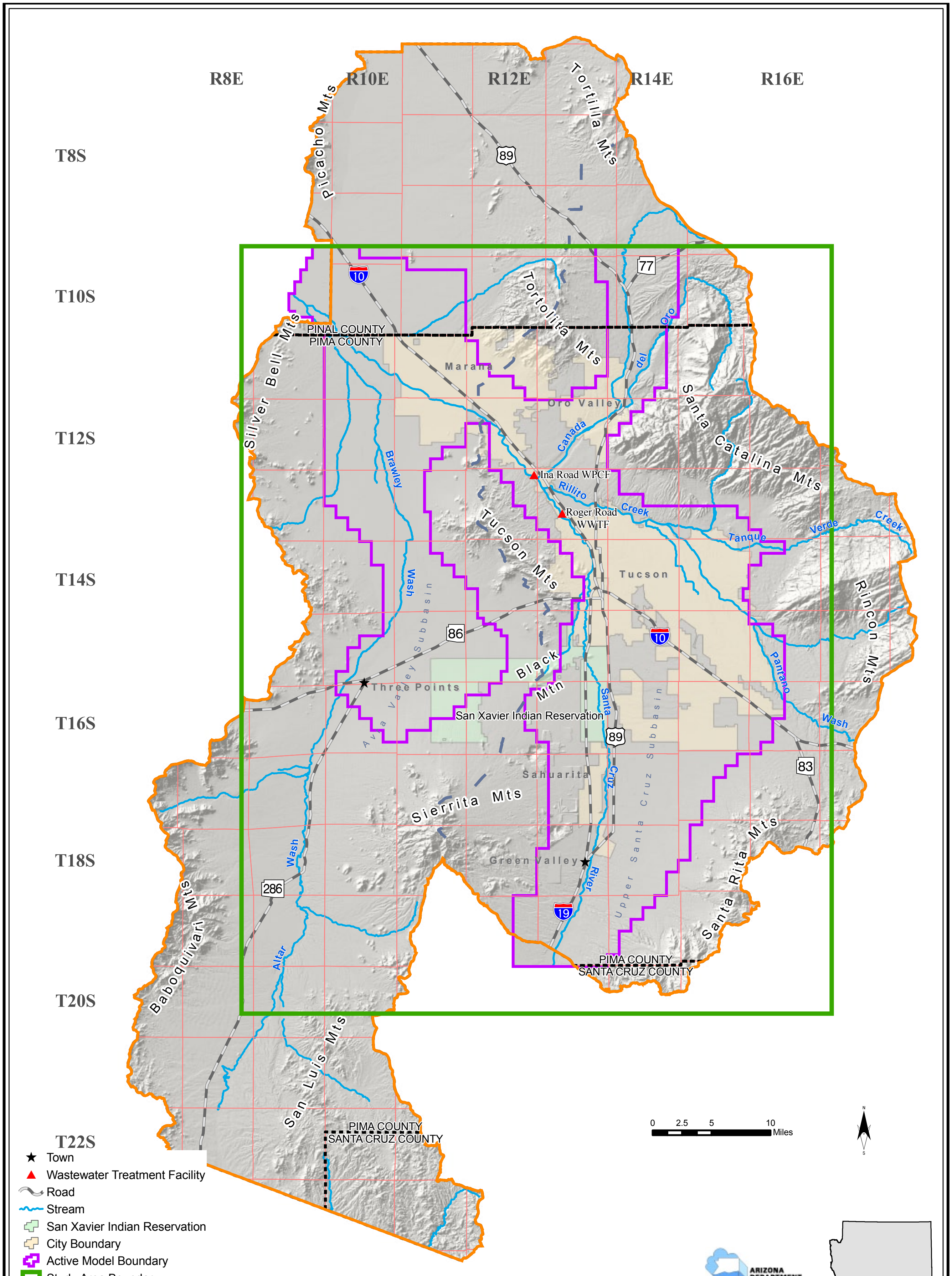

Figure 1.
Map showing location of study area,
Tucson Active Management Area (AMA), Arizona.

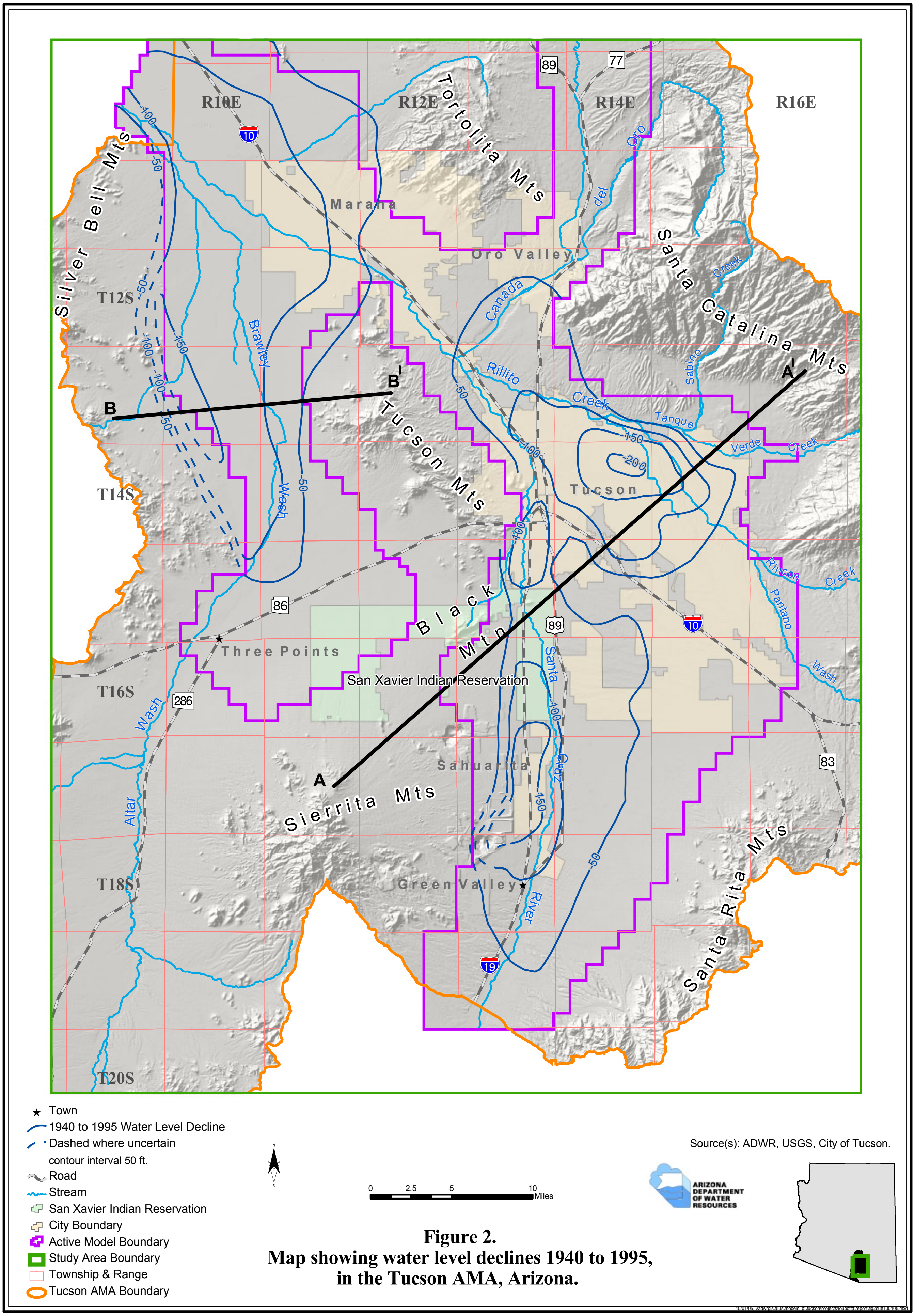

Figure 2.
Map showing water level declines 1940 to 1995, in the Tucson AMA, Arizona.

specific pumpage data from 1984 to 1999, and other hydrologic data developed since the last modeling project was completed in 1990.

The objectives of this project are to develop a regional groundwater flow model that accurately simulates the regional hydrologic flow regime and to accumulate updated hydrologic, geologic, and water use data. The Tucson AMA staff and local water use managers can then use the updated model to analyze the effect of different water supply and demand scenarios on the regional aquifer. Projecting future water levels based on assumed water management scenarios would allow local water managers determine if the planning scenarios help the AMA reach its goal of safe yield.

General Description of Model Area

The Tucson AMA is located in southeastern Arizona and encompasses approximately 4,000 square miles (Figure 1). The AMA consists of two parallel north-south trending alluvial basins that are separated by block-faulted mountains. The two alluvial basins divide the AMA into two sub-basins, the Upper Santa Cruz (USC) sub-basin and the Avra Valley sub-basin (Figure 1). The USC sub-basin contains the Tucson metropolitan area, which is the major urban population center in the Tucson AMA. The Avra Valley sub-basin consists of Altar and Avra Valleys and contains a large agricultural area, which is centered in the central and northern sections of the sub-basin around Marana, Arizona (Figure 1).

The Tucson AMA is located within the Sonoran Desert sub-province of the Basin and Range physiographic province. The climate at the lower elevations is semiarid with sparse vegetation consisting of creosote, mesquite, and cacti at the lowlands. Higher rainfall totals in the upper elevations of the mountains around the Tucson AMA's margins support larger conifers and deciduous trees such as aspens, Douglas firs, and oaks. Annual rainfall ranges from 11 inches to 16 inches on the valley floors to as much as 30 inches in the surrounding mountains. In January, the mean daily maximum temperature is 75^{o} F (24^{o} C) and the mean daily minimum temperature is 50^{o} F (10^{o} C). In July, the mean daily maximum temperature is 105^{o} F (40.5^{o} C) and the mean daily minimum is 83^{o} F (28^{o} C) (Hydrodata, 2001).

Upper Santa Cruz Sub-basin

The USC sub-basin is a large alluvial valley that slopes to the north and northwest and is underlain with thick basin-fill deposits. The sub-basin has experienced long-term water level declines and some related land subsidence due to past groundwater withdrawals for irrigation and municipal demands (Figure 2). The Santa Cruz River is the main surface water drainage, entering the Tucson AMA from the south and exiting the sub-basin between the Tucson and Tortolita Mountains (Figure 1). Throughout most of the sub-basin the Santa Cruz is ephemeral, flowing only in response to local rainfall events. However, effluent discharges into the riverbed from two Pima County Waste Water Treatment plants have created a perennial reach downstream from the discharge points. During the winter months, effluent discharges are sufficient to maintain surface water flows all the way to the Tucson AMA - Pinal AMA boundary between the Silver Bell and Picacho Mountains. Major tributaries to the Santa Cruz River are Pantano Wash, Rillito Creek, Tanque Verde Creek, and Cañada del Oro (Figure 1).

Avra Valley Sub-basin

The Avra Valley sub-basin is a broad, flat alluvial valley that slopes to the north and northwest. Thick basin-fill deposits also underlie the sub-basin. The southern part of the alluvial valley is called Altar Valley; north of Three Points, Arizona, at about Township 16 South, Range 10 East, the valley narrows, and north of this point is called Avra Valley. The Altar Valley section of the sub-basin is sparsely developed and is not included within the active model boundary (Figure 1). The Avra Valley section of the sub-basin has been extensively developed, originally for agriculture and more recently for residential purposes. Water levels in the southern part of the sub-basin are generally stable; however, developed areas in the central and northern part of the sub-basin have experienced long-term water level declines (Figure 2). The sub-basin has two major surface water features, the Santa Cruz River in the north and Altar and Brawley Washes in the south. Altar Wash drains the Altar Valley section of the sub-basin; Altar Wash is renamed Brawley Wash where it enters the Avra Valley part of the sub-basin. The Santa Cruz River enters the sub-basin between the Tucson and Tortolita Mountains and flows to the northwest across the northern part of the sub-basin. Brawley Wash and the Santa Cruz River exit the Tucson AMA into the Pinal AMA between the Silver Bell and Picacho Mountains (Figure 1).

Previous Investigations

The Tucson AMA area has been extensively studied beginning in the early 1900's up to the present. Major topics of investigations conducted within the two basins include geology and stratigraphy, hydrogeology, water resources, and numerical groundwater modeling. Studies documenting geology and stratigraphy include Heindl and White (1965), Pashley (1966), Davidson (1973), and Anderson (1987, 1988, 1989). Hydrogeology and water resources studies include Smith (1910), Turner (1943), Turner and others (1947), Schwalen and Shaw (1957), White, Matlock, and Schwalen (1966), Burkham (1970), Condes de la Torre (1970), Matlock and Davis (1972), Osterkamp, (1973, 1974), Davidson (1973), Brown (1976), Hollett and Garrett (1984), Murphey and Hedley, (1984), Cuff and Anderson (1987), Leake and Hanson (1987), Hanson (1989), Anderson, Freethey, and Tucci (1990), Webb and Betancourt (1990), Hammett and Sicard (1996), and Pool (1999). Regional Groundwater flow modeling investigations include Moosburner (1972), Anderson (1972), Travers and Mock (1984), Hanson, Anderson, and Pool (1990), and Hanson and Benedict (1994).

This list is by no means an exhaustive references list for all hydrologic, geologic, or modeling studies for the Tucson area. The studies cited above were used to develop a conceptual understanding of the regional aquifer system in the Tucson AMA and helped in constructing the basic framework of the Tucson regional groundwater flow model.

Sources of Data

In addition to the literature cited above there is a wide variety of hydrogeologic information available for the area encompassed by the Tucson AMA. The information available includes water level data, well location and construction records, estimated and measured pumpage totals, annual effluent release data, crop census data, aquifer test results, stratigraphic interpretations and particle-size analysis derived from well cores, and data sets from previous modeling studies. Much of this data had been gathered or developed by previous investigators and was made available to the ADWR through the cooperation of the USGS, the City of Tucson, and Pima County. Additional data was obtained from ADWR's own files and databases, which contain an extensive amount of well-related data and are maintained as part of ADWR's regulatory and administrative responsibilities.

ADWR maintains four databases that contain well-related information that were used in developing well locations and pumpage values for the regional model. The **G**round**W**ater **S**ite **I**nventory (GWSI) database, State Well Registry database (called the 55 File), and **R**egistry of **G**roundwater **R**ights (RGR) database are active databases and were important sources of well and pumpage data used in this report. A fourth database, the old State Land Department Well Registry, (called the 35 File), which was a precursor to the current ADWR Well Registry, was also used in developing historic well data.

The GWSI database contains field-checked data on selected wells that have been visited by personnel from ADWR's Basic Data section or the USGS. Information in GWSI includes measured water levels, construction data on selected wells, well perforation data, and well location coordinates. Water level data from the GWSI was used in constructing water level contour maps used in the steady-state and transient model calibration. The Well Registry database contains well completion data, well use information, well locations, and ownership information. Well construction and location data from the Well Registry and the GWSI were used to assign pumpage to cells and distribute pumpage by layer in the steady-state and transient model simulations.

The water rights system implemented through the GMA requires that pumpage from all large water production wells, those wells with a capacity of over 35 gallons per minute or that irrigate more than 2 acres, be reported to the ADWR and entered into the RGR database. Wells that irrigate less than 2 acres or have a capacity of less than 35 gallons per minute are exempt from reporting requirements. Since 1984, all pumpage from non-exempt wells in the AMA's have been reported to the RGR database. Model pumpage files for the transient model period of 1984 to 1999 were constructed using data from the RGR pumpage files.

Information provided by the City of Tucson and the USGS were very useful in developing the ADWR model. Pumpage estimates for the 1940 steady-state period and the transient period of 1941 to 1983 were developed from data provided by the USGS, the City of Tucson, and from ADWR files. The City of Tucson provided well-specific pumpage data from 1956 to 1983 from their well production files, well log data, aquifer test results, and water level data. The USGS provided well log data that was used to develop the basic model layer structure and vertical hydraulic conductance inputs to the model. Pumpage estimates, transmissivity and aquifer storage distributions, and natural recharge estimates developed for the USGS regional groundwater flow models by Mooseburner (1972), Anderson (1972), Hanson and others (1990), and Hanson and Benedict (1994) were important sources of data used to develop the ADWR model inputs.

Travers and Mock (1984) gathered a large amount of hydrologic data during the development of the first ADWR Tucson regional groundwater flow model completed in 1984. The Travers and Mock data included pumpage data from the Cortaro-Marana Irrigation District (CMID), Farmers Investment Co-Operative (FICO) and crop census and well inventory data from the University of Arizona's (U of A) Agricultural Engineering College. The U of A was actively gathering a wide variety of agricultural production information in the Tucson area from the 1930s through the 1970s. The pumpage data, crop census information, and transmissivity data gathered in the ADWR files by Travers and Mock were very useful in developing water budget information and model data sets for the early transient period of 1941 to 1983.

Chapter 2

Regional Hydrogeologic Setting

General Overview of Regional Hydrogeology

The Tucson AMA is in the Basin and Range physiographic province, which is characterized by block-faulted mountains separated by basins filled with alluvial sediments. As previously discussed, the Tucson AMA contains two separate alluvial basins, which divide the AMA into two groundwater sub-basins (Figure 1). The block-faulted mountains are composed of Precambrian through Tertiary age granitic, metamorphic, volcanic, and consolidated sedimentary rock. The sedimentary deposits that fill the intervening basins are collectively termed basin-fill deposits and are of Tertiary to Quaternary age. The basin-fill deposits are composed of volcanic deposits and unconsolidated to consolidated sediments consisting of gravel, sand, silt, and clay with minor amounts of gypsiferous and anhydrous sediments. The basin-fill sediments are generally coarse-grained along the basin margins, and grade into finer-grained and evaporite deposits in the central parts of the basins. Generalized geologic cross-sections for each sub-basin are presented in Figures 3 and 4.

Previous investigators have divided the basin-fill sediments into a lower basin-fill and an upper basin-fill unit based on their general hydrogeologic characteristics (Davidson, 1973; Pool, 1986; Hanson and others, 1990; Hanson and Benedict, 1994). The basin-fill has also been subdivided into stratigraphic units based on lithologic descriptions, structural relationships, and depositional history (Davidson, 1973, Pool, 1986, Anderson, 1987, 1988, 1989). In ascending order the lower basin-fill unit has been divided into the Pantano Formation and the lower and middle Tinaja beds, and the upper basin-fill unit has been divided into the upper Tinaja beds, Fort Lowell Formation and surficial alluvial deposits, which include stream-channel deposits, described by Anderson (1987, 1988, 1989) and Davidson (1973).

Structural Geology and Tectonic History

The physical landscape and sedimentary deposits of the Tucson AMA have been strongly affected by tectonic activities during the Tertiary Period. The mid-Tertiary orogeny and the subsequent Basin and Range disturbance during the late Tertiary combined to create the current landscape and the sedimentary units that make up the Tucson AMA regional aquifer. The alluvial sediments deposited during these disturbances make up the lower and upper basin-fill units.

The mid-Tertiary tectonic activity, which began about 35 million years ago, is characterized as a period of regional uplifting, extensive sedimentation, and widespread intensive volcanism (Anderson, 1987). The metamorphic core complex rocks that make up the Rincon, Santa Catalina, Tanque Verde, and Tortolita Mountains were uplifted and deformed during the mid-Tertiary orogeny (Anderson, 1987). Sedimentary rocks related to the mid-Tertiary orogeny are highly faulted, folded, and interbedded with volcanic rocks and include conglomerates, gravels, mudstones, and evaporite deposits. The sedimentary units deposited during and immediately after this tectonic episode include the Pantano Formation and the lower Tinaja beds of the lower basin-fill unit.

In the Tucson area the Basin and Range disturbance began about 12 million years ago and included two distinct periods of faulting and sedimentation (Anderson, 1987). The first episode of faulting featured block faulting along deep-seated, high-angle normal faults that formed a landscape of deep, closed structural troughs, called grabens, surrounded by high block faulted mountains (Anderson, 1987; Davidson, 1973). In the USC sub-basin this period of block faulting created the Santa Cruz fault and a parallel series of faults along the north and east sides of the present day valley (Figure 5). Thousands of feet of coarse-grained to fine-grained basin-fill sediments were deposited in the troughs by rivers flowing into the closed

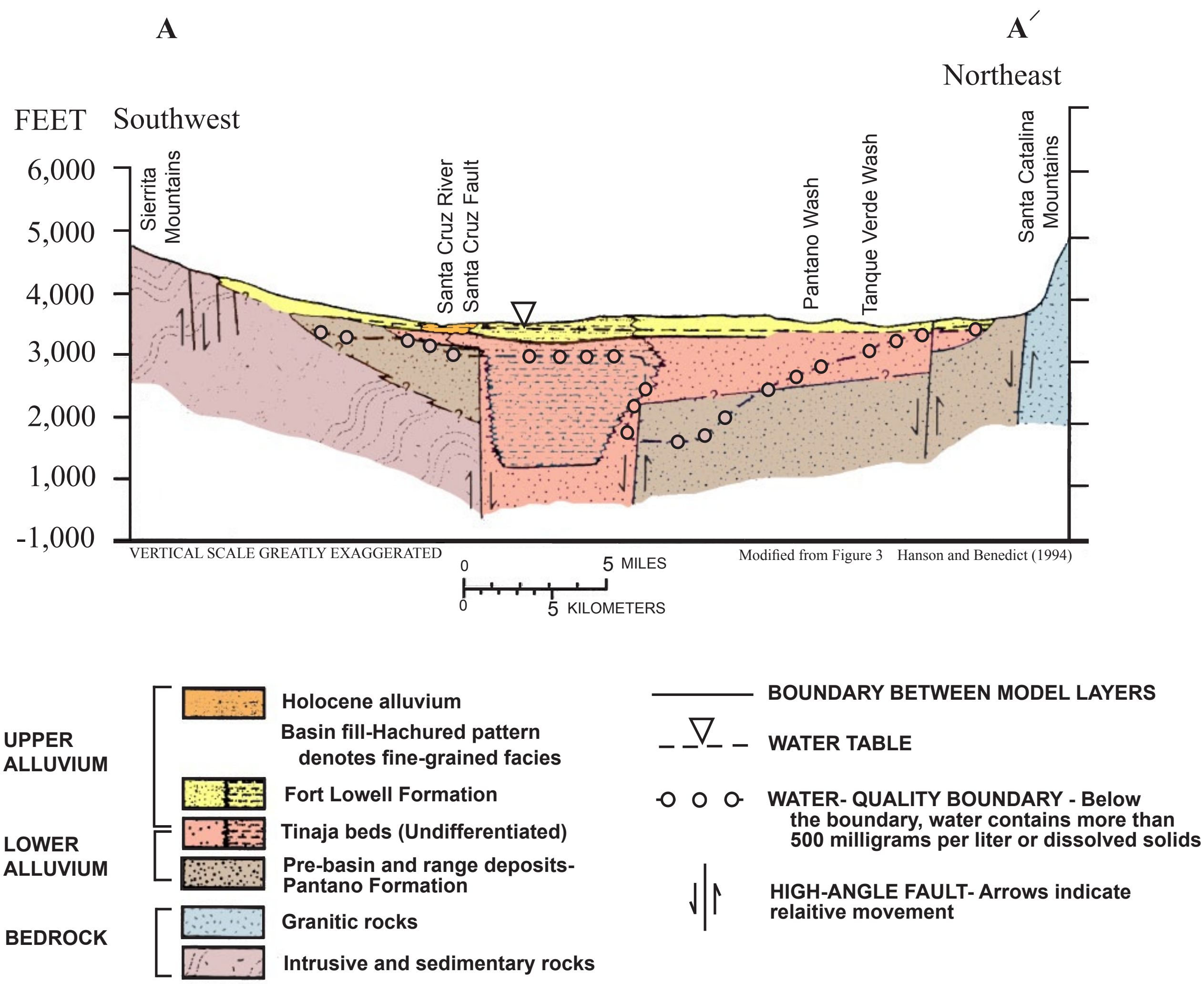

Figure 3. Generalized hydrogeologic cross-section of the Upper Santa Cruz Sub-basin, Tucson AMA, Arizona.

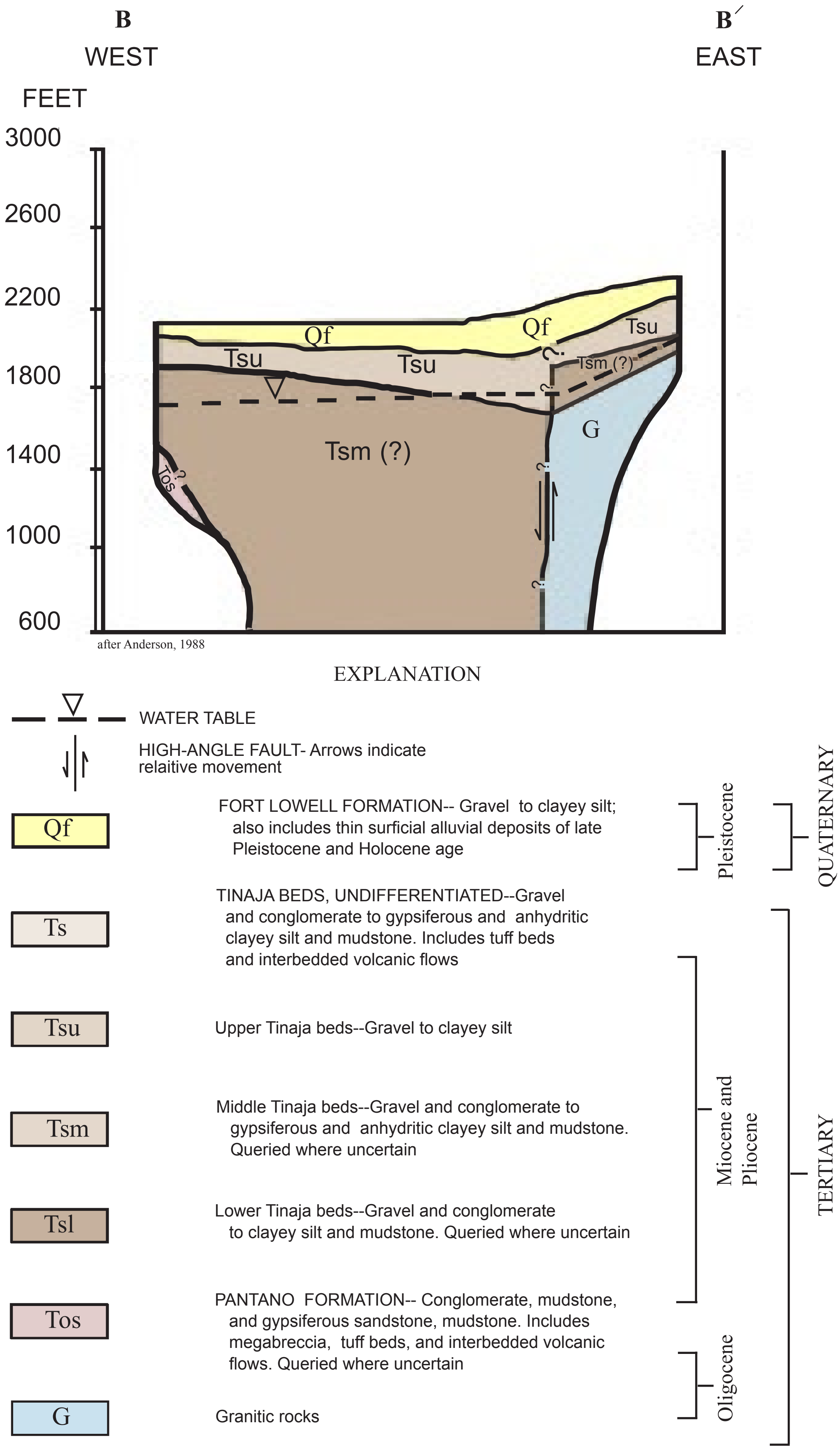

Figure 4. Generalized hydrogeologic cross-section of the Avra Valley Sub-basin, Tucson AMA, Arizona.

basins. The internal drainage system that developed during this time deposited coarse-grained materials in alluvial fans near the mountain-fronts and finer-grained sediments in the centers of the troughs. The fine-grained deposits include evaporite sequences that were deposited by playas and intermittent lakes that formed along the trough's central axis (Davidson, 1973; Anderson, 1987). Sediments that make up the middle Tinaja beds of the lower basin-fill unit were deposited as a result of this first episode of Basin and Range block faulting.

About 5 million years ago, following a period of erosion, a second period of regional uplift and faulting occurred (Davidson, 1973; Anderson, 1987). The previously deposited lower basin-fill sediments were faulted or folded and covered by a new sequence of alluvial sediments that are several hundreds of feet thick. Once again, coarse alluvial sediments eroded from the uplifted areas were deposited along the margins of the basin near the uplifted areas and the finer-grained materials were deposited along the central axis of the basins. The fine-grained sediments deposited during this tectonic event lack the evaporite deposits found in the older, lower basin-fill deposits. The upper Tinaja beds of the upper basin-fill unit were deposited during this last episode of Basin and Range faulting. Figure 5 shows the locations of known or suspected faults in the Tucson AMA study area that formed during the Tertiary orogenic events.

About 1.5 to 2 million years ago the Basin and Range tectonic activity gradually diminished. As tectonic activity ended a period of regional erosion began and the internal drainage system in the previously closed basins evolved into one that featured through-flowing rivers. The Fort Lowell Formation, the overlying surficial alluvium, and the current stream-channel deposits were deposited during and after the development of the through flowing river system.

The relationship between the Tucson AMA hydrologic units, stratigraphic units and orogenic events is presented in Table 1. For a more detailed description of the hydrologic units, stratigraphic, structural, and geologic history of the Tucson area the reader is referred to Pashley (1966), Davidson (1973), Pool (1986, 1999), Anderson (1987,1988, 1989), and Anderson and others (1990).

Hydrogeology

As described above, the Tucson AMA contains a wide variety of igneous, metamorphic, and sedimentary rocks and unconsolidated sedimentary material. The mountains surrounding the AMA are composed of crystalline and sedimentary rocks that generally yield very little water and are not considered part of the regional aquifer, and are therefore, not part of this study. The basin-fill sediments are composed of consolidated to unconsolidated sedimentary material of Tertiary to Quaternary age. The thickness of the basin-fill deposits range from a thin veneer along the mountain-fronts to as much as 9,000 ft thick in the Avra Valley sub-basin and 11,200 ft thick in the USC sub-basin (Davidson, 1973; Anderson, 1987, 1988, 1989; Hanson and others, 1990; Hanson and Benedict, 1994). As described above, the basin-fill has been divided into a lower basin-fill unit and an upper basin-fill unit based on regional hydrogeologic characteristics, and further sub-divided into stratigraphic units based on lithology and deposition environment by Pashley (1966), Davidson (1973), Pool (1986), and Anderson (1987, 1988, 1989). The general characteristics of the basin-fill deposits are described below.

Upper basin-fill

The upper basin-fill unit ranges from several hundred feet to as much as 1,000 ft thick in both sub-basins. The unit consists mostly of semi-consolidated to unconsolidated gravel, sands, and clayey silt. In the Avra Valley sub-basin the upper basin-fill consists largely of finer grained material in the north and central parts of the sub-basin (Mooseburner, 1972; Anderson, 1988). The upper basin-fill is generally coarser in the southern part of Avra Valley. In the USC sub-basin the upper basin-fill is generally coarser north of Township 13 South and finer grained throughout the rest of the sub-basin (Hanson and Benedict, 1994). The upper basin-fill is correlated to the upper Tinaja beds, the Fort Lowell Formation, and the surficial alluvium deposits as described by Anderson (1987, 1988, 1989) and Davidson (1973).

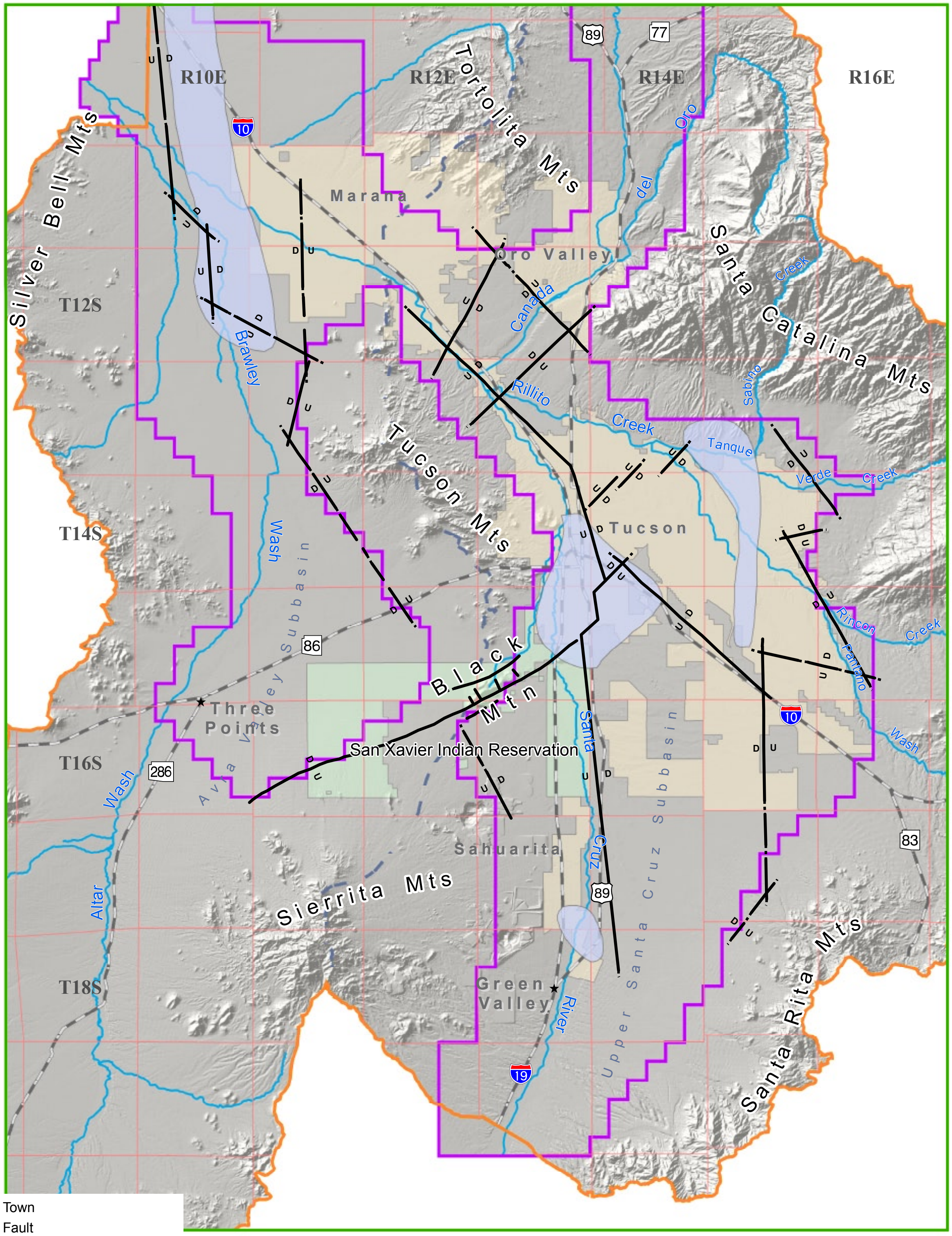

★ Town
Fault
Dashed where uncertain
Road
Stream
San Xavier Indian Reservation
City Boundary
Township & Range
Perched Area
Active Model Boundary
Study Area Boundary
Subbasin Boundary
Tucson AMA Boundary

0 2.5 5 10 Miles

Source(s): Davidson (1973) and Hollett and Garrett (1984).

ARIZONA DEPARTMENT OF WATER RESOURCES

Figure 5.
Map showing locations of known or suspected major geologic faults and areas of perched water zones, Tucson AMA, Arizona.

Table 1. Correlation of stratigraphic units and Tucson AMA model units to orogenic events.

<table>
<tr><th>Stratigraphic Units</th><th>Hydrologic Unit</th><th>Orogenic Events</th><th>Geologic Age</th><th>Geologic Period</th></tr>
<tr><td rowspan="8">Surficial Alluvium
0.01 – 1.3 m.y.a
-------- unconformity ------
Fort Lowell Formation
1.3 – 2.2 m.y.a.
-------- unconformity ------
Upper Tinaja Beds
2.2 – 5.8 m.y.a.
-------- unconformity (?)----
Middle Tinaja Beds
5.8 - 12 m.y.a.
-------- unconformity (?)---
Lower Tinaja Beds
12 – 24 m.y.a
-------- unconformity ------
Pantano Formation
24 – 35 m.y.a.
-------- unconformity ------
Pre-Oligocene Igneous, Sedimentary, and Metamorphic Rocks</td><td rowspan="3">Upper Basin-Fill</td><td rowspan="2">General tectonic stability and development of through flowing drainage</td><td>Holocene</td><td rowspan="2">Quaternary</td></tr>
<tr><td>Pleistocene
1.7 – 2.2 m.y.a.</td></tr>
<tr><td>Second phase of Basin and Range faulting, 5.8 m.y.a and transition to tectonic stability by 2.2 m.y.a</td><td>Pliocene
4.9 – 5.3 m.y.a.</td><td rowspan="6">Tertiary</td></tr>
<tr><td rowspan="5">Lower Basin-Fill</td><td>Basin and Range faulting
12 – 2.2 m.y.a.</td><td rowspan="2">Miocene
23 – 26 m.y.a.</td></tr>
<tr><td>Transition from Mid-Tertiary Orogenic event to Basin and Range Disturbance, 24 – 12 m.y.a.</td></tr>
<tr><td>Mid-Tertiary Orogenic Event
35 - 24 m.y.a.</td><td>Oligocene
34 –38 m.y.a.</td></tr>
<tr><td rowspan="2">Pre-Oligocene Geologic Event</td><td>Eocene
54 – 56 m.y.a.</td></tr>
<tr><td>Pre-Eocene</td></tr>
</table>

After Anderson, 1987, Plate 1.
Million Years Ago – m.y.a.

The surficial alluvial deposits are composed of gravels, sands and silty sands and include alluvial-fan, terrace and stream-channel deposits. The surficial deposits are not hydrologically significant except for the stream-channel deposits, which are usually referred to as the Younger Alluvium. The Younger Alluvium is very permeable and ranges from 40 to 100 ft thick (Davidson, 1973). During pre-development times, the Younger Alluvium was probably partially-to-fully saturated along most of the Santa Cruz River and its tributaries. By 1940, water level declines from localized groundwater pumpage had drained much of the Younger Alluvium along the Santa Cruz River and its tributaries. However, the Younger Alluvium remains hydrological important because it serves as a conduit for floodflow recharge that infiltrates into the underlying regional aquifer

The sediments of the Fort Lowell Formation are generally flat lying and are at most 300 ft to 400 ft thick (Davidson, 1973; Anderson, 1988, 1989). The Fort Lowell Formation is generally unconsolidated to weakly cemented and composed of gravel, sands and clayey silt. In the northern areas of the USC sub-basin the sediments of the Fort Lowell Formation are coarser-grained than in the central and southern parts of the sub-basin. In the Avra Valley sub-basin the unit is generally more coarse-grained in the southern part of the sub-basin and finer-grained in the central and northern parts of the sub-basin.

The upper Tinaja beds are several hundred ft thick and consist of unconsolidated to slightly cemented gravels, sands and clayey silts. In well cuttings it is hard to differentiate the contact between upper Tinaja and the Fort Lowell Formation due to their similar lithologies. The choice of selecting a boundary between the Fort Lowell and the upper Tinaja beds is based, in part, on changes in color, cementation, and mineralogy. In the USC sub-basin the sediments of the upper Tinaja beds are coarsest in the northern section of the sub-basin, becoming finer-grained in the central and southern section of the sub-basin. The upper Tinaja beds are coarser in the central and southern parts of the Avra Valley sub-basin and grade into finer grained deposits in the northern part of the sub-basin.

Deposition of the upper Tinaja beds occurred during the late Basin and Range faulting episode. As a result, the upper Tinaja beds are thickest in the downthrown blocks and thinner on the upthrown blocks of the structural basins in the USC and Avra Valley sub-basins (Figures 3 and 4). A complete sequence of upper, middle, and lower Tinaja beds can be found in the downthrown block, whereas the middle Tinaja beds are generally missing from the sedimentary sequence on the upthrown blocks (Anderson, 1987, 1988, 1989).

Lower Basin-fill

The lower basin-fill is several thousand feet thick and consists of conglomerates, gravels, sands, silts, anhydritic clayey silts, and mudstones. In the Avra Valley sub-basin the lower basin-fill grades from mostly sands, gravels, and conglomerates in the southern part of the sub-basin to anhydritic clayey silts and mudstones in the central and northern parts of the sub-basin (Anderson, 1988; Hanson and others, 1990). The lower basin-fill is more coarse-grained in the northern part of the USC sub-basin with finer grained deposits, including extensive evaporite deposits, occurring in the central grabens of the USC sub-basin (Davidson, 1973; Anderson, 1989; Hanson and Benedict, 1994). The lower basin-fill is equivalent to the Pantano Formation and the lower and middle Tinaja beds described by Anderson (1987, 1988, 1989).

The middle and lower Tinaja beds are several hundred to several thousand feet thick and their composition ranges from gravels and conglomerates to gypsiferous and anhydritic clayey silts, and mudstones. The sediments of the middle and lower Tinaja beds are found in the downthrown blocks of the structural basins in the USC sub-basin and the northern part of the Avra Valley sub-basin. The middle Tinaja sediments are generally not present on the upthrown blocks, having been removed by erosion between periods of Basin and Range faulting (Anderson, 1987). In the downthrown blocks the middle and lower Tinaja sediments are generally fine-grained and can contain thick deposits of gypsiferous and anhydritic clayey silts.

The Pantano Formation consists of semiconsolidated to consolidated conglomerates, sandstones, mudstones and gypsiferous mudstones (Davidson, 1973, Anderson, 1987, 1988, 1989). The total thickness of the Pantano Formation is not known, but it is estimated to be several thousands of feet thick (Davidson, 1973). The unit is usually deeply buried by overlying Tinaja beds along the central axis of the USC sub-basin in the downthrown structural blocks. Along the basin's margins, on the upthrown fault blocks, the Tinaja beds are much thinner, and the Pantano Formation is closer to the surface and sometimes exposed at the surface.

Chapter 3

Regional Groundwater Flow System

Conceptual Model of the Regional Aquifer System

The upper and lower basin-fill sediments within the Tucson AMA are saturated at depth and form the regional aquifer system. Groundwater in the regional aquifer is generally unconfined or partially confined to depths of about 1,000 ft (Davidson, 1973; Hanson, 1988, 1989). Localized confining conditions occur in areas where fine-grained materials in the basin-fill sediments exist. Localized perched zones have also been observed in the regional aquifer (Figure 5). Water level declines due to excessive groundwater withdrawals and/or deep percolation of excess agricultural irrigation are the probable mechanisms for creating the perched areas. For example, fine-grained layers in the basin-fill may strand existing groundwater in areas of large water level declines, or trap irrigation recharge that is percolating through the vadose zone. Perched areas generally occur in the central and northern parts of the Avra Valley sub-basin and in the central and southern parts of the Upper Santa Cruz (USC) sub-basin.

Inflow into the regional aquifer system occurs as groundwater underflow from the SCAMA, mountain-front recharge, stream infiltration, infiltration of effluent released into the bed of the Santa Cruz River, and deep percolation of excess agricultural irrigation water. Central Arizona Project CAP surfacewater became available in the early 1990's and is currently being utilized by the agricultural, industrial, and municipal sectors within the Tucson AMA. CAP water is also being recharged into the regional aquifer at artificial recharge sites located on both the Avra Valley and USC sub-basins. Groundwater is discharged from the regional aquifer through pumpage, evapotranspiration, and as underflow into the Pinal AMA (PAMA). During the winter months some of the effluent released into the channel of the Santa Cruz River from the Pima County Wastewater Treatment Plants exits the Tucson AMA as surface flow.

Groundwater movement within the regional aquifer is generally to the north and northwest, except in the Cañada del Oro drainage, where groundwater moves south before entering the main part of the USC sub-basin. Groundwater enters the USC sub-basin in the south from the Santa Cruz AMA and from the east through the narrow gap between the Rincon and Santa Rita Mountains near Vail, Arizona. Groundwater exits the sub-basin through the Rillito narrows between the Tucson and Tortolita Mountains, moving into the northern part of the Avra Valley sub-basin. Groundwater in the Avra Valley sub-basin also flows to the north-northwest from the southern source areas in Altar Valley to the northern Avra Valley where it exits the Tucson AMA into the Pinal AMA through the gap between the Silver Bell and Picacho Mountains (Figure 1).

Precipitation falling in the mountains and along the valley floors of the two sub-basins is the largest source of natural inflows to the Tucson AMA regional aquifer. Water from precipitation generates mountain-front recharge and flow events in ephemeral streams and washes along the valley floor. Numerous studies have shown that in semi-arid and arid environments low-lying topographic areas such as ephemeral streams and dry washes serve as preferred pathways for recharge. These streambeds and washes typically contain highly permeable sands and gravels, which allow relatively rapid infiltration of runoff from precipitation events. The rapid infiltration allows some water to infiltrate down past the root zone and beyond the effects of high evaporation rates that are present along the valley floor. Very little, if any, of the precipitation that infiltrates directly into the vadose zone away from low-lying areas is believed to recharge the regional aquifer. Most water that infiltrates the vadose zone away from the stream channels in the lower valley floor is absorbed by the soil and then lost through evaporation or transpired by plants.

Annual average precipitation ranges from about 11 inches along the valley floor to as much as 30 inches in the higher elevations of the surrounding mountains (Hydrodata, 2000). Monthly precipitation totals for lower elevations along the valley floor can range from zero to almost 8 inches (Table 2).

Table 2. Average monthly precipitation totals for Tucson, Arizona 1894-2000.

Month	Monthly Average (inches)	Monthly Minimum (inches)	Year	Monthly Maximum (inches)	Year
January	0.89	0	1972	5.58	1993
February	0.85	0	1999	4.15	1905
March	0.76	0	1984	3.88	1905
April	0.38	0	1993	3.53	1905
May	0.18	0	2000	1.34	1931
June	0.27	0	1998	2.07	1938
July	2.05	0.05	1995	7.56	1984
August	2.14	0.08	1924	5.61	1935
September	1.17	0	1973	4.41	1996
October	0.76	0	1982	5.78	1983
November	0.78	0	1999	4.61	1905
December	0.99	0	1996	5.85	1914
Year	11.3	5.07	1924	24.17	1905

Data Source: Hydrodata, 2001

Precipitation occurs in southern Arizona in two distinct seasons; a summer wet season from July to late September, referred to locally as the monsoon season, and a winter wet season from November to April (Figure 6). Beginning in late June to early July, the summer rainy season of isolated, localized thunderstorms provides a break from the spring dry season. Moisture drawn into southern Arizona from the Gulf of California and the Pacific Ocean combines with rising hot air to generate high-intensity, short-term thunderstorms. During the last stages of the summer rainy season, in September and October, dissipating tropical cyclones that originate in the Pacific Ocean off Mexico occasionally make their way into southern Arizona. The tropical cyclones generate large regional storm events that can cause intense precipitation and occasional flooding in southern Arizona. During the winter rainy season, from November to April, widespread low-intensity precipitation events are generated by large-scale regional low-pressure frontal systems. Individual winter precipitation events generally don't produce large rainfall totals; however, under certain conditions winter storms can produce substantial rainfall totals and severe flooding.

Aquifer System

The Tucson AMA regional aquifer system consists of the upper and lower basin-fill as previously described. The Younger Alluvium, the Fort Lowell Formation, and upper Tinaja beds of the upper basin-fill are the most productive units within the basin fill. Most high capacity wells that provide water for municipal, industrial, or irrigation are completed in one or all of these units. As discussed above, the Younger Alluvium is not considered a significant aquifer due to its limited extent and water level declines. However, it may still be saturated in some localized areas, and it is hydrologically significant because it serves as a pathway for stream infiltration into the regional aquifer. The middle and lower Tinaja beds and Pantano Formation of the lower basin-fill are generally not highly productive and have not been widely developed as a source of groundwater. This is due to several reasons, which may include depth of burial, increased consolidation, and presence of large percentages of fine materials. Wells developed in the middle and lower Tinaja beds and Pantano Formation generally produce only small to moderate amounts of water. However, there are areas along the basin margins where the middle and lower Tinaja and Pantano formation are an important source of groundwater. The crystalline and metamorphic units that make up the basement bedrock and the mountains surrounding the alluvial basins provide only small amounts of groundwater for local use and are not considered a part of the Tucson AMA regional aquifer.

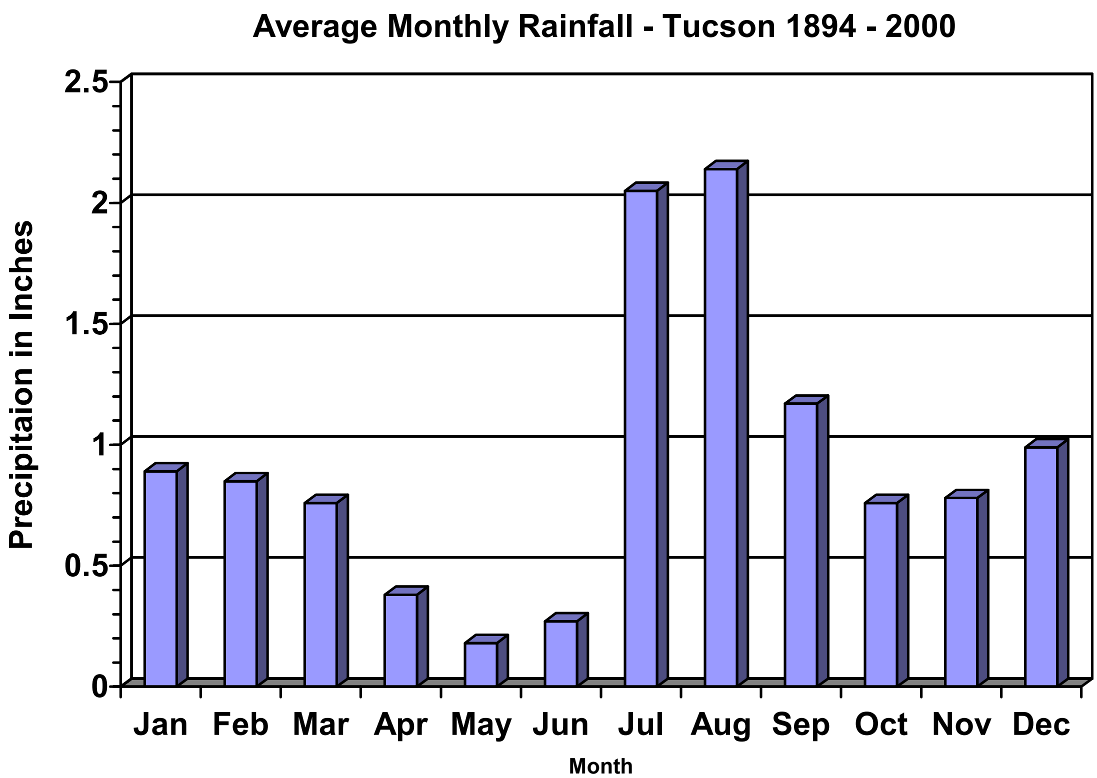

(Source: Hydrodata, 2001).

Figure 6. Average monthly rainfall 1896-2000, Tucson, Arizona.

Fort Lowell Formation

The Younger Alluvium, where it is saturated, the Fort Lowell Formation and the upper Tinaja beds forms the most productive unit in the Tucson AMA aquifer system. Wells completed in the Fort Lowell Formation are capable of producing 500 to 1,500 gallons per minute (Davidson, 1973; Anderson, 1988, 1989). The Fort Lowell Formation has significant saturated thickness throughout most of the USC sub-basin and in the northern parts of the Avra Valley sub-basin, and is considered the main regional aquifer. Groundwater in the Fort Lowell Formation generally occurs under unconfined or water table conditions. Localized perching conditions, caused by interbedded layers of fine-grained sediments, are known to exist in the USC sub-basin just north, south, and east of Black Mountain, and in the northern sections of the Avra Valley sub-basin (Figure 5) (Babcock and others, 1982; Anderson, 1988, 1989). Hydraulic conductivity and storage values for the Fort Lowell Formation vary widely and are dependent on the particle-size distribution and degree of cementation within the unit. Reported hydraulic conductivity values generally range from less than 5 to over 700 ft per day and transmissivity values ranging 1,500 to 40,000 ft^2 per day (Hanson and others, 1990; Hanson and Benedict, 1994). The highest conductivity and transmissivity values generally occur in the Younger Alluvium along the streambed of the Santa Cruz River and its main tributaries. Estimates of specific yields for the upper basin-fill, which includes the Younger Alluvium, Fort Lowell Formation and the upper Tinaja beds, generally range from 0.05 to 0.25 and average about 0.15 (Hanson and others, 1990; Hanson and Benedict, 1994).

Upper Tinaja beds

The upper Tinaja beds and the Fort Lowell Formation form the most productive unit of the Tucson AMA regional aquifer. The upper Tinaja beds have become a more important aquifer in areas where water level declines have reduced the saturated thickness of the Fort Lowell Formation. Well yields and the hydrologic properties of the upper Tinaja beds are generally similar to those of the Fort Lowell Formation. In well cuttings it is hard to differentiate the contact between upper Tinaja and the Fort Lowell Formation due to their similar lithologies. The choice of selecting the boundary between the Fort Lowell and the upper Tinaja beds is based in part on color, cementation, and mineralogy rather than hydrologic parameters. Throughout much of Avra Valley the Fort Lowell Formation is either not saturated or has a smaller saturated thickness than in the USC sub-basin. As a result, the upper Tinaja beds, along with the middle and lower Tinaja beds, are more significant aquifers in the Avra Valley Sub-basin. This is particularly true in the southern portions of the Avra Valley sub-basin where the Fort Lowell Formation is unsaturated and the Tinaja beds consist of thick sequences of coarse-grained sand deposits. In this area the Tinaja beds can be very productive and are the main water-bearing unit.

Middle and lower Tinaja beds

Wells completed in the middle and lower Tinaja beds generally produce only small to moderate amounts of water (Davidson, 1973; Hanson and others, 1990; Hanson and Benedict, 1994). In the USC sub-basin the presence of large amounts of fine-grained material and increased consolidation of the two units reduces their ability to transmit large amounts of water to wells. As a result, these two units generally have not been highly developed as a source of water in the USC sub-basin, except along the basin margins where the Fort Lowell doesn't exist. However, in Avra Valley the Tinaja beds are an important source of groundwater (Anderson, 1987).

Transmissivity and storage properties vary greatly in the middle and lower Tinaja beds depending on their location and composition. Estimated hydraulic conductivity values for the lower basin-fill, which includes the middle and lower Tinaja beds, range from 1 to over 200 ft per day and transmissivities range from 1,000 to over 40,000 ft^2 per day (Davidson, 1973; Hanson and others, 1990; Hanson and Benedict, 1994). Storage properties for the lower basin-fill are difficult to determine and are largely based on estimates from previous modeling studies. Specific yield values are at the low end of reported estimates, probably ranging from 0.03 to 0.10. Storage coefficients for the lower basin-fill below 1,000 ft are estimated to be about 1×10^{-4} (Davidson, 1973; Hanson and others, 1990; Hanson and Benedict, 1994).

Pantano Formation

The Pantano Formation is capable of producing small to moderate amounts of water to wells (Davidson, 1973, Anderson, 1987, 1988, 1989). The unit is generally not an important water-producing unit within the regional aquifer because it is usually too deeply buried by overlying sediments and wells do not penetrate the unit. This is especially true in the downthrown structural blocks where the Pantano Formation is overlain by thousands of feet of sediments from the upper, middle, and lower Tinaja beds. However, near the basin margins on some of the upthrown blocks, particularly west of the Santa Cruz Fault in the USC sub-basin where the Tinaja beds are either missing or much thinner, the Pantano Formation and the overlying Tinaja beds combine to form the main aquifer (Figure 3). Wells completed in the Pantano Formation in these areas can produce moderate amounts of water (Davidson, 1973). Transmissivity and storage values for the Pantano Formation are similar to those reported for the lower Tinaja beds by previous investigators.

Predevelopment Groundwater System

Prior to about 1900, the Tucson AMA regional aquifer system was in a state of dynamic equilibrium with the long-term natural recharge balanced by long-term natural discharge. Groundwater withdrawals during this period were small and limited to domestic and stock uses. Groundwater development in the Tucson AMA began in the early 1900s when the first irrigation wells were constructed in the USC sub-basin to supplement surface water flows diverted from the Santa Cruz River (Schwalen and Shaw, 1957; Hanson and Benedict, 1994). Many of the early irrigation wells were drilled close to the Santa Cruz River and its tributaries because that is where land had been cleared for farming and the water table was shallow (Schwalen and Shaw, 1957; Davidson, 1973). Irrigated agriculture began in the Avra Valley sub-basin in the early 1920s, and by 1937 about 6,000 acres of land was in production in the area around Marana, Arizona (Andrews, 1937). Irrigation water was supplied to these agricultural lands from wells located in the USC sub-basin and transported via canals (White and others, 1966). High capacity irrigation wells were not drilled in the Avra Valley sub-basin until after 1937.

There is consensus among previous investigators that the Tucson AMA regional aquifer system was still in a state of dynamic equilibrium until about 1940 (Anderson, 1972; Moosburner, 1972; Davidson, 1973; Hanson and others, 1990; Hanson and Benedict, 1994). Water budget and water level data support this conclusion. Figure 7 presents estimated pumpage in the Tucson AMA area from 1915 to 1940, and indicates that prior to about 1920, pumpage was, at most, only about 10,000 ac-ft/yr. From 1920 to 1940, pumpage was relatively constant, averaging about 35,000 ac-ft/yr. The relatively uniform stress over that time period probably allowed the regional aquifer system to adjust to withdrawals and maintain an approximate state of equilibrium between inflows and outflows (Davidson, 1973, Hanson and Benedict, 1994). The balance between inflows and outflows was probably maintained by a decrease of evapotranspiration from riparian areas approximately equal to the amount of pumpage plus a small loss of aquifer storage from areas near pumping centers. Schwalen and Shaw (1957) constructed hydrographs of wells with water level data available from the early 1930s through the early 1940s that indicate water level declines were relatively small and concentrated along the Santa Cruz River where the majority of irrigation and municipal wells were located. As a result, any loss of aquifer storage probably affected a relatively small area of the aquifer system, mostly the Younger Alluvium, and probably did not seriously affect the larger regional flow system.

For this modeling study the condition of the Tucson AMA regional aquifer system in 1940, is considered generally representative of predevelopment times and is used as the steady-state period. Figure 8 is a water level contour map developed by ADWR from water level data for the period 1939 to 1940. The map is similar to contour maps of 1940-water levels developed by Moosburner (1972), Anderson (1972), Hanson and others (1990), and Hanson and Benedict (1994), and represents the initial water level surface for the steady-state period. A conceptual steady-state water budget for 1940 developed from numerous sources is discussed below and presented in Table 4.

Inflows

During predevelopment times inflows to the Tucson AMA regional aquifer occurred as groundwater underflow, mountain-front recharge, and streambed infiltration from flow events along the Santa Cruz River and its' major tributaries. Table 3 presents previous estimates of natural recharge from studies that included part or all of the areas included in the Tucson AMA's groundwater basins. Previous investigators' estimates of natural recharge vary widely because of the varying size of the study areas and different methods employed to generate the estimates; therefore, some recharge estimates are not directly comparable to this study's estimates.

Mountain-Front Recharge

Mountain-front recharge occurs in streams at upper elevations of the mountains surrounding the Tucson AMA and through alluvial fans along the mountain-fronts. Rainfall and snowmelt generate surface flows that infiltrate into the alluvial material under the streams and washes that flow from the mountains and cross the alluvial fans. Some water also infiltrates directly into the fans during sheet flow events (Bouwer, 1989). Groundwater then flows into the regional aquifer system through the alluvial fans at the base of the mountains.

Estimates of mountain-front recharge in the Tucson AMA area by previous investigators are not easily compared to this study's estimates. Many previous study areas do not coincide with the current model area and the assumptions used to develop past water budgets are different than those used in this study. Table 3 presents inflow and outflow estimates from investigators whose study areas most closely match the ADWR study boundaries. The mountain-front recharge estimates are listed by sub-basin and for the USC sub-basin range from 28,000 ac-ft per year to 32,000 ac-ft per year. Estimates for the Avra Valley sub-basin range from 500 ac-ft per year to about 9,000 ac-ft per year.

The initial mountain-front recharge estimates for the ADWR model are 29,600 ac-ft/yr for the USC sub-basin and 3,500 ac-ft per yr for the Avra Valley sub-basin for a total of 33,100 ac-ft per year (Table 3). The USC sub-basin estimates are similar to the values developed by Anderson (1972), Davidson (1973) and Hanson and Benedict (1994). The conceptual mountain-front recharge estimates for the Avra Valley sub-basin are based on values developed from a water budget analysis of the sub-basin by Osterkamp (1973).

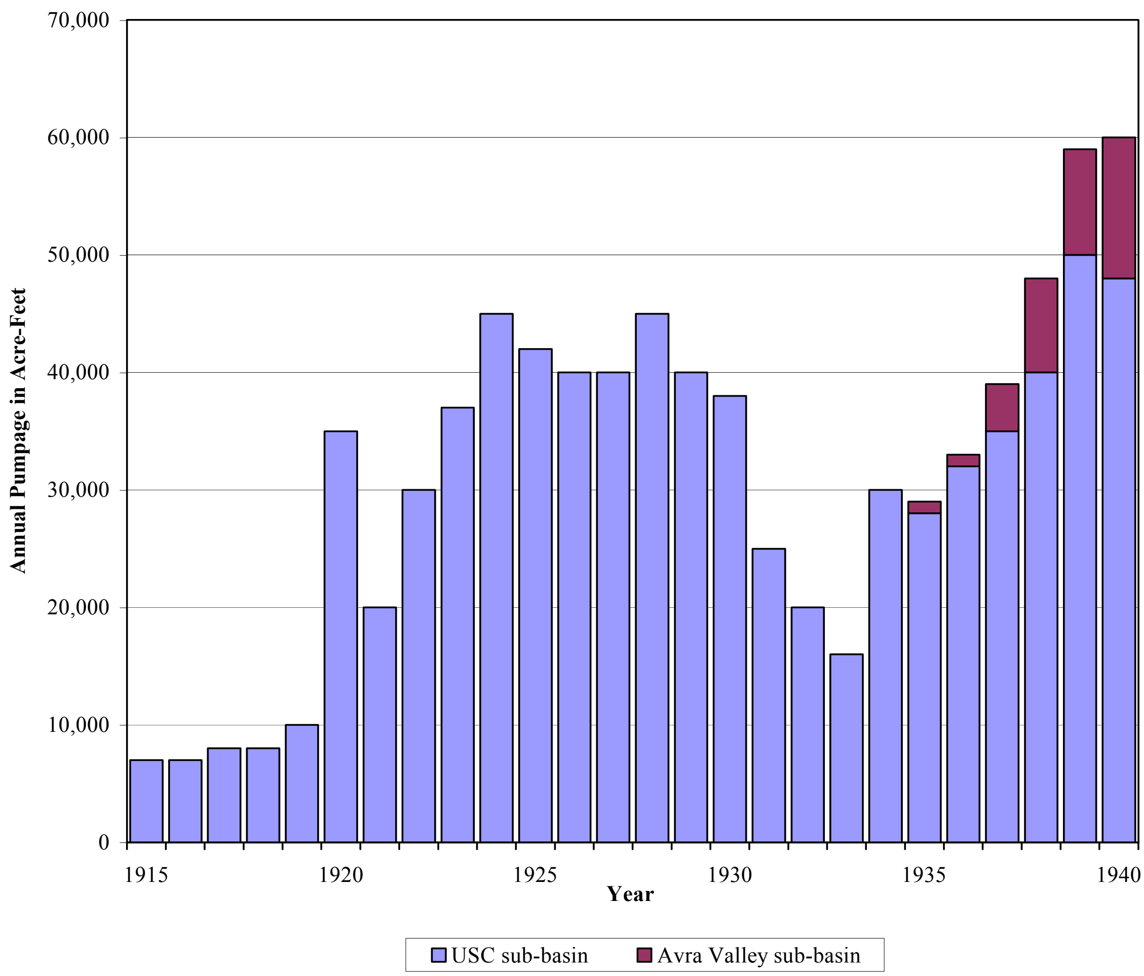

(source: Anning and Duet, 1994)

Figure 7. Estimated pumpage in the Tucson area, 1915 to 1940.

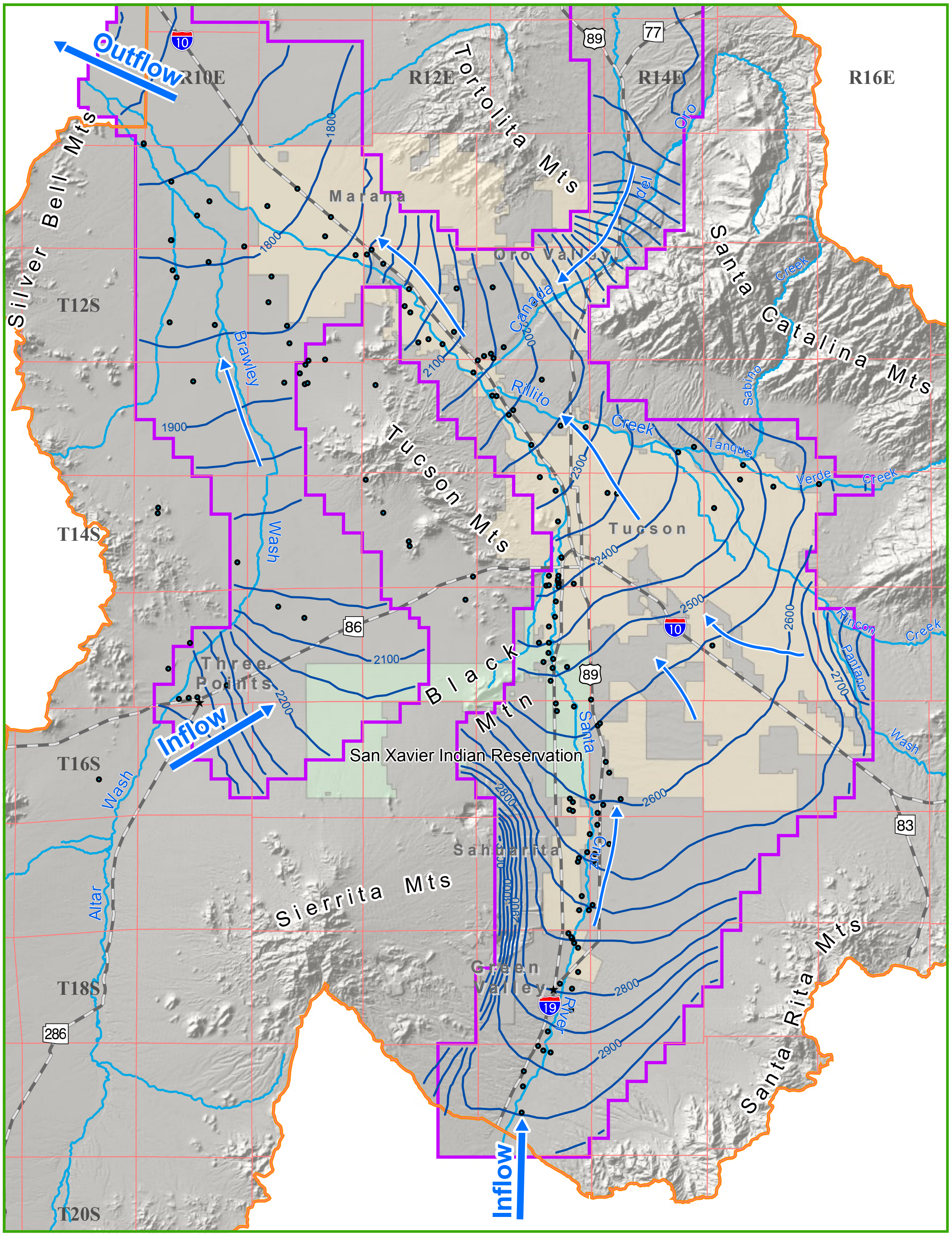

- 1940 Water Level Location
- Town
- 1940 Measured Water Level - ft. above MSL contour interval = 50 ft
- Direction of groundwater flow
- Road
- Stream
- San Xavier Indian Reservation
- City Boundary
- Township & Range
- Active Model Boundary
- Study Area Boundary
- Tucson AMA Boundary

0 2.5 5 10 Miles

Source(s): ADWR, Groundwater Site Inventory.

ARIZONA DEPARTMENT OF WATER RESOURCES

Figure 8.
Map showing groundwater levels in 1940, locations of 1940 water level data, and locations of groundwater underflow, Tucson AMA, Arizona

Table 3. Summary of estimated predevelopment groundwater budget components for the Santa Cruz and Avra Valley sub-basins, Tucson AMA, Arizona. (values are in acre-feet per year)

			Inflows						Outflows		
Time Period	**Source**	**Mountain-Front Recharge**	**Stream Flow Infiltration**	**Groundwater Underflow**	**Other Sources of Recharge**	**Total Inflow**		**Evapotranspiration**	**Underflow**	**Pumpage**	**Total Outflow**
	Santa Cruz sub-basin										
1940 - 65	Anderson (1972)	28,000 [1]	19,000 [1]	10,000 (7,800) [1, 2]	----------	64,800		----------[3]	17,500	47,500	65,000
1940	Clifton (1981)	----------	----------	----------	----------	----------		----------	11,450	----------	----------
1940 - 84	Hanson and others (1990)	----------	----------	----------	----------	----------		----------	9,000	----------	----------
1940	Hanson and Benedict (1994)	29,840	34,020	7,500 (5,430)[2, 4]	----------	76,790		7,890	15,260	53,000	76,150
1936 –65	Osterkamp (1973)	31,900 [6]	63,020 [6]	----------	----------	94,920		----------	----------	----------	----------
1936 - 63	Davidson (1973) [7]	31,000 [8]	51,000 [9]	10,000 (7,800) [2]	17,300 [10]	117,100		6,000 – 15,000 [11]	10,000	176,700 [12]	202,200
1940	Moosburner (1972)	----------	----------	----------	----------	----------		----------	13,000	----------	----------
1940	Whallon (1983)	----------	----------	----------	----------	----------		----------	20,100	----------	----------
1940	ADWR Steady-State Model	31,198	33,655	13,900	0	78,753		17,170	14,380	47,280	78,830
	Avra Valley sub-basin										
1940	Anderson (1972)	----------	----------	17,500 [13]	----------	----------		----------	----------	----------	----------
1940	Clifton (1981)	500	----------[3]	11,450 (6,790) [14]	0	18,470		0	18,470	0	18,470
1940	Freethey and Anderson (1986) [5]	9,000	5,000	12,400 [14]	0	26,400		7,400	19,000	0	26,400
1940	Moosburner (1972)	< 3,000 [15]	----------[3]	13,000 (9,000) [14]	0	22,000		----------[3]	22,000	10,000 [15, 16]	22,000
1940	Osterkamp (1973)	7,100	14,700	----------[3]	----------[3]	21,800		----------[3]	----------[3]	----------[3]	----------[3]
1940	Hanson and Benedict (1994)	----------[3]	----------[3]	15,260	----------[3]	----------[3]		----------[3]	----------[3]	----------[3]	----------[3]
1940	Hanson and others (1990)	0	0	9,000 (9,900)[14]	0	18,900		0	18,900	0	18,900
1940	Whallon (1983)	----------[3]	----------[3]	20,100 (16,600)[14]	0	36,700		----------[3]	34,700	----------[3]	34,700
1940	ADWR Steady-State Model	3,227	5,790	14,380 (10,255)[14]	0	33,652		0	21,191	12000	33,191

Notes:

1. Value simulated in electric-analog model steady-state model.
2. The first value is simulated flow from the Santa Cruz AMA. If provided a second value in parenthesis is underflow simulated along the northern part of the model as underflow coming from the Canada del Oro (CDO) drainage.
3. Budget component was not estimated, simulated, or was considered negligible.
4. The Hanson and Benedict (1994) model's southern boundary was south of Tubac, approximately 12 miles south of the southern boundary of the ADWR model.
5. Basin estimate includes Altar Valley and may not be directly comparable to other values in this report.
6. Value represents recharge for an area that is approximately the same as the Hanson and Benedict (1994) model. Recharge values for the current ADWR model study area would be less.
7. Values represent the mean values for the time period listed.
8. Value is from Anderson (1972).
9. Value is based on Burkham (1970).
10. Value represents 8,300 acre-feet per year of estimated effluent recharge and 9,000 acre-feet per year of estimated incidential recharge from industrial uses.
11. Estimated value from early 1960s.
12. Estimated pumpage for 1965.
13. Underflow from USC sub-basin, Altar Valley was not in study area.
14. The first value is simulated flow from the Upper Santa Cruz sub-basin. If provided a second value in parenthesis is simulated underflow from Altar Valley.
15. Inflow or outflow estimates reported by investigator but not used in report.
16. Pumpage estimate reported from White and others (1965).

Stream Infiltration

Stream infiltration occurs at the lower elevations when precipitation creates flow events that infiltrate into the normally dry beds of the Santa Cruz River and it's tributaries. Individual flow events generated by direct precipitation falling in the valleys are usually of short duration, especially during the summer thunderstorm season. Some winter storms may last for several days and can generate prolonged flow events that may produce large amounts of recharge. Flow events associated with winter storms are believed to contribute more recharge to the regional aquifer than summer storms (Gallaher, 1979).

During predevelopment times stretches of the Santa Cruz River flowed intermittently within the study area due to groundwater discharging from the Younger Alluvium into the riverbed. Cienegas, marshes fed by intermittent flow, occurred near the San Xavier Mission and within the current City of Tucson boundaries (Webb and Betancourt, 1990; Parker, 1993). However, since the early 1900s, a combination of streambed entrenchment along the Santa Cruz River and declining water levels due to groundwater development has impacted the river . A cycle of floods and droughts in the late 1800s and the early 1900s caused headcutting and entrenchment of the river's main channel through much of present day Tucson, destroying the cienegas (Webb and Betancourt, 1990; Parker, 1993). The combination of river entrenchment and early groundwater development, which was concentrated near the river, drained much of the Younger Alluvium. The lowering of the local water table resulted in the regional aquifer becoming hydrologically disconnected from the riverbed, ending natural discharge to the river. By 1940, most sections of the river channel in the Tucson area were deeply entrenched, much of the Younger Alluvium had been dewatered, and the Santa Cruz River flowed only in response to precipitation events.

Estimates of annual stream infiltration into the two sub-basins by previous investigators vary widely and are not easily compared to each other or with the infiltration estimates of this study. Most investigators study areas' did not coincide with the current model area, and assumptions used to develop their stream infiltration estimates may have been different than those used for the ADWR model. Estimates of annual stream infiltration in the Santa Cruz sub-basin range from 19,000 ac-ft to about 63,000 ac-ft, and values in Avra Valley range from 5,000 ac-ft to 14,700 ac-ft annually (Table 3). ADWR's initial estimates of annual stream infiltration within the study area were developed using information from Burkham (1970), Anderson (1972), Davidson (1973), Osterkamp (1973), and Hanson and Benedict (1994). Initial estimates for the average long-term infiltration for the steady-state period are 34,200 ac-ft per year in the USC sub-basin and 6,000 ac-ft per year in the Avra Valley sub-basin (Table 4).

Groundwater Underflow

Underflow into the USC sub-basin occurs from the south across the Tucson AMA - Santa Cruz AMA boundary and to the east through the bedrock gap near Vail, Arizona, where Pantano Wash enters the Tucson AMA. Estimates of steady-state underflow crossing the southern boundary into the USC sub-basin range from 5,600 ac-ft/yr to 10,600 ac-ft per yr (Table 3). Estimates of underflow across the eastern boundary of the study area along the Pantano are small and were included in the stream recharge estimates for Pantano Wash it enters the study area. In the Avra Valley sub-basin groundwater underflow moves into Avra Valley from Altar Valley in the area of Township 16 South. Underflow into the Avra Valley portion of the study area from Altar Valley has been estimated to range from about 6,800 ac-ft per yr to about 16,600 ac-ft per yr (Turner, 1959; Mooseburner, 1972; Brown, 1976; Whallon, 1983; Clifton, 1981; Travers and Mock, 1984; Hanson and others, 1990). The initial estimates of steady-state groundwater underflow into the model from Santa Cruz County and the Altar Valley are 8,600 ac-ft per year and 10,000 ac-ft per year, respectively (Table 4). The initial underflow estimate from Santa Cruz County was calculated as the mid-point of the range of underflow estimates found in reference literature (Table 3). The initial estimate of underflow from Altar Valley was taken from the groundwater flow model developed by Hanson and others (1990).

Outflows

Steady-state groundwater discharge from Tucson AMA's regional aquifer system occurred as pumpage, underflow, and evapotranspiration. Previous estimates of groundwater discharge may not be directly applicable in this study due to differences between study areas and water budget assumptions. Table 3 provides a summary of outflow estimates from studies that cover all, or parts, of the study area.

Pumpage

Groundwater pumpage for agricultural, municipal, and industrial purposes were the single largest source of withdrawals from the regional aquifer in the steady-state period. Estimates of total annual pumpage from the Tucson AMA regional aquifer for the steady-state period, 1940, are about 61,000 ac-ft (Figure 7). Estimated withdrawals in the USC sub-basin were relatively consistent from 1915 until 1919, averaging about 8,000 ac-ft per year. Withdrawals increased in 1920, and ranged from 30,000 ac-ft per year to 45,000 ac-ft per year until 1930 (Figure 7). Withdrawals declined slightly in the early 1930s, to less than 20,000 ac-ft per year before increasing to about 60,000 ac-ft per year in 1940. The initial steady-state pumpage estimate for the USC sub-basin is 49,600 ac-ft (Table 4). The amount and general distribution of USC pumpage comes from previous modeling studies by Anderson (1972), Travers and Mock (1984), and Hanson and Benedict (1994). The initial pumpage estimates for the Avra Valley sub-basin for 1940 is 12,000 ac-ft and comes from the modeling report by Hanson and others (1990).

Underflow

Groundwater underflow exits the Tucson AMA aquifer through the gap between the Silverbell and Picacho Mountains. Underflow between the sub-basins moves to the northwest from the USC sub-basin into the Avra Valley sub-basin through the Rillito narrows between the Tucson and Tortolita Mountains. Previous investigator's estimates of groundwater underflow through the Silverbell and Picacho Mountains gap range from 18,670 ac-ft per year to 34,500 ac-ft per year (Table 3). The conceptual steady-state estimate of annual underflow leaving the Tucson AMA was originally set at 24,500 ac-ft. This estimate was later revised to 22,500 ac-ft based on estimates of mountain-front, stream infiltration, and groundwater underflow into the Avra Valley sub-basin. Estimates of underflow from the USC sub-basin into the Avra Valley sub-basin range from 3,000 to 20,100 ac-ft per year (Table 3). The conceptual steady-state underflow from the USC sub-basin to Avra Valley was set at 15,000 ac-ft per year.

Evapotranspiration

Estimates of evapotranspiration for the Tucson AMA area vary widely in previous investigations. Annual evapotranspiration estimates for predevelopment times in the USC sub-basin range from 15,000 ac-ft to 55,700 ac-ft (Table 3). Prior to the 1890s, water levels in the USC sub-basin along the Santa Cruz River and its major tributaries were shallow enough to support extensive mesquite bosques and cienigas (Bryon, 1922; Schwalen and Shaw, 1957; Parker, 1993). During that time stream infiltration along the Santa Cruz River and its tributaries was probably in balance with evapotranspiration and surface water outflow (Davidson, 1973; Hanson and Benedict, 1994). By 1940, the combination of streambed entrenchment, lowering of the water table near the Santa Cruz River due to groundwater withdrawals, and development in the floodplain had significantly reduced the areal extent of the remaining bosques and associated evapotranspiration. Davidson (1973) estimated evapotranspiration to be between 6,000 and 15,500 ac-ft per year in 1965. Hanson and Benedict (1994) simulated steady-state evapotranspiration at 7,890 ac-ft per year. The conceptual estimate for the Tucson AMA model steady-state ET was rounded up to 8,000 ac-ft per year.

There are no published estimates of evapotranspiration available for the Avra Valley sub-basin. Previous investigators have either assumed that evapotranspiration in Avra Valley was negligible, or did not estimate that component of their water budgets. Andrews (1937) reported the depth to water in the northern part of

Avra Valley along the Santa Cruz River was about 150 feet below land surface, which is too deep to support riparian vegetation. For the purposes of this study, the predevelopment water table in Avra Valley was assumed to be too deep to support riparian vegetation; therefore, evapotranspiration was not considered a component in the Avra Valley sub-basin water budget.

Table 4. Conceptual steady-state groundwater budget for study area.

	Upper Santa Cruz Sub-Basin	Ac-ft/yr.	Avra Valley Sub-Basin	Ac-ft/yr.	AMA Totals Ac-ft/yr.
Inflows					
	Mountain-Front Recharge	**29,600**	Mountain-Front Recharge	**3,500**	**33,100**
	Stream Infiltration	**34,200**	Stream Infiltration	**6,000**	**40,200**
	Underflow from		Underflow from		
	Santa Cruz AMA	8,600	Altar Valley	10,000	
	Pantano	200	USC sub-basin [1]	15,000	
	Total Underflow	**8,800**	Total	**25,000**	**18,800** [1]
	Total Inflows	**72,600**	Total Inflows	**34,500**	**92,100**
Outflows					
	Pumpage	**49,600**	Pumpage	**12,000**	**61,600**
	Evapotranspiration	**8,000**	Evapotranspiration	**0**	**8,000**
	Underflow to Avra Valley [1]	**15,000**	Underflow	**22,500**	**22,500**
	Total Outflows	**72,600**	Total Outflows	**34,500**	**92,100**
	In – Out	**0**	In - Out	**0**	**0**

1. Underflow from the USC sub-basin to the Avra Valley sub-basin is internal to the study area and is not included in the AMA totals calculation.

Groundwater in Storage

Estimates of groundwater in storage for the Tucson AMA regional aquifer during predevelopment times vary depending on assumptions regarding depth to bedrock and aquifer specific yield values. Groundwater storage estimates range from about 68 million ac-ft to about 76 million ac-ft. ADWR (1999a) estimated that total groundwater storage to a depth of 1,200 feet below land surface during predevelopment was about 70 million ac-ft. Groundwater in storage in the USC sub-basin to 1,000 feet below land surface during pre-development time was estimated at about 52 million ac-ft (Davidson, 1973; Hanson and Benedict, 1994). There are no published estimates of groundwater in storage for the Altar Valley section of the Avra Valley sub-basin due to a lack of data. However, estimates of groundwater in storage to a depth of 1,000 feet in the Avra Valley section of the sub-basin range from about 16.5 to 24 million ac-ft (White and others, 1966; Hanson and others, 1990).

Groundwater Development Period: 1941 – 1999

The period from 1941 to 1999 was selected as the groundwater development period for this modeling study. During this period increasing groundwater demands far in excess of natural recharge put the regional aquifer into an overdraft condition. Annual estimated pumpage in the Tucson AMA rose from about 60,000 ac-ft in 1941 to about 490,000 ac-ft in the mid-1970s at (Figure 9). Since the mid-1970s, annual groundwater withdrawals have generally declined to approximately 265,000 ac-ft in 1999.

Groundwater development in the Tucson AMA has altered the predevelopment flow system. Figure 10 shows the Tucson AMA groundwater level map for 1999. Municipal withdrawals from the City of Tucson's central well field, located in T 14 S, R 14 E, have created a large cone of depression in the central part of the USC sub-basin under central Tucson (Figure 10). A smaller elongated cone of depression has formed in the Sahuarita-Green Valley area due to agricultural, industrial, and municipal withdrawals (Figure 10). Heavy agricultural withdrawals in the northern part of the Avra Valley sub-basin between Marana and the Tucson AMA - Pinal AMA boundary have created widespread water level declines and decreased the groundwater flow gradient (Figure 10).

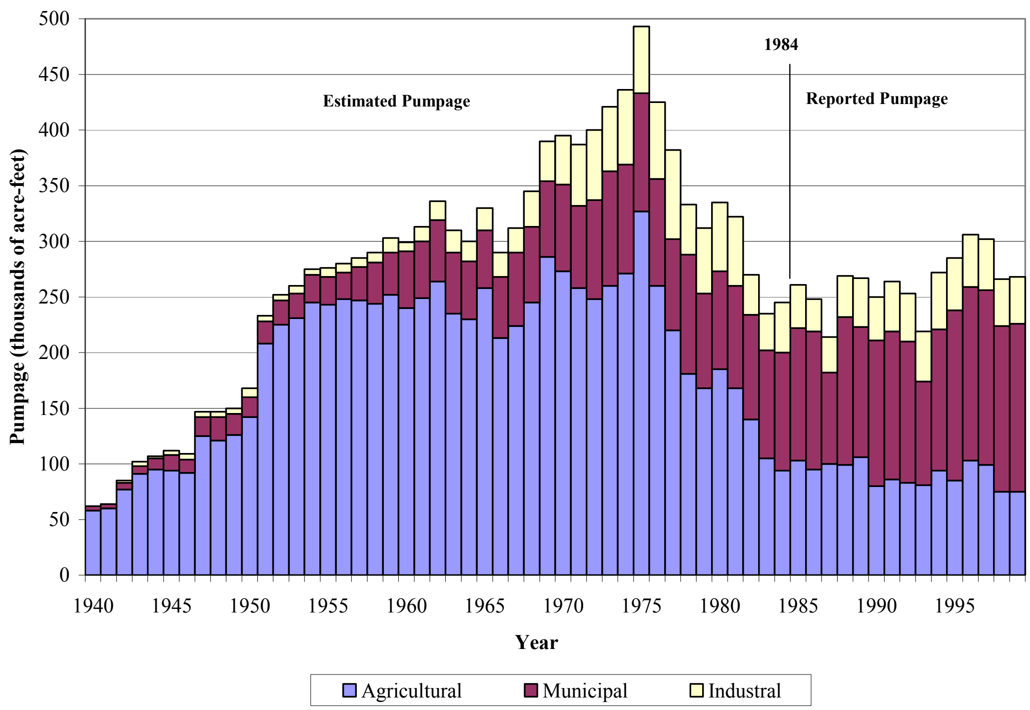

(source: Anning and Duet, 1994; ADWR Registry of Groundwater Rights)

Figure 9. Estimated and reported pumpage in the Tucson AMA: 1940 – 1999.

Initially most groundwater in the Tucson AMA was used for irrigation, but by the mid-1970s, irrigation withdrawals began declining as farms were retired for their water rights and municipal and industrial demands increased to meet population growth. By the mid-1980s, agriculture and municipal water use were about equal, with each accounting for about 40 percent of the total groundwater withdrawn. Industrial

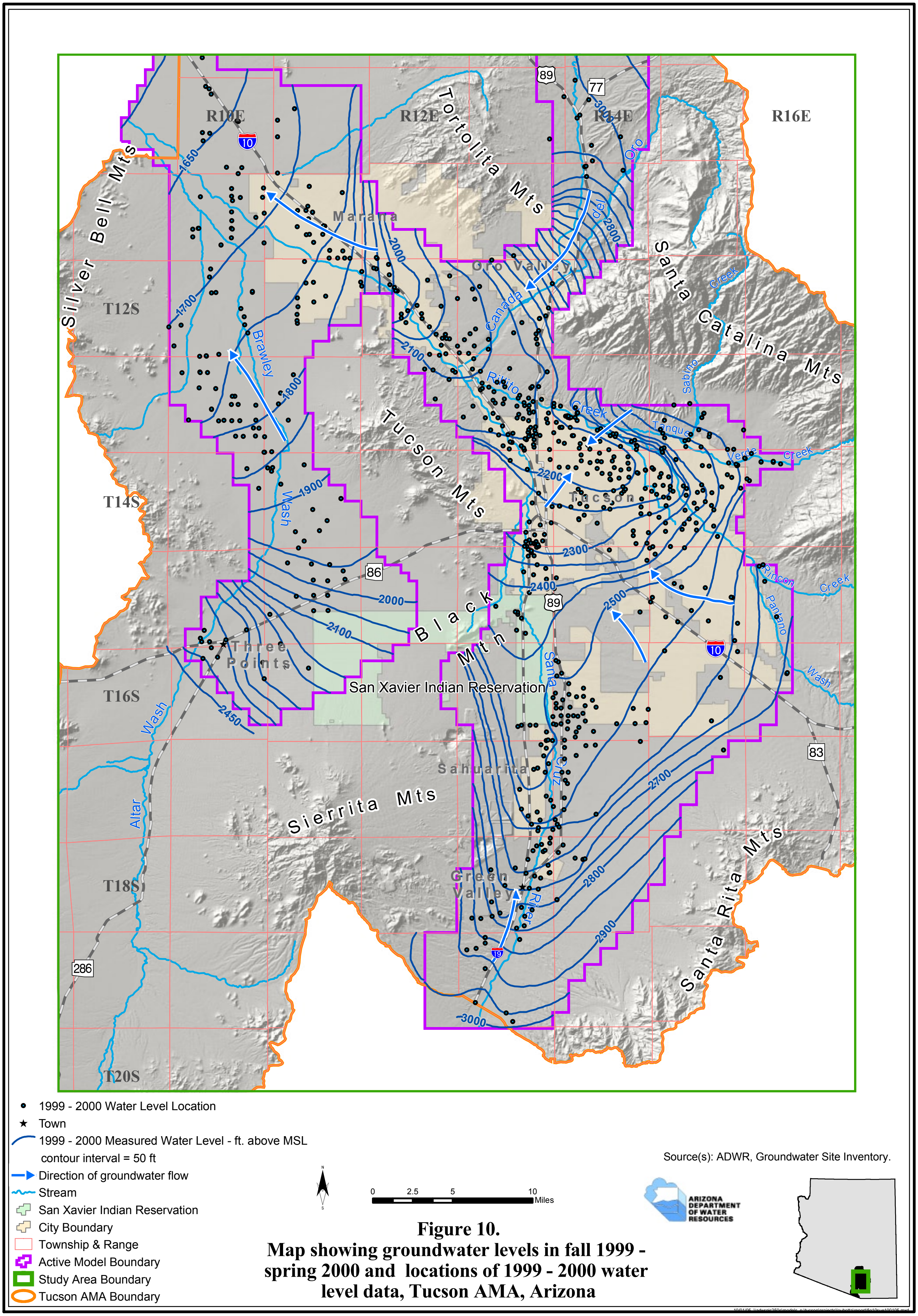

Figure 10.
Map showing groundwater levels in fall 1999 - spring 2000 and locations of 1999 - 2000 water level data, Tucson AMA, Arizona

use made up the remaining 20 percent (ADWR, 2000). By the late 1990s, municipal use surpassed agricultural use and accounted for 50 percent of all groundwater withdrawals. Agricultural use had declined to only about 30 percent of total withdrawals with industrial remaining at 20 percent of total pumpage (ADWR, 2000).

Inflows

Some components of inflow into the Tucson AMA regional aquifer have changed and new recharge components have been added as a result of groundwater development in the regional aquifer. Water level declines under streams and rivers have created a deeper vadose zone and increased potential storage for stream flow infiltration. Groundwater withdrawals have changed water level gradients across inflow and outflow boundaries, either increasing or decreasing underflow volumes into or out of the Tucson AMA.

New sources of recharge have been created by groundwater development. Incidental recharge from deep percolation of excess agricultural irrigation, infiltration of effluent released into the channel of the Santa Cruz River, and seepage from mine tailing ponds exceeded natural recharge by the mid-1960s. These new recharge sources will continue to be major sources of recharge in the Tucson AMA in the future. Artificial recharge projects that are on-line or are in the planning and permitting stages that will utilize CAP water and effluent will increase the importance of incidental recharge in the future. Sources of inflow to the Tucson AMA regional aquifer for the groundwater development period are discussed below.

Natural Recharge

Steady-state mountain-front recharge estimates represent long-term average annual recharge from precipitation in the mountains and is the only natural recharge component that is assumed to have not changed significantly during the developed period. Stream infiltration and underflow into the study area have changed during the post-development period.

Stream Infiltration

The long-term annual stream infiltration distribution developed for the steady-state period is representative for the period from 1941 to 1958. Average stream infiltration values are believed to have increased after 1959, along Rillito Creek and for the Santa Cruz River north of its confluence with the Rillito Creek. Hanson and Benedict (1994) increased stream infiltration values in their model after 1959 based on an analysis of stream flow by Webb and Betancourt (1990), and recharge investigations by Gallaher (1979) and Keith (1981). Gallaher (1979) studied stable isotopes from groundwater in the Tucson basin and determined that winter storms contribute more recharge to the regional aquifer than summer storms. Webb and Betancourt (1990) determined that there was a change in the dominant regional storm-types from summer monsoonal storms to fall-winter cyclonic storms after 1959. Their analysis also suggests an increase in winter precipitation and runoff since 1959. Webb and Betancourt's (1990) work is in agreement with the work of Keith (1981), which also indicated an increase in winter stream flows since 1960, and that more recharge occurs in the winter along drainages that originate in the mountains than in the summer. To maintain consistency between the Hanson and Benedict (1984) and the ADWR update, ADWR stream infiltration values were increased for areas along the Santa Cruz River, Rillito Creek, and Tanque Verde Creek for 1958 to 1999.

Groundwater Underflow

Groundwater underflow across the Santa Cruz AMA – Tucson AMA boundary has changed due to water level fluctuations in the southern part of the Tucson AMA and the northern part of the Santa Cruz AMA. Water level declines and recoveries in the boundary area have altered the predevelopment water table gradient and affected the groundwater flux across the study's southern boundary. Water levels in the southern part of Avra Valley sub-basin along the study area boundary have changed little since predevelopment times so there probably has been no significant change in underflow across that boundary. The potential change in groundwater underflow along the Santa Cruz AMA – Tucson AMA boundary and how the groundwater flow model simulates those changes during the developed period are discussed in Chapter 4.

Incidental and Artificial Recharge

For the purposes of this report, incidental recharge is defined as water that recharges the regional aquifer during the course of its use for agricultural, industrial, or municipal purposes. This includes water that is recharged as a result of irrigation activities, wastewater effluent that is released into the Santa Cruz River or used to irrigate crops and turf facilities, and water infiltrating from mine tailings ponds. Artificial recharge is defined as water that is recharged to the regional aquifer by direct, managed, or in lieu recharge projects permitted by the ADWR.

Agricultural Recharge

Water applied to crops that is not utilized by the plant for consumptive use, lost to evaporation, or held by the soil, percolates below the plant root zone and is termed agricultural recharge. Through deep percolation the excess water eventually reaches the water table and recharges the regional aquifer. For the Tucson AMA model, the maximum potential agricultural recharge was estimated to be equal to the average annual irrigation inefficiency (1 minus the average irrigation efficiency) multiplied by the total annual water applied for irrigation (Corell and Corkhill, 1994). The total annual water applied to agricultural crops or turf facilities (parks and golf courses) includes pumped groundwater, CAP surface water, and effluent.

The estimated average irrigation efficiency of the Tucson AMA has ranged from a low of 65 percent to a high of 75 percent during the developed period. Irrigation efficiencies were estimated to be only 65 percent during the early part of groundwater development in the 1940s through 1960s. Low efficiency values were due to a number of factors; which include poor field preparation, over application of water, and poor water conservation practices. Irrigation efficiencies improved in the 1970's and 1980's with the advent of laser leveling of fields, the implementation of better water management and farming practices, and the economic pressure of rising pumping costs. The estimated annual maximum potential agricultural recharge available for the developed period is presented in Figure 11.

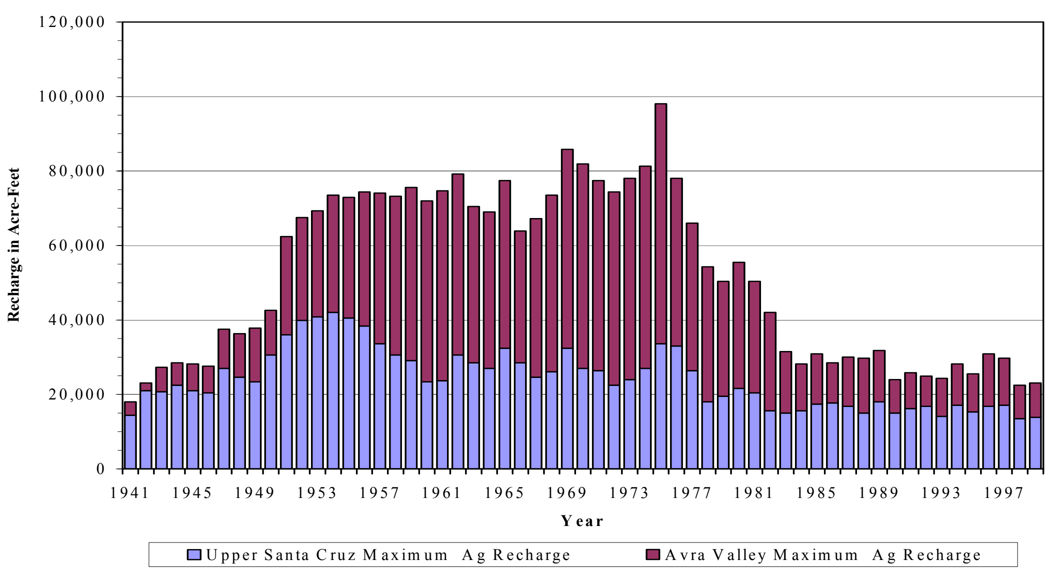

Figure 11. Maximum potential agricultural recharge in Tucson AMA, 1940 - 1999.

Agricultural recharge became a major source of recharge to the regional aquifer by the early 1950s. The estimated annual irrigation recharge has ranged from 60,000 to 80,000 ac-ft during the 1950s and 1960s, peaking in the late 1970's at over 90,000 ac-ft. Irrigation recharge decreased in the 1980's due to increased irrigation efficiency and decreasing agricultural production brought on by increasing agricultural production costs and urbanization of former farmlands. Since the early 1980s, the volume of annual agricultural recharge has been estimated at between 20,000 and 40,000 ac-ft.

Artificial Recharge

Prior to 1993, pumped groundwater was the main source of water in Tucson AMA. CAP surface water was introduced in 1993 and is being utilized in several ways. The largest amount of CAP water is applied for either agricultural irrigation, or as artificial recharge. A small amount is directly used by the industrial sector. Figure 12 shows the annual volume of CAP surface water being utilized in the Tucson AMA. The CAP water is applied for irrigation either directly, in which case no future water credits are earned, or as *in lieu* water. In lieu water use is managed through the ADWR Groundwater Saving Facility (GSF) program. The GSF program allows agricultural customers to apply CAP water in lieu of pumping groundwater, for which they receive recharge credits that can be withdrawn at a future time. CAP water is also directly recharged into the aquifer at artificial recharge projects called Underground Storage Facilities (USFs). USFs recharge and store water that will be recovered in the future as the need arises.

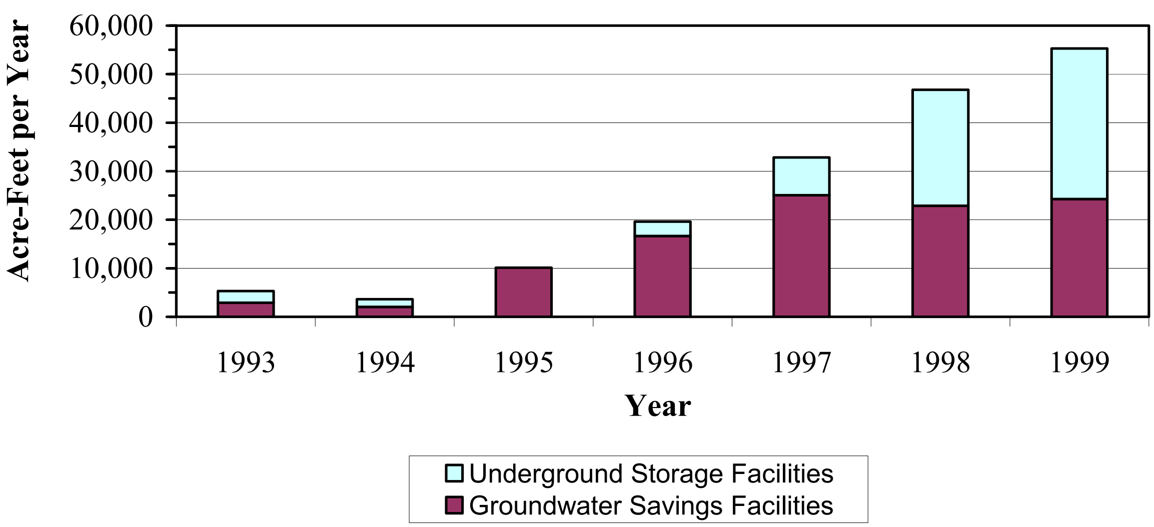

Source: ADWR Registry of Groundwater Rights

Figure 12. Annual CAP water use in Tucson AMA, 1993 - 1999.

Effluent Recharge

Effluent from wastewater treatment plants has been used for irrigation in the Tucson area since the early 1900s (Schladweiler, 2001). From 1917 to 1950, effluent, including raw sewage, was used to irrigate various city farmlands located within or near the city boundaries (Schladweiler, 2001). Effluent releases into the Santa Cruz River began in 1951 from the then just completed Roger Road Waste Water Treatment Plant (WWTP) (Figure 1). Between 1951 and 1956 effluent was diverted both to the river and to farms (Esposito and Thurnbald, 1981; Pima Association of Governments, 1983). From 1956 to 1969 most effluent produced by the Rogers Road WWTP was delivered to farms and little if any, was released directly to the riverbed. However, the farms redirected unused effluent back to the river when they could not utilize it, so there was an unknown amount of effluent recharge occurring through the riverbed during this time

(Esposito and Thurnbald, 1981; Pima Association of Governments, 1983). Due to water quality concerns, direct use of effluent for irrigation was discontinued in 1969, and the Rogers Road WWTP effluent was discharged into the Santa Cruz River.

In 1977, the Ina Road Water Pollution Control Facility (WPCF) became operational and began releasing effluent into the Santa Cruz River (Figure 1). Also in 1977, the Cortaro-Marana Irrigation District (CMID) began receiving secondary treated effluent for irrigation (Bookman-Edmonston, 1978). CMID has continued to receive effluent under contract from the Pima County Wastewater Management Department (PCWMD). The PCWMD and the City of Tucson have also developed a reclaimed water distribution system that supplies effluent to some turf facilities (parks, golf courses, and cemeteries) within Tucson AMA.

Data on effluent releases into the Santa Cruz River bed was provided by PCWMD from 1978 to 1999 (Glenn Petersen, Pima County, personal communications, 2002). Release data from 1950 to 1978 was developed from water quality studies done by the Pima Association of Governments (PAG) (Esposito and Thurnbald, 1981; Pima Association of Governments, 1983). Effluent releases have increased from an initial level of about 800 ac-ft/yr in 1951 to over 50,000 ac-ft/yr in the late 1990s. The releases have increased the amount of stream infiltration recharged into the regional aquifer and have created a relatively consistent surface water outflow component out of the Tucson AMA during the winter months. Figure 13 shows the measured and estimated effluent releases from 1951 to 2000 and represents the maximum potential recharge available due to effluent releases.

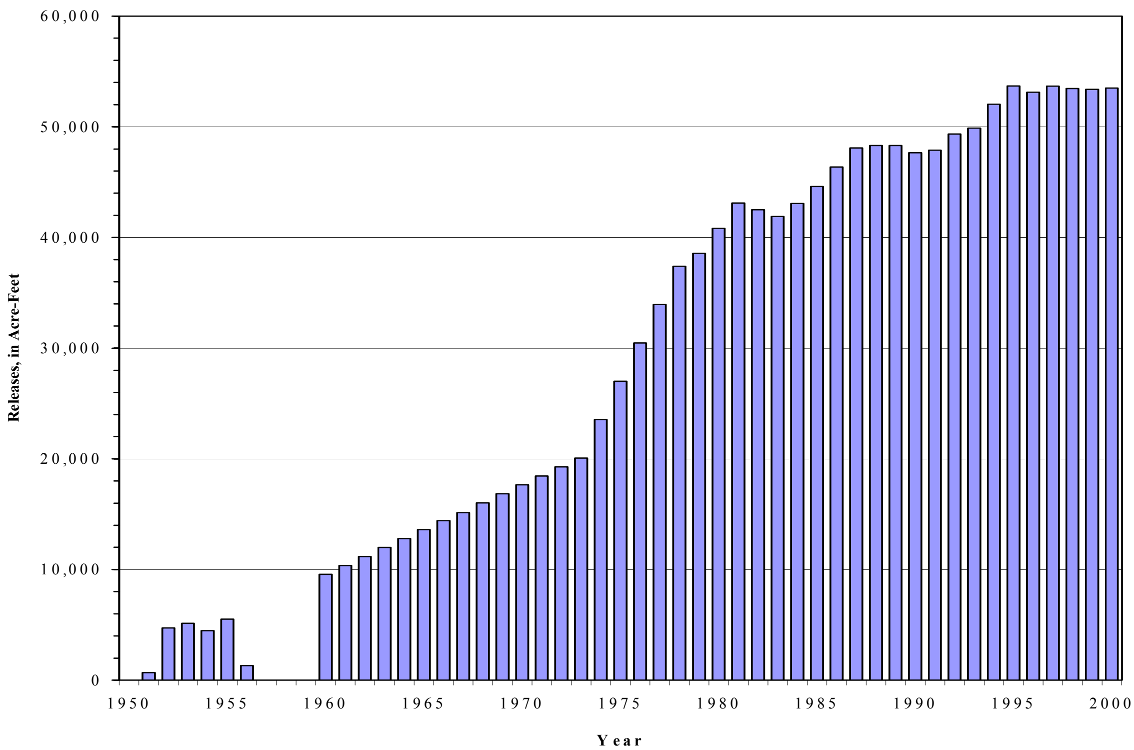

Sources: (Esposito and Thurnbald, 1981; PAG, 1983; Glenn Petersen, Pima County Wastewater Management Department personal communications, 2002)

Figure 13. Estimated and reported effluent releases into the Santa Cruz River 1950 – 2000

Mine Tailings Pond Recharge

Copper mining began in the late-1950s, along the eastern flanks of the Sierrita Mountains. Large volumes of water are used in the mining and milling the copper ore. Some water is returned to the aquifer through seepage from tailing ponds. For the period 1952 to 1984, estimates of mine withdrawals and incidental recharge from tailings ponds developed by Traverse and Mock (1984) and Hanson and Benedict (1994) were used as initial estimates in this study. Well specific pumpage reported to the ADWR ROGR system was used to develop withdrawal and recharge volumes for the period 1984 to 1999.

Outflows

The major sources of outflow from the Tucson AMA regional aquifer during the developed period were pumpage, groundwater underflow, and evapotranspiration. Between 1940 and the mid-1970s, annual groundwater pumpage in the Tucson AMA increased from about 60,000 ac-ft/yr to over 470,000 ac-ft/yr (Figure 9). The annual pumpage volume has far exceeded annual recharge since the mid-1940s, even accounting for increased incidental recharge from irrigation, mining activities and effluent releases. Groundwater underflow and evapotranspiration by riparian vegetation along the Santa Cruz River and its major tributaries have been affected by the large overdrafts during the development period (1941 – 1999). Groundwater flux leaving the Tucson AMA and evapotranspiration have both decreased from predevelopment levels due to water level declines related to the long-term overdraft of the aquifer.

Pumpage

The distribution and amount of annual pumpage prior to the mid-to-late 1960s is not well known. During the period of 1941 to 1960 few detailed records exist regarding the distribution and volume of individual well pumpage. Previous investigators (Anderson, 1972) estimated annual pumpage from 1940 to the early 1960s using power consumption records and crop distribution surveys. Beginning in the 1960s, more water users began keeping detailed withdrawal records for individual wells, so more is known about the amount and distribution of pumpage. However, there is some uncertainty in the pumpage estimates developed during this time period, which are still largely based on energy consumption and crop consumptive use data, rather than metered water usage.

Starting in 1984, the location and amount of pumpage for high-capacity wells in the Tucson AMA has been available. The GMA requires all non-exempt well owners to report well-specific annual pumpage to the ADWR. A brief discussion of historical pumpage during the development period (1941 – 1999) for each sub-basin is presented below.

Avra Valley sub-basin

Historically, about 95 percent of groundwater withdrawals have been used for agricultural irrigation in the Avra Valley sub-basin with the remaining 5 percent used by the municipal and industrial sectors. The dominance of irrigation use has changed in the last 20 to 30 years. During and following Word War II farm acreage increased dramatically and by the early to mid-1950s agricultural development reached a maximum with about 30,000 acres in production (White and others, 1965). The number of wells drilled to supply the increasing water demand also increased so that by 1954, more than 100 irrigation wells were pumping groundwater in the sub-basin (White and others, 1965). Although farm acreage peaked in the 1950s, groundwater withdrawals continued to increase until the mid-1970s due to water application practices and cropping schedules such as double cropping. Figure 14 shows the estimated and reported pumpage for the Avra Valley sub-basin from 1941 to 1999.

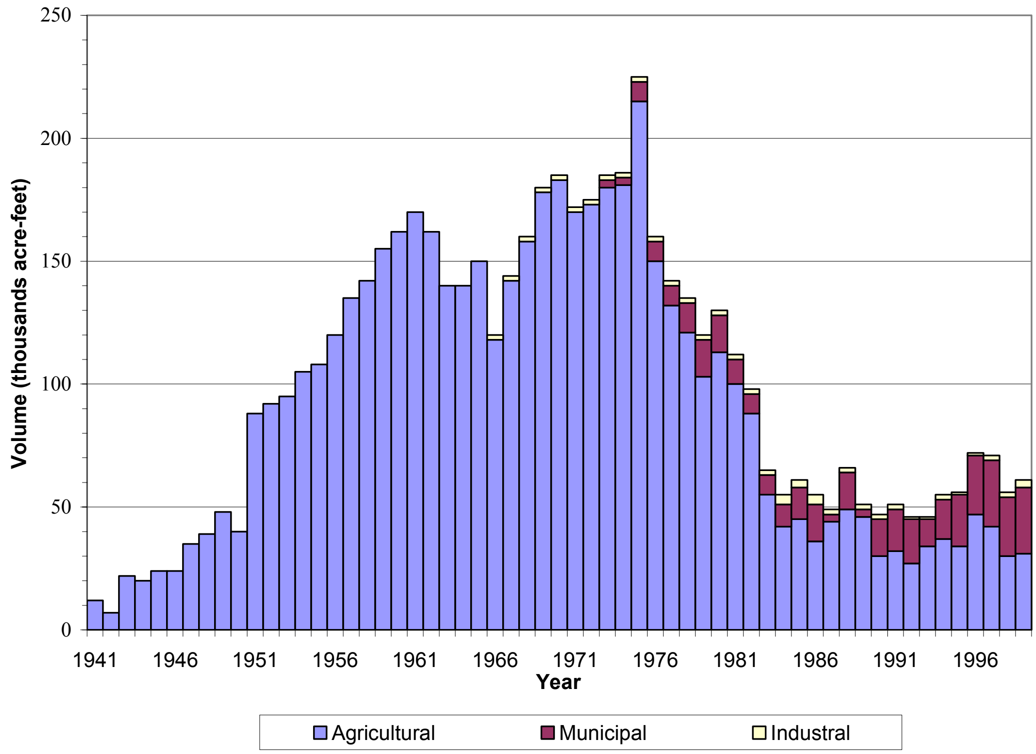

Figure 14. Estimated and reported pumpage in the Avra Valley sub-basin of the Tucson AMA, Arizona, 1941 - 1999

Annual groundwater withdrawals in the sub-basin have declined from a high of about 230,000 ac-ft in 1976, and have averaged about 55,000 ac-ft/yr since 1985. Groundwater withdrawals have declined significantly since the mid-1970s due to several factors. In the early 1970s the City of Tucson began purchasing and retiring farmland in Avra Valley, preserving the groundwater for future municipal use to meet its growing demand. A weakened farm economy and the urbanization of agricultural lands around the town of Marana have also contributed to a shift of water use from the agricultural sector to the municipal and industrial sectors in the sub-basin. In 1999, agriculture, industrial, and municipal use accounted for 48 percent, 47 percent , and 5 percent of water withdrawals in the Avra Valley sub-basin, respectively (ADWR, 2000).

Upper Santa Cruz sub-basin

Agricultural pumpage accounted for 80 to 90 percent of the total pumpage in the USC sub-basin until the mid-1950s (Figure 15). Since the mid-1950's the percentage of municipal and industrial pumpage has increased and the percentage of agricultural pumpage has decreased. The decline in agricultural withdrawals in the USC sub-basin reflects the shift in water use from farming to supplying municipal and industrial water to the growing population of the Tucson area.

Groundwater withdrawals in the USC sub-basin tripled from about 50,000 ac-ft/yr to over 170,000 ac-ft/yr from 1941 to the mid-1950s. Annual groundwater pumpage generally increased from the mid-1950s to the mid-1970s, peaking in 1976 at over 270,000 ac-ft/yr. Since 1976, groundwater withdrawals have generally declined, but from 1985 to the present have averaged just over 200,000 ac-ft/yr. Water use by sector for 1999 in the USC sub-basin was municipal 58 percent, agriculture 14 percent, and industrial 28 percent.

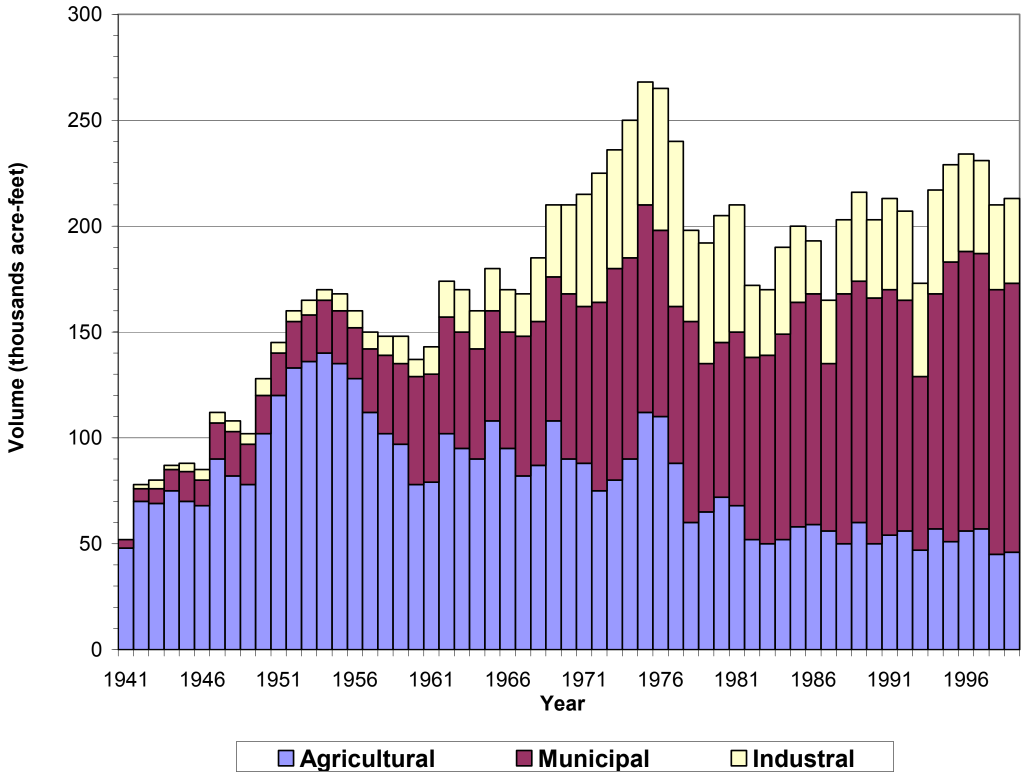

Figure 15. Estimated and reported groundwater pumpage in Upper Santa Cruz sub-basin, Tucson AMA, Arizona, 1941 - 1999.

Groundwater Underflow

Wide-spread water level declines in the northern part of the Avra Valley sub-basin from the early 1940s to the mid-1970s ranged from 50 to as much as 200 feet in some areas. These declines have reduced water level gradients and saturated thicknesses in the regional aquifer in the northern part of the sub-basin at the Tucson AMA – Pinal AMA boundary. The decrease in saturated thickness and gradient near the boundary reduced groundwater underflow leaving the Tucson AMA. Flow net analysis using historic water level data was used to estimate how much groundwater underflow may have been reduced. The flow net analysis indicated that groundwater underflow leaving the Tucson AMA may have been reduced by as much as 10,000 ac-ft/yr from the predevelopment (steady-state) flux of 22,500 ac-ft/yr.

Evapotranspiration

Evapotranspiration (ET) from riparian vegetation has generally declined during the developed period as water levels have dropped along the Santa Cruz River and its tributaries. Hanson and Benedict (1994) simulated a decrease in ET in the Tucson basin of about 5,500 ac-ft/yr, from a steady-state (1940) volume of 7,850 ac-ft/yr to 2,400 ac-ft/yr by 1986.

Transient Water Level Conditions

Water level declines during the groundwater development period (1941 – 1999) have had a large impact on the Tucson AMA regional aquifer. Widespread water level declines of 100 feet to 250 feet have occurred in both the Avra Valley and USC sub-basins, reducing overall aquifer storage and transmissivity. The loss of aquifer storage has caused aquifer compaction and associated land subsidence in both sub-basins. Water level declines associated with pumping centers have created large cones of depression changing the steady-state groundwater flow paths (Figure 10). Water level declines have also isolated shallow aquifers in some areas creating perched zones (Hanson and others, 1990; Hanson and Benedict, 1994) (Figure 5). The perched aquifers continue to receive recharge from natural and incidental sources.

Water levels in many areas of the USC sub-basin have generally exhibited a long-term downward trend. Groundwater withdrawals in the north central area of the USC sub-basin have resulted in historic water level declines of between 50 and 225 feet and the formation of a large cone of depression in the metropolitan Tucson area. This is an area referred to as the central well field, where a large concentration of high-capacity wells provides water to the City of Tucson. Many of the wells in this area have experienced steep, long-term declines. Several smaller, localized cones have formed in areas with high levels of groundwater withdrawals. In the Green Valley-Sahuarita area, located in the southern part of the USC sub-basin, a cone has formed that parallels the Santa Cruz River. This cone has been created by pumpage for mining and agricultural activities. Water levels in the Green Valley-Sahuarita area declined about 100 to 150 feet between 1940 and the early 1980's. However, water levels have shown recoveries of 50 to 75 feet since the early 1980's (Hammett and Sicard, 1996). The recovery may be due, in part, to a decrease in mine withdrawals as a result of a depressed mining economy in the early 1980's and infiltration of flood flows in the Santa Cruz River

Water levels in some agricultural wells in the northern part of the Avra Valley sub-basin have declined by 150 feet to 200 feet from 1940 to the mid-1970s. Since the mid 1970s, water levels in some areas have stabilized or recovered by as much as 75 feet (Hammett and Sicard, 1996). The water level recovery is due to several factors, which include a large decrease in pumpage in northern Avra Valley since the mid-1970s, and large volumes of agricultural recharge that is now reaching the water table after percolating through the unsaturated zone. Agricultural pumpage peaked in Avra Valley in the mid-1970s and has decreased from a high of about 230,000 ac-ft/yr to the current pumpage of about 55,000 ac-ft/yr. Artificial recharge projects that store CAP surface water in the northern and central sections of Avra Valley may have also contributed to recent water level recoveries in those areas.

Change in Storage

Consistent overdrafting of the Tucson AMA regional aquifer since the 1940s has resulted in a persistent, long-term loss in the volume of groundwater stored in the regional aquifer. The loss of storage in the regional aquifer since 1940 has been estimated to range from 6 to 8 million ac-ft (ADWR, 1999a). The estimated loss is similar to the total simulated aquifer storage losses in the Avra Valley and USC sub-basin of 6.8 million ac-ft from groundwater flow models by Hanson and others (1990) and Hanson and Benedict (1994) for the period 1941 to 1986. The estimated loss represents 8 to 11 percent of the estimated 70 million ac-ft of groundwater available to a depth of 1,200 feet below land surface in the Tucson AMA (ADWR, 1999a).

Chapter 4

Numerical Model

Modeling Approach

The Tucson AMA regional groundwater flow model study area is 3,250 square miles and includes portions of the Upper Santa Cruz and Avra Valley sub-basins. The study area boundaries and the lateral extent of the active model are presented in Figure 1. The model simulates steady-state (predevelopment groundwater) conditions in 1940, and transient (developed groundwater) conditions from 1941 to 1999. The transient period was divided into 59 annual stress periods from 1941 to 1999. The model units of length and time were feet and days, respectively. The regional aquifer was divided into three model layers to enable the model to simulate three-dimensional groundwater flow. The model simulates underflow into and out of the AMA, natural recharge from mountain-front and stream channel infiltration, incidental recharge from agricultural irrigation, effluent releases into the Santa Cruz River and mine tailings ponds, evapotranspiration from riparian vegetation, artificial recharge, and groundwater pumpage. The general characteristics of the Tucson AMA regional groundwater flow model are presented in Table 5. A detailed description of the model design is discussed below.

Model Code

The model code selected to simulate groundwater flow in the Tucson AMA was the Modular Three-Dimensional Finite Difference Groundwater Flow Model (MODFLOW) developed by the U.S. Geological Survey (McDonald and Harbaugh, 1988; McDonald and Harbaugh, 1996: Harbaugh and others, 2000). The MODFLOW code was selected for use in this project because: 1) MODFLOW has a modular format that allows specific hydrologic features and stress to be simulated, 2) The code can allow interconnection between multiple hydrologic units, 3) the documentation is complete and ADWR staff has experience with the code, and 4) the code is widely used and is accepted as a valid model for simulating groundwater flow. The initial calibration of the steady-state and transient models was done using MODFLOW 96. In the fall of 2000, when MODFLOW 2000 became available the steady-state and transient models were converted to the run using MODFLOW 2000. For a detailed explanation of the mathematical theory of MODFLOW and how to implement the code, please refer to McDonald and Harbaugh (1988, 1996) and Harbaugh and others (2000).

Model Development

Model Grid and Cell Definitions

The model study area is 50 miles east to west and 65 miles north to south and is oriented north-south following the Arizona township and range grid. The model grid was divided into a regular orthogonal grid consisting of 130 rows and 100 columns; each cell is 0.5 miles on a side and contains 160 acres (Figure 16).

There are three types of cells used in MODFLOW: no-flow cells (inactive cells), variable head cells (active cells), and constant head (specified-head) cells. No-flow cells are inactive and are not involved in the model solution process. Variable head cells are used to simulate saturated portions of a model where model heads, simulated water levels, vary with time. Constant head cells are used to simulate model heads that remain constant over either a specified time period, or the entire model simulation.

Table 5. Tucson model components**.**

Model Component	Description	Units
Steady-State Period	1940	Time = Days, Length = Feet
Transient Period	1941-1999	Time = Days, Length = Feet
Model Grid	130 Rows x 100 Columns	Model Cells = 0.5 mile square
Model Cell Types	No Flow, Constant and Variable Head	
Boundary Conditions	Constant Head and Specified Flux	
DIS Package	Specifies aquifer tops and bottoms and time discritization	1 Steady-State and 59 Transient Stress Periods, 12 Time Steps per Transient Stress Period
BAS Package	Specifies starting water levels and active model domain	
Block-Centered Flow (BCF) - Rewetting Active	Specifies hydrologic parameters and allows rewetting of cells that go dry prior to or during a simulation	Rewetting threshold: 20 Ft.
Layer 1 - 2198 active cells	Layer Type 1 - Unconfined Aquifer, Transmissivity = K x Thickness	K = Feet / Day
Layer 2 – 4266 active cells	Layer Type 3 – Confined-Unconfined Aquifer, Transmissivity = K x Thickness	K = Feet / Day
Layer 3 – 4811 active cells	Layer Type 2 – Confined-unconfined Aquifer, Constant Specified Transmissivity	T = $Feet^2$ / Day
Vertical Leakance	Assigned based on the areal distribution of percent fines in each layer	1 / Days
Specific Yield	Volume of water yielded per unit area per unit change of water level in unconfined aquifer	Dimensionless
Storage Coefficient	Volume of water yielded per unit area per unit change in a confined aquifer's potentiometric surface	Dimensionless
Pumpage	Assigned to all cell layers	$Feet^3$ / Day
Recharge	Applied to uppermost active cells; Specified in some cells during Transient Period,	Feet / Day
Evapotranspiration	Assigned rates per cell; Extinction Depth 25 Feet	Feet / Day
Numerical Solvers	Steady-State Calibration: Strongly Implicit Procedure (**SIP**)	Closure Criteria: 0.01 Feet
	Transient calibration: Preconditioned Conjugate Gradient Method (**PCG**)	Number of Interations: 100 Preconditioning Type: 5 Strongly nonlinear problem: 2 Closure Criteria: 0.01 Feet & 50 $Feet^3$ / Day

In the Tucson AMA model no-flow cells delineate the active model domain by representing bedrock areas or areas where groundwater flow is parallel to a model boundary. These conditions exist along the various mountain-fronts in the model domain. Variable head cells define the active model area that represents the regional aquifer in the study area. Constant head cells are specified along some model boundaries to simulate groundwater underflow into or out of the study area. Utilizing constant head cells along these boundaries allows groundwater fluxes can change in response to changing hydraulic gradients within the model. Constant head cells were assigned in all layers along the southern boundary and along the northwestern boundary to simulate underflow into the model from the Santa Cruz AMA and Altar Valley and to simulate groundwater underflow out of the model and into the Pinal AMA (Figure 16). The northern model boundary at the head of the Cañada del Oro Wash is believed to be a groundwater divide with no or very little groundwater flux and is modeled with variable head cells.

Model Layer Definitions

Three model layers were used to simulate the major water bearing aquifers in the Tucson AMA. The model layers were defined using well log information obtained from files from the USGS and the City of Tucson, previous modeling reports, and other geologic data (Anderson, 1987, 1988, 1989; Hanson and others, 1990; Hanson and Benedict, 1994). Some minor adjustments were made to the layer elevations during the calibration process. In this study, only the upper basin-fill and the upper portions of the lower basin-fill are considered hydrologically significant. Bedrock areas that yield only small amounts of water to wells are not considered part of the regional aquifer and are not within the active model domain. The lateral extent of each model layer is shown in Figure 16.

Model layer 1 is the saturated portion of the Younger Alluvium (stream channel and flood plain alluvium) and the Fort Lowell Formation. Layer 1 is present at the surface in the USC and Avra Valley sub-basins and is modeled as an unconfined water table aquifer (MODFLOW Layer Type 1) with a specified hydraulic conductivity value and specific yield value. The Fort Lowell Formation is the most productive and heavily utilized aquifer in the Tucson AMA.

Model layer 2 represents the upper Tinaja beds, which underlie the Fort Lowell Formation and make up the second most productive aquifer in the modeled area. Layer 2 is modeled as a MODFLOW convertible layer (Layer Type 3) that allows cells to convert from water table (unconfined) conditions to confined conditions. Hydraulic conductivities and storage values are specified and determined based on the head in a cell. If the head in a cell is above the top of the cell, then the cell is confined; cell transmissivity is calculated using the cell thickness and the specified conductivity and storage is determined using an assigned storage coefficient value. In the case where the initial head in a cell is above the top of the cell and falls below the cell top during a simulation, the cell converts to a water table condition cell. When this occurs transmissivity is calculated using the assigned conductivity and the saturated thickness of the cell and storage is determined using an assigned specific yield value. A cell can also convert from water table to confined conditions during a simulation. Model layer 2 extends from the basin centers to the margins of both sub-basins. Large areas of the Fort Lowell Formation have been dewatered since the 1940s, consequently, model Layer 2, the upper Tinaja beds, has become an increasing important source of water.

Model layer 3 simulates the water bearing basin-fill sediments below the upper Tinaja beds. This layer includes the middle and lower Tinaja beds and the Pantano Formation. Layer 3 is also modeled as a MODFLOW convertible layer (Layer Type 2) with a specified transmissivity. Any water level change in this type of layer is assumed to be small relative to its total saturated thickness, and therefore, the layer has no assigned thickness. Storage calculations for layer 3 are done in a manner similar to layer 2, where the head in the cell determines whether a storage coefficient or a specific yield value are used in calculating storage changes. Layer 3 exists through out the aquifer system, but is generally the least productive aquifer.

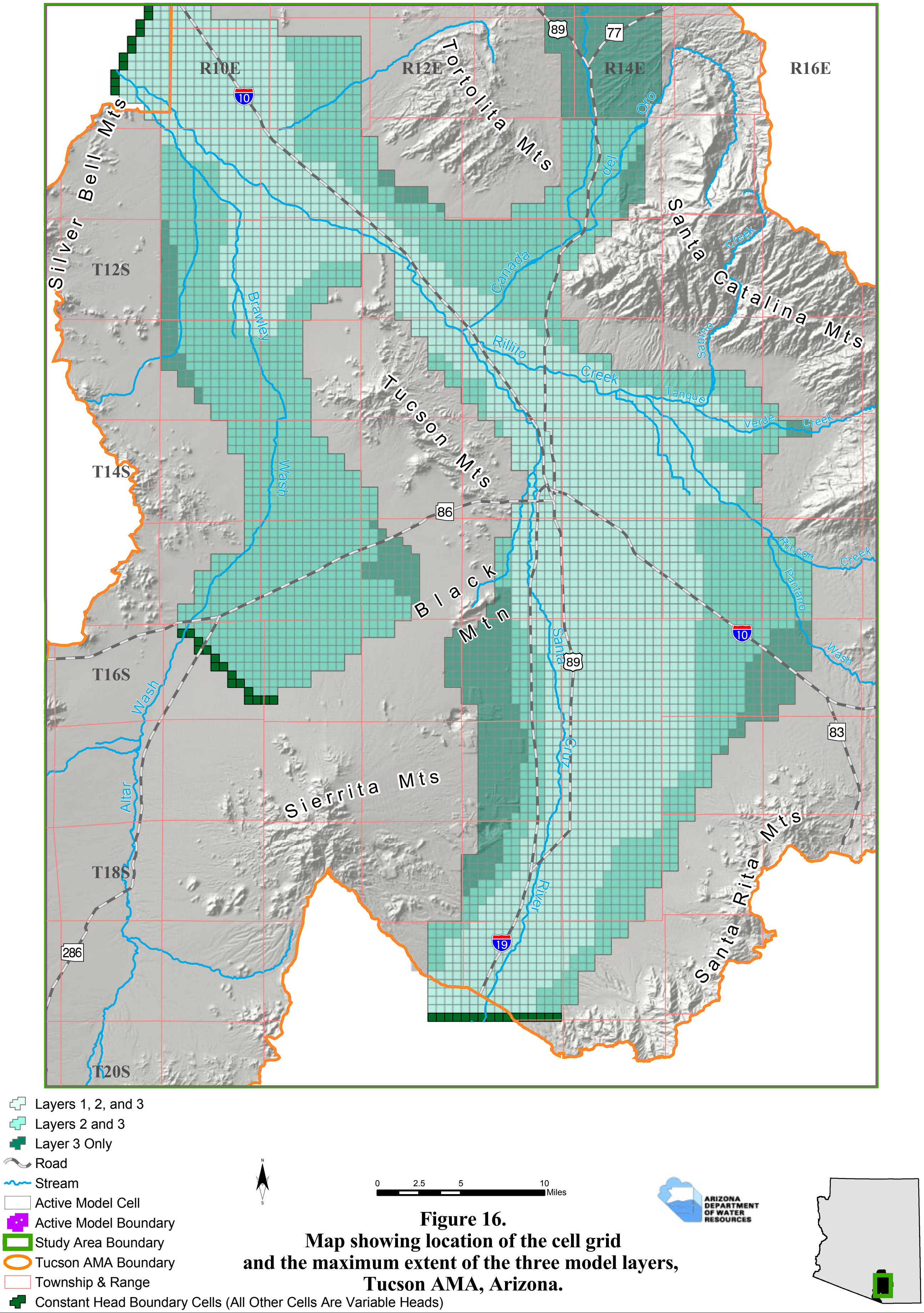

Figure 16.
Map showing location of the cell grid and the maximum extent of the three model layers, Tucson AMA, Arizona.

MODFLOW Packages

The Tucson AMA groundwater flow model utilizes seven packages and two numerical solvers that are available in MODFLOW 2000. The packages are: Basic (BAS), Block-Centered Flow (BCF), Discritization (DIS), Well (WEL), Recharge (RCH), Evapotranspiration (EVT), and the Time-Variant Specified-Head Package (CHD). Numerical solvers used included the Strongly Implicit Procedure (SIP) and the Preconditioned Conjugate Gradient Procedure (PCG). The brief discussion below describes how each package was used in modeling the Tucson AMA regional aquifer.

- The BASIC (**BAS**) package designates the active model domain and the starting water levels for each active cell. The package defines cells as no-flow, variable head, or constant head. In the steady-state simulation cells along inflow and outflow boundaries were defined as constant head values.

- The Block-Centered Flow (**BCF**) package defines the cell-centered hydraulic parameters of the model. The hydraulic parameters defined in the BCF package are the cell-specific horizontal hydraulic conductivities or transmissivities, vertical conductance, and storage terms. The BCF package also controls the cell Rewetting option, which is used to establish the condition under which a model cell that had gone dry can be rewetted. The BCF package calculates the conductance values for the finite-difference equation that determines flow between active model cells. If a simulation is transient the movement of water into and out of storage is also calculated.

- The Discretization (**DIS**) package establishes the physical layout of a model. The package assigns the number of model rows and columns, the number of model layers, the physical dimensions of each cell and the layer tops and bottoms. The DIS package also assigns the model time and length units, the number of stress periods and the length of time for each stress period, and whether a model simulation is steady-state or transient or contains both steady-state and transient stress periods.

- The Well (**WEL**) package is used to simulate water that is withdrawn from or added to a model, usually by a well. The well is assigned a specified rate for a given stress period and is located within the model based on a row and column designation. The discharge can also be assigned to individual layers within the model.

- The Recharge (**RCH**) package can be used to add areally distributed water to selected cells within a model. Usually the recharge package is used to simulate precipitation that percolates into the aquifer, mountain-front recharge, or various incidental recharge sources

- The Evapotranspiration (**ET**) package is used to simulate groundwater outflow that is transpired by riparian vegetation or direct evaporation of groundwater at the land surface.

- The Time-Variant Specified-Head (**CHD**) package is used to simulate time-varying specified heads. The package allows constant head cells to be assigned different values at different times during the model simulation, which allows boundary fluxes to vary through time based on the hydraulic gradient between the specified-head and variable heads within the model.

- Numerical solvers are used by MODFLOW to solve the large system of linear finite-difference groundwater flow equations needed to calculate movement of water into and out of the model cells. Two model solvers, the Strongly Implicit Procedure (**SIP)** and Preconditioned Conjugate Gradient (**PCG)** packages, were used in the steady-state and transient models, respectively.

For documentation describing the mathematical theory and application of the MODFLOW packages and numerical solvers used in the Tucson AMA model the reader is directed to McDonald and Harbaugh (1988), Hill (1990), McDonald and others (1992), and Harbaugh and McDonald (1996).

Boundary Conditions

Selection of appropriate boundary conditions is important to the modeling process and should reflect the hydrologic conditions along model boundaries. To simplify the modeling process, boundaries for the Tucson AMA model were selected along mountain fronts and at points of underflow into and out of the AMA (Figure 16). The inflow-outflow boundaries were selected at or as close as possible to the AMA boundaries, and where possible the inflow-outflow boundaries were selected to coincide with previous model boundaries so that current and previous model inflow and outflow fluxes could be compared.

Mountain-fronts were simulated as no-flow boundaries with specified flux boundaries representing mountain-front recharge. Recharge volumes were assigned to cells using MODFLOW's Recharge Package. Underflow into and out of the model was simulated using constant head cells and as specified fluxes. Simulated fluxes into or out of the model across the constant head boundaries were proportional to the hydraulic gradient and conductance between the constant head cells and adjacent variable head cells. Fluxes across selected model boundaries were simulated using specified fluxes using the Well Package during the transient model. The locations and types of model boundaries used in the steady-state and transient model simulation are discussed in more detail in Chapter 5.

Model Data Development

As discussed in Chapter 1 there is a large amount of data available from numerous hydrogeologic studies for the Tucson AMA area. The data include both generalized information that is useful in developing a conceptual understanding of the regional groundwater flow system, and more detailed site specific data that can be used in developing a groundwater flow model. Initial model data sets for the Tucson AMA model were largely developed using data sets from modeling studies by Travers and Mock (1984), Hanson and others (1990), and Hanson and Benedict (1994). In many cases the raw information used to construct those data sets were available along with more current information. A discussion of sources of data used to develop the initial ADWR model data sets is presented below.

Water Levels

Water level data was used to create target water level maps and establish observation heads for the steady-state and transient model simulations. Target water level maps are created from observed water level data and can be compared with maps of model-simulated heads (water levels) to determine if the model is able to generally reproduce observed regional flow paths. Observation heads are selected water levels from wells that can be compared to model simulated heads. A statistical analysis of the difference (residual) between observation and simulated heads can be used to describe the average error and identify areas of unacceptably large error for a particular model simulation.

Water level data for target water level maps and observation heads were obtained from the ADWR GWSI database. The GWSI water level database contains over 36,000 water levels from 3,200 wells in the Tucson AMA. A 1940, steady-state water level contour map was developed using approximately 157 water level data points (Figure 8). The map is similar to water level maps of 1940, developed by Anderson (1972), Moosburner (1972), Hansen and others (1990) and Hansen and Benedict (1994). The 1940 water level contour map was used to estimate cell-centered model water levels that were used as initial starting conditions for the steady-state simulation.

Maps were constructed for water level conditions in 1960, 1983, and 1999, using existing maps by Davidson (1973), Hedley and Murphy (1986) and water level data from the GWSI. The 1960 and 1983 water level maps were used as intermediate calibration targets during the transient model calibration. A water level contour map for the final year of the transient period, 1999, was developed from observed water level data points collected during the fall of 1999 and early spring of 2000 (Figure 10). The 1940 and 1999 observed water levels from the GWSI were used as model calibration targets for the steady-state and transient model calibrations.

Aquifer Parameters

Initial estimates of the model aquifer parameters of hydraulic conductivity and storage values for this study were developed from previous modeling studies, geohydrologic studies, and aquifer test results. Model data sets from studies by Travers and Mock (1984), Hanson and others (1990), Marra (1992) and Hanson and Benedict (1994) greatly facilitated the development of the initial hydrologic parameters for the Tucson AMA model. Hanson and others (1990) and Hanson and Benedict (1994) developed two-layer models of the two sub-basins within the Tucson AMA. The study by Hanson and others (1990) covered the Avra Valley sub-basin and the Hanson and Benedict (1994) study encompassed the USC sub-basin.

Model layer 1 in this study, and in Hanson and others (1990) and Hanson and Benedict (1994) are approximately the same. Initial hydraulic conductivity and aquifer storage values for model layer 1 were assigned directly from Hanson and others (1990) and Hanson and Benedict (1994). The second layers from Hanson and others (1990) and Hanson and Benedict (1994) represent the lower basin-fill deposits and are equivalent to layers 2 and 3 in this study. The layer 2 transmissivity values from Hanson and others (1990) and Hanson and Benedict (1994) were split between layers 2 and 3 in this study. The initial transmissivity split between layers 2 and 3 was 70 percent and 30 percent, respectively. The initial hydraulic conductivity values for layer 2 cells were calculated by dividing the Hanson and others (1990) or Hanson and Benedict (1994) layer 2 transmissivity value by each cell's 1940, saturated thickness and multiplying by 0.7. The initial Layer 3 transmissivity values were assigned by multiplying the Hanson and others (1990) or Hanson and Benedict (1994) layer 2 transmissivity values by 0.3.

The calibrated distributions of hydraulic conductivity for layers 1 and 2, the transmissivity for layer 3, and the total composite model transmissivity are presented in Figure 17. The calibrated hydraulic conductivity values for layer 1 ranged from 2 to 300 feet per day (ft/d)(Figure 17a), and for layer 2 from 1 to 139 ft/d (Figure 17b). The calibrated transmissivity distribution for layer 3 ranged from 30 feet squared per day (ft^2/day) to 10,000 ft^2/day (Figure 17c). The calibrated total composite transmissivity for 1940 is presented in Figure 17d along with the composite transmissivity from Hanson and others (1990) and Hanson and Benedict (1994). The total composite transmissivity ranges from less than 200 ft^2/day to about 47,500 ft^2/day. The calibrated composite transmissivity is generally similar to the composite transmissivity distributions of Anderson (1972) Moosburner (1972) Travers and Mock (1984), Hanson and others (1990) and Hanson and Benedict (1994).

Storage properties for model layers 1, 2, and 3 were based on available well log data, aquifer compaction studies by Anderson (1987, 1988), and studies by Hanson and others (1990) and Hanson and Benedict (1994). Model layer storage properties were simulated using specific yield for layer 1 and also for layers 2 and 3 where these layers were the uppermost active layer. Specific yield values for layers 1, 2 and 3 are presented in Figure 18. Specific yield distributions ranged from 6 percent to 22 percent for layer 1 and were generally largest near the Santa Cruz River and its major tributaries and lowest in the central part of the USC sub-basin (Figure 18a). Layer 2 was modeled as a convertible layer, which allows cells to convert from confined (fully saturated) conditions to unconfined (water table) conditions depending on the overlying cell. Specific yields for unconfined cells in layer 2 ranged from 4 percent to 18 percent and followed a similar pattern as the layer 1 specific yield distribution (Figure 18b). Layer 3 was also modeled as a convertible layer with specific yields ranging from of 3 percent to 15 percent (Figure 18c). The storage coefficient assigned to cells in layers 2 and 3 that are confined was 0.0001 ($1 X10^{-4}$), which is the storage coefficient value used by Hanson and others (1990) and Hanson and Benedict (1994). The specific yield and storage coefficient values were within the ranges of estimates by previous investigators (White and others, 1966; Moosburner, 1972; Anderson, 1972; Davidson, 1973; Traverse and Mock, 1984; Hanson and others 1990; Hanson and benedict, 1994).

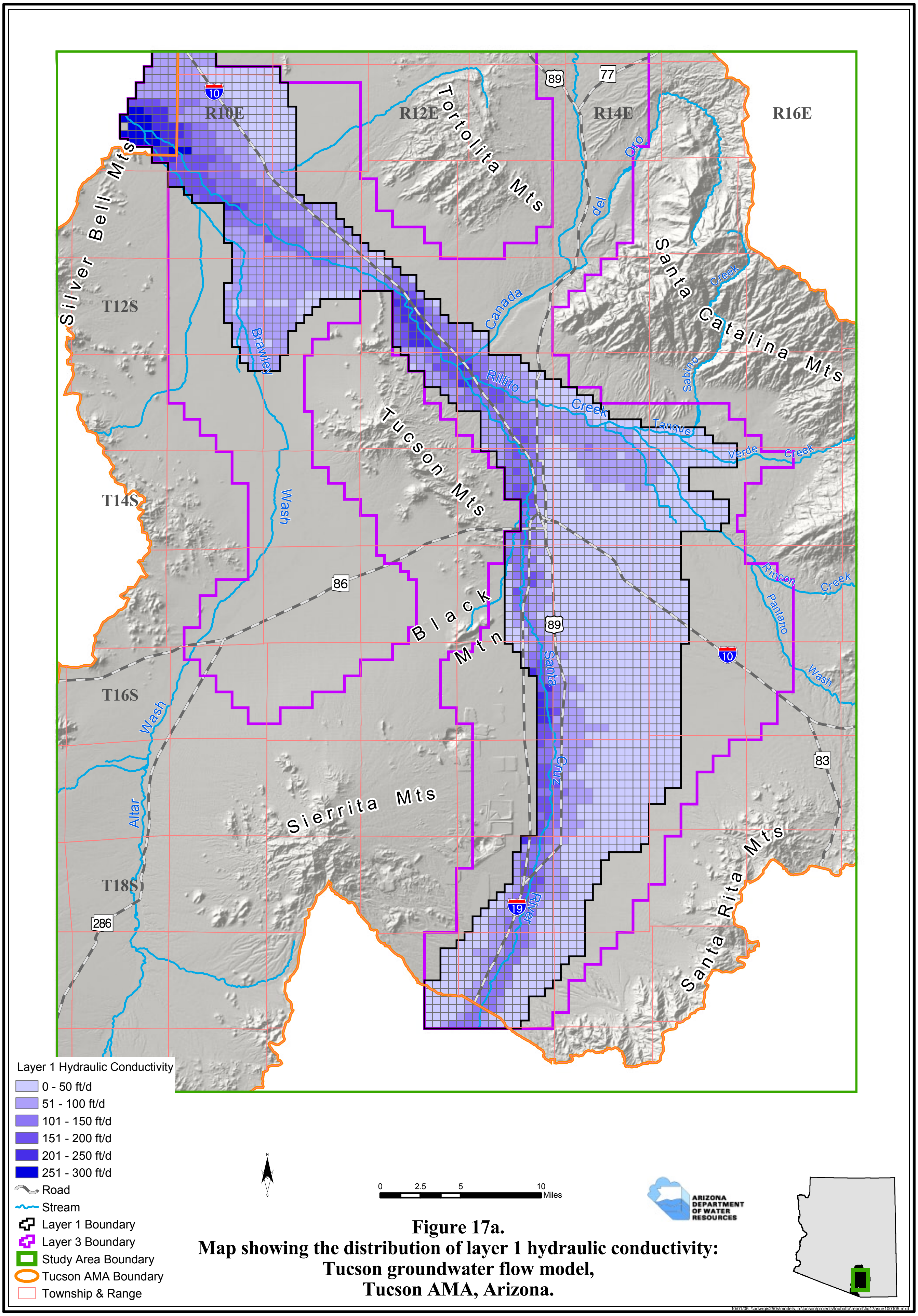

Figure 17a.
Map showing the distribution of layer 1 hydraulic conductivity:
Tucson groundwater flow model,
Tucson AMA, Arizona.

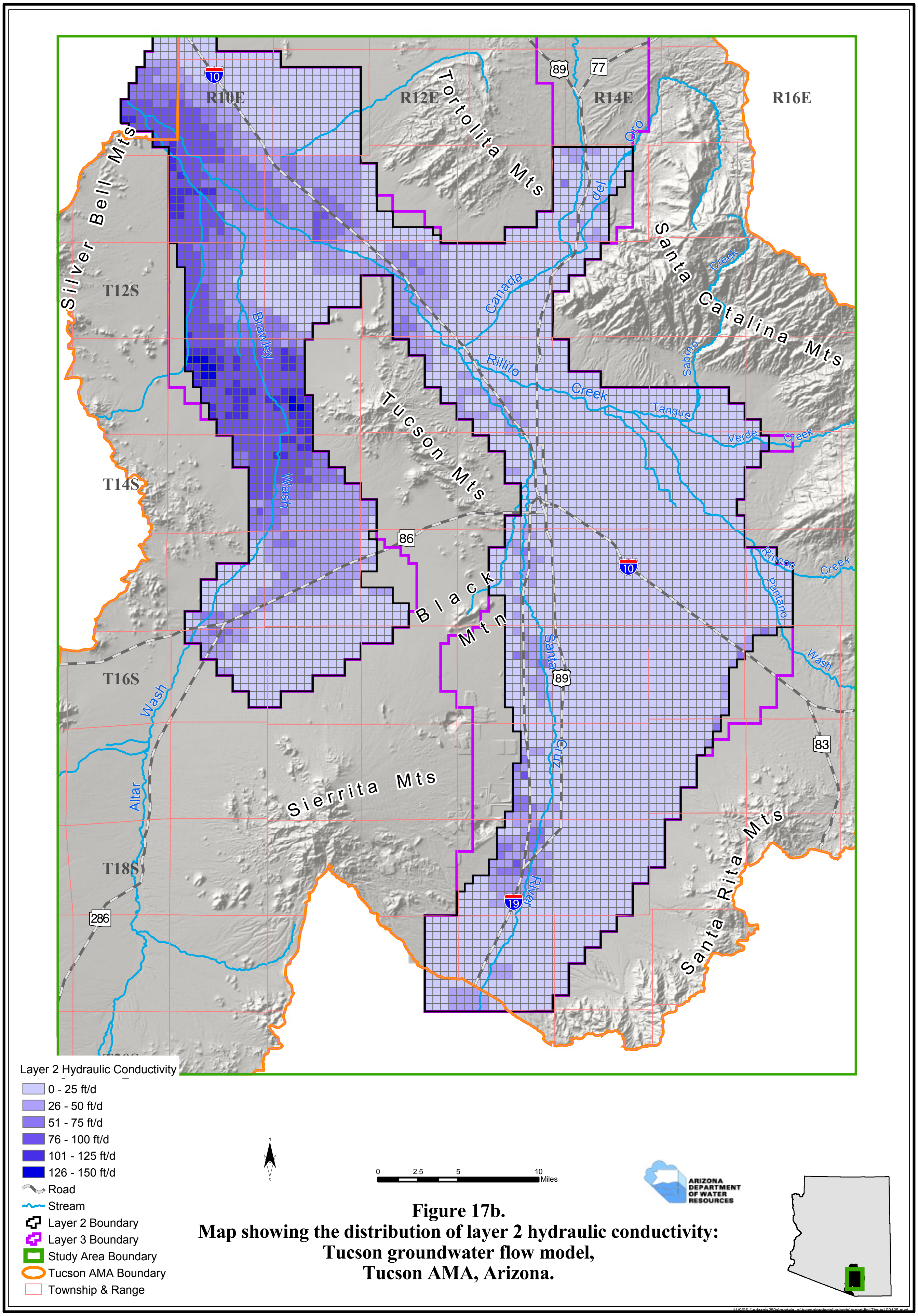

Figure 17b.
Map showing the distribution of layer 2 hydraulic conductivity:
Tucson groundwater flow model,
Tucson AMA, Arizona.

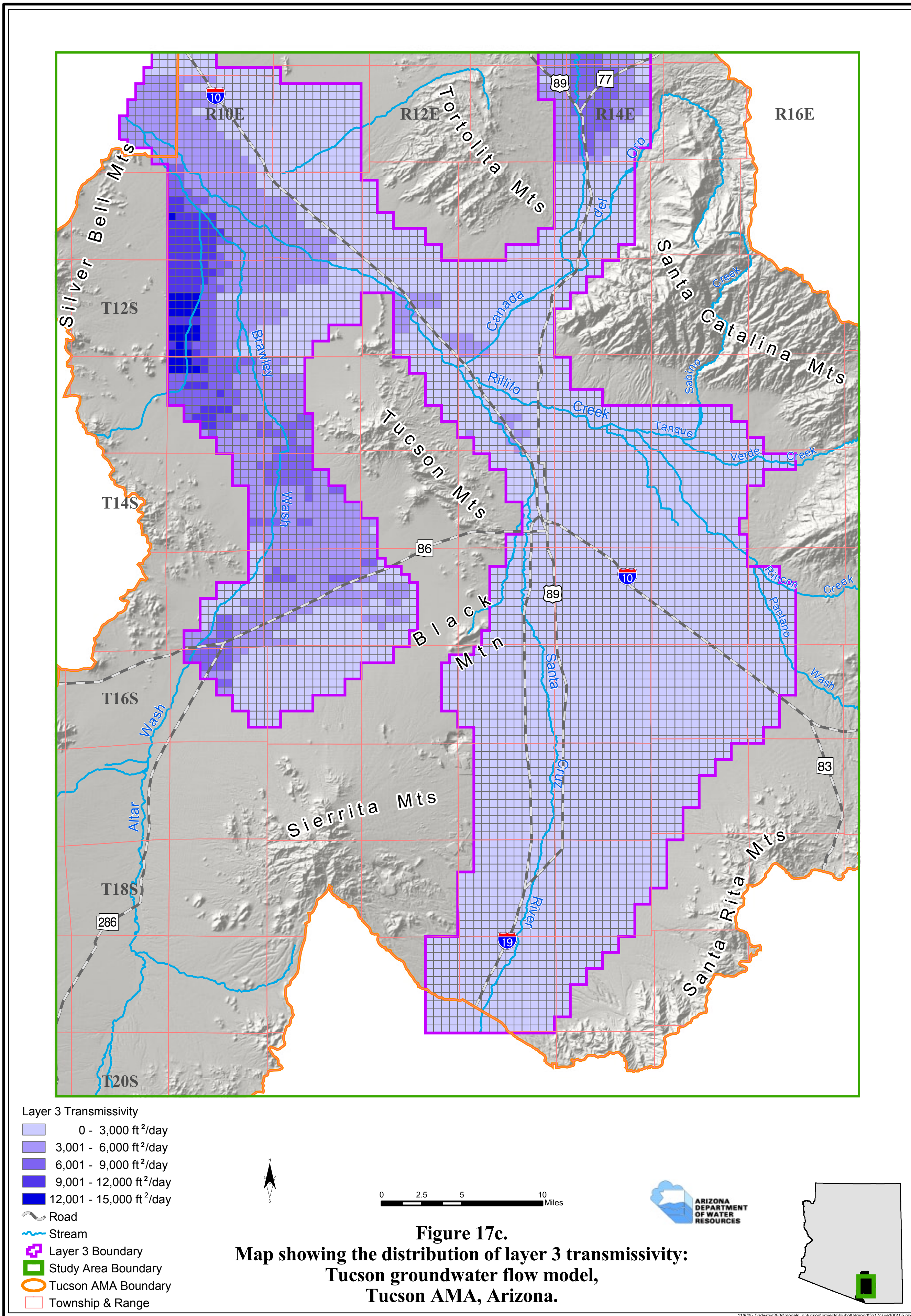

Figure 17c.
Map showing the distribution of layer 3 transmissivity:
Tucson groundwater flow model,
Tucson AMA, Arizona.

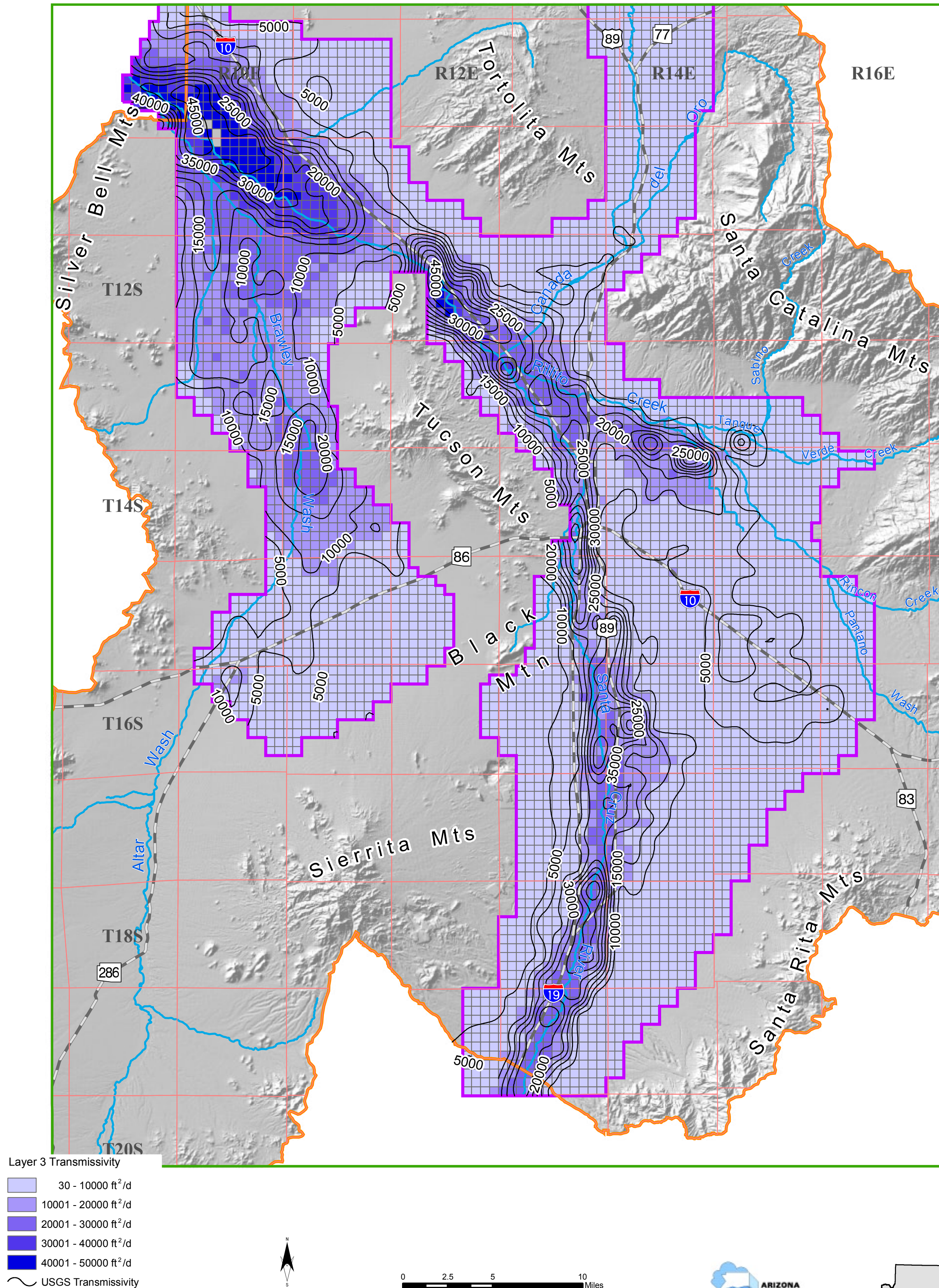

Figure 17d.
Map showing the 1940 distribution of total composite model transmissivity: Tucson groundwater flow model, Tucson AMA, Arizona.

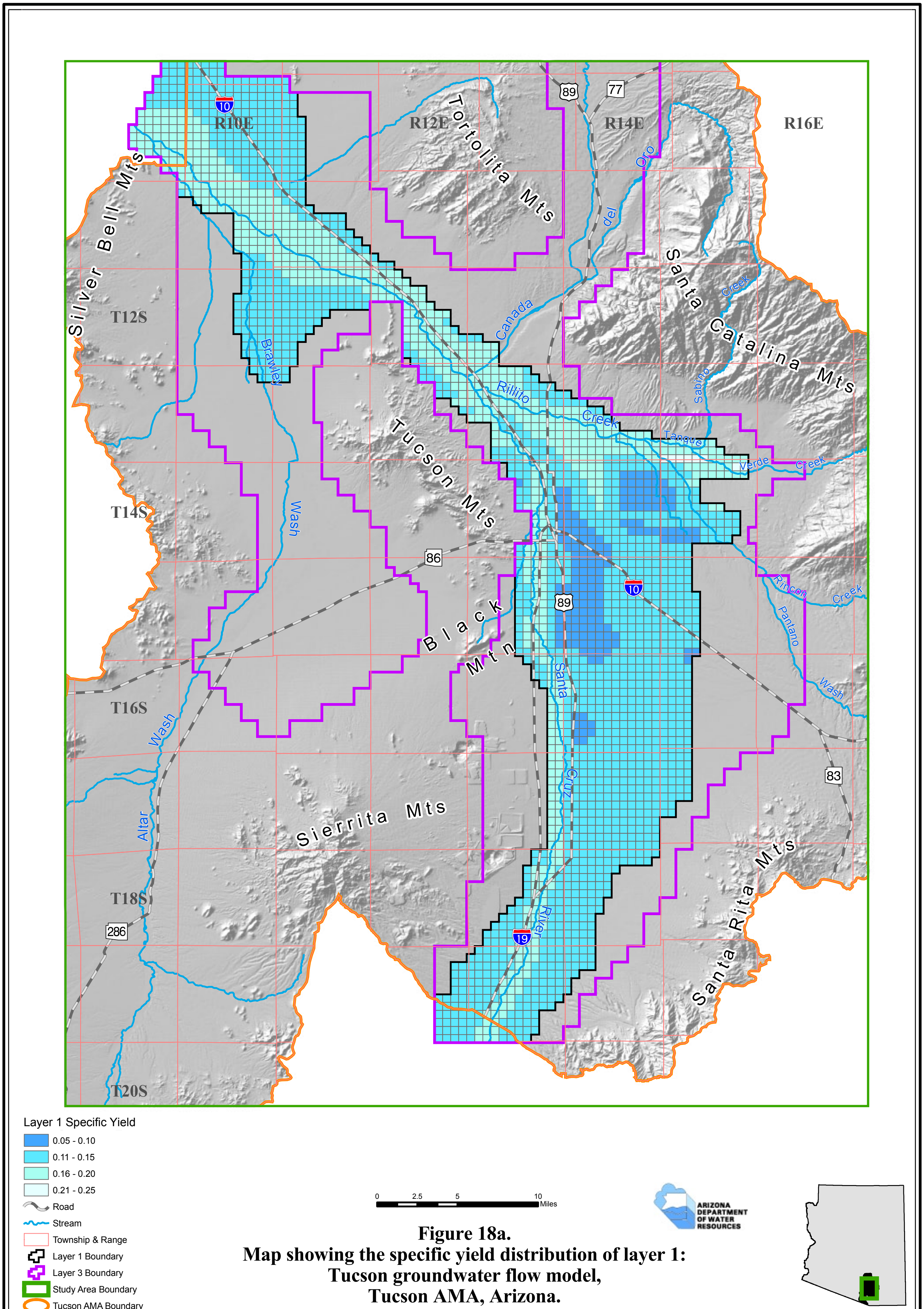

Figure 18a.
Map showing the specific yield distribution of layer 1: Tucson groundwater flow model, Tucson AMA, Arizona.

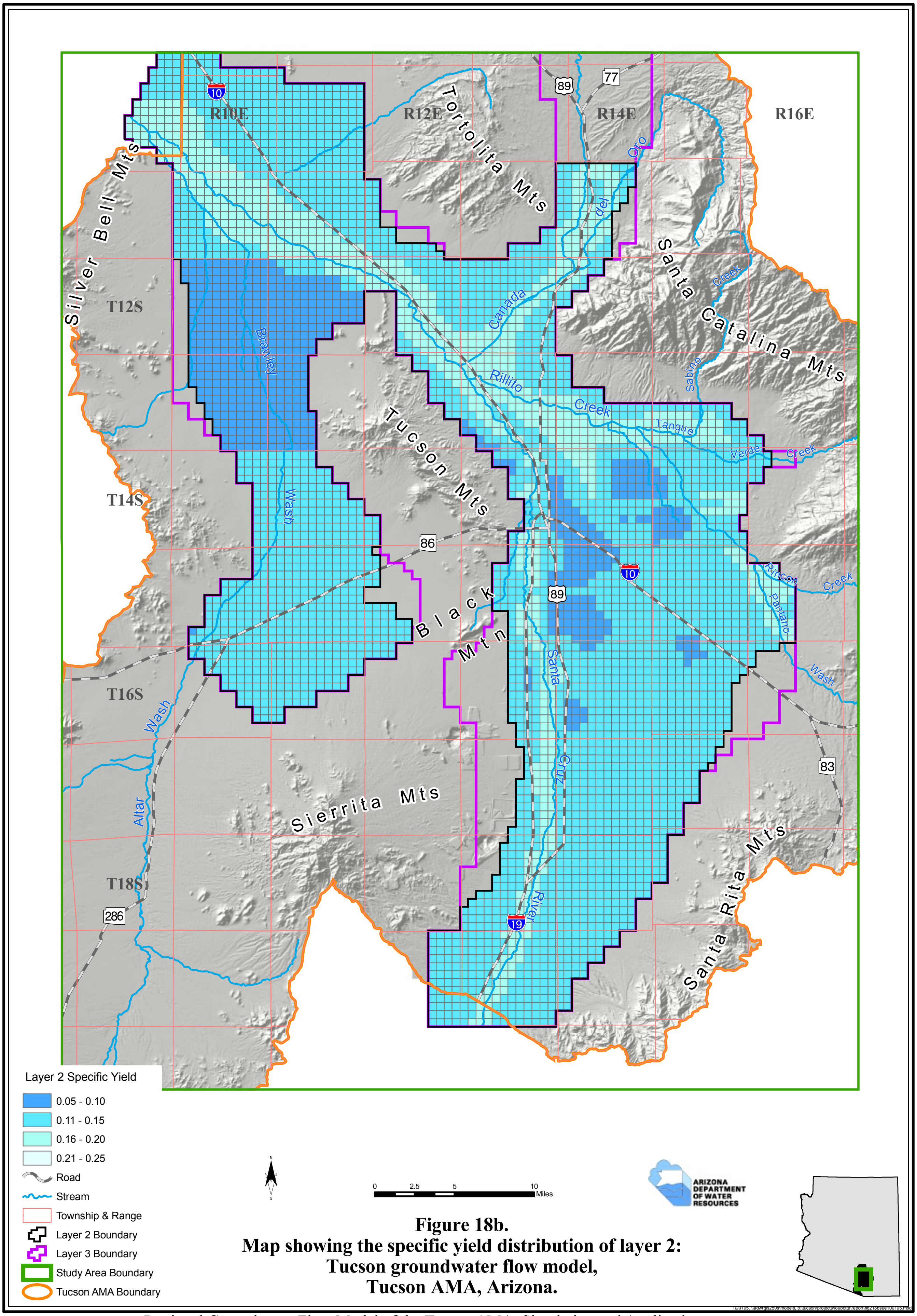

Figure 18b.
Map showing the specific yield distribution of layer 2: Tucson groundwater flow model, Tucson AMA, Arizona.

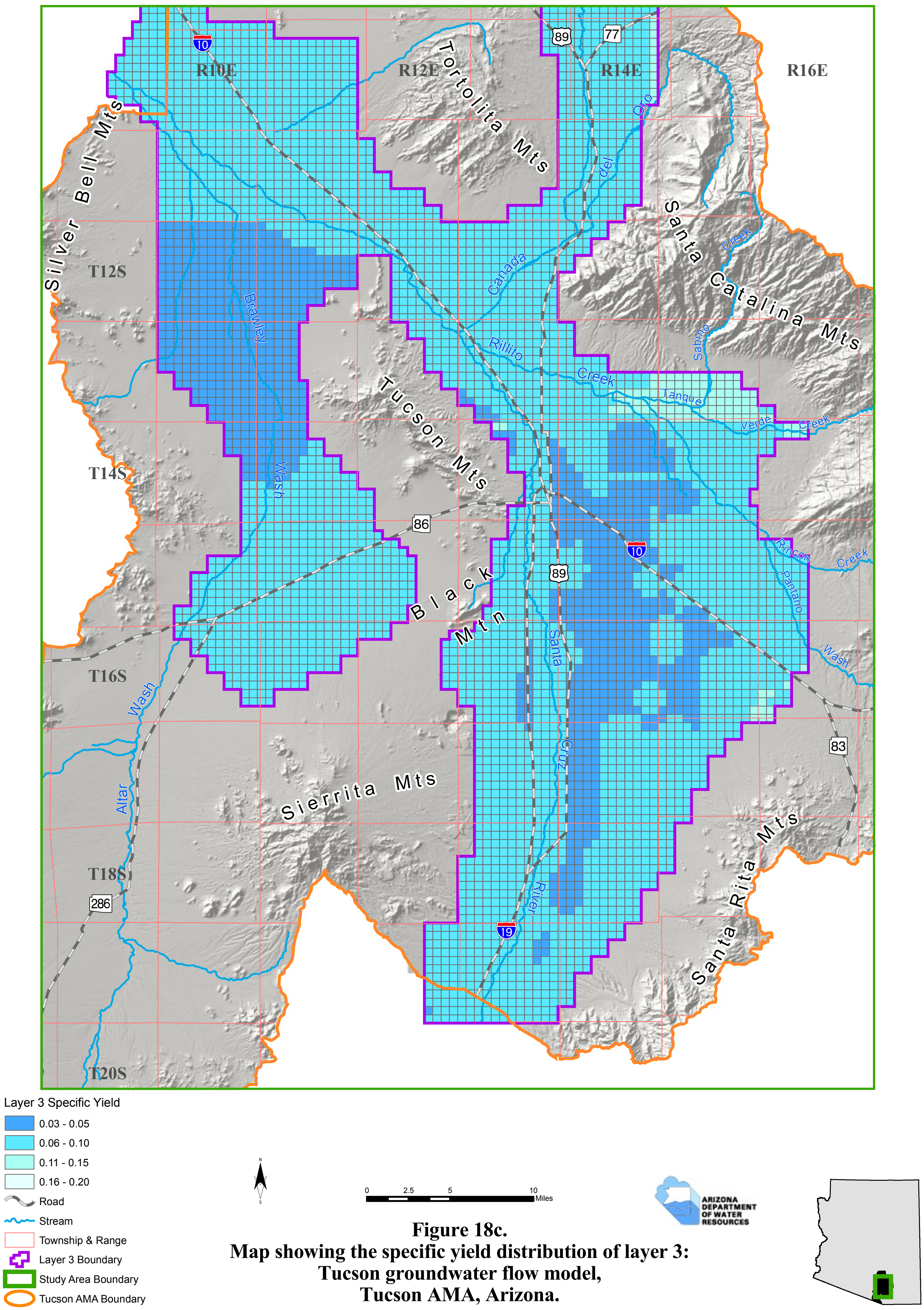

Figure 18c.
Map showing the specific yield distribution of layer 3: Tucson groundwater flow model, Tucson AMA, Arizona.

The vertical movement of groundwater, or leakance, in MODFLOW is controlled by an assigned vertical leakance value called the **Vcont**. The Vcont term incorporates a cell's vertical hydraulic conductivity, thickness, and cell area. Initial leakance distributions for layers 1 and 2 were assigned based on silt-and-clay (percent fines) content maps for the Fort Lowell Formation (model layer 1) and the upper Tinaja beds (model layer 2) developed by Anderson (1988, 1989), model data set from Hanson and others (1990) and Hanson and Benedict (1994). Each active model cell was assigned a leakance value based on a relationship between the percentage of silt and clay and leakance values developed by Hanson and Benedict (1994). There was very little data available on the percent fine content of model layer 3, which consists of the middle and lower Tinaja beds and the Pantano Formation. The existing percent fines data suggest that, on average, sediments from model layer 3 have a slightly lower percentage of fine material than the upper Tinaja beds (model layer 2). An average cell-centered percent fines value for model layer 3 was calculated by reducing layer 2 values by 5 percent, and a cell-centered leakance value was assigned as described above for layers 2 and 3. The vertical conductance values and the corresponding percent fines are listed in Table 6 and are comparable to the values used in studies by Hanson and others (1990) and Hanson and Benedict (1994).

For the purposes of this study, the vertical leakance between two layers is the average vertical leakance of the two layers. The cell-centered leakance terms between layers 1 and 2 and layers 2 and 3 were calculated as the average of the vertical leakance value of adjoining cells. The resulting leakance terms ranged from 0.0065 d^{-1} (feet/day/foot) to 0.0344 d^{-1} (ft/d/ft) between layers 1 and 2, and from 0.0043 d^{-1} (ft/d/ft) to 0.0344 d^{-1} (ft/d/ft) between layers 2 and 3. These vertical leakance values assigned for this model are comparable to the range of values used by Hanson and others (1990) in the Avra Valley groundwater flow model and by Hanson and Benedict (1994) in the Upper Santa Cruz basin groundwater flow model. For a more complete description of the Vcont term the reader is directed to McDonald and Harbaugh (1988). The final calibrated vertical leakance (Vcont) values between layers 1 and 2 and layers 2 and 3 are presented in Figure 19a and 19b.

Table 6. Vertical conductance values used in the Tucson AMA, Arizona.

Percent Fines	Leakance (Vcont) Value in ft/d/ft
< 20	0.0344
21 - 40	0.0258
41 - 60	0.0172
61 - 80	0.0086
> 80	0.0043

Pumpage Data

The location and volume of pumpage were distributed within the active model domain based on well locations from the ADWR Well Registry and GWSI databases, previous water resource studies, and the model pumpage data sets from Hanson and others (1990) and Hanson and Benedict (1994). Other sources of pumpage values and locations include the City of Tucson, White and others (1966); Anderson (1972); Moosburner (1972), and Travers and Mock (1984). Crop survey data for Pima and Pinal Counties, collected by the University of Arizona Agricultural Engineering Department, was also a valuable source of information for double-checking the distribution and amount of agricultural pumpage within the model area.

Previous model studies were based on mile square model grids that were aligned to coincide with the sections of the township and range grid. In this study, model cells are one-half mile in length and width, and also aligned with the township and range grid, so that each model cell represented a 160-acre quarter section. Reassigning the pre-1984 pumpage from the 640-acre cells of the previous models to the 160-acre cells in the current model was accomplished using location, construction date, and water use data for large-capacity wells from the Arizona State Land Department's well registry (the 35 File), the current ADWR

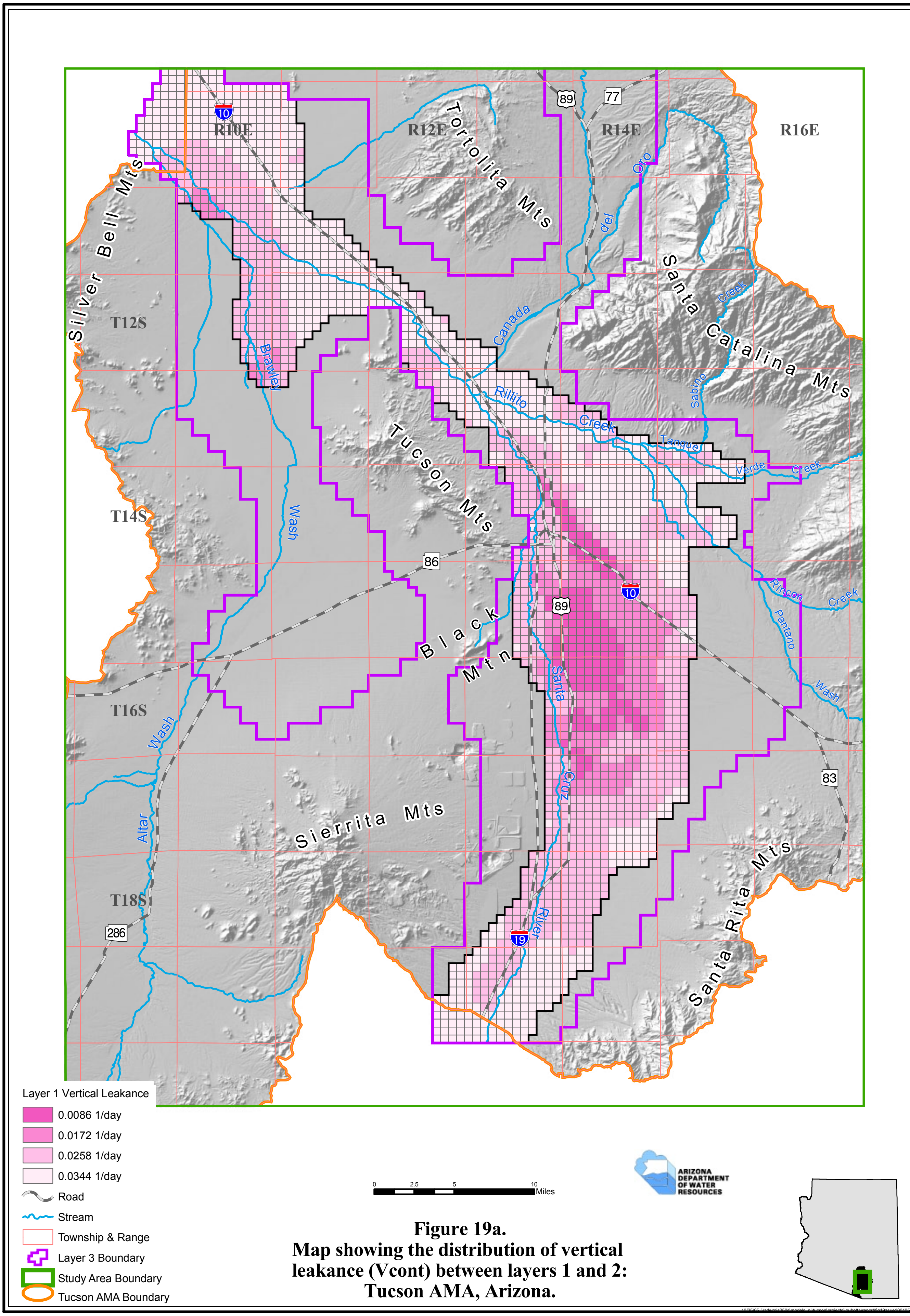

Figure 19a.
Map showing the distribution of vertical leakance (Vcont) between layers 1 and 2: Tucson AMA, Arizona.

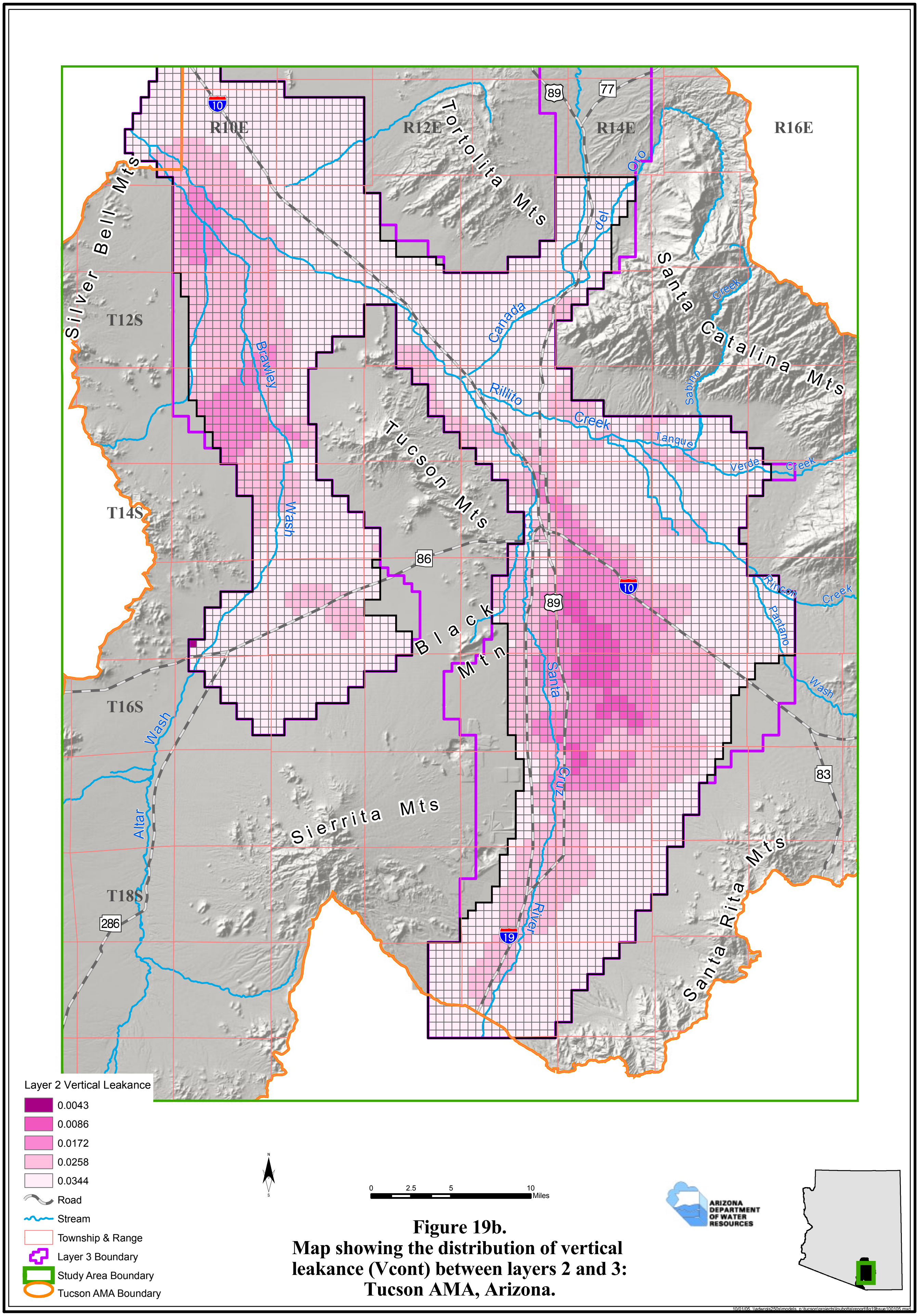

Figure 19b.
Map showing the distribution of vertical leakance (Vcont) between layers 2 and 3: Tucson AMA, Arizona.

Well Registry (the 55 File), and the GWSI database. Each of these sources records a well's location to at least the nearest 10-acre parcel. A time line was developed that contained the location and completion date of known large-capacity wells. Pumpage from the previous model studies was assigned to well(s) located in a section based on its construction date and water use. If a section had pumpage, but there were no well(s) with known construction dates available, the pumpage was assigned equally to well(s) that were known to exist but had no known construction date. If there were no known wells in a section, the pumpage was distributed evenly into each quarter section that represented the current model cells.

The initial distribution and volume of pumpage for the model from 1941 to 1983 were based on the pumpage data sets developed by Hanson and others (1990) and Hanson and Benedict (1994), which were based on the work of Anderson (1972), Mooseburner (1972) and Travers and Mock (1984). For the period of 1940 to the early 1960's, these investigators used power consumption records and crop distribution surveys to develop estimates for the areal distribution and volume of pumpage. From the early 1960s, until the early 1980s, pumpage records were generally better and more well-specific pumpage data were available; however, much of the pumpage during this time is estimates based on power consumption records and crop census data. For the period of 1984 to 1999, the distribution and amount of pumpage for the current model was assigned directly from the ADWR ROGR database, which contains annual well-specific withdrawal volumes. Most non-exempt wells were assigned to cells based on their cadastral location, or legal description. However, some non-exempt wells have been field checked and assigned Universal Transverse Mercator (UTM) coordinates, which were used to assign cell locations. See Anderson (1972); Mooseburner (1972), and Travers and Mock (1984) for details on the development of the areal distribution and pumpage volumes for their models.

Layer specific pumpage was assigned to wells in one of three ways depending on how much information was known about the well's construction. Wells with known perforation intervals had pumpage percentages assigned to each layer by dividing the theoretical yield from each layer (saturated length of perforated interval times layer transmissivity) by the total theoretical yield for the well (the sum of the yields for each layer). Where only the depth of the well was known, pumpage was assumed to come from the entire saturated depth of the well and the procedure described above was used to calculate layer specific percentages. If there was no known depth for a well then pumpage was distributed to each layer based on each layers percentage of the total cell transmissivity.

Evapotranspiration

Water levels in the Avra Valley sub-basin are generally too deep to support riparian vegetation. Therefore, evapotranspiration (ET) in this study is simulated only in the USC sub-basin. GIS techniques were used to develop the initial model ET distributions. The distribution of ET rates developed by Hanson and Benedict (1994) were used to create the initial ET rate distribution for this study. The model grid for the Hanson and Benedict (1994) study was overlain with the major river drainages and riparian corridors and rediscretized into the current model grid. The ET surface elevation for each ET cell was determined by subtracting the ET extinction depth (25 feet) from the cell's land surface elevation. Average land surface elevations for each cell were calculated using Triangular Irregular Network (TIN) interpolation techniques from USGS digital elevation maps (DEM).

Natural Recharge

The initial estimates of mountain-front recharge and stream infiltration for the USC sub-basin were based on natural recharge values from Hanson and Benedict (1994). The mountain-front recharge and stream infiltration values from Hanson and Benedict (1994) were rediscretized into the Tucson AMA model grid using GIS techniques. The rediscretization involved overlaying the current model grid and model grid from Hanson and Benedict (1994) with a digitized cover of the Tucson AMA model grid. The initial mountain-front recharge distribution was created by projecting the cell-specific Hanson and Benedict (1994) mountain-front recharge values evenly into the corresponding four cells in this study. Stream infiltration values were assigned to each cell by multiplying the percentage of the river length per cell by the infiltration value of the Hanson and Benedict (1994) model cell.

A steady-state groundwater flow model of the Avra Valley by Hanson and others (1990), which did not include mountain-front recharge or stream infiltration values, was used to develop recharge estimates for the Avra Valley sub-basin. A recharge package that included mountain-front recharge and stream infiltration was developed using regional recharge estimates by Osterkamp (1973). The model was then recalibrated by adjusting hydraulic conductivity, transmissivity, mountain-front recharge, and stream infiltration values until water level and water budget calibration targets were met. The Tucson AMA model grid has a finer cell mesh than the Hanson and others (1990) model grid; each cell in Hanson and others (1990) model contains four model cells from this study. Geographic Information Systems (GIS) mapping techniques were used to rediscretize the cell-specific recharge values from the modified Hanson and others (1990) model into the appropriate model cells in this study. The resulting mountain-front recharge and stream infiltration values were then used as initial values for the Tucson AMA steady-state model.

Incidental Recharge

As discussed previously recharge from excess water applied to crops, from mine tailings ponds, and from effluent used to irrigate crops or released into the Santa Cruz River is termed incidental recharge. By the late 1960s, incidental recharge had become a major component of the Tucson AMA water Budget. The development of incidental recharge estimates is discussed below.

Agricultural Recharge

The areal distribution of recharge from excess agricultural irrigation for the development period (1941 to 1999) was constructed using agricultural pumpage locations from previous modeling efforts, crop census reports from the U of A, and the location of current **I**rrigation **G**rand**f**athered **R**ights (IGFRs) in the Tucson AMA. Prior to the mid-1980s, the U of A Crop Survey data and agricultural pumpage locations from previous modeling projects were deemed the best available source of data for distributing irrigation recharge. Since the 1980's the IGFR system administered by the ADWR was used to determine the spatial distribution of irrigation water use and recharge.

Water applied to irrigated crops that is not consumed, evaporated, or lost to soil moisture will eventually recharge the aquifer. The estimated maximum potential agricultural irrigation recharge for the transient model period was previously discussed and is presented in Figure 11. Deep percolation of the irrigation recharge to the water table may take many years and is dependent on a number of factors such as irrigation techniques, cropping history, subsurface geology, and depth to the water table. The concept of using a time-lag when applying agricultural recharge to a model to account for deep percolation travel time was introduced by Corell and Corkhill (1994). The addition of lag-time to the recharge estimates was necessary because MODFLOW has no provision for unsaturated flow. Recharge applied in a MODFLOW model arrives instantaneously at the water table no matter how deep the water table actually is. Corell and Corkhill (1994) reasoned that there must be a lag time between the application of irrigation water and its' arrival at the water table in areas where the water table is deep, and that the transit time of irrigation recharge through the vadose zone has to be accounted for when applying transient recharge using MODFLOW. Using an estimated travel time to an average depth to water of about 200 feet below land surface Corell and Corkhill (1994) applied an average lag-time of 10 years (a deep percolation rate of 20 feet per year) to irrigation recharge in the ADWR Salt River Valley (SRV) regional groundwater flow model. See Corell and Corkhill (1994) for a detailed discussion of how that percolation rate was developed.

Anderson (1982) compared actual well hydrographs to model generated hydrographs for models developed for 11 basins in south-central Arizona. In 9 of the 11 basins examined there was a need for an additional source of recharge during the later calibration periods. The need for additional recharge with increasing time indicates that time-delayed deep percolation of irrigation recharge is a factor in many developed basin. Anderson's study included both the Avra Valley and USC sub-basins, and concluded that travel time for deep percolation in the Avra Valley sub-basin was on the order of 15 to 20 years and that deep percolation became significant in the northern part of the sub-basin in the mid-1960s (Anderson, 1982).

The initial lag-time used for applying irrigation recharge due to deep percolation for the transient model was calculated using a percolation rate of 20 feet per year and the simulated 1940, depth to water. Cell-specific lag values were calculated for all cells that had agricultural pumpage, and therefore, would have agricultural recharge. The cell-specific lag values ranged from 1 to 30 years and averaged 8 years. The average lag time was 10 years in the Avra Valley sub-basin and 5 years in the USC sub-basin. The cell-specific lag applied to the initial pumpage estimates resulted in lagged agricultural recharge peaking in the USC sub-basin in the late 1950s and early 1960s at about 40,000 ac-ft per year. Lagged agricultural recharge in the Avra Valley sub-basin reached a maximum of about 50,000 ac-ft per year in the mid-1960s and remained at about that volume until 1980, when the recharge began to decline. The period of maximum lagged recharge in the Avra Valley coinciding with Anderson's (1982) estimate of when deep percolation of agricultural recharge indicates that the deep percolation rate of 20 feet per year may be a reasonable estimate.

The actual amount of irrigation recharge and its' arrival is difficult to determine and is dependent on many factors. The volume and timing of irrigation recharge are model components that were adjusted during the model calibration process. It is important to recognize that when using the lag-time approach, the total volume of recharge that is applied to the model over the transient calibration period is always slightly less than the estimated maximum potential recharge, assuming that the transient period begins from an initial steady-state, and that the time-lag is implemented to delay the arrival of estimated agricultural recharge until later in the transient period.

Mine Tailings Pond recharge

Incidental recharge from mine tailings ponds was included in the developed period (1941 – 1999). The location and initial estimates of the volume of recharge mine tailings pond was developed based on the modeling efforts by Travers and Mock (1984) and Hanson and Benedict (1994). Initial estimates of tailings pond recharge where 20 percent of total mine pumpage. The tailings pond recharge was also lagged using the 20-foot per year travel time.

Effluent Recharge

As previously discussed effluent from WWTPs was released into the Santa Cruz River for a short period in the early 1950s, and then again beginning in the late 1960s. Using estimated and reported release data recharge due to the effluent releases was distributed to cells downstream for the WWTPs. The effluent recharge was also lagged based an average depth to water and the deep percolation rate of 20 feet per year.

Chapter 5

Simulation of Groundwater Flow

Model Calibration Process

The model calibration process involved varying model inputs within reasonable real-world acceptable ranges to obtain a realistic match between model-simulated data and field-observed or estimated data. The purpose of the calibration process is to minimize the difference, or error, between simulated data and observed data, yet still maintain a set of hydrogeologic input data that is consistent with independent estimates or observed data. Model inputs that were adjusted include cell-centered hydrogeologic parameters, boundary conditions, and stresses imposed on the model. Hydrogeologic parameters that were varied during the calibration included horizontal hydraulic conductivity and transmissivity values, vertical leakage (Vcont) between layers, storage values, layer tops and bottoms, and initial head values. Model boundaries and stresses were simulated using different MODFLOW packages. Model boundaries were simulated using the Recharge and Time-Variant Specified-Head (CHD) Packages. Stresses were simulated using the Well, Recharge, and Evapotranspiration packages. Model boundaries and stresses were adjusted to constrain the amount of water entering or leaving the model to within conceptual water budget values.

Calibration Criteria and Model Error

Anderson and Woessner (1992) recommend establishing calibration criteria prior to model calibration as a method for evaluating model simulations. The calibration criteria consists of observed or estimated data that is evaluated against model simulated data and are used to judge when a model simulation adequately replicates the natural flow system. The calibration criteria should include individual calibration targets; for example, water levels or fluxes, which have a measured or estimated value and an associated acceptable calibration tolerance (or error). Using a calibration target and its associated error as a guideline, calibration levels can be defined for each calibration target. The calibration levels can then be used to define the calibration criteria that determine when a model's error is minimized; at which point the model can be regarded as adequately calibrated. Model calibration criteria were established for the steady-state and transient model calibrations prior to the beginning of running model simulations.

Anderson and Woessner (1992) also discuss several common statistical-based measures that can be used to evaluate the average error for a model simulation. The measures include using model head residuals, the difference between simulated heads and observed heads, to describe the average model error. The mean of the head residuals describes the mean error (ME) of a simulation and the mean of the absolute value of the head residuals describes the absolute mean error (AME) of a model simulation. The root mean squared error (RMSE), also called the standard deviation of the residuals, is a good measure of error if the error is normally distributed about the mean (Woessner and Anderson, 1992). Another useful measure of model error is the ratio of the RMSE to the total head loss in the system being modeled. The ratio is calculated by dividing the RMSE of the head residuals by the total head loss across the system being modeled. If this value is low, less than 10 percent is a generally accepted threshold, then the model error is considered to represent only a small part of the overall model response. See Woessner and Anderson (1992) Chapter 8, for a detailed discussion on evaluation of a model calibration.

The statistical methods described above give an indication of the average error of a model simulation. However, it is also important to examine the spatial distribution of model error to determine if there are areas in the model with excessive error. The occurrence of spatial bias in model error can indicate potential problem areas in the model, which can then be focused on during the calibration process. In this model study, water level contour maps of simulated heads for steady-state and transient model simulations were compared to the steady-state (1940) or transient (1999) water level contour maps. This was done to determine how closely the simulated heads replicated the generalized regional groundwater flow pattern. The residuals from each simulation were also plotted on a map to determine if there were any obvious spatial trends in the residual head data. Scatter plots of the residuals and observed head pairs were also created as a further check for any spatial trends.

Calibration Targets

Water level data and the conceptual water budget components were used to establish calibration targets for this study. The water level calibration targets were established as an observed head, plus or minus an average associated error of 10 feet. The water budget calibration targets were set as having the conceptual water budget component within the range of published estimated values (Table 3).

Water level elevations in GWSI are calculated using the elevation of the land surface at the wellhead minus the measured depth to water. Possible sources of error in determining a water level elevation include the wellhead elevation and the water level measurement itself. Each GWSI site is assigned an elevation either by field personnel from a map or based on a known land survey elevation. ADWR field procedures state that wellhead elevations determined in the field from maps can be estimated to within one-half the map contour interval during field investigations (Reg Barnes, personal communication, 2003). Each site is also assigned an altitude accuracy based on the method used to determine the site altitude. Sites with elevations determined from maps are assigned an altitude accuracy of one-half of a maps contour interval, as described above, and sites with surveyed elevations are assigned an accuracy based on the land survey method. Since most wellhead elevations in GWSI have been determined from 7.5-minute quadrangle maps, which generally have contour intervals of 20 feet, the average estimated error for GWSI water level elevation is assumed to be ±10 feet. Experienced field staff can measure water levels to within about 0.1 foot, making the wellhead elevation determination the largest factor controlling potential water level measurement error.

For this modeling project the average error for observed water levels was set at ±10 feet. Therefore, the calibration levels for model simulated water levels were set using multiples of the 10-foot error value as:

Level 1 – simulated water level within ± 10 feet of observed water level
Level 2 – simulated water level within ± 20 feet of observed water level
Level 3 – simulated water level within ± 30 feet of observed water level
Level 4 – simulated water level within ± 40 feet of observed water level
.
Level N – simulated water level within ± (N * 10) feet of observed water level

Additional calibration targets were developed using the results of the Observation Process from MODFLOW-2000, which allows various model-simulated components to be compared with observed data (Hill and others, 2000). In this study, the Hydraulic-Head Observation (HOB) option of the BASIC package was utilized to compare simulated heads with observed water levels (heads). The HOB option provided several important functions that include: 1) a weighting option that allows water level observations deemed more accurate to be assigned more significance, or weight, than observations that are believed to be less accurate, 2) the ability to interpolate simulated heads at the location of observed heads, and 3) using model head residuals to calculate several statistical measures that describe how well the model results compare to expected normal distribution results. If the weighting option is used in the HOB process then the statistical measures are calculated using the weighted head residuals.

The statistical measures calculated by MODFLOW-2000 using the head residuals include the correlation coefficient and a run test. The correlation coefficient is a measure that describes the match between the simulated and observed heads and can be presented as a value and displayed graphically as a scatter plot. The closer the correlation value is to 1.0, the greater the correlation between observed and simulated heads, or the closer an observed head is to a simulated head. Hill (1998) recommends that the correlation coefficient be greater than 0.90. The run test is a summary statistic that tests the weighted residuals for randomness. Ideally, residuals plotted on a graph should show no discernable pattern. If a pattern is observable than the residuals are biased, which can indicate a problem with the model calibration (Hill, 1998), or the conceptual model.

In this study, the weighting method suggested by Hill (1998), which evaluates the accuracy of the observation point's altitude error, was utilized to determine the weighting factor of each observed water level. As described above, the average accuracy of an observation point's altitude can be determined using the assigned altitude accuracy for each observation point. The altitude accuracies in the GWSI for the Tucson AMA range from less than one foot to as much as fifty feet, and averaged about 10 feet. The site altitude accuracy value was used to calculate the estimated standard deviation of a water level elevation measurement error for each observation point after Hill (1998). The resulting weighting factors ranged from 0.033, for observation points with very inaccurate altitudes, to 1.0, for observation points with very accurate altitudes. An explanation of the head weighting procedure and head weighting values used in the model is included in Appendix B, and a more detailed discussion of weighting observed data can be found in Hill (1998).

Observation heads rarely coincide with cell center locations, so to provide accurate comparisons between simulated and observed data the HOB package uses geometric interpolation to calculate what a simulated head would be at the location of an observed head. The methods used to calculate the interpolated heads can vary depending on the presence and location of dry cells in relation to observed head. The reader is directed to Hill and others (2000) for a detailed explanation of the interpolation procedures. Results from the HOB option include the observed heads and their associated interpolated simulated heads, and the difference (residual) between observed and simulated heads. If the weighting option is used, the results, observed heads, simulated heads and residuals, are multiplied by the assigned weighting factor.

For this study the weighted residuals from the HOB package were used in the statistical and frequency distribution analysis and to determine the calibration level of an observation points. The weighted residual (difference) between the interpolated model simulated head (water level) and observed water level was determined using the formula:

$$R_i = H_s - H_m$$

where:

R_i = the residual, in feet
H_s = the interpolated model simulated head value at the location where H_i was observed, in feet
H_m = the observed head at point *i*, in feet

If the residual is positive, then the simulated head is higher than the observed head; and if the residual is negative, the simulated head is lower than the observed head. The head residuals form the basis of many of the calibration criteria. See Hill (1998) and Hill and others (2000) for a detailed discussion of issues related to parameter weighting and implementation of the Observation Processes in MODFLOW 2000.

Steady-State Calibration

The steady-state Tucson AMA regional model was calibrated to conditions, as they existed in 1940. The steady-state calibration required 95 model runs before an acceptable calibration was obtained. During the calibration process cell-specific hydraulic parameters and model stresses were adjusted within reasonable ranges to achieve a better match between the observed water levels and estimated flux targets. Model properties that were adjusted were conductivity values (Layers 1 and 2), transmissivity values (Layer 3), vertical conductivity values, initial head values and layer tops and bottoms. Model stresses that were adjusted included mountain-front recharge, stream infiltration, pumpage volume and location, and ET values.

During the initial calibration runs the model was divided into several zones and the various model inputs were adjusted for each zone. Once the analysis of the model results began to approach the calibration targets, the model inputs were adjusted on a cell-by-cell basis within the established zones. Each steady-state simulation was analyzed using the methods described below to determine if the established calibration criteria were met.

Steady-State Calibration Criteria

The calibration criteria established for this study required both qualitative and quantitative analysis of model simulations. Quantitative analysis of model simulations involved a statistical and frequency distribution analysis of model head residuals (simulated heads minus observed heads). The qualitative analysis of the steady-state calibration included comparing contour maps of simulated water level data to observed water level data and examining the spatial distribution of the model head residuals to determine if any spatial bias existed in the model.

The steady-state model was considered adequately calibrated when the following criteria were met:

1). The AME of the weighted residuals is equal to or less than 10 feet (Level 1 Calibration).
2). The percent error in the MODFLOW mass balance water budget is less than or equal to 0.1 percent.
3). Model simulated water budget components are within the range of conceptual estimates.
4). The ratio of the RMSE to the overall head loss in the system is 5 percent or less.
5). The absolute value of the maximum residuals is less than 75 feet (5 percent of the head loss in the system).
6). The correlation coefficient calculated by MODFLOW-2000 is greater than or equal to 0.90.
7). There is no obvious spatial bias in the distribution of the weighted residuals.
8). The simulated heads produced a water level contour map that reasonably replicated the hand contoured water level map based on 1940 water level data.

Steady-State Model Results

Water levels

The steady-state groundwater table map (Figure 8) and the observed water level data from GWSI were used for qualitative and quantitative comparisons to the final calibrated model simulated heads. The final steady-state model water level contours are presented in Figure 20. The water level contour map shows that the model-simulated head contours are similar to the regional flow pattern of hand-contoured observed heads for 1940. The location and relative magnitude of the steady-state weighted residuals are also plotted on Figure 20. The plotting symbol for each weighted residual is proportionally scaled based on the absolute value of the weighted residual.

The summary statistical analysis of the steady-state weighted residuals is presented in Table 7 and the weighted residuals are listed in Appendix B. There was a close match between the final simulated heads and the 118 observed target heads as indicated by the weighted head residuals, which ranged from -16 feet to +20 feet. The mean error (ME) of all the weighted head residuals was 0.4 feet, the mean of the absolute error (MAE) was 3.0 feet, and the standard deviation (RMSE) was 4.7 feet. The MAE is only 0.2 percent of the total head relief in the Tucson model (about 1540 feet) and is well below the calibration target of 5 percent. The low positive mean error indicates that the steady-state model slightly over-simulated average heads model-wide. The MAE represents the average difference between observed and simulated heads and is a good measure of the average error for a model. As previously discussed, the ME and MAE of the residuals are two general measures of average model error. The other commonly used measure of average model error, the ratio of the RMSE to total head loss in the system, is 0.0031 (0.31 percent), well below the calibration target of 0.05 (5 percent). The model calibration was better in the USC sub-basin than in the Avra Valley sub-basin. The ME, MAE, and RMSE for Avra Valley are 0.4 feet, 3.6 feet, and 4.8 feet, respectively. The ME for the USC sub-basin was 0.4 feet, the MAE for the USC sub-basin was 2.8 feet, and the RMSE was 4.7 feet.

The slight over-simulation of simulated heads indicates that there is either too much recharge or not enough transmissivity to move water through the model. The residual analysis indicates that Avra Valley has the largest model error and; therefore, is probably the area where the transmissivity and recharge relationship are most out of balance. Avra Valley was also the most difficult area of the model to calibrate during the steady-state model calibration.

The spatial distribution of model error is often biased due to hydraulic gradients within the regional flow system. In areas where the gradient is relatively flat the head change across a single model cell is small and can be accurately simulated. However, in areas where steep gradients occur, such as near mountain-fronts or model boundaries, larger residuals can be expected because models tend to over or under simulate heads in these areas due to the large head changes across single model cells. This is a scale problem caused by model cell-size and can be resolved to some extent by the selection of appropriate cell-size dimensions.

Table 7. Statistical summary of steady-state model weighted residual, Tucson AMA, Arizona.

Weighted Residual Statistical Analysis (all values are in feet)						
	Model-Wide	Avra	USC	Layer 1	Layer 2	Layer 3
Mean Error	0.4	0.4	0.4	0.2	0.2	1.5
Stan Dev	4.7	4.8	4.7	4.7	4.9	3.4
Absolute Mean Error	3.0	3.6	2.8	2.8	3.1	2.9
Max	20	7	20	20	13	7
Min	-16	-15	-16	-16	-15	-5
Count	118	28	90	50	55	13

The spatial distribution of model error can be observed in Figure 20, which shows the location and relative magnitude of the weighted residuals. Examination of the distribution indicates that no well-defined areas with a consistently large model error are present in the final calibrated steady-state model. Two individual residuals with large absolute values are located in southern and north central Avra Valley stand out, but there are no areas with concentrations of large residuals that would indicate areas where the model calibrated poorly.

A histogram of the weighted residuals frequency distribution also indicates that the model is biased towards positive residuals (Figure 21). The positive trend in residuals can be seen clearly in Figure 21 where a majority of the residuals fall in the zero to +10-foot range. Ideally, the residuals would be more evenly distributed on either side of the zero point. The frequency distribution of the absolute value of the weighted residuals is presented in Table 8. The frequency distribution analysis uses intervals of 10 feet to match the calibration level intervals. Model wide, about 92 percent of the weighted residuals fell within the first calibration level of ±10 feet and 100 percent of residuals were in the first three calibration levels, or within ± 30 feet of an observed head (Table 8).

Table 8. Frequency distribution of the absolute value of the steady-state weighted residuals, Tucson AMA, Arizona.

	Absolute Value of Model Wide Weighted Residuals		
	Range (Ft)	*Frequency*	Cumulative %
Level 1	0 to 10	110	93%
Level 2	10 to 20	7	99.8%
Level 3	20 to 30	1	100%
Level 4	30 to 40	0	100%
Count		118	

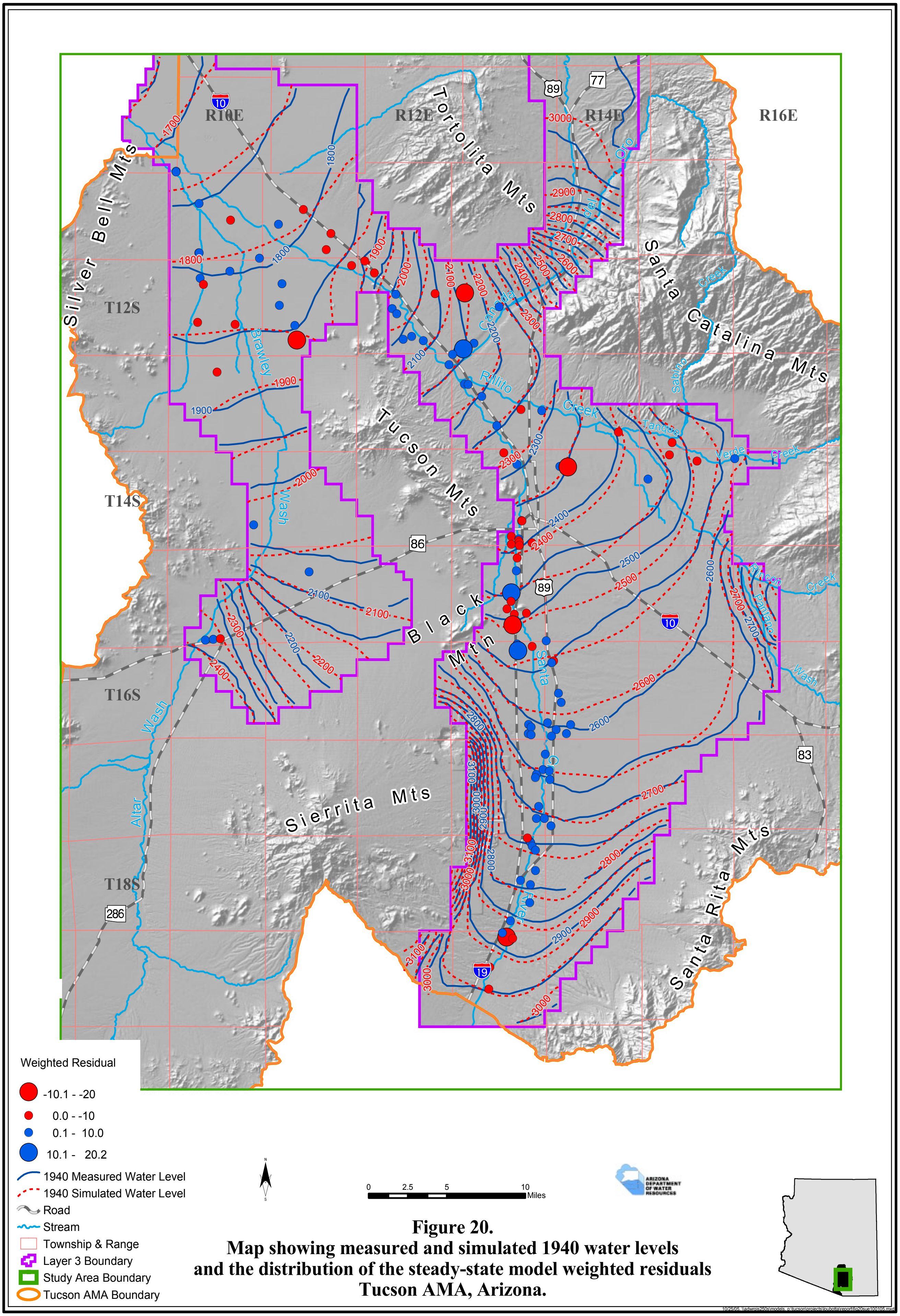

Figure 20.
Map showing measured and simulated 1940 water levels and the distribution of the steady-state model weighted residuals Tucson AMA, Arizona.

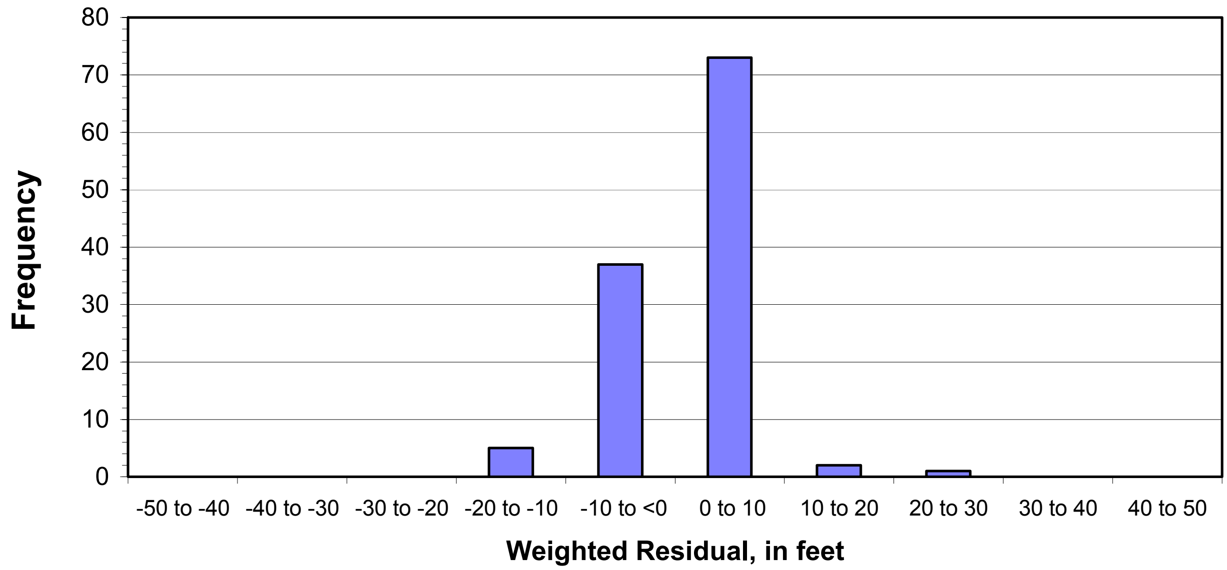

Figure 21. Steady-state weighted residual histogram Tucson AMA, Arizona.

There is a good correlation between weighted simulated and weighted observed heads (Figure 22a) for the steady-state model. The correlation coefficient is 0.85, which is slightly below the minimum value (0.90) recommended by Hill (1998). The results of small weighting factor for some observed heads can be seen in the low weighted head values in figure 22a. The HOB process of MODFLOW-2000 uses a run test to examine the distribution of residuals for randomness. The results of the run test for the steady-state simulation indicate that the weighted residuals are not randomly distributed. Ideally, a graph of weighted residuals and unweighted observed heads (Figure 22b) should show no discernable pattern. If a pattern is observable then the residuals are biased, which can indicate a problem with the model calibration (Hill, 1998). There are two general trends in the distribution of the weighted residuals in Figure 22b. At an elevation of between about 2600 and 2800 feet, located in the southern area of the USC sub-basin, the weighted residuals consistently fall at or slightly above the zero line, indicating that the model consistently over-simulated the observed heads in this area. The second trend occurs in the northern part of the Avra Valley sub-basin between 1700 feet and 1900 feet in elevation. In this area, the residual data points are again generally above the zero line, indicating that the simulated heads in the northern part of Avra Valley are slightly higher than the observed heads.

Water Budget

The final cumulative model water budget and separate water budgets for each sub-basin are presented in Appendix A. Table 9 presents a comparison of the 1940 conceptual steady-state water budget components to the final simulated water budget components. Most conceptual and simulated water budget components were very similar and fall within the range of estimated values presented in Table 3. The simulated underflows into the Tucson AMA across the southern boundary from the Santa Cruz AMA and evapotranspiration values are larger than conceptual estimates (Table 9). The reasons these values are larger than conceptual estimates are discussed below. The final simulated water budget was within the calibration criteria with a cumulative difference between inflows and outflows of -31 ac-ft, or 0.03 percent of the total simulated flux in the model.

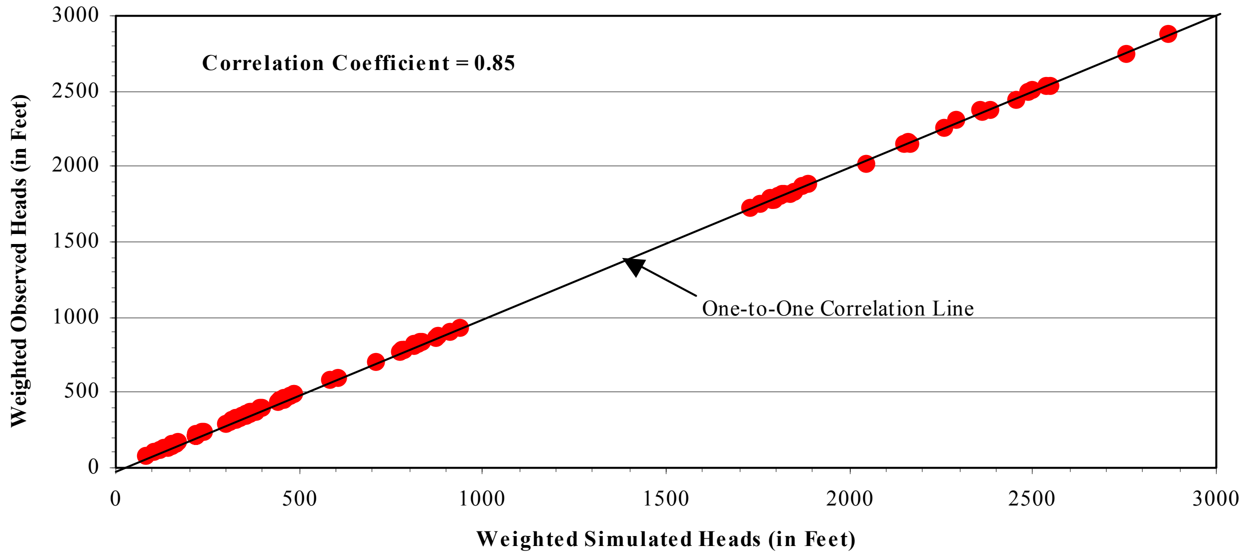

Figure 22. a) Scatter plot of steady-state weighted observed heads vs. weighted simulated heads.

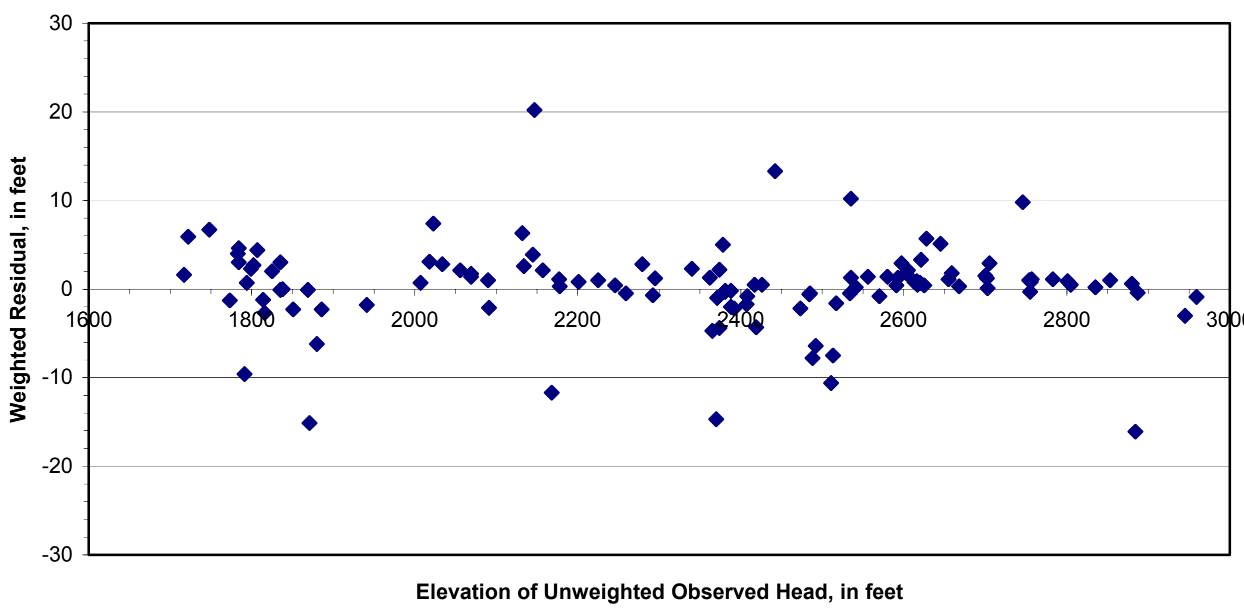

Figure 22. b) Scatter plot of steady-state weighted residuals vs. unweighted observed heads.

Groundwater underflow into and out of the model was simulated using constant head cells and constrained to the range of estimated values by adjusting the elevations and the cell-specific model transmissivities of the constant head cells along the boundaries. The recharge package was used to distribute mountain-front recharge along model boundaries and to simulate long-term average stream infiltration. Outflow components of the water budget, evapotranspiration and pumpage, were simulated using MODFLOW's ET and well packages, respectively. The distribution of calibrated steady-state recharge and discharge points is presented in Figure 23a and 23b.

Inflows

Model inflows included natural recharge (mountain-front recharge and stream infiltration) and groundwater flux across model boundaries from Altar Valley and the Santa Cruz AMA (Figure 23a). Simulated annual steady-state inflows totaled 98,025 ac-ft; about 73,670 ac-ft (76 percent of total inflows) was applied using MODFLOW's recharge package, which simulated mountain-front recharge and stream infiltration. Groundwater flux into the model was simulated using constant head boundaries and accounted for 24,135 ac-ft (24 percent) of the total inflow. Mountain-front recharge totaled 34,425 ac-ft (37 percent of total inflows), with the Avra Valley sub-basin receiving 3,227 ac-ft (4 percent of total inflows) and the USC sub-basin receiving 31,198 ac-ft (33 percent of total inflows). The simulated mountain-front recharge for the USC sub-basin is similar to estimates by Davidson (1973) and Osterkamp (1973) and from groundwater models developed by Anderson (1972) and Hanson and Benedict (1994). The amount of mountain-front recharge for the Avra Valley sub-basin is similar to that estimated by Moosburner (1973). Stream infiltration for the model totaled 39,247 ac-ft (42 percent of total inflows) and represents the long-term average recharge from stream flows. The USC sub-basin received 33,457 ac-ft (36 percent of total inflows) and the Avra Valley received 5,790 ac-ft (6 percent of total inflows) of stream infiltration. The volume of stream recharge for the USC and Avra Valley sub-basins is similar to that of previous investigators (Table 3).

The simulated groundwater flux into the model from the Santa Cruz AMA and Altar Valley were 13,880 ac-ft (14 percent of total inflows) and 10,250 ac-ft (10 percent), respectively. A small amount of underflow into the model along the northern model boundary at the head of the Canada del Oro area was specified using the well package. The groundwater flux across the SCAMA boundary was originally constrained to about 8,500 ac-ft per year based on estimates from previous studies. However, early results of the transient model simulation indicated that a larger groundwater flux across the boundary was needed to accurately simulate observed water levels from the 1950s and early 1960s in the southern portions of the USC sub-basin. The steady-state constant heads were readjusted based on historic water levels and model transmissivity values were modified in this area to allow more groundwater flux across the boundary. The final simulated flux was 13,880 ac-ft per year, which is larger than the highest estimated flux of 10,500 ac-ft, allowed both steady-state and the transient simulated water levels to better match observed water levels along the southern boundary (Table 3).

Zone budget analysis of the groundwater flux from the USC sub-basin into the Avra Valley sub-basin indicated that the flux was 14,580 ac-ft, which is larger than simulated by Hanson and others (1990) but slightly smaller than the flux simulated by Hanson and Benedict (1994). Inflow to the steady-state model by Hanson and Benedict (1994) from the Cañada del Oro drainage was controlled by constant heads and amounted to 5,430 ac-ft per year. Zone budget analysis of the simulated flux across the same boundary within the ADWR model produced a slightly smaller value of 4,130 ac-ft per year. Overall, the inflow components of the model groundwater budget were similar to previous studies estimates and model results.

Outflows

Model discharge included groundwater flux across the northwest boundary into the Pinal AMA, ET, and pumpage (Figure 23b). Total steady-state simulated outflows are 98,056 ac-ft; individual annual outflow components are pumpage: 59,700 ac-ft (61 percent of total outflows), underflow out (simulated as constant heads): 21,126 ac-ft (21 percent of total outflows) and ET: 17,170 ac-ft (18 percent of total outflows). The steady-state pumpage was distributed in the USC sub-basin based on previous modeling studies of Anderson (1972) and Hanson and Benedict (1994) and totaled 47,280 ac-ft (50 percent of total outflows).

Simulated pumpage in the Avra Valley sub-basin was 12,420 ac-ft (13 percent) and is slightly higher than estimates by Moosburner (1972). Avra Valley pumpage was assigned based on the location of known wells and

Table 9. Comparison between 1940 conceptual water budget and steady-state simulated water budget, Tucson AMA, Arizona.

Budget Component	Conceptual Water Budget	Model Water Budget	Percent Difference
Inflows (Ac-ft/yr)			
Mountain-Front Recharge	33,100	34,425	4.0%
Stream Infiltration	40,200	39,445	-2.4%
Groundwater Underflow	18,700	24,155	29.1%
Santa Cruz AMA	8,600	13,880	61.4%
Altar Valley	10,000	10,255	2.5%
Canada del Oro	>100	20	
USC into Avra Valley*	13,000	14,580	12.2%
Total Inflow	**92,100**	**98,025**	6.4%
Outflows (Ac-ft/yr)			
Pumpage	61,600	59,695	-3.1%
Evapotranspiration	8,000	17,170	114.6%
Groundwater Underflow	22,500	21,191	-6.1%
Total Outflow	**92,100**	**98,056**	6.5%
In – Out	0	-31	

* Flow between the two sub-basins is internal to the study area and is not included in the total inflow or outflow calculation.

estimates of agricultural pumpage by White and others (1965) and Moosburner (1972). As previously stated, all ET was limited to the USC sub-basin with the majority of the ET, 15,520 ac-ft (90 percent of the total ET), coming from layer 1. Estimates of ET in the USC sub-basin vary widely. The final ET volume is slightly higher than the estimated average range for 1936 to 1965 by Davidson (1973) of 6,000 to 15,000 ac-ft per year. Groundwater flux out of the model and into the Pinal AMA was within the range of previous estimates and very close to the initial conceptual estimates. Figure 23b shows the locations of well pumpage, ET, and the constant head discharge boundary.

Simulated head differences between layers were very small, but there was net vertical flow upwards in both sub-basins. In the USC sub-basin net vertical flow from layer 2 into layer 1 was 31,820 ac-ft, or about 41 percent of total inflows in the sub-basin. Net flow upwards from layer 3 to layer 2 was about 7,980 ac-ft, (13 percent of total inflows to the sub-basin). The model layering and area covered are different between this study and the Hanson and Benedict (1994) model. However, the vertical flow in Hanson and Benedict (1994) of 42,500 ac-ft is very close to the net vertical flow in the USC sub-basin of 39,800 ac-ft. The net

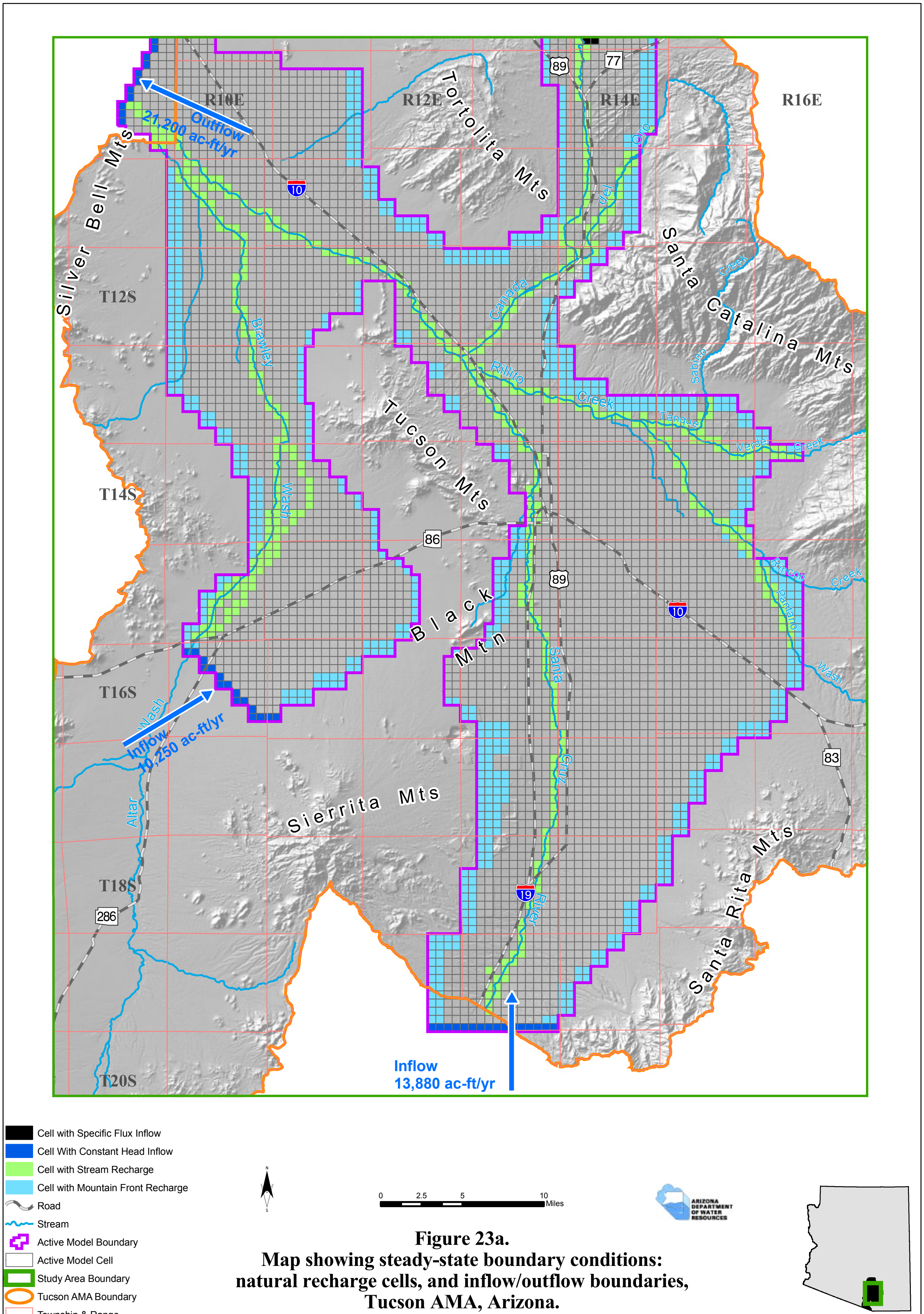

Figure 23a.
Map showing steady-state boundary conditions: natural recharge cells, and inflow/outflow boundaries, Tucson AMA, Arizona.

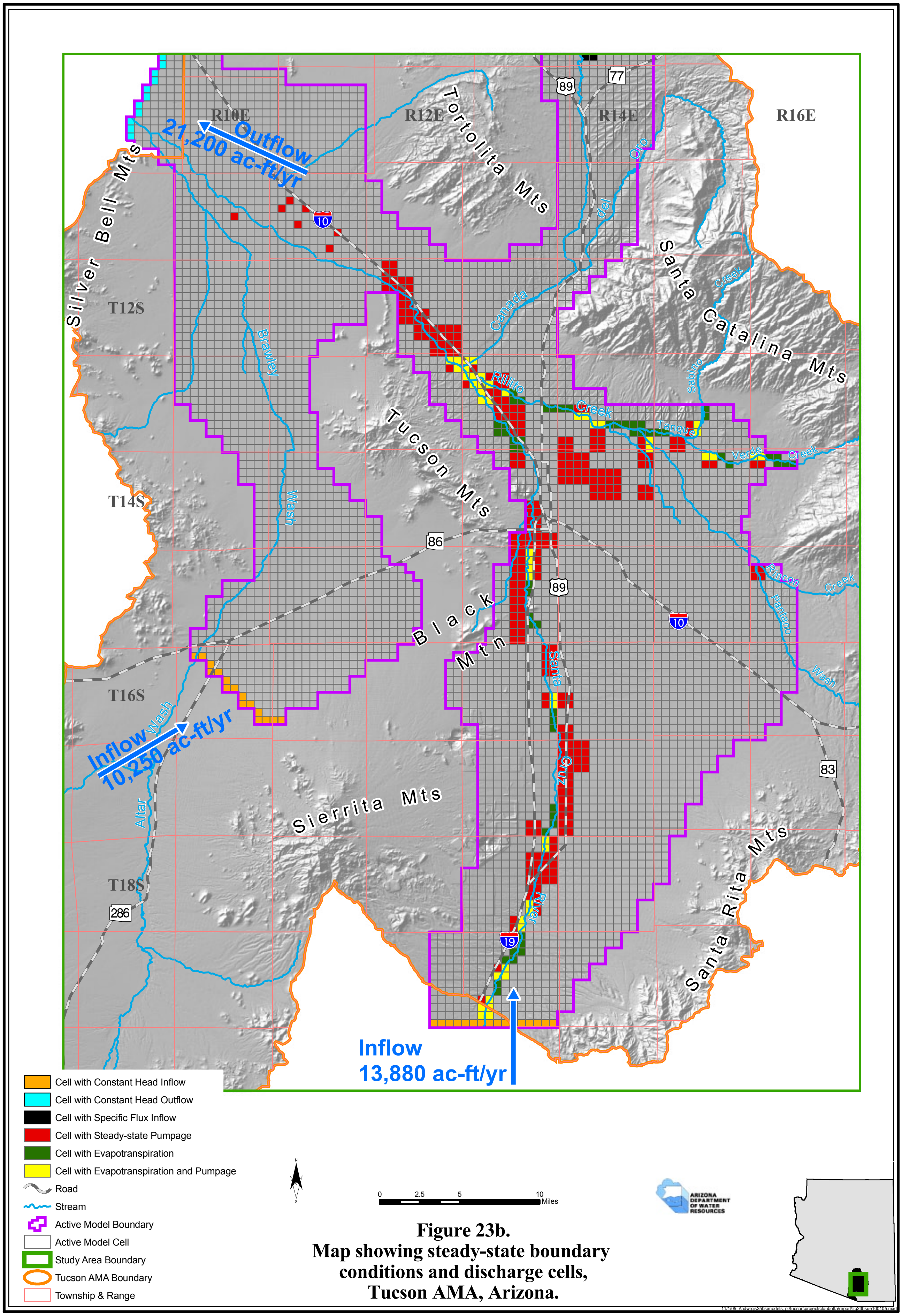

Figure 23b.
Map showing steady-state boundary conditions and discharge cells, Tucson AMA, Arizona.

vertical flow in the Avra Valley between all layers was also upwards and totaled 3,020 ac-ft between layer 1 and 2 and 2,790 ac-ft between layer 2 and 3. The smaller volume of vertical flow in the Avra Valley sub-basin is probably due to the large amount of fine-grained material present in the central and northern parts of the sub-basin, which would tend to inhibit vertical flow.

Transient Calibration

The transient model simulated the response of the regional aquifer system to changing stress conditions that existed for the period of groundwater development from 1941 to 1999. The transient model calibration involved making reasonable adjustments to model stresses (pumpage and incidental recharge) and storage terms (specific yield). Incidental recharge components that were adjusted included agricultural recharge, effluent infiltration, and mine tailings pond recharge. Pre-1984 pumpage was adjusted to improve the calibration between 1941 and 1983. After 1984, pumpage totals reported through the ROGR database were incorporated directly into the model pumpage data sets. As discussed previously, the only adjustment to the natural recharge values for the transient period was to increase stream infiltration values for reaches north of and downstream from Rillito Creek after 1959.

The simulated final heads from the steady-state model were used as the initial heads for the transient model simulation. The use of the final steady-state heads as initial transient heads provides internal consistency between the steady-state and transient models. The transient model simulation was divided into three calibration phases; 1941 to 1960, 1961 to 1983 and 1984 to 1999. The first calibration phase, 1941 to 1960, represents a time when pumpage stresses and distributions are not well documented. The second calibration period covers a time period when the volume and distribution of pumpage stresses were better known. However, some uncertainty still remains as to the volumes and distribution of pumpage. The last calibration period, 1983-1999, covers the recent past when the location and magnitude of pumpage were better known.

Transient Calibration Criteria

The transient calibration criteria were less rigorous than the steady-state criteria due to significant uncertainties in some of the model inputs. Calibration criteria for the transient model simulation were developed based on an analysis of results from previous ADWR regional modeling studies. The transient calibration targets were set as:

1) No weighted residuals greater than 100 feet (7 percent of the head loss in the system).
2) 95 percent of the absolute value of weighted residuals shall be less than 75 feet (5 percent of the head loss in the system).
3) The MAE for weighted residuals will be less than 30 feet (2 percent of the head loss in the system).
4) The ratio of the Root Mean Square Error (RMSE) to the overall head loss in the system will be equal to or less than 5 percent.
5) A reasonable match between hydrographs of selected wells and simulated heads during the simulation.
6) The simulated heads produce a water level contour map that reasonably replicates the hand contoured water level map based on 1999 observed water levels.
7) The percent error in the MODFLOW water budget is less than or equal to 0.1 percent.

Transient Calibration Process

As previously discussed, the storage and stress components were adjusted by trial and error during the three transient model calibration periods. The secondary storage (specific yield) terms were adjusted for each model layer and were limited to the range of values used by previous modeling studies. Transient stresses that were adjusted included annual pumpage volumes (including the vertical distribution), agricultural recharge, mine tailings recharge, and effluent infiltration. After 1984, pumpage reported to the ADWR through the ROGR system was used. Some post-1984 pumpage was adjusted, but any changes were limited to only ±5 percent, which is a reasonable approximation of the error for any of the approved meters used to total pumpage volumes.

Agricultural and mine pumpage and their associated incidental recharge volumes were increased and decreased in tandem so that recharge volumes were consistent with pumpage volumes. The agricultural efficiency factors used to calculate the volume of agricultural recharge and the lag factor used to time the application of the incidental recharge were also adjusted during the calibration process. The final calibrated agricultural efficiency values are 33 percent for the period 1941 to 1970, 28 percent for 1971 to 1980, and 25 percent for 1984 to 1999. The final lag times for all incidental recharge is based on a deep percolation rate of 20 feet per year. Cell-specific lag times were calculated using the deep percolation rate and the initial depth to water for cells receiving agricultural, effluent, and mining recharge. The cell-specific lag times yielded agricultural lag times that ranged from 1 to 30 years and averaged 6 years. Lag times in the Avra Valley sub-basin ranged from 6 to 27 years and averaged 10 years. In the USC sub-basin lag times ranged from 1 to 30 years, but averaged only 5 years. Lag times for recharge from artificial recharge projects was assigned at 1 year, mine tailing pond lag times averaged 10 years, and effluent recharge lag averaged 5 years.

The vertical distribution of pumpage for each cell was based on the same method used to apportion pumpage between layers in the steady-state model as previously described. The percentage of pumpage that was lost in each stress period due to cells going dry was calculated for each simulation. If non-simulated pumpage losses exceeded 3 percent, then the model was checked for dry cells and pumpage from those cells that went dry was moved down into the next model layer. By 1984, model cell dewatering in layer 1 combined with numerical instability problems made it necessary to assign all pumpage to either layers 2 or 3. Assigning all pumpage to layers 2 and 3 reflects the loss of saturated thickness in the upper model layer due to over drafting of the regional aquifer.

Transient Calibration Results

The final transient calibration run was analyzed both quantitatively and qualitatively to determine the acceptability of the simulation to the established calibration criteria. The final transient calibration met most of the selected calibration criteria and was able to generally reproduce historically observed water level declines and estimated groundwater storage changes for the Tucson AMA regional aquifer.

Water levels

About 970 water levels, measured during late 1999 and early 2000 by the ADWR, were used to develop a hand-contoured water level map of the 1999 water table. The hand-contoured map was used as a qualitative tool for comparison to model simulated heads. Only 728 of the water level observations were made at wells that had well depth or well perforation information and fell within the active model domain. These well points were used as target head observation points for the final stress period of the transient calibration. The head observation for each well with a perforation or depth record was assigned to either a single layer or multiple layers based on its perforation intervals or well depth. If only a well's depth was known, the observation head was assigned to the lowest layer that the well penetrated. Head observations for wells lacking perforations or well depth information were discarded from the set of observation points.

A water level contour map of the 1999 simulated water levels was superimposed over the hand-contoured map of 1999 observed water level data points and is presented in Figure 24. The map shows that the simulated water levels are similar to the hand contoured values in most areas and indicated that the transient simulation adequately reproduced the regional groundwater flow pattern of 1999. A statistical analysis of 1999 weighted head residuals is presented in Table 10 and the weighted residuals are listed in Appendix B. Only 507 of the 728 observation water levels were available for a statistical analysis due to model cells going dry. The ME of all weighted head residuals was –2.2 feet and the MAE of the weighted residuals was 12.6 feet, or about 0.8 percent of the head loss across the study area. The residuals ranged from + 46 feet to – 126 feet and had a RMSE of 18.6 feet. The ratio of RMSE to the total head change in the model is 0.0124 (1.24 percent). The ME for the Avra Valley and the USC sub-basins are –3.1 and –1.9 feet, respectively. Layer specific weighted residual statistics are also presented in Table 10.

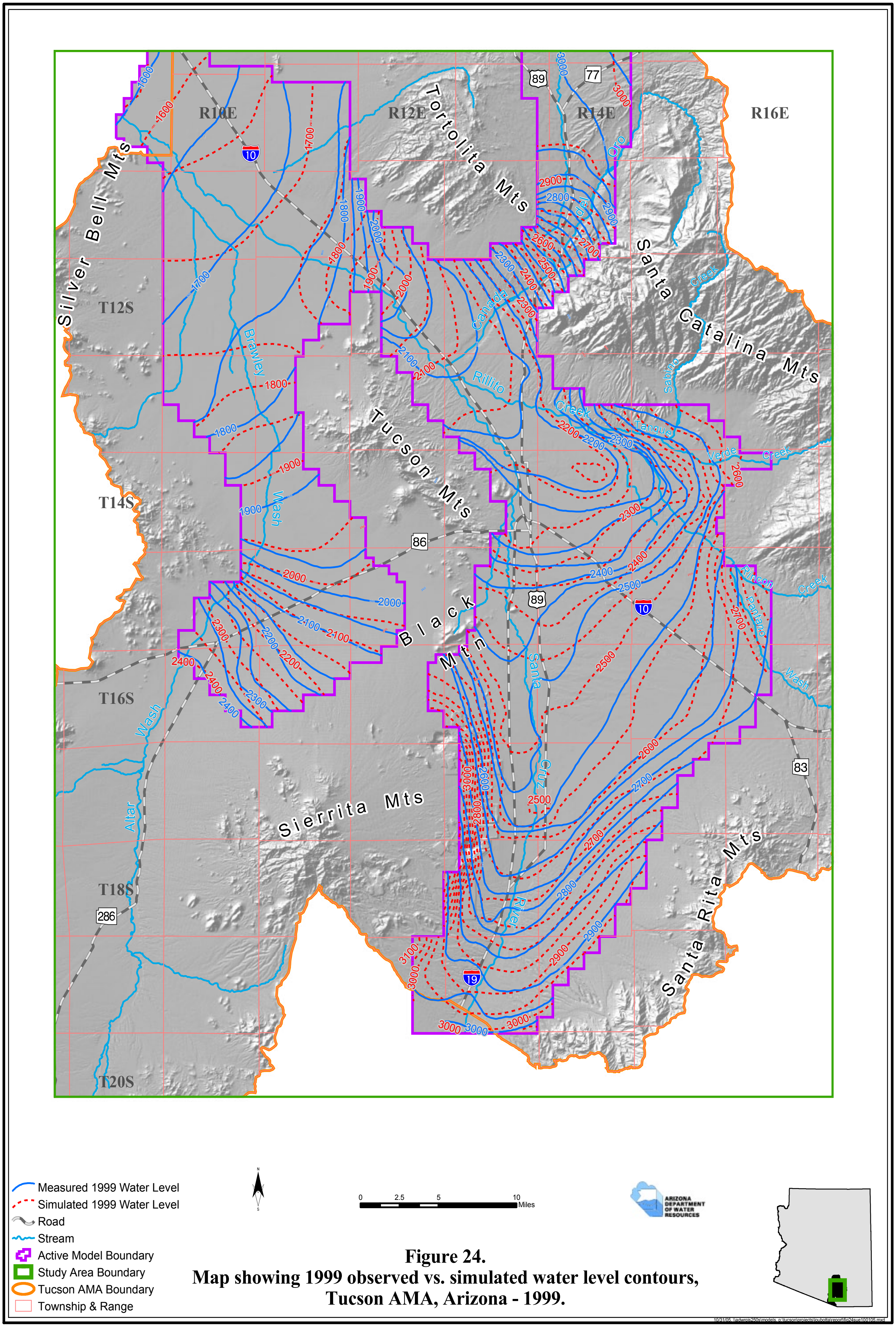

Figure 24.
Map showing 1999 observed vs. simulated water level contours, Tucson AMA, Arizona - 1999.

Layer 1, which had the smallest number of observed heads, had the largest ME, MAE, and RMSE. Some of the largest residuals, both positive and negative residuals, were from observation wells that were assigned to Layer 2. The low negative ME (-2.2 ft) and the residual distribution (Figure 25) indicates the model slightly under simulated the aquifer conditions in 1999.

The frequency distributions of the absolute value of the weighted residuals for the entire model and their calibration levels are presented in Table 11. The frequency distribution of all transient weighted residuals is presented as a histogram in Figure 25. The frequency distribution of the weighted residuals was calculated using intervals of 10 feet to match the calibration level intervals. For the transient simulation 61 percent of weighted residuals fell within calibration level 1, within 0 to ± 10 feet of an observed head, and 94 percent were within ± 40 feet of an observed head, or a level 4 calibration (Table 11). The statistics and frequency distributions all fell within the calibration criteria established for the transient model.

Table 10. Statistical summary of transient model weighted head residuals

Weighted Residual Statistical Analysis (all values are in feet)

	Model-Wide	Avra	USC	Layer 1 Wells	Layer 2 Wells	Layer 3 Wells	Multi-Layer Wells
ME	-2.2	-3.1	-1.9	-8.1	-4.5	-3.3	2.2
RMSE	18.5	15.9	19.2	21.8	21.5	14.9	15.9
MAE	12.6	11.5	12.9	17.3	14.4	9.9	11.5
Median	-1.4	-0.9	-0.8	-7.9	-1.2	-0.7	2.9
Max	46	46	45	44	45	42	46
Min	-126	-48	-126	-44	-126	-66	-48
Count	507	110	397	33	186	127	161

There is a good match between weighted simulated and weighted observed heads (Figure 26a) with the correlation coefficient equal to 0.92, slightly above the recommended lower limit suggested by Hill (1998). The results of the run test indicated that the transient residuals are not randomly distributed. The weighted residuals are presented in a scatter plot of weighted residual versus observed head elevation in Figure 26b and plotted on a map in Figure 27. In Figure 27, the weighted residuals are color-coded and sized proportional to value for easier interpretation.

The weighted residuals are about evenly distributed between positive (44%) and negative (56%) values (Figure 25). However, several spatial trends in the data are evident from examining data in Figures 26b and 27. First there are two distinct trends in the Avra Valley sub-basin. In the northern part of the Avra Valley sub-basin, T 9 to 12 S, R 9 to 11 E, the majority of weighted residuals are negative, and in the central part of the sub-basin, T13 and 14, R 10 and 11, the majority of residuals are positive. The residuals indicate that the model generally under simulated heads in this the northern section of the sub-basin and over simulated heads in the central area of the sub-basin.

A second observed trend is that residuals in the USC sub-basin south of T 14 N are generally negative and almost entirely positive north of T 14 N. The mean simulated head residual for the USC sub-basin is –2.2 feet, indicating that the model generally under simulated head elevations in the sub-basin. Examination of Figure 27 indicates that in T 13 S, R 13 E there is an area of consistently large residuals that range up to 40 feet. The confluence of the Santa Cruz River and Rillito Creek occurs in is in the northwestern corner of T 13 S, R 13 E, and almost all high positive residuals occurred in the area between the Santa Cruz and Rillito Creek. In this area the transient model may have over-simulated heads due to the combined effects of over-estimation of agricultural recharge, stream, and/or effluent recharge along the Santa Cruz River and stream recharge along Rillito Creek, or the presence of fine material in the basin-fill sediments that lie above the water table as reported by Hoffman and others (2001). The fine materials in the upper basin-fill sediments may create perching conditions that the model may not be able to accurately simulate.

Table 11. Frequency distribution of the absolute value of the 1999 weighted residuals.

Calibration Level	*Absolute Range (Ft)*	*Frequency*	*Cumulative Percent*
Level 1	0 to 10	308	61%
Level 2	10 to 20	92	79%
Level 3	20 to 30	46	88%
Level 4	30 to 40	31	94%
Level 5	40 to 50	23	98.6%
Level 6	50 to 60	1	98.8%
Level 7	60 to 70	4	99.6%
Level 8	70 to 80	1	99.8%
Level 9	80 to 90	0	99.8%
Level 10	90 to 100	0	99.8%
Level 11 or more	> 100	1	100%
	Count	507	

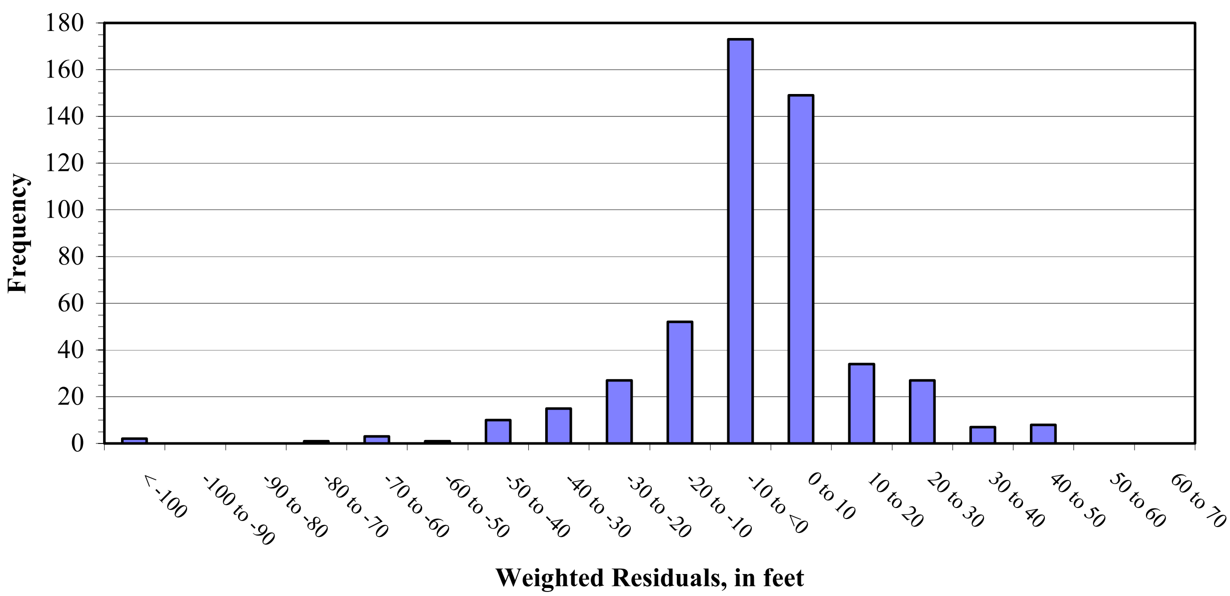

Figure 25. Histogram of 1999 weighted residuals Tucson AMA, Arizona.

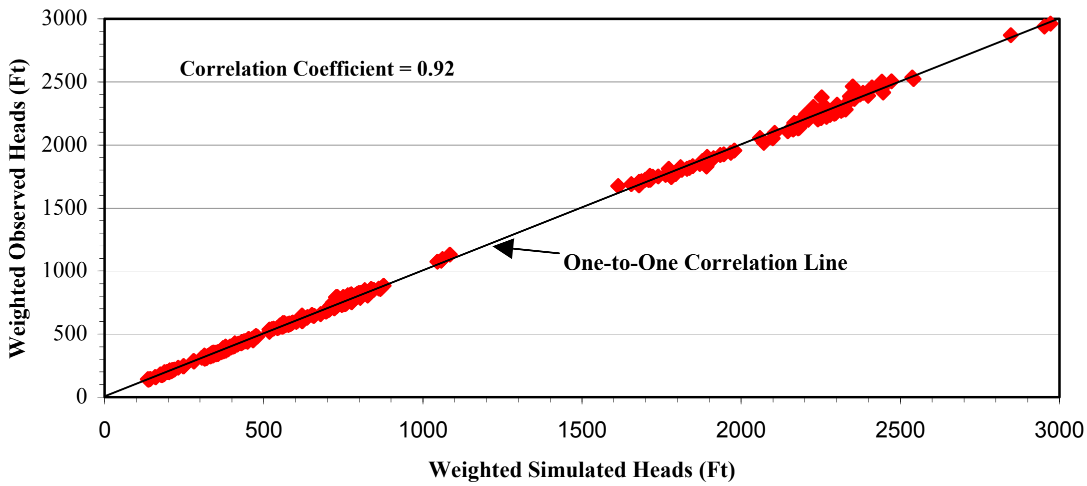

Figure 26. a) Scatter plot of transient weighted observed heads vs. weighted simulated heads.

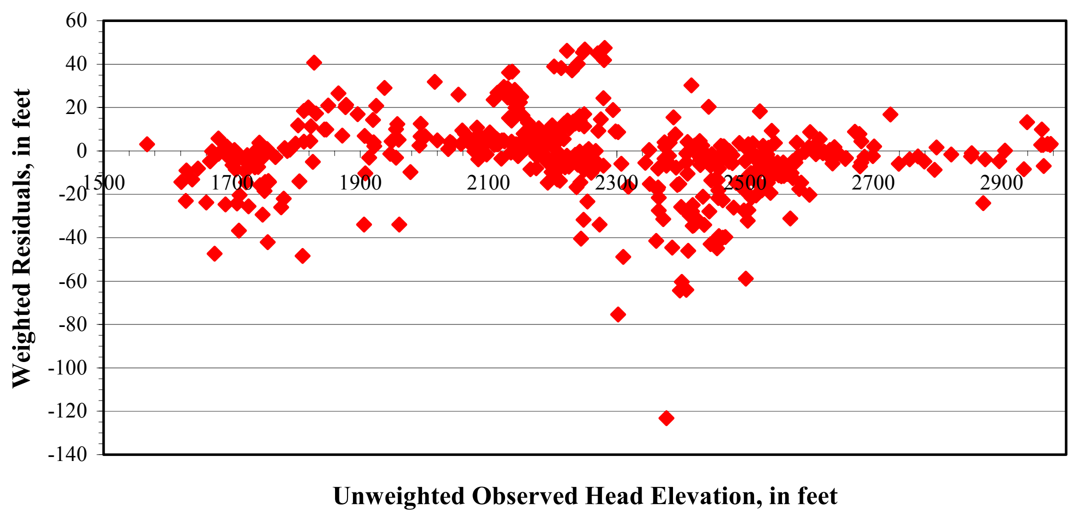

Figure 26. b) Scatter plot of transient weighted residuals vs. unweighted observed heads Tucson AMA, Arizona.

Other areas of large residuals in the USC sub-basin are located in T. 14 S., R. 15 E. and T.15 S., R. 13 E. and 14 E. The residuals in these areas include both large positive and negative. The grouping of large residuals in T.14 S., R. 15 E are generally located close to areas with steep hydrologic gradients (Figure 24). Geologic faults and suspected areas of perched groundwater also occur in these areas. The residuals in T 15 S, R 13 and 14 E, also have both large positive and negative residuals and are in an area of suspected perched groundwater and near the Santa Cruz Fault, which runs southeast to northwest through the area.

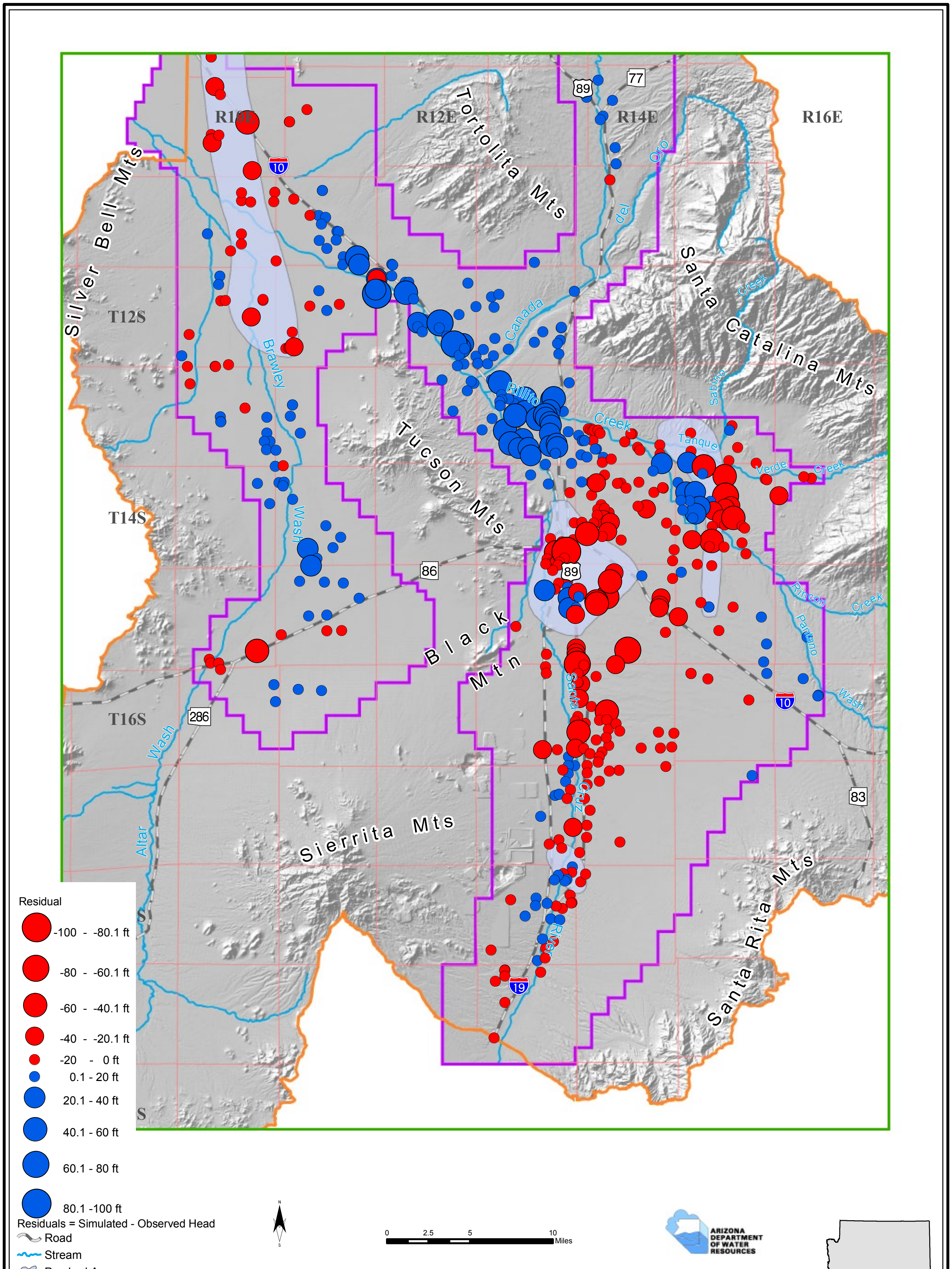

Figure 27.
Map showing distribution of simulated transient head residuals, Tucson AMA, Arizona.

Hydrographs

Another method of evaluating the transient model simulation is to examine its ability to simulate past aquifer response by comparing hydrographs of observed water levels verses simulated water levels. Hydrographs of 26 wells with long-term water level records and a locator map are presented in Appendix C. In most areas the simulated heads replicated observed groundwater levels with reasonable accuracy. The best match between hydrographs and simulated heads occurred in the northern sections of the Avra Valley sub-basin, the central well field area (T 14 S, R 14 E) and in the southern portions of the USC sub-basin. Hydrographs A through F represent wells in the agricultural areas of northern Avra Valley. Most hydrographs show long-term water level declines from the 1940s into the early 1970s, then water levels generally stabilized or begin recovering. The model was generally able to simulate the long-term water level declines and recoveries that began in the late 1970s. Even in wells where the observed and simulated water levels differed by 15 to 20 feet, the slopes of the simulated water levels generally parallel the observed water levels, and the break in slope that marks the late 1970s recovery period also generally coincided. Hydrographs of simulated heads vs. observed heads from wells in the USC sub-basin generally matched (Hydrographs J through Z). Hydrographs in the central well field area, T. 14 S., R. 14 E., matched well indicating that the model was able to accurately simulate the historic aquifer response in that area. Several wells located close to the Santa Cruz River show water level rises that are probably in response to recharge from flood flow events that occurred in 1983 and again in 1993 (Hydrographs J and X). The model was unable to replicate these transient effects due to the long-term average stream infiltration values that are used in the transient model simulation.

The transient simulation period included three calibration periods: 1) 1941 to 1960, 2) 1961 to 1983, and 3) 1984 to 1999. A comparison of the model head residuals through time is another means of determining how well the model replicated observed, historic aquifer conditions. A statistical comparison of the head residuals for each calibration period is presented in Table 12. Examination of the weighted residuals show that for the entire model both the MAE and RMSE increased from 1960 to 1999, indicating the model calibration error increased through time. However, the trend of the model calibration error is different for the two sub-basins. The MAE and RMSE for the Avra Valley sub-basin both decreased from 1960 to 1983, then increase slightly from 1983 to 1999. In contrast, the MAE and RMSE for the USC sub-basin both increased over the calibration period. The weighted head residuals for each calibration period are presented in Appendix B. The final model calibration went from slightly over-simulating water level in 1960 (ME = 4.9 feet) to slightly under-simulating regional water levels by 1999 (ME = -2.2 feet).

Table 12. Weighted head residuals for the transient period 1941- 1999, Tucson AMA. Arizona.

Model-Wide Residuals (ft)					
	ME	MAE	RMSE	Range	RMSE Ratio
1960	4.9	8.9	14.0	65 to –49	0.0094
1983	2.7	10.2	16.1	94 to –77	0.0107
1999	-2.2	12.6	18.6	48 to –126	0.0124
Avra Valley Residuals (ft)					
1960	5.7	15.0	20.0	65 to –49	NA
1983	0.8	10.4	13.9	24 to -54	NA
1999	-3.1	11.5	15.9	46 to – 49	NA
USC sub-basin Residuals (ft)					
1960	4.8	8.0	12.9	41 to –38	NA
1983	3.0	10.2	16.4	94 to –77	NA
1999	-1.9	12.9	19.2	48 to -126	NA

Water Budget

Table 13 presents the simulated annual model water budget for the transient calibration period; the final cumulative water budget is presented in Appendix A. Most simulated water budget components were close to estimated conceptual volumes. From 1941 through 1983, model simulated pumpage was generally less than initial pumpage estimates and generally less than was simulated by Hanson and others (1990) and Hanson and Benedict (1994). As previously discussed, the pumpage from 1984 to 1999 that was reported to the ADWR was used with only slight modification.

Inflows

Simulated transient inflow consists of natural recharge, incidental recharge, and underflow across the Santa Cruz AMA – Tucson AMA and Avra - Altar Valley boundaries. Natural recharge components include mountain-front recharge and stream infiltration. Mountain-front and stream infiltration recharge was held constant at the steady-state values, except for stream infiltration after 1959, which was increased as previously discussed. Incidental recharge included agricultural irrigation recharge, infiltration of effluent releases, recharge from artificial or managed recharge projects, and recharge from mine tailing ponds. The location of effluent, agricultural, and mine tailings pond recharge components for 1999 is presented in Figure 28.

Incidental Recharge

As discussed in Chapter 3, incidental recharge comes from water recharged to the regional aquifer during the course of its use for agricultural, industrial, or municipal uses. Incidental recharge increased steadily through the transient period peaking in the mid-1970s through the mid-1980 at about 100,000 ac-ft per year (Table 13). Since the mid-1960s incidental recharge has been as large as or larger than natural recharge, making it an important component of the water budget in the Tucson AMA. Zone budget analysis indicates that incidental recharge has a larger impact on the Avra Valley sub-basin than the USC sub-basin due to the large volume of agricultural pumpage.

Agricultural Recharge

Agricultural recharge was applied one of two ways depending on whether the pumpage was from a private farm or associated with one of the two active irrigation districts in the model area. Recharge associated with private farms was applied to cells that contained wells that were assigned agricultural pumpage. Annual recharge from the Cortaro-Marana Irrigation District (CMID) and Farmers Investment Coop (FICO) was based on reported water applied by the districts. GIS techniques were used to estimate the percentage of a district's total irrigated acres occupied by a cell. The district's total annual recharge was calculated from the water applied and then distributed to cells based on their assigned percentage of total acres. The year that agricultural recharge was applied was calculated by adding a cells lag factor to the year the water was applied. Total lagged agricultural recharge started at about 14,000 ac-ft in 1941, peaked in the mid-1960s, at about 86,000 ac-ft per year, and declined to about 24,000 ac-ft in 1999. In the USC sub-basin the lagged agricultural recharge peaked in 1960 at about 40,000 ac-ft and steadily declined to about 11,000 ac-ft in 1999. The lagged agricultural recharge peaked later in the Avra Valley and stayed at or near the peak value longer than in the USC sub-basin. In Avra Valley the lagged recharge peaked in 1965 at about 53,000 ac-ft and stayed at about 50,000 ac-ft per year until 1982, since then agricultural recharge has declined sharply to about 12,000 ac-ft in 1999.

Effluent Recharge

Effluent released into the Santa Cruz River was distributed into cells with stream recharge located downstream from the WWTPs. Initial estimated of effluent infiltration were based on values developed from an effluent infiltration study by Galyean (1996). Adjusting cell-specific effluent infiltration rates during the transient calibration controlled effluent infiltration. This allowed the total volume of simulated

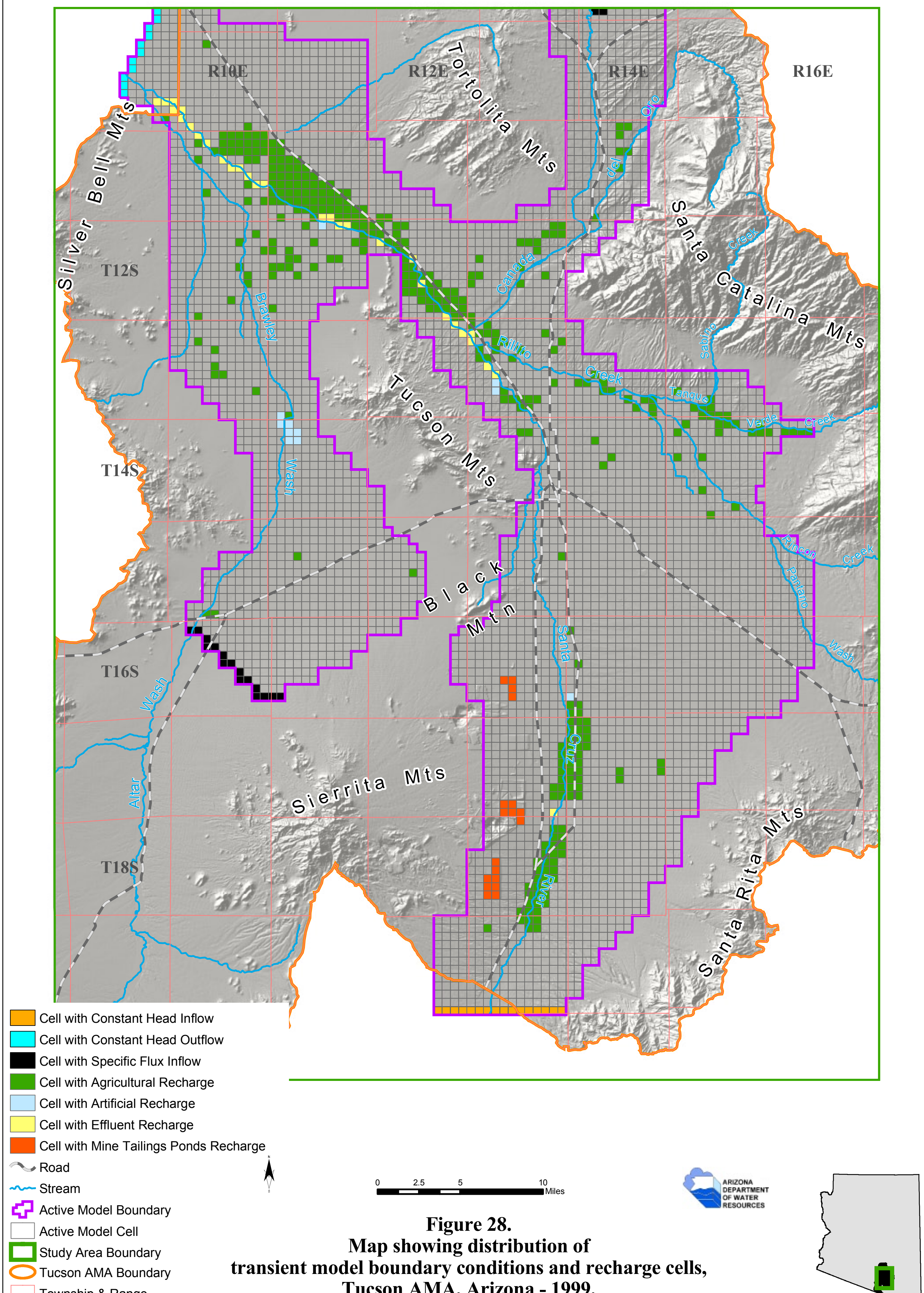

Figure 28.
Map showing distribution of
transient model boundary conditions and recharge cells,
Tucson AMA, Arizona - 1999.

Table 13: Annual simulated model water budget 1941 - 1999 for the Tucson AMA.

Report Units: Acre-Feet/Year

Year	Model Simulated Recharge	Specified Mountain-Front Recharge	Specified Stream Infiltration	Incidental Recharge	Constant Head Inflow	Altar Valley Inflow	Canada del Oro Inflow	Total Water Budget Inflows	Constant Head Outflows	Pumpage Out of Model	ET	Total Water Budget Outflows	Annual Change In Storage	Cumulative Change In Storage
1941	87382	34,445	39,270	13,667	14,342	10,252	20	111,996	20,804	105,256	22,079	148,140	-36,147	-36,147
1942	87935	34,445	39,270	14,220	13,306	10,255	20	111,515	21,574	116,501	23,841	161,916	-50,411	-86,558
1943	90225	34,445	39,270	16,510	11,227	10,255	20	111,727	22,037	119,184	26,240	167,461	-55,733	-142,291
1944	90876	34,445	39,270	17,161	10,099	10,255	20	111,250	22,728	124,455	27,056	174,239	-62,989	-205,280
1945	92931	34,445	39,270	19,216	9,783	10,255	20	112,988	21,186	128,311	25,674	175,171	-62,185	-267,465
1946	96126	34,445	39,270	22,411	9,836	10,255	20	116,237	20,948	137,412	23,893	182,254	-66,018	-333,483
1947	96752	34,445	39,270	23,037	9,577	10,255	20	116,605	20,745	160,173	22,011	202,929	-86,328	-419,811
1948	101126	34,445	39,270	27,411	9,938	10,255	20	121,338	20,659	174,138	19,558	214,355	-93,021	-512,832
1949	106953	34,445	39,270	33,238	10,746	10,255	20	127,974	16,773	181,702	17,611	216,086	-88,111	-600,943
1950	111987	34,445	39,270	38,272	11,609	10,255	20	133,870	16,495	192,876	15,365	224,736	-90,865	-691,809
1951	113949	34,445	39,270	40,234	12,894	10,255	20	137,118	18,183	230,753	12,511	261,447	-124,336	-816,144
1952	115530	34,445	39,270	41,815	14,038	10,255	20	139,842	18,051	260,695	10,255	289,001	-149,165	-965,309
1953	116499	34,445	39,270	42,784	15,026	10,255	20	141,799	17,564	270,526	8,106	296,195	-154,401	-1,119,710
1954	119916	34,445	39,270	46,201	15,142	10,255	20	145,332	17,667	283,617	6,598	307,882	-162,558	-1,282,268
1955	126021	34,445	39,270	52,306	14,744	10,255	20	151,040	17,704	279,049	5,726	302,479	-151,443	-1,433,711
1956	134733	34,445	39,270	61,018	14,670	10,255	20	159,677	18,138	298,701	5,213	322,052	-162,376	-1,596,088
1957	137714	34,445	39,270	63,999	14,350	10,255	20	162,338	18,506	321,456	4,903	344,865	-182,525	-1,778,613
1958	141577	34,445	39,270	67,862	14,170	10,255	20	166,022	18,240	331,823	5,029	355,093	-189,057	-1,967,670
1959	152039	34,445	49,800	67,794	14,693	10,255	20	177,007	17,750	331,494	5,915	355,159	-178,172	-2,145,842
1960	157049	34,445	49,800	72,804	15,178	10,255	20	182,502	18,960	335,404	6,408	360,772	-178,291	-2,324,133
1961	155294	34,445	49,800	71,049	14,541	10,255	20	180,110	19,632	312,448	6,915	338,994	-158,893	-2,483,026
1962	153913	34,445	49,800	69,668	15,149	10,255	20	179,336	18,788	331,867	6,955	357,611	-178,270	-2,661,296
1963	153014	34,445	49,800	68,769	15,221	10,255	20	178,510	19,936	316,074	6,754	342,763	-164,234	-2,825,530
1964	158501	34,445	49,800	74,256	15,469	10,255	20	184,244	19,957	314,464	6,542	340,963	-156,729	-2,982,259
1965	160868	34,445	49,800	76,623	16,206	10,255	20	187,348	17,115	331,949	6,416	355,480	-168,139	-3,150,398
1966	162743	34,445	49,800	78,498	17,729	10,255	20	190,747	17,484	271,483	6,331	295,299	-104,568	-3,254,967
1967	167979	34,445	49,800	83,734	17,825	10,255	20	196,079	17,726	305,579	7,012	330,317	-134,246	-3,389,213
1968	168647	34,445	49,800	84,402	19,719	10,255	20	198,640	17,719	318,512	7,153	343,384	-144,758	-3,533,970
1969	167275	34,445	49,800	83,030	20,282	10,255	20	197,832	17,386	332,899	7,263	357,549	-159,724	-3,693,694
1970	171224	34,445	49,800	86,979	20,717	10,255	20	202,216	18,842	342,918	6,691	368,451	-166,237	-3,859,931
1971	167514	34,445	49,800	83,269	21,278	10,255	20	199,067	16,338	331,735	6,003	354,076	-155,012	-4,014,944
1972	166629	34,445	49,800	82,384	21,288	10,255	20	198,192	16,371	342,414	5,552	364,336	-166,140	-4,181,084
1973	165767	34,445	49,800	81,522	21,517	10,255	20	197,559	15,346	326,267	5,307	346,920	-149,362	-4,330,445
1974	173991	34,445	49,800	89,746	21,287	10,255	20	205,553	14,214	347,831	5,027	367,072	-161,522	-4,491,967
1975	183799	34,445	49,800	99,554	21,587	10,255	20	215,660	14,265	364,058	4,576	382,899	-167,241	-4,659,208
1976	190348	34,445	49,800	106,103	21,948	10,255	20	222,570	15,440	356,648	4,227	376,316	-153,747	-4,812,956
1977	189847	34,445	49,800	105,602	22,867	10,255	20	222,988	15,353	322,796	4,052	342,202	-119,212	-4,932,168
1978	181605	34,445	49,800	97,360	23,169	10,255	20	215,048	14,850	261,792	3,957	280,599	-65,553	-4,997,721
1979	179100	34,445	49,800	94,855	24,031	10,255	20	213,406	16,100	275,044	3,986	295,130	-81,718	-5,079,439
1980	179299	34,445	49,800	95,054	23,915	10,254	20	213,488	16,342	287,430	4,110	307,882	-94,384	-5,173,823
1981	181447	34,445	49,800	97,202	24,832	10,254	20	216,554	15,716	291,437	4,508	311,660	-95,099	-5,268,922
1982	184268	34,445	49,800	100,023	25,119	10,254	20	219,661	15,950	250,255	4,896	271,102	-51,430	-5,320,352
1983	182264	34,445	49,800	98,019	26,100	10,254	20	218,639	14,340	216,358	5,255	235,953	-17,315	-5,337,667
1984	180592	34,445	49,800	96,347	25,249	10,254	20	216,116	16,863	250,409	5,988	273,261	-57,139	-5,394,806
1985	181786	34,445	49,800	97,541	26,399	10,254	20	218,459	16,690	271,776	5,340	293,806	-75,344	-5,470,149
1986	174059	34,445	49,800	89,814	25,618	10,254	20	209,951	15,853	258,590	5,212	279,655	-69,695	-5,539,844
1987	170782	34,445	49,800	86,537	24,463	10,254	20	205,520	15,440	225,729	4,807	245,976	-40,450	-5,580,294
1988	165826	34,445	49,800	81,581	23,755	10,254	20	199,855	15,459	282,446	4,968	302,873	-103,011	-5,683,305
1989	165844	34,445	49,800	81,599	23,574	10,254	20	199,693	15,143	281,372	4,654	301,169	-101,474	-5,784,779
1990	159832	34,445	49,800	75,587	24,251	10,254	20	194,358	14,623	264,653	4,436	283,712	-89,371	-5,874,150
1991	157043	34,445	49,800	72,798	24,718	10,254	20	192,035	14,681	282,304	4,216	301,201	-109,154	-5,983,304
1992	155373	34,445	49,800	71,128	24,294	10,254	20	189,941	14,638	268,625	4,323	287,586	-97,640	-6,080,944
1993	153423	34,445	49,800	69,178	24,749	10,254	20	188,447	15,768	235,695	4,173	255,636	-67,193	-6,148,137
1994	151852	34,445	49,800	67,607	26,018	10,254	20	188,145	15,195	287,004	3,931	306,130	-117,972	-6,266,109
1995	152385	34,445	49,800	68,140	27,324	10,254	20	189,983	15,036	303,488	3,790	322,314	-132,333	-6,398,441
1996	153423	34,445	49,800	69,178	26,734	10,254	20	190,431	15,834	320,245	3,599	339,678	-149,250	-6,547,691
1997	156573	34,445	49,800	72,328	25,407	10,254	20	192,255	16,100	315,457	3,233	334,790	-142,530	-6,690,221
1998	157711	34,445	49,800	73,466	24,900	10,254	20	192,885	16,020	285,379	2,893	304,292	-111,401	-6,801,623
1999	174185	34,445	49,800	89,940	24,990	10,254	20	209,449	15,229	292,254	2,753	310,235	-100,789	-6,902,412
Totals 1941-1999		2,032,255	2,748,660	4,052,430	1,129,607	605,022	1,180	10,569,147	1,018,494	15,961,210	491,796	17,471,504	-6,902,411	

Notes: 1) Altar Valley and Canada de Oro inflows are specified using the well package
2) Constant head inflows are generally representative of underflow into the model across the southern boundary from the Santa Cruz AMA.
3) Constant head outflows are generally reresentative of underflow out the model across the northern boundary into the Pinal AMA.

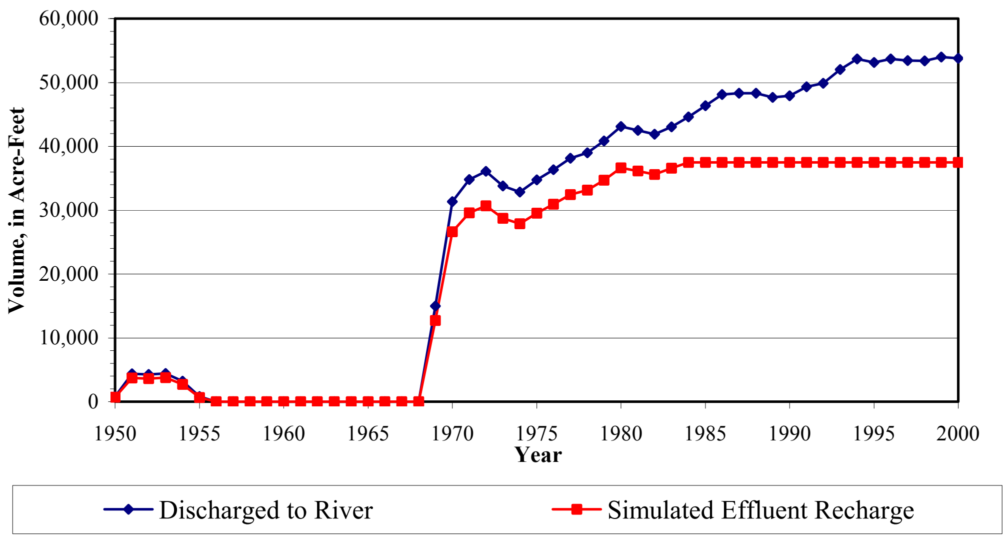

Figure 29. Graph showing total effluent released and simulated effluent infiltrated into the Santa Cruz River – 1951 to 1999.

effluent infiltration to be controlled in an attempt to match simulated heads to observed water levels in cells near the river. The total infiltration along these river segments comes from a combination of both natural and effluent flows. Figure 29 shows the total effluent released to the river and the effluent infiltration simulated in the model. Prior to about 1978, all the effluent released into the river was included as stream infiltration inside the Tucson AMA. After 1978, not all the release volume was included in the stream recharge totals. This is water that does not infiltrate within the model domain, but exited as surface water flows. The percentage of effluent not included in the model as recharge ranged from 4 to 17 percent of annual releases.

Mine Tailings Pond Recharge

Tailings pond recharge was calculated based on a mine's estimated or reported pumpage and distributed to cells that contain tailings ponds associated with the mine (Figure 28). The calibrated tailings pond recharge value was only 10 percent of the pumpage and the average lag factor was 10 years. The simulated tailings pond recharge peaked in mid-1980s, at about 6,000 ac-ft and declined to slightly more than 2,500 ac-ft by 1999.

Groundwater Underflow

Water levels in wells near the Altar Valley – Avra Valley model boundary were generally stable during the transient period; therefore, the flux across this boundary was held constant at the steady-state values using specified fluxes in the well package. Groundwater underflow along the Santa Cruz AMA – Tucson AMA inflow boundary was simulated using the Time-Variant Specified-Head (CHD) Package, which allows inflows to change as water levels near the boundary fluctuated over the transient period. Water level changes in the CHD package were assigned based on hand-contoured water levels and examination of hydrographs from wells near the model boundary. Groundwater underflow into the Tucson AMA across the model's southern boundary was examined using the MODFLOW post-processing program Zone Budget. The zone budget analysis indicated that the simulated inflows remained relatively consistent until the early 1960s, averaging about 12,400 ac-ft per year. Simulated inflows gradually increased through the 1960s, 1970s, and 1980s. Average inflows were 15,300 ac-ft per year during the 1960s, 19,500 ac-ft per year during the 1970s, and 22,900 for the 1980s. The final simulated Santa Cruz inflow is just over 24,000 ac-ft per year.

The increasing inflows from the Santa Cruz AMA reflect an increasing water table gradient along the boundary caused by generally stable water levels in the northern part of the Santa Cruz AMA and declining water levels due to pumping in the southern area of the Tucson AMA. Water levels have remained generally stable in the northern part of the Santa Cruz AMA due, in part, to regular releases of effluent into the Santa Cruz River. Raw sewage and/or effluent has been released into the Santa Cruz River or its tributaries by Nogales, Arizona and Nogales, Sonora, Mexico since the early 1950s (ADWR, 1999b). The Nogales International Wastewater Treatment Plant (NIWWTP) has been treating sewage from the twin cites of Nogales, Arizona and Nogales, Sonora and releasing it into the Santa Cruz River since 1972 (ADWR, 1999b). This steady source of water has generally stabilized water levels in the area between the NIWWTP and the Santa Cruz AMA – Tucson AMA boundary (Nelson and Erwin, 2001). The simulated flux across the Santa Cruz AMA – Tucson AMA boundary for 1999 is very similar to the outflow from a groundwater flow model being developed for the northern area of the Santa Cruz AMA by the ADWR (Keith Nelson, personal communication, 2004). Preliminary results from the Santa Cruz AMA model indicate a groundwater flux across the Santa Cruz AMA – Tucson AMA boundary for the quasi-steady-state of 1997 to 2002 of about 22,000 ac-ft/yr.

Outflows

Simulated transient discharges consisted of pumpage, ET and boundary outflows. The distribution of transient model discharges for 1999 is presented in Figure 30. As previously discussed, groundwater pumpage within the Tucson AMA has varied widely both in volume and spatial distribution throughout the developed period. Pumpage represents groundwater withdrawn from the aquifer to meet municipal, industrial and agricultural demands within the Tucson AMA. Natural outflows during the transient period included groundwater outflows into the Pinal AMA at the northwestern model boundary and ET.

Pumpage

The final simulated transient pumpage increased steadily from 1941 to 1958, reaching 328,000 ac-ft in 1958. The increase in pumpage reflected the increasing amount of irrigated acreage during the 1940s and 1950s. Pumpage peaked in 1975, and then began to decline as agricultural irrigation, especially in the Avra Valley sub-basin, began to decline. The general decline continued until the mid-1980s, when increasing municipal demand reversed the trend and total water use begin to increase again. As discussed earlier, decreasing agricultural pumpage has been offset by increasing municipal demand since the mid-1980s, resulting in a gradual increase in total annual pumpage. Pumpage over the transient period totaled almost 16 million ac-ft, with about 6 million occurring in the Avra Valley sub-basin and about 10 million in the USC sub-basin.

Groundwater Outflow

Groundwater outflow out of the model was simulated using the CHD package. Water level changes through time were assigned based on hand-contoured water levels, examination of hydrographs of wells near the boundary, and previously simulated water level changes (Hanson and others, 1990). The simulated flux across this boundary was analyzed using the zone budget program and found to generally have mimicked the historic water level trends. The boundary flux remained relatively stable during the 1940s, averaging about 20,500 ac-ft per year. The flux declined during the 1950s, 1960s, and 1970s, during the time of water table declines in the northern Avra Valley. By the 1970s, the average annual flux had decreased to about 12,600 ac-ft per year. In the 1980s and 1990s, during the water level recovery period, the flux gradually increased and averaged about 14,500 ac-ft per year during the 1990s.

Evapotranspiration

The ET input estimates, both areal locations and rates, were held constant throughout the transient simulation. Simulated ET declined through the developed period simulation, reflecting both the long-term water level declines experienced in the USC sub-basin and possible urbanization activities along the Santa Cruz River and its tributaries. Simulated ET declined from over 22,000 ac-ft per year to slightly less than 3,000 ac-ft per year by 1999. Simulated ET along the Santa Cruz River declined from 16,350 ac-ft per year

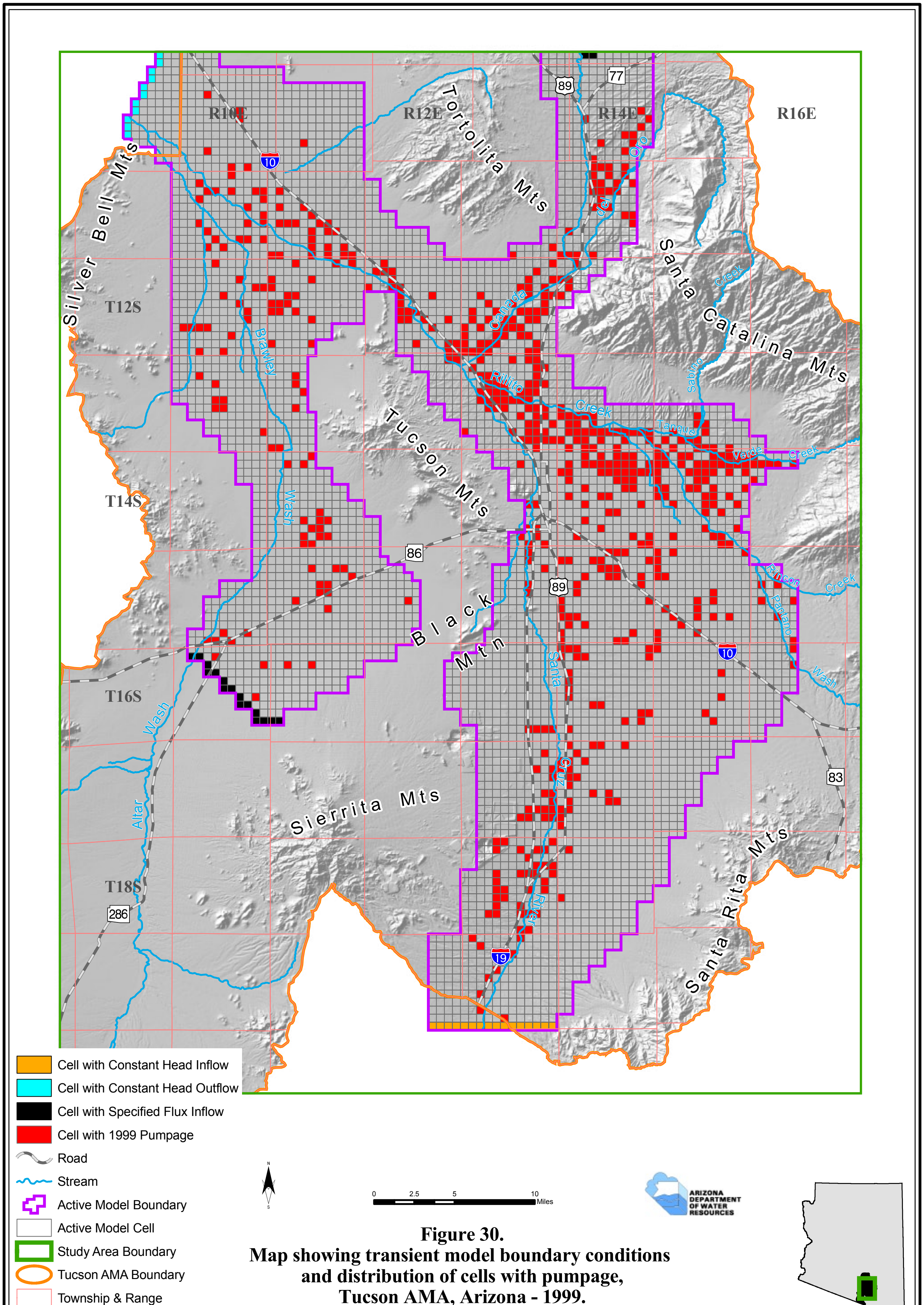

Figure 30.
Map showing transient model boundary conditions and distribution of cells with pumpage, Tucson AMA, Arizona - 1999.

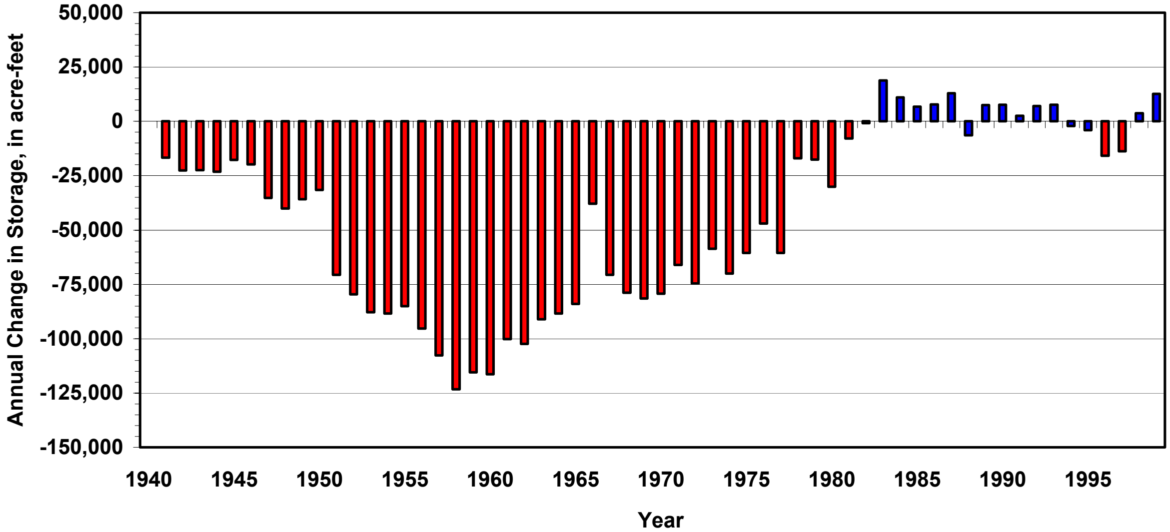

Figure 31. Graph showing simulated annual change-in-storage for Avra Valley sub-basin 1941 - 1999, Tucson AMA, Arizona.

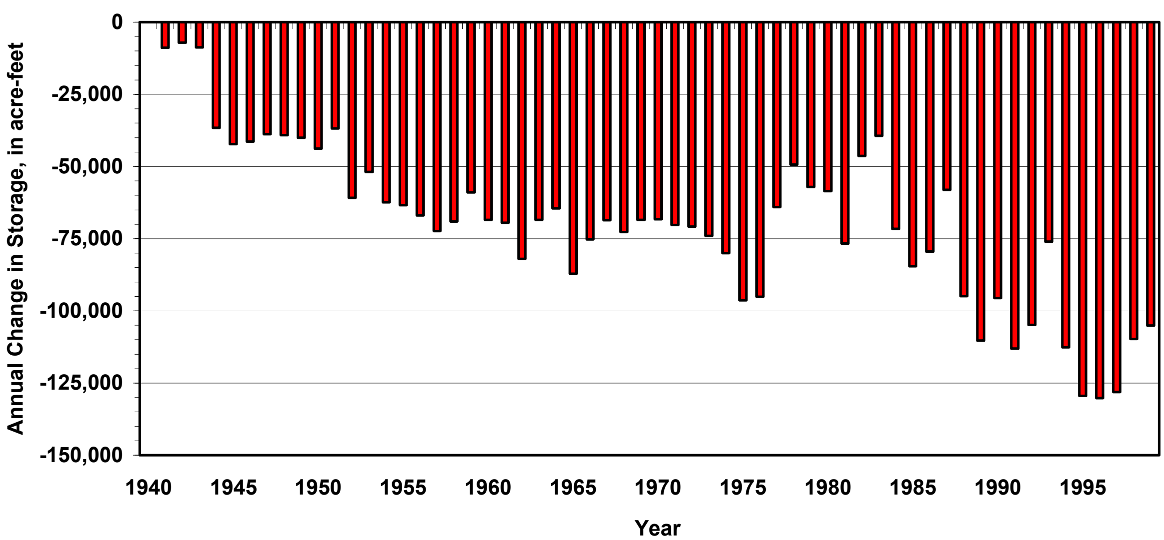

Figure 32. Graph showing simulated annual change-in-storage for USC sub-basin 1941-1999, Tucson AMA, Arizona.

in 1940 to about 2,800 ac-ft per year in 1999, and was confined to T. 19 S., R. 13 E. Simulated ET along the Pantano, Sabino, and Tanque Verde Creeks also declined, decreasing from about 4,900 ac-ft per year in 1940 to less than 500 ac-ft per year in 1999.

Change in Storage

The total loss of storage during the transient simulation period totaled 6.9 million ac-ft, which is similar to reported estimates of loss of storage during the developed period (ADWR, 1999a). Model simulated storage loss from 1941 to 1999 in the Avra Valley and USC sub-basins was about 2.5 million ac-ft and 4.4 million ac-ft, respectively. This study simulated aquifer storage losses similar to those from Hanson and others (1990) for the Avra Valley sub-basin and Hanson and Benedict (1994) in the USC sub-basin. Simulated storage depletion values for 1941 to 1984 in the Avra Valley sub-basin are: Hanson and others (1990): 3.4 million ac-ft; this study: 2.5 million ac-ft. Simulated storage depletion values for the USC sub-basin from 1941 to 1986 are; Hanson and Benedict (1994): 3.4 million ac-ft; this study: 3.0 million ac-ft.

The transient model generally replicated the historic long-term water level decline, stabilization and recovery observed in the northern and central sections of Avra Valley. The water level declines reflect the period from the 1940s to the early 1970s during which severe overdrafting of the aquifer occurred. Water level recoveries began in the mid to late 1970s as pumpage decreases combined with deep percolation from agricultural recharge, which probably began reaching the water table in large volumes at this time, began reducing the overdraft (Anderson, 1982). Simulated annual storage depletion in the Avra Valley sub-basin followed the general pattern of historic water levels. Simulated annual storage depletions steadily increased from 1941, peaking in the late 1950s at more than 123,000 ac-ft/year, and then remained between 80,00 and 100,000 ac-ft/year throughout the 1960s (Figure 31). Simulated and observed water levels declined through this period reflecting the large annual storage depletion (Appendix C, Hydrographs A through H). The large annual storage depletions began decreasing in 1970, and by the early 1980s, storage depletions in the Avra Valley sub-basin had reversed and the aquifer began recording net surpluses. The trend of increasing aquifer storage in the sub-basin continued until the end of the model simulation in 1999 (Figure 31). The transition from large annual storage depletions to surplus conditions is also reflected in water level hydrographs (Appendix C) and in the increasing boundary flux out of the model as discussed above (Table 13). It should be noted that the change from aquifer depletion to gain is not due to “new” water, but is the result of lagged agricultural recharge being applied to the model.

The USC sub-basin has experienced continual overdraft conditions through the developed period (Figure 32). Annual overdrafts varied through the development period, peaking in the early 1970s, then declined as agricultural development declined before increasing again as municipal demands increased in the 1980s and 1990s. The overdrafts have resulted in long-term drawdowns in most wells in the sub-basin, as can be observed in Hydrographs J through Z in Appendix C. Wells in the floodplain of the Santa Cruz River and its major tributaries generally have smaller overall declines due to stream infiltration during wet periods, for example beginning in the 1980s, or as a result of major flood events (Hydrographs J, X and Y).

The combination of pumpage and incidental recharge greatly altered vertical flow within the model during the developed period. Net vertical flow reversed in both sub-basins from the steady-state to the end of the transient simulation period in 1999. In the USC sub-basin the upward vertical flow between layers 1 and 2 declined by 68 percent and vertical flow from layer 3 to layer 2 increased by 44 percent. The net upward flow from layer 2 to layer 1 during pre-development times reversed going from a net 31,000 ac-ft/year upward to a net downward flow of about 96,000 ac-ft/year (layer 1 to layer 2). Upward vertical flow between layers 2 and 3 also reversed from a net upwards flow of about 10,000 ac-ft/year during the steady-state to a net downward flow of about 72,500 ac-ft/year. The upward vertical flow between layer 1 and 2 inthe Avra Valley sub-basin decreased by over 94 percent between 1940 and 1999, and the net upwards vertical flow went from 2,600 ac-ft/year (layer 2 to layer 1) to a net downward flow of 15,400 ac-ft/year. The net flow between layers 2 and 3 reversed, changing from a net upwards flow of 3,700 ac-ft/year to a net downward flow of 17,900 ac-ft/year. The reversal in both sub-basins may be largely due to the deepening of wells in the in the 1970s and 1980s, which is reflected in the assignment of all pumpage to model layers 2 and 3 after about 1985.

Chapter 6

Sensitivity Analysis

Model Sensitivity

A sensitivity analysis provides a means of evaluating uncertainty that exists in the model inputs. The response of a model to changes in the various input parameters can be used to evaluate the sensitivity of a model solution to a particular model input parameter. The Tucson AMA steady-state and transient calibrations were based, in part, on direct information collected through time, for example water levels and pumpage data, and indirect information that were derived using statistical techniques, estimation, or interpretation. Examples of indirect information include recharge estimates (mountain-front and stream infiltration, agricultural recharge), timing of agricultural recharge (the lag factor), aquifer parameters (hydraulic conductivity, transmissivity and storage values), and boundary conditions (groundwater inflow and outflows). The interpretation of the indirect data introduces a source of uncertainty in the model. Increasing or decreasing the value of these indirect parameters and observing the effect on the model results helps identify parameters that may have measurable impacts on the model simulation.

Sensitivity Procedures

The sensitivity to changes in model input parameters was tested for both the steady-state and transient models using simulated residuals and water budget components as comparison points. Model simulations, called sensitivity runs, were made where only one model input was changed over a reasonable range of values. Changes in simulated residuals and water budget values between a sensitivity run and the final calibrated model runs (both steady-state and transient) provided quantitative measures of the model's sensitivity to an input parameter. The model input parameters that were evaluated for model sensitivity during the steady-state sensitivity analysis were the hydraulic conductivity of Layers 1 and 2, transmissivity of Layer 3, mountain-front recharge, stream recharge, and inflow boundary fluxes. The transient sensitivity analysis consisted of changing the specific yield and the volume of agricultural recharge.

The hydrologic input parameters, their range of variation, and the quantitative measurements for each sensitivity run are presented in Table 14. Measurements used to examine the impact of input change for each sensitivity run include the change in model residuals and selected water budget components. The residuals and water budgets components are grouped separately for presentation in Tables 14a and 14b, respectively. The residual measures examined included the change in ME, MAE, and RMSE between the final model run and a sensitivity run. The simulated water budget parameters that were evaluated include net change in component and the percent of change in the water budget component. Water Budget components evaluated included ET, underflow between the USC and Avra Valley sub-basins, underflow into the model, and underflow out of the model. The value of each budget component should change as heads within the model change in response to changing the input parameters.

Steady-State Sensitivity Analysis

In general, the steady-state model was most sensitive to changes in mountain-front recharge and stream infiltration and least sensitive to changes in boundary conditions along the southern boundary between the Tucson AMA and Santa Cruz AMA. The model was less sensitive to changes in the hydraulic conductivity of Layer 1, changes in the transmissivity of layer 3, and changes in boundary conditions along the Avra – Altar Valley boundary. The model was least sensitive to changes in Layer 2 hydraulic conductivity. Model sensitivities were also found to vary by sub-basin. For example, heads in the Upper Santa Cruz sub-basin were more sensitive to changes in Layer 1 hydraulic conductivities than heads in the Avra Valley sub-basin. This is probably due to the limited extent of layer 1 in the Avra Valley sub-basin. Conversely, heads in the Avra Valley sub-basin were more sensitive to changes in Layer 3 transmissivities and Layer 2 hydraulic conductivities than heads in the USC sub-basin. Sub-basin specific reactions were also observed when the inflow flux across the Santa Cruz AMA and Altar - Avra Valley boundaries were varied. Substituting specified fluxes for the constant heads at the boundaries allowed the model to react to increasing or decreasing flux volumes. Increasing or decreasing inflow volumes generally had the greatest effect on the sub-basin where the flux was varied. Impacts on model heads were largest when the Altar – Avra Valley inflows were changed. Increased boundary inflows from the Santa Cruz AMA were largely taken up by ET in the southern part of the model, which resulted in very small head increases in the USC sub-basin and model-wide.

Transient State

The impact on the transient model results caused by changes in specific yield, agricultural recharge, and pumpage prior to 1960 were analyzed and are presented in Table 14. In general, the model is most sensitive to changes in Layer 1 specific yield and least sensitive to changes in agricultural recharge. The model was only slightly less sensitive to changes in agricultural recharge volume than the Layer 2 specific yield. Simulated heads in the Upper Santa Cruz sub-basin were more sensitive than heads in the Avra Valley sub-basin to changes in Layer 1 specific yield, due to the larger extent of Layer 1 in the USC sub-basin. Conversely, simulated heads in the Avra Valley sub-basin were more sensitive to changes in Layer 2 specific yield, which is the primary aquifer in much of the Avra Valley sub-basin. Model-wide water levels were slightly less sensitive to changes in agricultural recharge and pre-1960 pumpage than to changes in Layer 2 storage values; however, changes in agricultural recharge and pumpage had a larger effect on the change in storage and model outflows than changes in layer 2 storage values. The relative sensitivity of the model water budget to agricultural recharge and pre-1960 pumpage indicates that more research into irrigation efficiency and travel time to the water table for deep percolation of irrigation recharge and better estimates of pre-1960 pumpage may improve the model calibration.

Table 14a. Sensitivity analysis of the steady-state and transient model parameters: change in model residual error (all changes are in feet)..

Hydrologic Parameter	Change Factor	Model Wide Change in Residual			Avra Valley Change in Residual			USC Change in Residual			Layer 1 Change in Residual			Layer 2 Change in Residual			Layer 3 Change in Residual		
		ME	MAE	RMSE	ME	MAE	RMSE	ME	MAE	RMSE	ME	MAE	RMSE	ME	MAE	RMSE	ME	MAE	RMSE
Layer 1 Hydraulic Conductivity	-50%	-4.5	6.9	7.9	-5.4	5.4	5.2	-3.8	8.1	9.4	-4.0	7.8	8.9	-5.3	5.6	5.9	-3.1	4.4	5.8
Layer 1 Hydraulic Conductivity	-25%	-2.0	3.1	3.5	-2.6	2.6	2.5	-1.5	3.5	4.1	-1.6	3.4	4.0	-2.4	2.6	2.7	-1.3	2.0	2.7
Layer 1 Hydraulic Conductivity	+25%	1.5	2.6	3.0	2.3	2.3	2.2	0.8	2.7	3.4	1.1	2.8	3.3	2.1	2.2	2.3	1.3	1.9	2.7
Layer 1 Hydraulic Conductivity	+50%	2.7	4.8	5.5	4.4	4.4	4.0	1.3	5.0	6.1	1.8	5.1	6.1	4.0	4.3	4.2	2.1	3.5	4.9
Layer 2 Hydraulic Conductivity	-50%	3.9	5.2	7.5	6.9	8.0	9.3	1.6	3.1	4.5	1.2	2.9	4.1	8.0	8.8	9.5	2.7	3.8	7.3
Layer 2 Hydraulic Conductivity	-25%	1.6	2.2	3.1	2.8	3.2	3.6	0.7	1.5	2.2	0.6	1.3	2.0	3.3	3.6	3.7	0.9	1.7	3.0
Layer 2 Hydraulic Conductivity	+25%	-1.3	1.8	2.4	-2.2	2.4	2.6	-0.7	1.4	2.0	-0.5	1.2	1.7	-2.3	2.8	2.8	-0.5	1.1	2.4
Layer 2 Hydraulic Conductivity	+50%	-2.5	3.4	4.3	-4.0	4.3	4.5	-1.3	2.7	3.8	-1.1	2.4	3.4	-4.6	4.9	4.8	-1.0	2.2	4.1
Layer 3 Transmissivity	-50%	-5.2	6.3	7.0	-11.3	12.0	6.0	0.5	1.9	3.0	-2.1	3.3	5.2	-9.8	10.9	6.8	-3.5	6.5	8.2
Layer 3 Transmissivity	-25%	-2.6	3.0	3.3	-5.5	5.8	2.8	-0.4	0.9	1.5	-1.1	1.6	2.5	-4.8	5.2	3.2	-1.7	3.0	3.9
Layer 3 Transmissivity	+25%	2.4	2.8	3.0	5.0	5.2	2.4	0.3	0.9	1.5	1.0	1.5	2.3	4.5	4.8	2.7	1.7	2.7	3.5
Layer 3 Transmissivity	+50%	4.6	5.4	5.8	9.8	10.0	4.4	0.7	1.8	3.0	1.9	2.9	4.4	8.7	9.2	5.2	3.3	5.1	6.6
Input Parameter																			
Stream Recharge	-50%	-25.5	25.5	11.6	-24.4	24.4	12.3	-26.3	26.3	11.0	-26.0	26.0	10.1	-24.7	24.7	13.5	-18.8	18.8	13.3
Stream Recharge	-25%	-11.8	11.8	6.1	-13.0	13.0	6.4	-10.8	10.8	5.8	-11.2	11.2	6.1	-12.6	12.6	6.5	-8.8	8.8	6.6
Stream Recharge	+25%	10.2	10.2	4.9	11.3	11.3	5.1	9.4	9.4	4.6	9.7	9.7	4.7	11.0	11.0	5.2	7.9	7.9	5.8
Stream Recharge	+50%	17.6	17.6	8.0	19.6	19.6	8.7	16.2	16.2	7.1	16.8	16.8	7.3	18.9	18.9	8.8	13.7	13.7	9.4
Mountain-Front Recharge	-50%	-23.3	23.3	10.8	-20.7	20.7	9.5	-25.3	25.3	11.3	-24.7	24.7	10.8	-21.3	21.3	10.5	-18.4	18.4	11.1
Mountain-Front Recharge	-25%	-10.8	10.8	5.5	-10.5	10.5	4.8	-11.1	11.1	5.9	-10.9	10.9	5.6	-10.7	10.7	5.3	-8.4	8.4	5.4
Mountain-Front Recharge	+25%	9.7	9.7	4.7	9.7	9.7	4.2	9.7	9.7	5.1	9.6	9.6	4.9	9.8	9.8	4.5	7.6	7.6	5.1
Mountain-Front Recharge	+50%	16.4	16.4	7.6	17.0	17.0	7.0	15.9	15.9	8.0	15.9	15.9	7.7	17.0	17.0	7.5	13.1	13.1	8.4
Boundary Conditions																			
Scama Specified Flux	+20%	0.2	0.2	0.5	0.0	0.0	0.0	0.4	0.4	0.6	0.3	0.3	0.5	0.0	0.0	0.2	0.3	0.3	0.6
Scama Specified Flux	+10%	0.0	0.1	0.3	0.0	0.0	0.0	0.1	0.1	0.4	0.1	0.1	0.4	0.0	0.0	0.0	0.1	0.1	0.3
Scama Specified Flux	-10%	-0.8	0.8	1.3	0.0	0.0	0.2	-1.3	1.3	1.5	-1.1	1.1	1.5	-0.2	0.2	0.6	-0.7	0.7	1.2
Scama Specified Flux	-20%	-1.3	1.3	2.2	-0.1	0.1	0.2	-2.2	2.2	2.5	-1.9	1.9	2.5	-0.3	0.3	0.9	-1.2	1.2	2.04
Altar Valley Specified Flux	+20%	6.3	6.3	8.2	13.9	13.9	7.4	0.6	0.6	1.4	1.7	1.7	3.2	13.5	13.5	8.5	11.7	11.7	11.7
Altar Valley Specified Flux	+10%	3.3	3.3	4.3	7.2	7.2	3.9	0.3	0.3	0.8	0.9	0.9	1.7	7.0	7.0	4.4	6	6.1	6.0
Altar Valley Specified Flux	-10%	-2.6	2.6	3.5	-5.9	5.9	3.1	-0.2	0.2	0.6	-0.7	0.7	1.4	-5.7	5.7	3.6	-5.1	5.13	5.29
Altar Valley Specified Flux	-20%	-5.5	5.5	7.3	-12.3	12.3	6.5	-0.5	0.5	1.1	-1.5	1.5	3.0	-11.9	11.9	7.5	-11.3	11.33	11.6
Hydrologic Parameters																			
Layer 1 Specific Yield	+50%	8.9	3.6	2.5	3.2	2.1	0.9	10.5	2.9	3.1	9.1	1.3	2.6	9.9	2.0	1.2	5.8	4.2	5.2
Layer 1 Specific Yield	+25%	4.8	1.4	1.1	1.7	1.3	0.7	5.7	1.4	1.4	7.1	-0.4	0.7	5.0	0.7	0.8	3.0	2.2	2.6
Layer 1 Specific Yield	-25%	-3.9	-0.2	-0.1	-1.7	-0.7	-0.1	-4.8	0.0	-0.3	0.0	-2.7	-5.1	-5.1	-0.7	-0.9	-4.4	-0.1	-0.6
Layer 1 Specific Yield	-50%	NA	NA	NA	NA	NA	NA	NA	NA	NA	NA	NA	NA	NA	NA	NA	NA	NA	NA
Layer 2 Specific Yield	+50%	4.8	1.3	0.4	7.0	5.4	2.6	4.2	0.1	-0.3	3.1	0.5	1.1	5.8	-0.2	-0.7	4.2	1.9	0.7
Layer 2 Specific Yield	+25%	2.8	0.8	0.4	4.0	3.2	1.6	2.4	0.1	0.0	3.1	0.1	1.4	2.9	0.1	0.0	2.2	1.0	0.2
Layer 2 Specific Yield	-25%	-2.4	-0.9	-0.9	-5.0	-2.4	-0.5	-1.7	-0.5	-0.7	1.3	-2.5	-6.3	-2.5	-0.5	-0.3	-3.5	-0.4	0.3
Layer 2 Specific Yield	-50%	NA	NA	NA	NA	NA	NA	NA	NA	NA	NA	NA	NA	NA	NA	NA	NA	NA	NA
Ag Recharge	+20%	3.3	1.6	1.5	7.3	5.8	3.5	2.1	0.3	0.5	1.4	-0.9	-1.1	2.6	0.9	0.9	4.3	2.1	3.0
Ag Recharge	-20%	-2.6	-0.6	-0.7	-7.7	-2.9	-1.2	-1.1	0.0	-0.3	2.3	-2.0	-5.4	-2.2	0.5	0.7	-3.9	-1.9	-1.4
Pumpage - 1941-1960	+25%	-3.3	-1.5	-2.1	-6.8	-2.6	-0.9	-2.3	-1.2	-2.1	0.8	-2.4	-5.8	-2.6	-1.4	-1.9	-4.6	-0.8	-1.1
Pumpage - 1941-1960	-25%	4.6	1.9	1.8	6.7	5.1	3.1	4.0	1.0	1.3	5.0	-0.5	-0.3	4.4	0.7	1.4	3.8	2.8	2.8

Notes:

1) residual and water budget changes are calculated as sensitivity simulation values minus calibrated simulation values.

Table 14b. Sensitivity analysis of the steady-state and transient model parameters: Model water budget changes (all units in acre-feet/year, transient values use final model year - 1999)

		Inflows:						Outflows:					
		Underflow into Model				Underflow Between		ET		Underflow out of Model		Cumulative	
Hydrologic	Change	From SCAMA		From Altar Valley		USC and Avra Valley				into Pinal AMA		Change in Storage	
Parameter	Factor	Change	% Change	Change	% Change	Change	% Change	Change	% Change	Change	% Change	Change	% Change
Layer 1 Hydraulic Conductivity	-50%	-2,903	-32.1%	9	0.1%	-2,846	-20.9%	789	6.8%	-3,695	-18.5%	NA	NA
Layer 1 Hydraulic Conductivity	-25%	-1,471	-16.3%	4	0.0%	-1,410	-10.4%	408	3.5%	-1,880	-9.4%	NA	NA
Layer 1 Hydraulic Conductivity	+25%	1,540	17.0%	-4	0.0%	1,380	10.1%	-386	-3.3%	1,924	9.7%	NA	NA
Layer 1 Hydraulic Conductivity	+50%	3,134	34.7%	-7	-0.1%	2,713	19.9%	-774	-6.7%	3,904	19.6%	NA	NA
Layer 2 Hydraulic Conductivity	-50%	-1,489	-16.5%	-2,921	-31.0%	-3,705	-27.2%	1,347	11.7%	-5,767	-28.9%	NA	NA
Layer 2 Hydraulic Conductivity	-25%	-743	-8.2%	-1,414	-15.0%	-1,885	-13.9%	662	5.7%	-2,826	-14.2%	NA	NA
Layer 2 Hydraulic Conductivity	+25%	740	8.2%	1,367	14.5%	1,931	14.2%	-634	-5.5%	2,753	13.8%	NA	NA
Layer 2 Hydraulic Conductivity	+50%	1,482	16.4%	2,710	28.8%	3,913	28.8%	-1,227	-10.6%	5,426	27.2%	NA	NA
Layer 3 Transmissivity	-50%	-686	-7.6%	-2,294	-24.4%	-1,379	-10.1%	697	6.0%	-3,675	-18.4%	NA	NA
Layer 3 Transmissivity	-25%	-342	-3.8%	-1,143	-12.1%	-677	-5.0%	337	2.9%	-1,821	-9.1%	NA	NA
Layer 3 Transmissivity	+25%	339	3.8%	1,121	11.9%	653	4.8%	-314	-2.7%	1,781	8.9%	NA	NA
Layer 3 Transmissivity	+50%	675	7.5%	2,221	23.6%	1,283	9.4%	-609	-5.3%	3,510	17.6%	NA	NA
Input Parameter													
Stream Recharge	-50%	651	7.2%	157	1.7%	-4,288	-31.5%	-10,102	-87.7%	-6,087	-30.6%	NA	NA
Stream Recharge	-25%	287	3.2%	83	0.9%	-2,005	-14.7%	-5,809	-50.4%	-3,291	-16.5%	NA	NA
Stream Recharge	+25%	-255	-2.8%	-90	-1.0%	1,553	11.4%	6,904	59.9%	2,983	15.0%	NA	NA
Stream Recharge	+50%	-456	-5.0%	-179	-1.9%	2,476	18.2%	14,209	123.3%	5,273	26.5%	NA	NA
Mountain-Front Recharge	-50%	994	11.0%	294	3.1%	-3,517	-25.8%	-8,970	-77.8%	-4,690	-23.5%	NA	NA
Mountain-Front Recharge	-25%	453	5.0%	152	1.6%	-1,845	-13.6%	-4,936	-42.8%	-2,393	-12.0%	NA	NA
Mountain-Front Recharge	+25%	-345	-3.8%	-162	-1.7%	1,577	11.6%	5,901	51.2%	2,270	11.4%	NA	NA
Mountain-Front Recharge	+50%	-645	-7.1%	-317	-3.4%	2,632	19.3%	12,173	105.6%	4,009	20.1%	NA	NA
Boundary Conditions													
Scama Specified Flux	No Change	27	0.3%	1	0.0%	-4	0.0%	504	4.4%	-4	0.0%	NA	NA
Scama Specified Flux	+20%	1,818	20.1%	0	0.0%	5	0.0%	2,206	19.1%	6	0.0%	NA	NA
Scama Specified Flux	+10%	907	10.0%	0	0.0%	1	0.0%	1,299	11.3%	2	0.0%	NA	NA
Scama Specified Flux	+30%	2,717	30.1%	0	0.0%	7	0.1%	3,113	27.0%	8	0.0%	NA	NA
Scama Specified Flux	-10%	-892	-9.9%	1	0.0%	-15	-0.1%	-505	-4.4%	-14	-0.1%	NA	NA
Scama Specified Flux	-20%	-1,801	-19.9%	1	0.0%	-25	-0.2%	-1,403	-12.2%	-23	-0.1%	NA	NA
Altar Valley Specified Flux	No Change	0	0.0%	-4	0.0%	-4	0.0%	3	0.0%	89	0.4%	NA	NA
Altar Valley Specified Flux	+20%	0	0.0%	1,883	20.0%	-75	-0.6%	76	0.7%	1,896	9.5%	NA	NA
Altar Valley Specified Flux	+10%	0	0.0%	972	10.3%	-39	-0.3%	40	0.3%	994	5.0%	NA	NA
Altar Valley Specified Flux	-10%	0	0.0%	-942	-10.0%	31	0.2%	-31	-0.3%	-816	-4.1%	NA	NA
Altar Valley Specified Flux	-20%	0	0.0%	-1,883	-20.0%	63	0.5%	-62	-0.5%	-1,723	-8.6%	NA	NA
Hydrologic Parameters													
Layer 1 Specific Yield	+50%	-780	-4.7%	0	0.0%	175	1.1%	238	6.7%	1,994	12.9%	-243,058	4.2%
Layer 1 Specific Yield	+25%	-401	-2.4%	0	0.0%	52	0.3%	24	0.7%	1,005	6.5%	-135,341	2.3%
Layer 1 Specific Yield	-25%	469	2.8%	0	0.0%	-311	-1.9%	-309	-8.6%	-971	-6.3%	126,733	-2.2%
Layer 1 Specific Yield	-50%	NA	NA	NA	NA	NA	NA	NA	NA	NA	NA	NA	NA
Layer 2 Specific Yield	+50%	-199	-1.2%	0	0.0%	-179	-1.1%	144	4.0%	946	6.1%	-169,361	2.9%
Layer 2 Specific Yield	+25%	-66	-0.4%	0	0.0%	-71	-0.4%	12	0.3%	528	3.4%	-105,897	1.8%
Layer 2 Specific Yield	-25%	131	0.8%	0	0.0%	-25	-0.2%	-321	-9.0%	-610	-4.0%	121,550	-2.1%
Layer 2 Specific Yield	-50%	NA	NA	NA	NA	NA	NA	NA	NA	NA	NA	NA	NA
Ag Recharge	+20%	-416	-2.5%	0	0.0%	-55	-0.3%	95	2.7%	1,593	10.3%	524,218	-9.0%
Ag Recharge	-20%	506	3.1%	0	0.0%	-475	-2.9%	-91	-2.5%	-1,460	-9.5%	-545,725	9.3%
Pumpage - 1941-1960	+25%	254	1.5%	0	0%	56	0.3%	-199	-5.6%	-1,783	-11.6%	-701,169	12.0%
Pumpage - 1941-1960	-25%	-126	-0.8%	0	0%	-135	-0.8%	-41	-1.1%	1,972	12.8%	661,372	-11.3%

Notes: 1). The model solution would not converge when the specific yield as decreased by 50% in Layers 1 and 2.

2). A negative value in the Cumulative Change in Storage column indicates that the net loss of storage increased and a positive value indicates the net loss of storage decreased.

Chapter 7

Base Case Future Model Simulation

Introduction

One of the main purposes for updating the Tucson AMA groundwater flow model is to provide a decision making tool for developing long-term water resource planning and management strategies. Future development in the Tucson AMA is tied to a limited resource, groundwater in the regional aquifer and imported CAP surface water; therefore, it is important that water resource managers understand the impact on the aquifer from water management decisions. To utilize the model as a predictive tool, the ADWR modeling and Tucson AMA staff worked with local water providers to develop basic water demand and supply estimates for the period 2000 to 2025, the time when the Tucson AMA is scheduled to achieve "Safe Yield".

The usefulness and validity of the predictive model simulations are tied to developing realistic and reliable water supply and demand assumptions. To start the process of developing the information necessary to run the model out to 2025, the Tucson AMA staff began researching future water use projections through meetings with water providers and other selected agencies. The Tucson AMA staff organized individual interviews and small group meetings with municipal water providers and large industrial and agricultural water users to obtain their estimates on the quantity, timing, and sources of future water demand. The major water providers that supplied information for the base case scenario are listed in Table 15. Other smaller providers and users were interviewed and provided information. For ease in planning, the 2000-2025 model projection period was broken down into five, 5-year stress periods. Information from the meetings and additional staff research was compiled into a series of spreadsheets detailing future supply and demand projections. This data provided the model stresses used in the "Base Case" water use scenario for the time period 2000 - 2025.

The future projection stresses were appended to the transient period stresses (1941 – 1999) and a model simulation was run from 1941 to 2025. The result of the model simulation is a set of predicted water levels in the regional aquifer at five-year increments from 2000 to 2025 and model water budgets from 2000 to 2005. The predicted water level changes reflect the impact of the water management assumptions that went into the 2000 – 2025 supply and demand data. Projected water level changes from 2000 to 2025 are calculated by subtracting to 1999 simulated heads from the 2025 simulated heads.

Base Case Water Demands

Each water provider or agency was asked to provide estimates of their future water demands, the timing of their demands, and the source of the water to supply their projected demands. The assumptions used by each water provider varied depending on their size, projected future demands, access to CAP or other renewable water supplies, and whether they supplied water to the municipal, industrial, or the agricultural sector. However, a number of generalized assumptions were used to simplify the model data sets necessary to run the predictive scenario. Those general assumptions are discussed below.

Well Pumpage Distribution

Future well pumpage for water providers was spread among existing wells based on multi-year averages for each well's contribution to the provider's total pumpage. Some providers were able to supply information on future well locations; however, most were unable to provide this information. When future well locations were not available, future demand in excess of existing well capacity was assigned to the same well. The assumption being that new capacity would be met by either deepening existing wells or by developing a new well in the same model cell.

Table 15. Water providers in the Tucson AMA participating in developing the Base Case projection data

Industrial Sector:	Municipal Sector:	Agricultural Sector:
ASARCO-Mission	AZ State Prison	Cortaro-Marana Irrigation District
ASARCO-Silverbell	Davis-Monthath AFB	Farmers Investment Company
Phelps-Dodge	University of Arizona	Avra Valley Irrigation District
Tucson Electric Power	AZ Water Company	
	Avra Water Company	
	Community Water Company	
	Eagle C.R. Water Company	
	Farmers Water Company	
	Forty-Niner Water Company	
	Flowing Wells Irrigation District	
	G.V. Water Company	
	Lago del Oro Water Company	
	Las Q.S. Water Company	
	Marana Water District	
	MDWID & Hub (Metro)	
	Native American domestic needs	
	Queen Creek Water Company	
	R. Sahuarita	
	Ray Water Company	
	Ridgeview Water Company	
	Spanish Trail Water Company	
	Thim U. & W.C.	
	Town of Marana	
	Town of Oro Valley	
	Tucson Water	
	Vail	
	Voyager Water Company	

Municipal Water Demand

The method for projecting future municipal sector water demand varied depending on the individual municipal provider. Water demand was tied to population growth rates and expected water use based on gallons per day per capita (GPCD) from the Tucson AMA Third Management Plan (TMP). Expected population growth for municipal providers came from a variety of sources. In many cases expected growth rates developed by the providers were used in the Base Case. In other cases, future water demands were based on information filed with applications for Assured Water Supply Designations or Certificates. Population growth estimates based on the TMP or based on staff judgments were used in other cases. Figure 33 is a graph of Base Case population growth developed in the model area, which is expected to increase from the current 850,000 people to about 1.5 million people by 2025.

Agricultural Water Demand

Agricultural water demand for the projection period is based on estimates made for the TMP. In the TMP, demand from large agricultural users is based on a projected reduction of irrigated acres by 50 percent between 1995 and 2025, and a slight increase in utilization rate over that time period. The model projections were modified from the initial TMP estimates based on discussions with agricultural interests, past usage patterns, staff judgments, and projected urbanization trends. It was assumed that most small agricultural water users will go out of business due to economics and urbanization pressures. The projected total agricultural water demand for the Base Case projection and the sources of water supplies are presented in Figure 34. Total agricultural water use is expected to decrease by about 45 percent during the Base Case projection period, with groundwater use expected to decrease by 47 percent as CAP water gradually replaces groundwater.

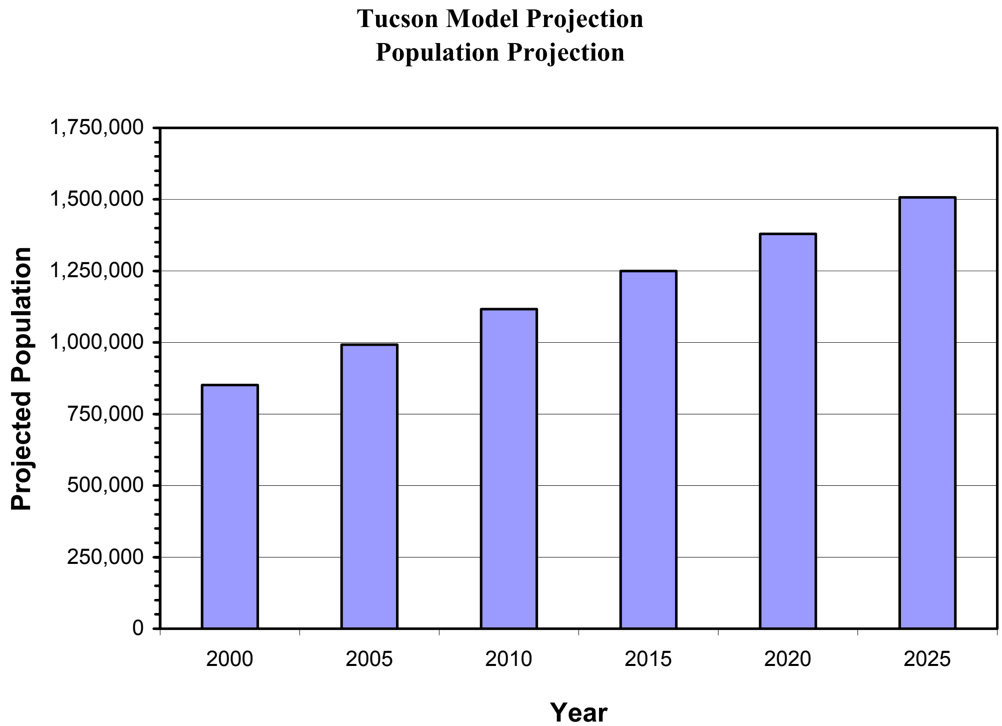

Figure 33. Projected population for Tucson AMA model area, 2000 – 2025.

Industrial Water Demand

Metal ore mining is one of the primary industrial water uses in the Tucson AMA. Water demand projections were provided by mining representatives and were based on economic and business projections. The economic projections are based on the world metals prices, which are very volatile and can fluctuate rapidly. As a result, the water use projections from the mining companies, while reasonable for the economic conditions when they were developed, are a best guess of future conditions in the mining industry. Future water demands for the existing mining facilities were developed based on the ore production projections and the assumption that water use is directly proportional to ore extraction. In the Base Case, ASARCO is expecting to be utilizing approximately 8,000 ac-ft of CAP water by 2004. Phelps-Dodge has expressed an interest in using CAP water, though due to their location, may not be able to develop necessary infrastructure to utilize CAP water. Phelps-Dodge expects to continue to rely on groundwater to meet its water demand for the Base Case projection.

Electrical power generation is another large industrial water demand in the AMA and water use projections for Tucson Electric Power were developed from meetings with company representatives. Water demand for other industrial users, such as sand and gravel mines, were developed based on past use histories and expected growth trends.

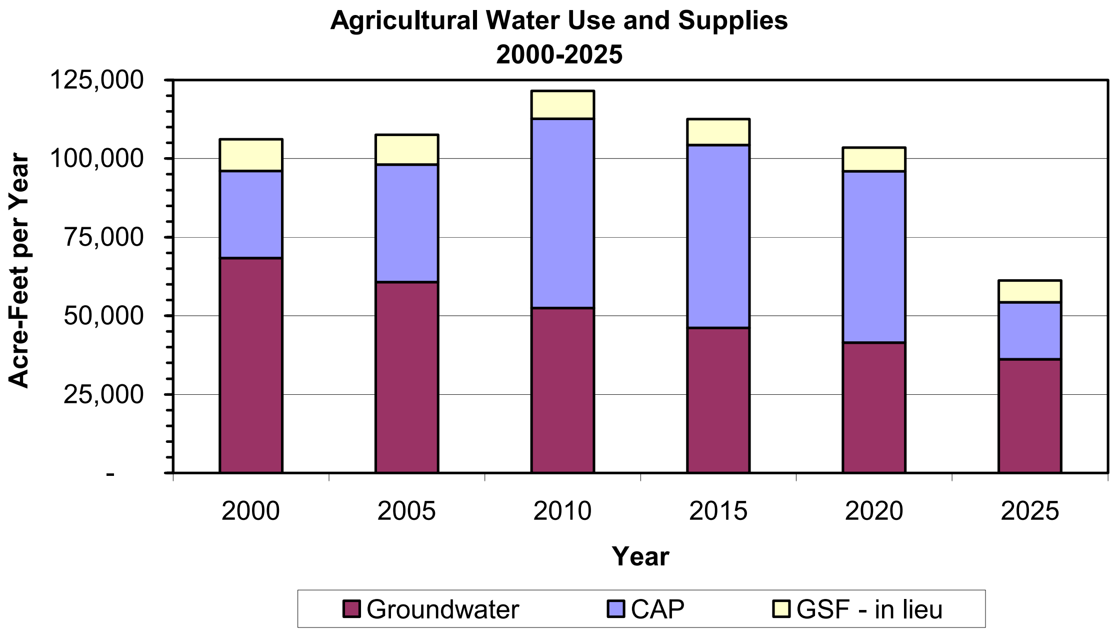

Figure 34. Projected future agricultural water use and supply sources, 2000 – 2025.

Miscellaneous Water Demands

There are many small water users that are not specifically addressed in the Base Future Water Demand projection. These include small water providers, small industrial users, and many small agricultural operations. The future water demand for these small users was assumed to remain constant throughout the projection period, with the exception of the agricultural users. Their demand was phased out as described above. An analysis of past trends in this small provider class supported flat-lining the demands from many of the small providers.

Base Case Water Supplies

Water supplies for the Base Future Water Demand projection included groundwater, CAP surface water, and treated effluent. The future projection assumed that there would be no transfer of water rights from one holder to another. This means that water-users with the right to pump groundwater would continue to withdraw groundwater to serve their own facilities or service area.

CAP Surface-water

Renewable surface-water supplies provided by the CAP are an important component of future projection water supplies. The total renewable supply used in the projection stress periods is the sum of all designated and certificated replenishment obligations for each stress period. Replenishment water is assumed to be CAP surface-water, except for the limited displacement of CAP use through the marketing of effluent credits earned on the Santa Cruz River. CAP surface-water is assumed to be available through recovery from various existing recharge facilities listed in Table 16. No direct delivery of CAP water for municipal use is anticipated in the Base Case projection.

Table 16. Permitted recharge projects in the Tucson AMA.

Permit Type	Project Name and Description	Permit Holder
Underground Storage Facility	Sweetwater Wastewater Treatment Plant: effluent recharge project	City of Tucson
Underground Storage Facility	Santa Cruz Managed Recharge Facility: effluent recharge project	City of Tucson/U.S. Bureau of Reclamation
Underground Storage Facility	Lower Santa Cruz Replenishment Project: CAP surface-water recharge project	Central Arizona Water Conservation District (CAWCD)
Underground Storage Facility	Central Avra Valley Storage and Recovery Project (CAVSARP)	City of Tucson
Underground Storage Facility	Marana High Plains Effluent Recharge Project: effluent recharge project	Pima County Flood Control District
Underground Storage Facility	Avra Valley Recharge Project: CAP surface-water recharge project	CAWCD
Underground Storage Facility	Pima Mine Road Recharge Project: CAP surface-water recharge project	CAWCD
Underground Storage Facility	Robson Ranch Quail Creek: effluent recharge project	Robson Ranch Quail Creek
Groundwater Savings Facility	In Lieu recharge of CAP surface-water to CMID lands	Cortaro-Marana Irrigation District)
Groundwater Savings Facility	In Lieu recharge of CAP surface-water to BKW & Milewide farms	CAWCD
Groundwater Savings Facility	In Lieu recharge of CAP surface-water to Kai farms in Picacho	Herb Kai
Groundwater Savings Facility	In Lieu recharge of CAP surface-water to Avra Valley Irrigation District (AVID)	Herb Kai
Groundwater Savings Facility	In Lieu recharge of CAP surface-water to Farmers Investment Company (FICO)	FICO

The location of CAP recharge facilities was limited to those present in the year 2000, assuming that their total capacity was not a limiting factor. CAP water use by Groundwater Saving Facilities (GSFs) followed assumptions regarding a facilities ability and willingness to receive CAP water in-lieu of pumping groundwater. As GSFs are typically cheaper to operate than Underground Storage Facilities (USFs), all available GSF capacity was used in the future projection. The remaining recharge was spread proportionally among the USFs based on capacity. All USFs, except Tucson Water's Clearwater Facility, were assigned an equal percentage of capacity in a stress period. The Clearwater facility received additional renewable CAP supplies that Tucson Water projects to have available for recharge. The estimated volume of renewable water available in the future was beyond the Clearwater facility's current capacity, so it was assumed that the facilities capacity would be expanded to meet the estimated available CAP water. For modeling purposes it was assumed that the impact to the aquifer of long-term versus short-term credits and from losses was negligible for all recharge projects. In the Base Case projection the annual volume of renewable CAP surface water available for recharge is expected to reach about 100,000 ac-ft by 2025 (Figure 35).

The Arizona Water Bank was projected to run through 2016 before exhausting its available funding sources. The assumption is based on estimated incentive prices and storage cost fees that were estimated from groundwater withdrawal fees of $2.50 per ac-ft and ad valorem property taxes, which include $3.5 million in the Bank's account and a tax rate of 0.7 mills per year. Incentive prices and storage fees were averaged for each stress period based on projected future costs (ADWR, Projected CAGRD Obligations and Advanced Replenishment Costs). The model assumed that none of the water stored by the Bank is recovered during the projection period.

Effluent

Reuse of effluent will be an important component of future water supplies, and effluent production and use are important components of the base water demand projections. Historic effluent release data for the Pima County and other smaller outlying wastewater treatment facilities (WWTF) were obtained from Pima County staff in order to estimate future production. Volumetric release data, discharge location, and service area for the following WWTF's were included in the effluent analysis: Ina Road, Rogers Road, Arivaca Junction, Avra Valley, Corona de Tucson, Desert Museum, Fairgrounds, Green Valley, La Puerta del Norte, Marana, Mt. Lemon, and Rillito Vista. The historic release data were analyzed and compared to Tucson AMA population figures and an effluent generation value of 79 gallons per person per day was calculated. A net annual effluent discharge per facility was calculated based on projected population, the effluent generation figure, and subtracting out estimated effluent reuse by each facility. Facilities producing less than 100 ac-ft per yr were not included in developing the net effluent discharge estimates.

The Ina and Rogers Road WWTFs (Figure 1) effluent releases were analyzed differently because they are the only facilities that do not have a contained location for their discharges. Effluent recharge was applied at the discharge location for the other WWTFs. The Ina and Roger Road facilities discharge directly into the channel of the Santa Cruz River. The effluent discharge supports flows in the river channel that can persist to the Tucson AMA border and beyond into the Pinal AMA. To determine how future effluent releases may affect the aquifer, an estimate of effluent recharge per river mile was developed based on similar work done for the transient (1941 – 1999) model simulation. See Chapter 5 for an explanation of how the distribution of historic effluent releases was developed. Using an infiltration rate per mile approach developed for the transient period allowed the length of river channel receiving effluent to vary annually with the estimated volume of effluent generated. The technique predicted that some effluent would continue to leave the Tucson AMA, which has been observed in the past.

Storage of effluent in the future depends on permits issued for storage along the Santa Cruz River and in other managed wetlands projects. The projections did not include any specific assumptions about permitted recharge projects, managed versus constructed, along the section of the Santa Cruz River downstream of the Ina Road and Rogers Road WWTF's. The Base Case future scenario assumes that recovery wells are limited to their present locations. However, more recovery wells may be constructed along the Santa Cruz River north of Rogers Road. The model assumes that the Santa Cruz Managed Recharge Project, located between Ina and Rogers Roads, and the Sweetwater effluent recharge project are both used to capacity after 2000. Storage of effluent remained constant at about 15,000 ac-ft annually for the Base Case projection.

Water providers with Assured Water Supply (AWS) designations are required to meet renewable supply obligations. Tucson AMA staff prepared estimates for those providers who were unable to supply detailed renewable supply plans for the projection period. Pumped groundwater was assigned to those providers, up to their mined groundwater allotments, then renewable water was assigned to make up any shortfall in projected demand.

Average replenishment rates for each of the five stress periods were used for certificated developments rather than predict specific percentages for each provider in each stress period. During the projection period all new developments were assumed to be certified and to have a replenishment obligation. For each projection stress period it was assumed that only the minimum replenishment obligation would be met. The replenishment schedule starts at 20 percent in 2000 and increases each year until 2015, when the obligation reaches 100 percent. However, since demand is growing each year the actual obligation would be greater than the averages calculated for the first three stress periods. Therefore, it was decided to increase the replenishment averages to reflect larger populations in the later years of each stress period. The revised replenishment obligations for the first three stress periods are 30 percent, 50 percent, and 65 percent, respectively.

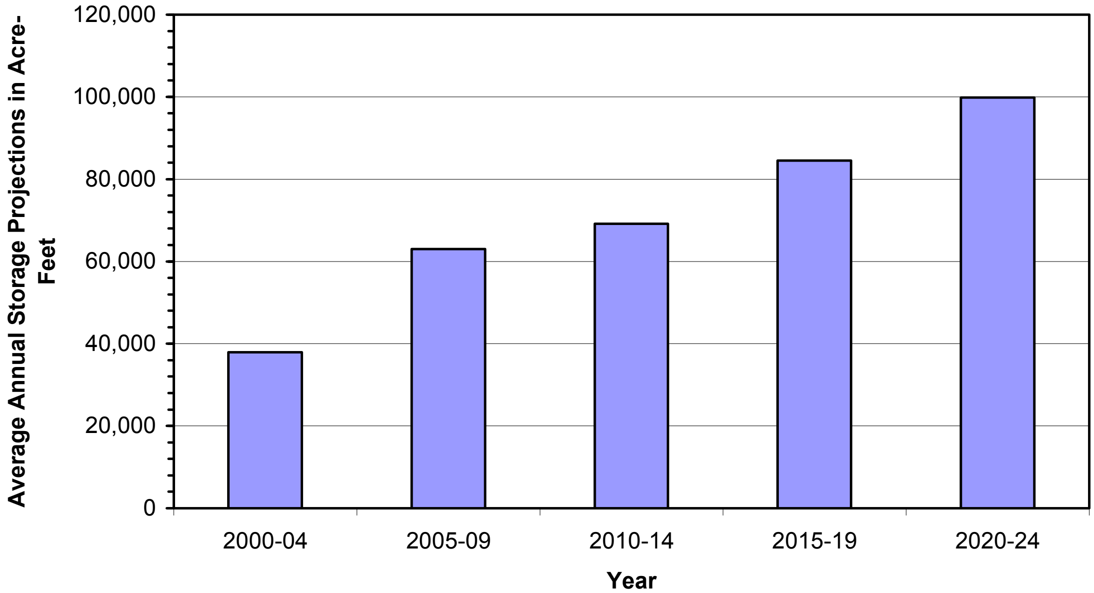

Figure 35. Annual CAP surface-water recharge allocations (recharge and In Lieu use) by stress period for the Base Case projection.

Base Case Future Scenario Predictions

Using information supplied by water providers, which ranged from general supply assumptions to specific withdrawal information, the AMA staff developed supply and demand data for the Base Case future water use scenario for 2000 – 2025. The Base Case model water budget reflects increasing utilization of renewable CAP water supplies and reuse of effluent to meet demand through the first 15 years of the projection period time. Overall demand declines through this period. During the last 10 years of the projection period the amount of non-renewable groundwater used to meet demand increases as the renewable supplies reach their limits. The Base Case simulation results are presented as water level change maps in Figure 36 and the water budget is presented in Table 17.

Water Budget

The 2000-2025 Base Case model water budget reflects the response of the regional aquifer system to the increased utilization of renewable CAP water supplies. The Base Case model water budget indicates that for the 2000 – 2025 projection period the Tucson AMA regional aquifer will have an overall cumulative decrease in storage of approximately 592,800 ac-ft (Table 17). The AMA-wide annual storage depletions decline sharply as renewable water supply use is implemented in 2000, and by 2011, overdrafts are projected to be between 14,000 and 15,000 ac-ft per year. Annual storage losses remain about 15,000 ac-ft until after 2020, increasing to about 20,000 ac-ft per year for the final 5 years of the projection period (Table 17). Although AMA-wide the model projects a net loss in storage for the projection period, the Avra Valley sub-basin is projected to continue to record positive aquifer storage changes. The projected change in aquifer storage for each sub-basin is presented in Figures 36 and 37. The net increase in aquifer storage recorded in the 1980s and 1990s in the Avra Valley sub-basin is expected to continue through the projection period (Figure 36). The net increase in storage for the Avra Valley sub-basin ranges from 5,000 ac-ft/year to about 25,000 ac-ft/year during the projection period and totals 453,000 ac-ft. The USC sub-basin is expected to continue to experience a net loss of storage throughout the projection period. The net storage depletion in the USC sub-basin decreases to about 40,000 ac-t per year and generally remains at that level for the duration of the projection period. The net storage depletion for the USC sub-basin totals just over 1,000,000 acre-feet for the Base Case simulation.

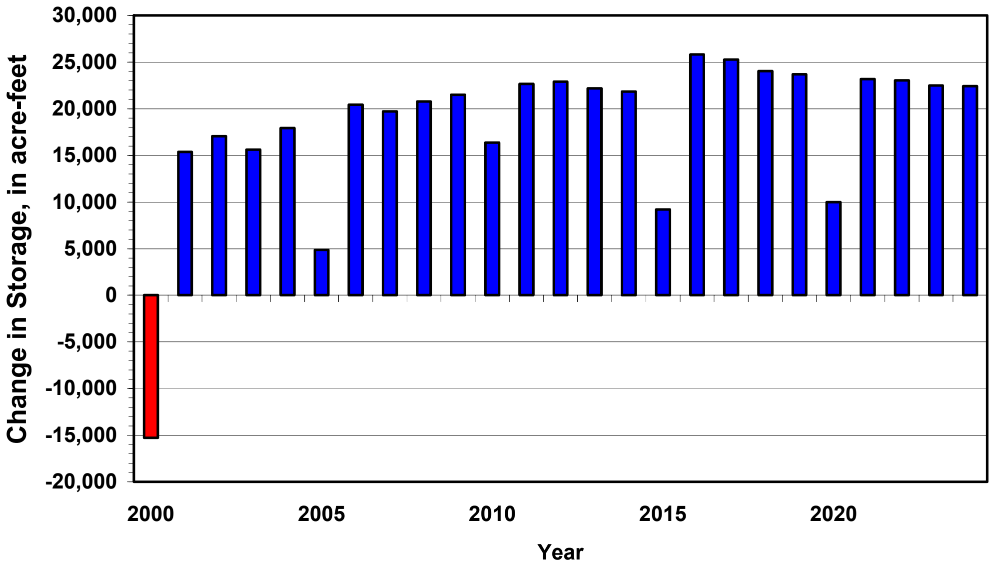

Figure 36. Annual projected change in storage 2000 - 2025, Avra Valley sub-basin, Tucson AMA, Arizona

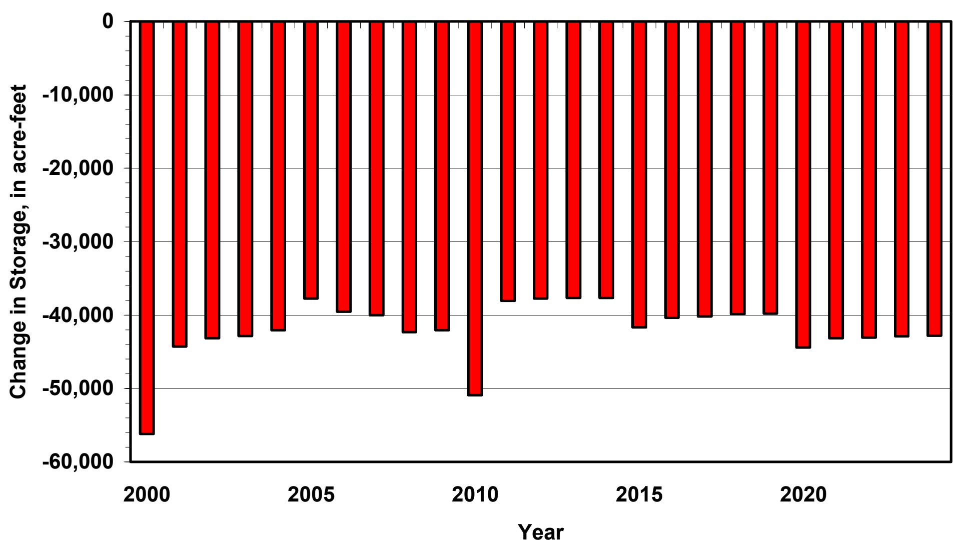

Figure 37. Annual projected change in storage 2000 - 2025, USC sub-basin, Tucson AMA, Arizona

Table 17. Annual simulated model water budget 2000 - 2024 for the Base Case projection, Tucson AMA.

Year	Specified Mountain-Front Recharge	Specified Stream Infiltration	Incidental Recharge	Constant Head Inflow	Altar Valley Inflow	Canada del Oro Inflow	Total Water Budget Inflows	Constant Head Out	Pumpage Out of Model	ET	Total Water Budget Outflows	Annual Change In Storage	Cummulative Change In Storage
2000	34,445	49,770	95,133	23,737	10,273	20	213,358	16,614	263,847	3,042	283,502	-70,161	-70,161
2001	34,445	49,770	137,470	23,522	10,273	20	255,479	18,022	263,147	3,151	284,321	-28,850	-99,011
2002	34,445	49,770	140,566	23,596	10,273	20	258,650	18,596	262,704	3,141	284,440	-25,799	-124,810
2003	34,445	49,770	139,068	23,671	10,273	20	257,226	18,923	262,451	3,120	284,494	-27,261	-152,071
2004	34,445	49,770	142,381	23,751	10,273	20	260,619	19,237	262,093	3,095	284,425	-23,806	-175,877
2005	34,445	49,770	143,049	23,948	10,273	20	261,485	19,389	273,855	3,061	296,304	-34,824	-210,701
2006	34,445	49,770	159,541	24,206	10,273	20	278,234	19,643	273,757	3,026	296,426	-18,191	-228,892
2007	34,445	49,770	158,404	24,368	10,273	20	277,259	19,901	274,403	3,002	297,305	-20,056	-248,948
2008	34,445	49,770	157,862	24,484	10,273	20	276,833	20,035	274,971	2,981	297,987	-21,148	-270,096
2009	34,445	49,770	158,783	24,573	10,273	20	277,844	20,250	274,950	2,962	298,163	-20,323	-290,419
2010	34,445	49,770	157,663	24,773	10,273	20	276,925	20,527	288,319	2,914	311,760	-34,838	-325,257
2011	34,445	49,770	176,710	25,036	10,273	20	296,234	20,707	287,889	2,861	311,458	-15,233	-340,490
2012	34,445	49,770	177,324	25,206	10,273	20	297,018	20,946	287,874	2,828	311,648	-14,645	-355,135
2013	34,445	49,770	176,774	25,332	10,273	20	296,593	21,198	287,799	2,802	311,799	-15,219	-370,354
2014	34,445	49,770	176,485	25,432	10,273	20	296,405	21,405	287,799	2,779	311,983	-15,587	-385,941
2015	34,445	49,770	177,278	25,516	10,273	20	297,282	21,654	305,094	2,759	329,507	-32,226	-418,167
2016	34,445	49,770	195,387	25,589	10,273	20	315,464	21,903	305,085	2,739	329,727	-14,265	-432,432
2017	34,445	49,770	195,098	25,653	10,273	20	315,239	22,091	305,076	2,721	329,888	-14,656	-447,088
2018	34,445	49,770	194,448	25,711	10,273	20	314,647	22,390	305,076	2,704	330,170	-15,541	-462,629
2019	34,445	49,770	194,322	25,761	10,273	20	314,571	22,645	305,076	2,687	330,409	-15,852	-478,481
2020	34,445	49,770	193,582	25,807	10,273	20	313,877	22,841	322,511	2,671	348,023	-34,158	-512,639
2021	34,445	49,770	207,646	25,849	10,273	20	327,982	22,982	322,158	2,656	347,797	-19,829	-532,468
2022	34,445	49,770	207,357	25,885	10,273	20	327,730	23,110	321,979	2,642	347,732	-20,000	-552,468
2023	34,445	49,770	207,158	25,920	10,273	20	327,566	23,361	321,668	2,629	347,657	-20,100	-572,568
2024	34,445	49,770	207,014	25,951	10,273	20	327,452	23,360	322,354	2,615	348,329	-20,206	-592,774
Totals	861,125	1,244,250	4,276,503	623,277	256,825	500	7,261,972	521,730	7,261,935	71,588	7,855,254	-592,774	

Notes:
1) Altar Valley and Canada del Oro inflows are specified using the well package
2) Constant head inflows are generally representative of underflow into the model across the southern boundary from the Santa Cruz AMA.
3) Constant head outflows are generally representative of underflow out the model across the northern boundary into the Pinal AMA.

Water Level Changes

The model water budget reflects the over-all response of the regional aquifer system to the changes in supply and demand. To examine the aquifer response in specific areas, projected water level change maps from 1999 calibrated heads were developed. The result of increased utilization of renewable CAP surface water supplies anticipated in the Base Case projection is evident at the end of the first projection stress period.

Figure 38a shows the projected water level change from 2000 to 2005. Water levels near the CAVSARP recharge facility, located in north-central Avra Valley, are projected to decrease slightly as the City of Tucson begins to recharge its permitted volume of CAP water and shift pumpage from the central well field area to CAVSARP. The long-term historic water level declines in the central well field area, approximately Township 14 South, Range 14 East, level off and begin to rise as this pumpage shift occurs. Water levels are projected to rise in northern Avra Valley, near Marana, where several GFSs and USFs recharge CAP water. In the southern part of the USC sub-basin, just north of Sahuarita, water levels are also expected to rise due to the Pima Mine Road and FICO recharge facilities. An existing drawdown cone is expected to continue to deepen east of the Sierrita Mountains due to mine pumpage, and a small cone is projected to begin forming in eastern Tucson in T 14 S, R 15 E due to increased development that will rely on groundwater. Water levels in T 18 S, R 13 E, are projected to increase as tailings pond recharge exceeds well pumpage in that area.

At the end of the second stress period, 2010, water levels around the CAVSARP facility have decreased slightly as water being recovered increases at the recharge facility (Figure 38b). Water levels in the central well field area are predicted to continue to recover as pumpage from the area is reduced by about 80 percent from the current demand levels. Water levels near recharge projects in the Marana area and north of Sahuarita continue to rise as recharge exceeds pumpage in those areas. Water level declines are projected to continue east of the Sierrita Mountains and the cone east of Tucson is expected to continue to deepen and expand. A new cone of depression is projected to begin developing southeast of Tucson spanning T15 S, R 14 and 15 E in an area that will utilize groundwater.

At the end of 2015 and 2020, the same general trends in water levels observed in 2005 and 2010 continue. Water level rises continue near Marana and north of Sahuarita due to CAP recharge projects (Figures 38c and 38d). The water level recovery in the central well field is projected to reach its maximum by 2015 and then generally stabilize. Water level declines continue around the CAVSARP facility in central Avra Valley, and the cones east and southeast of Tucson continue to expand and deepen. The cone of depression east of the Sierrita Mountains from mine pumpage slowly expands and its center continues to deepen.

By 2025, the end of the Base Case projection, the projected increased utilization of renewable CAP water has altered large areas of the regional aquifer in Tucson AMA (Figures 38e). The water level recovery in the central well field area has stabilized due to increasing municipal demand that is projected to be supplied by wells in this area (Figures 40 and 41). Water level recovery near the recharge facilities in Marana has reached more than 75 feet. Figure 42 indicates that the general water level recovery in the northern section of the Avra Valley sub-basin has begun to slow as recharged water is recovered for municipal use. The slow water level declines continue near CAVSARP, reaching a maximum of over 100 feet. Southeast of Tucson the developing cone of depression has expanded and water level declines have reached over 100 feet in T 16 S, R 15 E. The small, localized withdrawals east of Tucson in T 14 S, R 15 E have created a decline of about 200 feet. Mine pumpage continues to deepen the cone of depression east of the Sierrita Mountains in the southwestern corner of T 17 S, R 13 E. The maximum water level rise has occurred north of Sahuarita where recharge projects are projected to increase water level elevations about 200 feet during the projection period. The project depth to water in the regional aquifer is presented in Figure 39, and ranges from about 50 feet in T 16 S, R 13 E to over 1,000 feet near the model boundaries in the southern Avra Valley sub-basin.

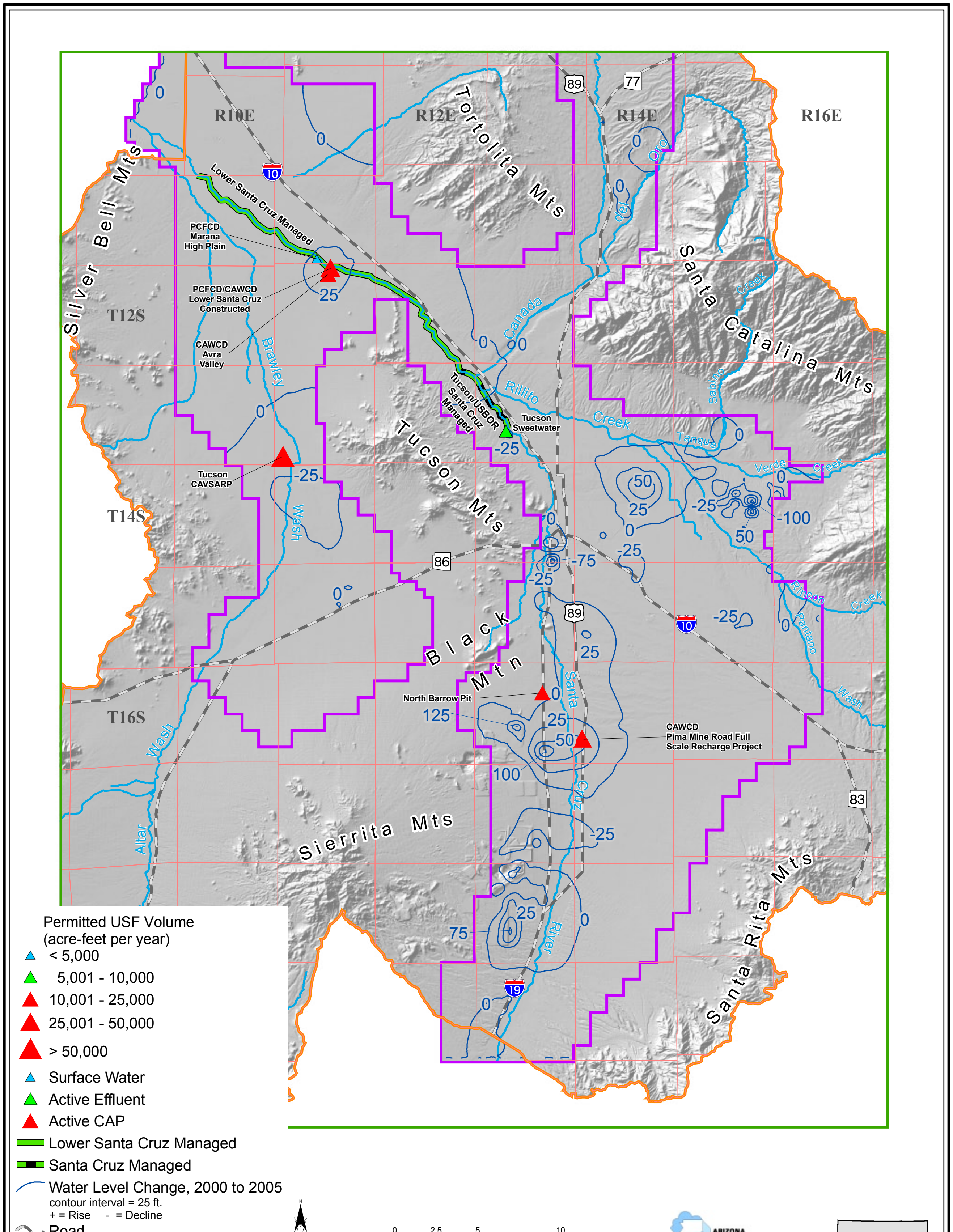

Figure 38a.
Map showing projected water level changes for Base Case Scenario Assumptions : 2000 - 2005, Tucson AMA, Arizona.

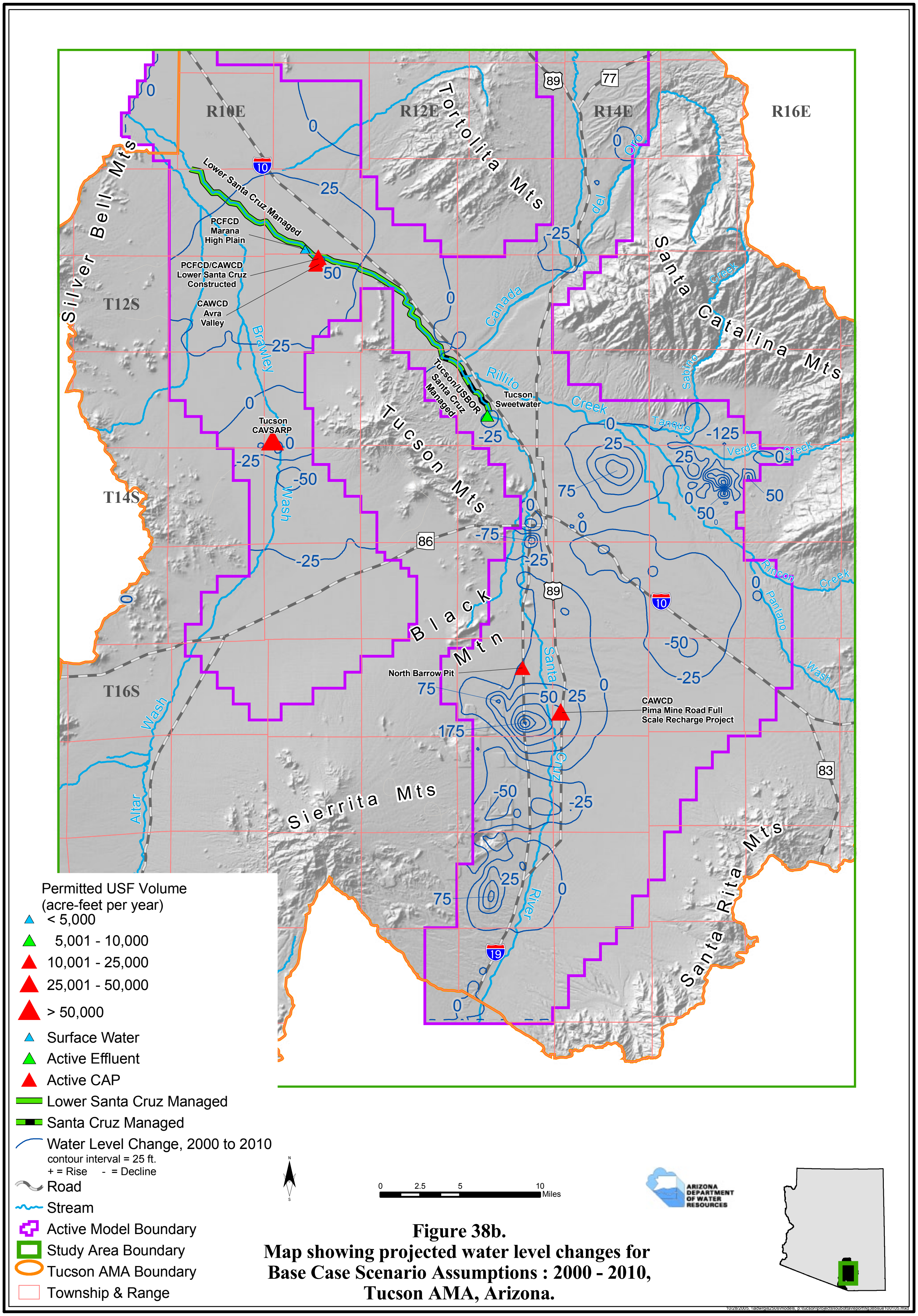

Figure 38b.
Map showing projected water level changes for Base Case Scenario Assumptions : 2000 - 2010, Tucson AMA, Arizona.

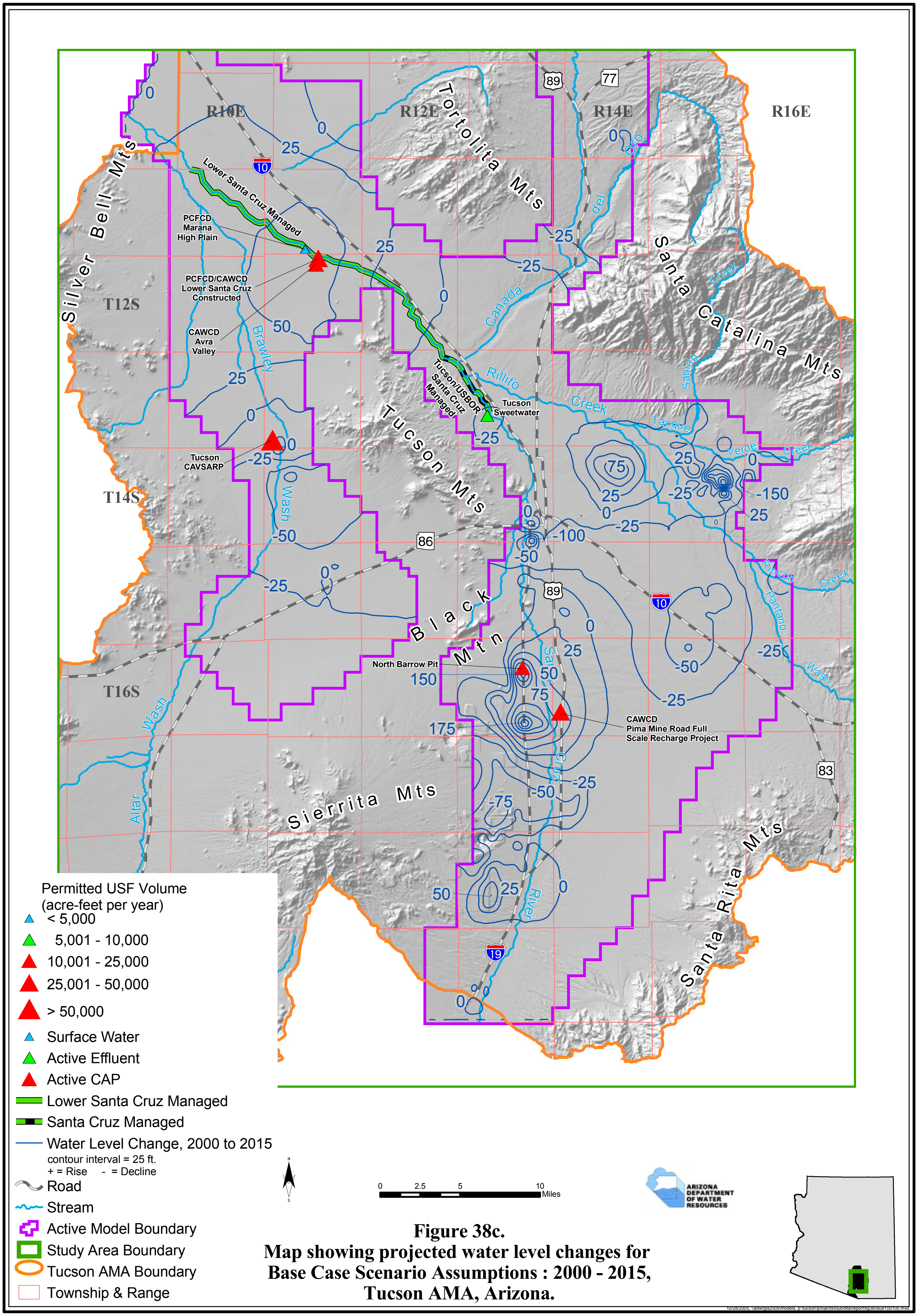

Figure 38c.
Map showing projected water level changes for Base Case Scenario Assumptions : 2000 - 2015, Tucson AMA, Arizona.

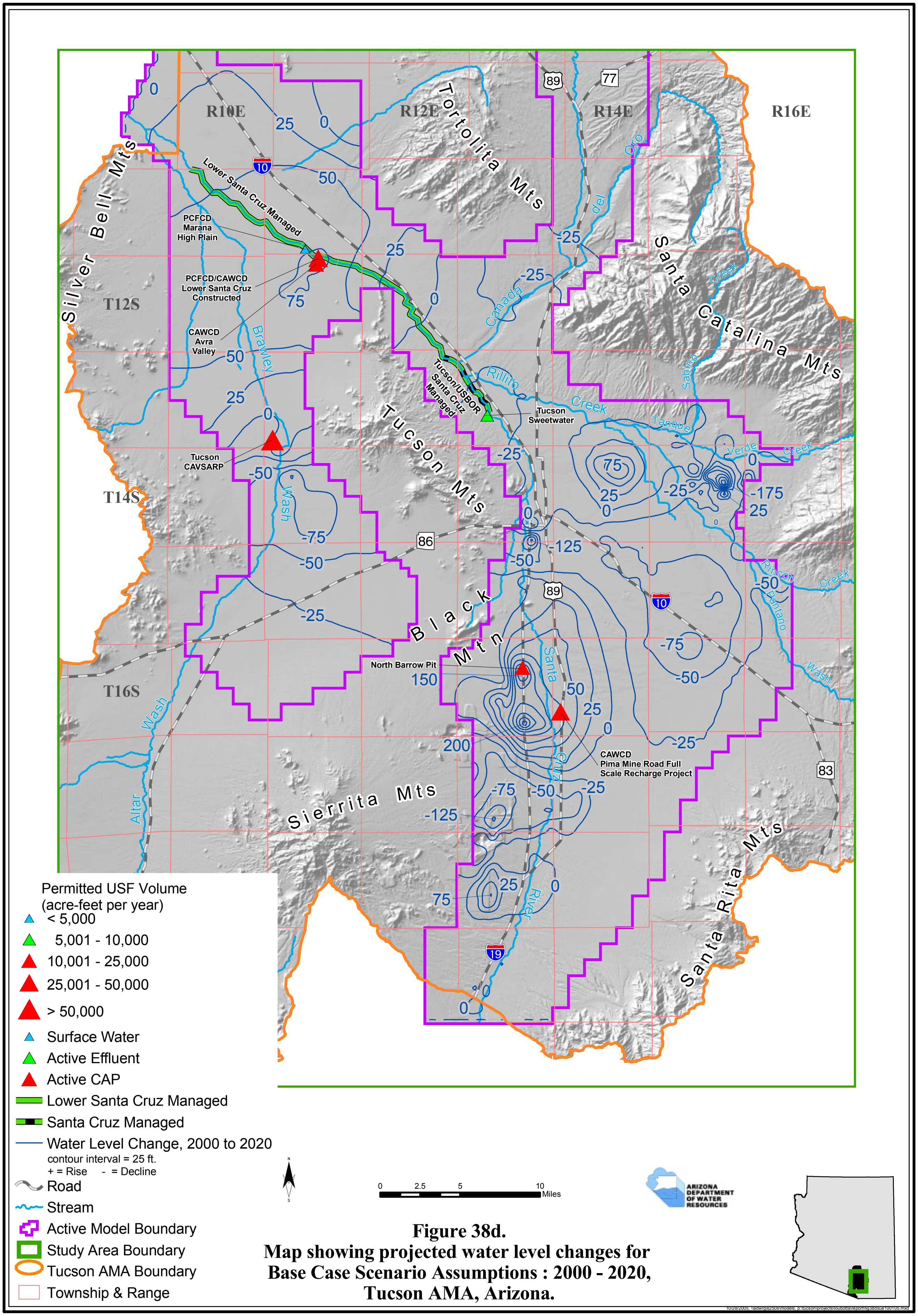

Figure 38d.
Map showing projected water level changes for Base Case Scenario Assumptions : 2000 - 2020, Tucson AMA, Arizona.

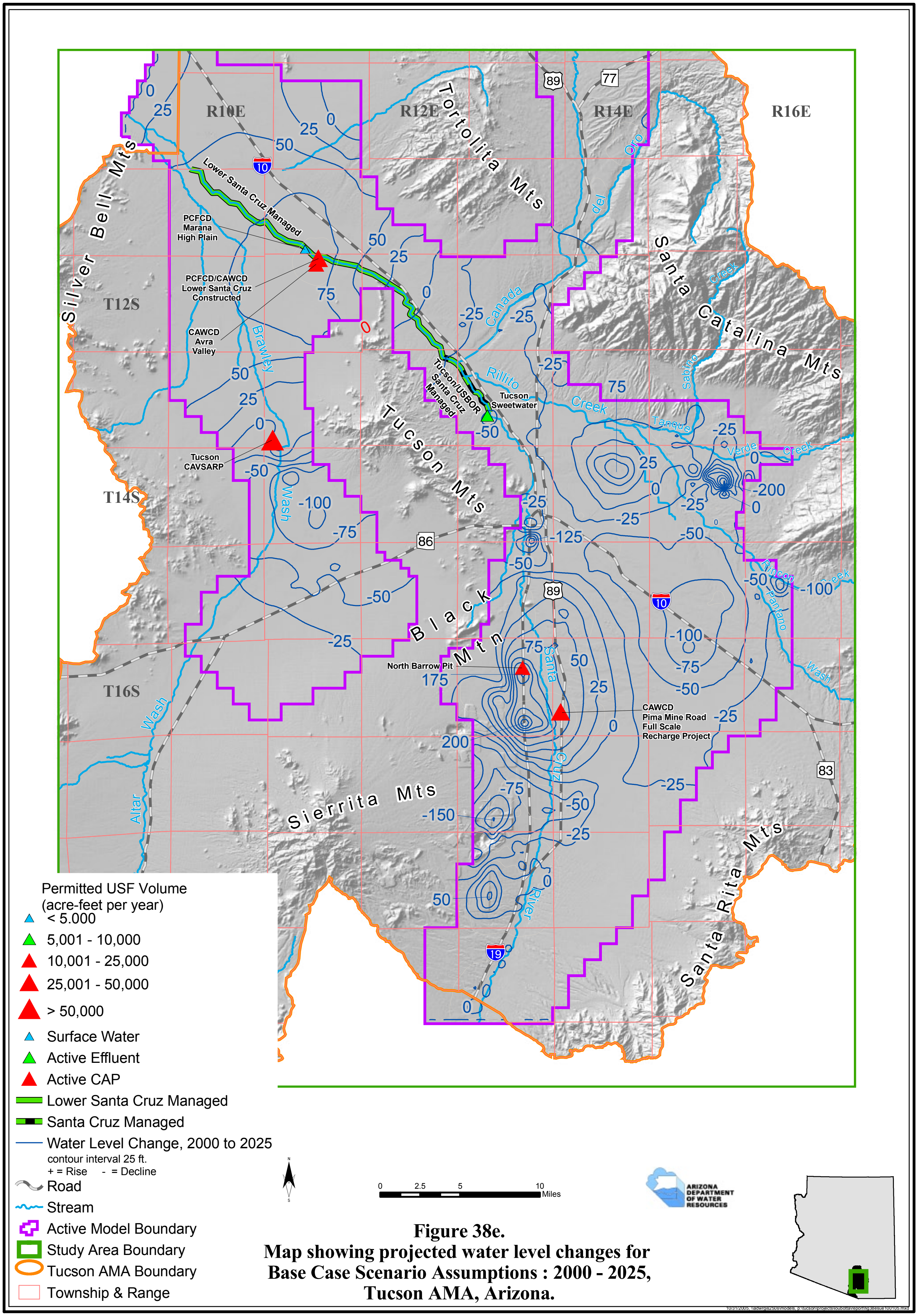

Figure 38e.
Map showing projected water level changes for Base Case Scenario Assumptions : 2000 - 2025, Tucson AMA, Arizona.

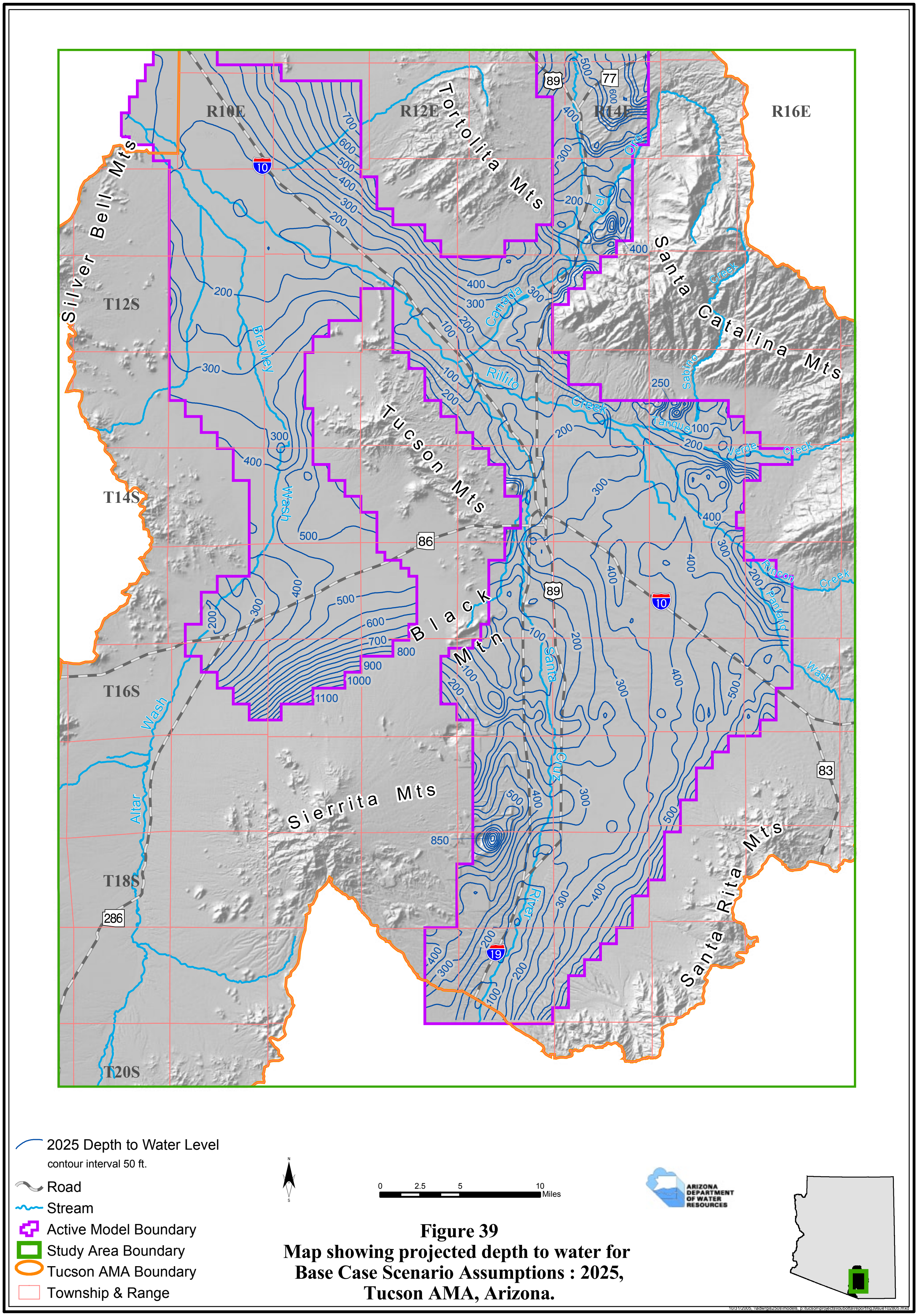

Figure 39
Map showing projected depth to water for Base Case Scenario Assumptions : 2025, Tucson AMA, Arizona.

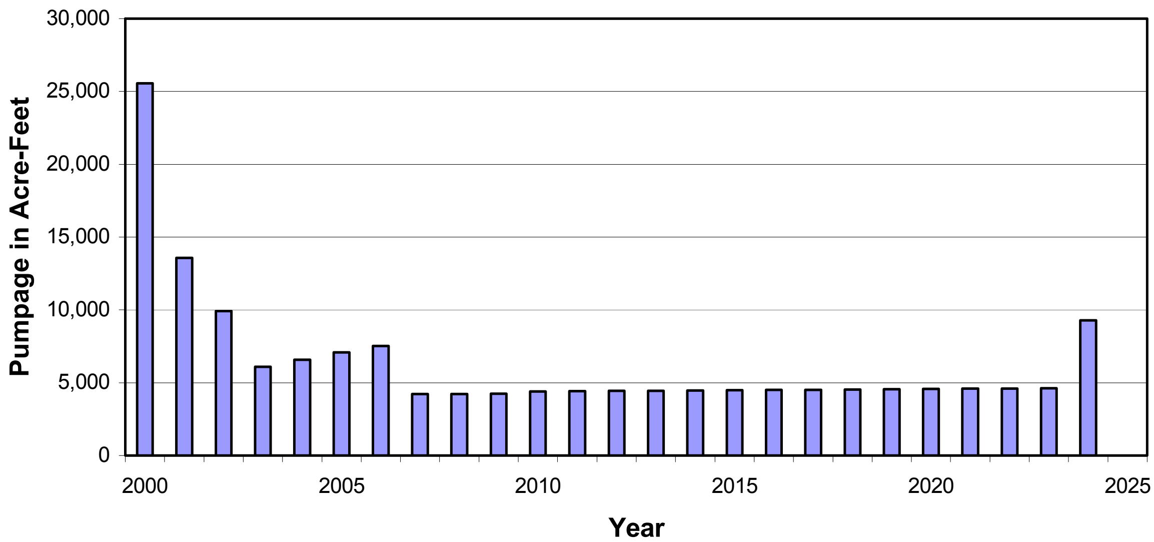

Figure 40. Estimated annual pumpage in the central well field area for the Base Case projection.

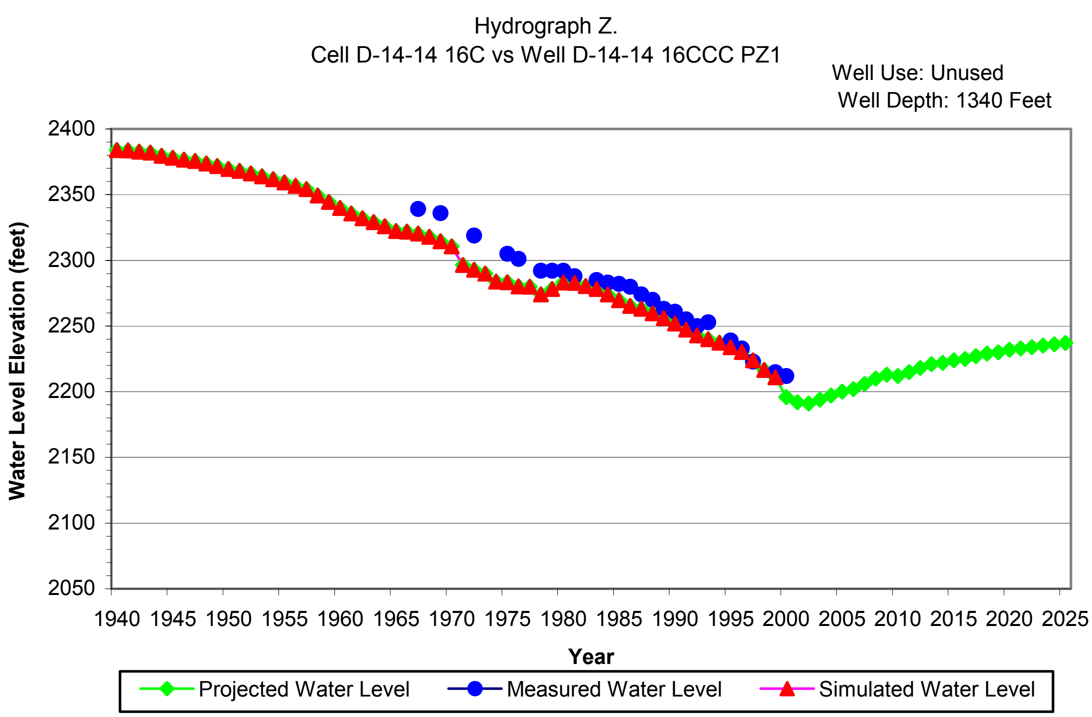

Figure 41. Hydrograph of measured, simulated, and projected water levels for well D-14-14 16ccc in the central well field area.

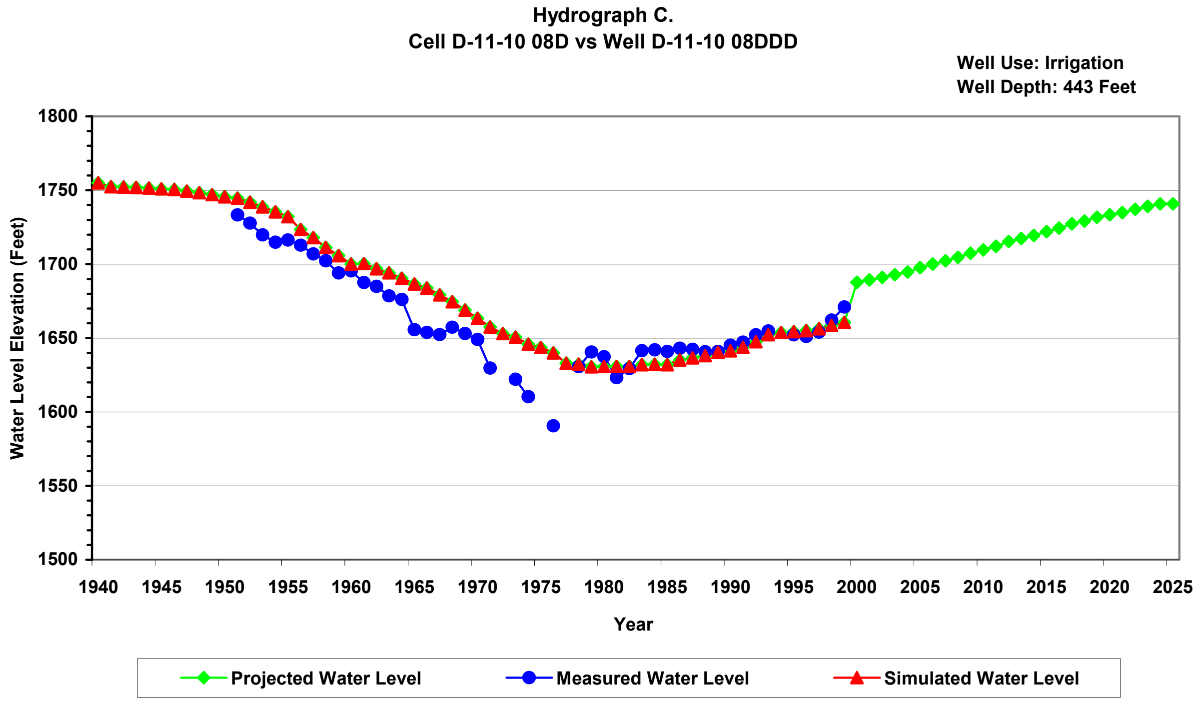

Figure 42. Hydrograph of measured, simulated, and projected water levels for well D-11-10 08ddd in the northern Avra Valley.

Summary

The Base Case projection run simulated future water supply and demand assumptions for the period 2000 to 2025. A key element of the water supply during the projection period is the introduction and wide-spread, intensive use of renewable CAP surface water and aggressive reuse of effluent. The results of the Base Case simulation indicate that the Tucson AMA will not reach its AMA-wide goal of "Safe Yield" by 2025, under the water use and supply assumptions used in the Base Case projection. However, the simulation projects relatively small overdrafts compared to historic overdrafts, in the tens of thousands of acre-feet as opposed to hundreds of thousands. And although the AMA as a whole is projected to fail to achieve "Safe Yield", the Avra Valley sub-basin is projected to maintain a net positive change in storage through out the Base Case projection. The USC sub-basin is projected to continue to experience persistent, long-term annual overdrafts, which are sufficiently large enough to cause the AMA to experience a net overdraft condition.

The response of water levels in the Tucson AMA regional aquifer varies depending on the supply and demand factors in the Base Case projection for particular areas within the AMA. In areas near major recharge facilities water level are projected to rise in excess of 220 feet. In the central well field area, an area of long-term water level decline due to municipal withdrawals by the City of Tucson, water levels are projected to stabilize and the recover by as much as 90 feet by 2025. This is due to a large overall decrease in projected pumpage for the central well field area as future water demands are shifted to recovery wells associated with CAVSARP and other recharge facilities. Water levels in the northern sections of the Avra Valley sub-basin near Marana are projected to continue a slow recovery as agricultural demand decreases and CAP water is recharged and developed for municipal use in that area.

Several areas are projected to have large water level declines based on the Base Case assumptions. The large declines are project in areas where CAP surface water is not expected to be available and demand must be met with groundwater. The two areas most affected are south of Sahuarita and east of the Sierrita Mountains where mine pumpage is projected to create a deep narrow cone of depression. Water level declines in the area are projected to be at least 175 feet from 1999 to 2025 give the current mine pumpage assumptions. In the areas east and southeast of the City of Tucson water level declines during the projection period are predicted to be 200 feet and over 100 feet, respectively.

Chapter 8

Summary

Summary

The major objectives of the Tucson AMA regional groundwater modeling update were to develop a calibrated regional groundwater flow model that reasonably simulates the regional hydrologic flow regime and accumulate and organize the available hydrologic, geologic, and water use data into an easily available format. The AMA staff and local water resource managers can use the calibrated model as a tool to determine the potential impacts of projected future water demands. This will allow local water resource managers to develop and evaluate long-term water management plans for the Tucson Active Management Area.

The results of both the steady-state and transient model calibrations indicate that the Tucson AMA model reasonably simulates the regional groundwater flow system. The model is able to accurately simulate historic changes in the regional groundwater flow systems. The 1940 model simulated groundwater levels matched very closely observed water level data. The 1941 to 1999 model simulation and observed water levels are also very similar. Both the steady-state and transient model have very low overall average model errors, 0.75 percent and 1.24 percent RMSE to head loss ratios, respectively. The average absolute head residual (MAE), the absolute value of the difference between a model-simulated head minus an observed head, for the steady-state model is 3.0 feet and 12.6 feet for the transient model. The steady-state and transient model water budgets both very closely match conceptual estimates, and the transient model's simulated change in aquifer storage is similar to previously estimated change in storage values.

Using the calibrated transient model for initial conditions, a Base Case future scenario was run using general water use assumptions developed by the Tucson AMA staff in cooperation with local water providers and users. The Base Case scenario ran from 2000 to 2025 and included current and future planned recharge projects, utilization of CAP surface water supplies and reuse of treated effluent. The results of the Base Case projection model indicate that the net annual loss of aquifer storage (overdrafting) of the regional aquifer will continue, although the overdrafts will be much smaller than in the past. For example, annual aquifer storage losses range from high of about -70,000 ac-ft at the beginning of the projection period to as little as –14,200 ac-ft (Table 17). The loss of aquifer storage is confined to the USC sub-basin, which is projected to experience a net loss of storage totaling slightly more than 1 million ac-ft during the projection period. The Avra Valley sub-basin is projected to have a net increase in aquifer storage of 453,000 ac-ft. The projected net increase of storage in the Avra Valley sub-basin is due to recharge of large volumes of renewable CAP surface water. The net loss of storage for the AMA over the projection period is 593,000 ac-ft (Table 17).

In the Base Case scenario groundwater pumpage from the central well field is cut dramatically and shifted to recovery wells associated with Tucson Water's Clearwater Recharge Facility located in the Avra Valley sub-basin. Conceptually, water levels in the central Tucson area would be expected to rebound due to the reduced pumpage, and the model simulated a rebound of at least 100 feet in the central well field area. Groundwater pumpage is expected to supply increasing demand in areas southeast and east of Tucson due to future urbanization. The Base Case scenario simulated water level declines in this area as groundwater pumpage increased to supply the growing urban demand. The fact that the model was able to accurately replicate past conditions indicates that the model will be a useful tool for water resource management in the Tucson AMA.

Model Limitations

Numerical groundwater flow models are useful tools to determine how an aquifer responds to changing stresses over time. However, regional models are, by their nature, only approximations of natural flow system and represent averaged conditions over a large area based on known data. Large-scale regional model, such as this model, may not be suitable for site-specific applications. Cell-size limitation, the lack of localized data, and the regional scale of the analysis make it difficult for the model to accurately simulate localized conditions.

Model accuracy is related to the amount, accuracy and distribution of the data used to develop the model. Model error is evaluated by comparing measured heads to simulated heads and usually reflects small-scale heterogeneities within an aquifer that are difficult for a model to simulate due to cell-size or data limitations. Generally speaking, model error usually is greatest in areas with sparse data and smallest in areas with large amounts of data. Better estimates of model input data and/or more data points usually result in a smaller model error and greater confidence in the model results. The trial-and-error method of model calibration is somewhat subjective and does not produce a unique solution. Trial-and-error model solutions are subject to uncertainty due to the need to estimate many model input parameters and boundary conditions.

Recommendations

The Tucson AMA modeling effort has identified need for the ADWR and local water managers coordinate their long-term water management plans. The Tucson AMA staff and local water providers will only be able to effectively manage the regional aquifer by working together in an attempt to eliminate long-term overdrafts of the regional aquifer. The Base Case scenario demonstrates that the goal of safe yield can be met, at least temporarily, with the wise use of the available water supplies. However, wise use will require cooperation, coordination, and communication between the ADWR staff, water providers, and consumers in developing future water management plans.

The Tucson AMA regional groundwater flow model can be a useful tool in the planning process. During the model development and calibration process several data and model limitations were identified. In order for the model to remain useful the following recommendations are offered.

1. Aquifer test data and well logs need to be collected on a continuing basis. These data need to be complied and maintained at a central location for easy access and inclusion in future model updates to help refine the model layer geometry and aquifer parameters.

2. Water level monitoring needs to be expanded, especially in areas that are not currently urbanized, but are expected to urbanize in the future. An expanded water level collection program will provide baseline data for comparison to future model updates.

3. Agricultural irrigation practices, both historic and current, need to be researched to better define the volume of agricultural recharge. Deep percolation of excess irrigation water is the single largest source of recharge to the regional aquifer after about 1970. A better understanding of past and current agricultural practices and cropping patterns is needed to help refine the currently available estimates of agricultural recharge.

4. Attempt to develop methods for estimating flood flow frequency and their contribution to annual recharge, so that recharge from past flood flows may be incorporated into the model. The model response in areas near the Santa Cruz River may be improved by developing annualized stream infiltration values that include major flood flows.

5. The current numerical model software, MODFLOW, will need to be updated to keep pace with improvements in modeling techniques. New packages and features developed for MODFLOW-2000 need to be implemented, such as the inverse modeling using Parameter Estimation. These new techniques will result in a model with a better calibration and, therefore, less uncertainty.

6. Subsidence has been recorded in both Avra Valley and central Tucson. To account for subsidence the U.S. Geological Survey's new Subsidence package should be incorporated into the model.

Selected References

Anderson, Mary P. and Woessner William W., 1992, Applied groundwater modeling: Simulation of flow and advective transport, Academic Press Inc., Harcourt Brace Jovanovich publishers, 381 p.

Anderson, S.R., 1987, Cenozoic stratigraphy and geologic history of the Tucson basin, Pima County, Arizona: U.S. Geological Survey Water-Resources Investigations Report 87-4190, 20 p.

_____ ,1988, Potential for aquifer compaction, land subsidence, and earth fissures in the Tucson basin, Pima County, Arizona: U.S. Geological Survey Hydrologic Investigations Atlas HA-713, 3 sheets.

_____ , 1989, Potential for aquifer compaction, land subsidence, and earth fissures in the Avra Valley, Pima County, Arizona: U.S. Geological Survey Hydrologic Investigations Atlas HA-718, 3 sheets.

Anderson, T.W., 1972, Electric-analog analysis of the hydrologic system, Tucson basin, southeastern Arizona: U.S. Geological Survey Water-Supply Paper 1939-C, 34 p.

_____, 1982, Implications of deep percolation to ground-water systems in south-central Arizona based on numerical-model studies: Proceedings of the 1982 Deep Percolation Symposium, October 26, 1982: Arizona Department of Water Resources Report Number 4, p. 30-40.

Anderson, T.W., Freethey, G.W., and Tucci, Patrick, 1990, Geohydrology and water resources of alluvial basins in south-central Arizona and adjacent states: U.S. Geological Survey Open-File Report 89-378, 99 p.

Andrews, David A., 1937, Ground water in Avra-Altar Valley, Arizona: U. S. Geological Survey Water-Supply Paper 798-E, p. 163 – 180.

Anning, D.,W. and Duet, N.,R., 1994, Summary of ground-water conditions in Arizona, 1987-1990; U. S. Geological Survey Open-File Report 94-476, 1 sheet.

Arizona Department of Water Resources, 1999a, Third management plan 2000 – 2010: Tucson Active Management Area,

Arizona Department of Water Resources, 1999b, Third management plan 2000 – 2010: Santa Cruz Active Management Area,

Arizona Department of Water Resources, 2000, Registry of Groundwater Rights, well summary data for year 2000.

Bookman-Edmonston Engineering, Inc, 1978, Report on use of reclaimed water for irrigation, For Cortaro-Marana Irrigation District, Pima County, Arizona, Bookman-Edmonston Engineering, Inc., Phoenix, Arizona, 67 p., 1 plate.

Brown, S.G., 1976, Components of the water budget in the Tucson area, Arizona, 1970-72: U.S. Geological Survey Miscellaneous Investigations Series Map I-844-M, 1 sheet.

Burkham, D.E., 1970, Depletion of streamflow by infiltration in the main channels of the Tucson basin, southeastern Arizona: U.S. Geological Survey Water-Supply Paper 1939-B, 36 p.

Condes de la Torre, Alberto, 1970, Streamflow in the upper Santa Cruz River basin, Santa Cruz and Pima Counties, Arizona: U.S. Geological Survey Water-Supply Paper 1939-A, 26 p.

Cuff, Melinda K. and Anderson, S.R., 1987, Groundwater conditions in Avra Valley, Pima and Pinal Counties, Arizona – 1985: U.S. Geological Survey Water-Resources Investigations Report 87-4192, 3 sheets.

Davidson, E.S., 1973, Geohydrology and water resources of the Tucson basin, Arizona: U.S. Geological Survey Water-Supply Paper 1939-E, 81 p.

Esposito, D. and Thurnbald, T., 1981, Historical perspective on potential pollution sources in the Cortaro area, Pima Association of Governments and the Water Resources Research Center.

Gallaher, B.M., 1979, Recharge properties of the Tucson basin aquifer as reflected by the distribution of a stable isotope: University of Arizona, Tucson, Arizona, unpublished Masters Thesis, 92p.

Galyean, Ken, 1996, Infiltration of wastewater effluent in the Santa Cruz River channel, Pima County, Arizona, Water-Resources Investigation 96-4021, p. 82

Hammett, B.A. and Sicard, J.W., 1996, Groundwater conditions in the Santa Cruz and Tucson Active Management Areas, Pima, Pinal, and Santa Cruz Counties, Arizona: Arizona Department of Water Resources Open-File Report 8, 4 sheets.

Hanson, R.,T., 1989, Aquifer-system compaction, Tucson basin and Avra Valley, Arizona: U.S. Geologic Survey Water-Resources Investigations Report 88-4172, 69 p.

Hanson, R.T., Anderson, S.R., and Pool, D.R., 1990, Simulation of ground-water flow and potential land subsidence, Avra Valley, Arizona: U.S. Geological Survey Water-Resources Investigations Report 90-4178, 41 p.

Hanson, R.,T. and Benedict, J.,F., 1994 , Simulation of ground-water flow and potential for land subsidence, Upper Santa Cruz basin, Arizona: U.S. Geological Survey, Water-Resources Investigations Report 93-4196, 47 p.

Harbaugh, A.W., Banta, E. R., Hill, M.C., and McDonald, M.G., 2000, MODFLOW-2000, The U.S. Geological Survey modular ground-water model: user guide to modularization concepts and the ground-water flow process: U. S. Geological Survey Open-File Report 00-92, 121 p.

Heindl, L.A. and White, Natalie D., 1965, Hydrologic and drill-hole data San Xavier Indian Reservation and vicinity, Pima County, Arizona: Arizona State Land Department Water-Resources Report Number 20, 48 p.

Hill, M.C., Banta, E.R., Harbaugh, A.W., and Anderman, E.R., 2000, MODFLOW-2000, the U.S. Geological Survey modular ground-water flow model – user guide to the observation, sensitivity, and parameter-estimation process and three post-processing programs: U. S. Geological Survey Open-File Report 00-184, 209 p.

Hill, M.C., 1998, Methods and guidelines for effective model calibration: U. S. Geological Survey Water-Resources Investigation Report 98-4005, 90 p.

Hollett, K.J. and Garrett, Joanne M., 1984, Geohydrology of the Papago, San Xaiver, and Gila Bend Indian Reservations, Arizona – 1978-1981: U.S. Geological Survey, Hydrologic Investigations Atlas HA-660, 2 sheets.

Hoffman, J.P., Ripich, M.A., and Ellett, K.M., 2002, Characteristics of shallow deposits beneath Rillito Creek, Pima County, Arizona: U. S. Geologic Survey Water-Resources Investigations Repor01-4257, 51 p.

Hydrosphere Data Products, 2001, Summary of the day precipitation data: from the National Climatic Data Center, 1 CD.

Keith, S.J.S., 1981, Stream channel recharge in the Tucson basin and its implication for groundwater management: University of Arizona, Tucson, Arizona, unpublished Masters Thesis, 84p.

Leake, S.A., and Hanson, R.T., 1987, Distribution and movement of trichloroethylene in ground water in the Tucson area, Arizona: U.S. Geological Survey Water-Resources Investigations Report 86-4313, 40 p.

Marra, Ralph P., Jr., 1992, Preliminary steady-state modeling calibrations of Tucson Water's central well field flow model Tucson Basin, Southeastern Arizona; Tucson, University of Arizona, Master's thesis, 196 p.

Matlock, W.G. and Davis, P.R., 1972, Groundwater in the Santa Cruz Valley, Arizona: University of Arizona Agricultural Experiment Station Bulletin 194, 37 p.

Matlock, W.G. and Morin, George C.A., 1976, Groundwater in Avra and Altar Valleys, Arizona: University of Arizona Agricultural Experiment Station Bulletin 232, 59 p.

McDonald, M.G. and Harbaugh, A.W. 1988, A modular three-dimensional finite-difference ground-water flow model: U.S. Geological Survey Techniques of Water-Resources Investigations, Book 6 Modeling Techniques, Chapter A1, 586 p.

_____ , 1996, User's documentation for MODFLOW-96, an update to the U.S. Geological Survey modular finite-difference ground-water flow model, : U.S. Geological Survey Open-File Report 96-485 56 p.

Moosburner, Otto, 1972, Analysis of the ground-water system by electric-analog model, Avra Valley, Pima and Pinal Counties, Arizona: U.S. Geological Survey Hydrologic Investigations Atlas HA-215, 2 sheets.

Murphy, B.A., and Hedley, J.D., 1984, Maps showing groundwater conditions in the upper Santa Cruz basin area, Pima, Santa Cruz, Pinal, and Cochise Counties, Arizona – 1982: Arizona Department of Water Resources Hydrologic Map Series Report Number 11, 3 sheets.

Nelson, Keith and Erwin, Gretchen, 2001, Santa Cruz Active Management Area 1997-2001 Hydrologic Monitoring Report: Arizona Department of Water Resources, 44 p.

Osterkamp, W.R., 1973, Ground-water recharge in the Tucson Area, Arizona: U.S. Geological Survey Miscellaneous Investigations Series Map I-844-E, 1 sheet.

Osterkamp, W.R., 1974, Map showing ground-water velocities in the uppermost saturated alluvium deposits of the Tucson area, Arizona: U.S. Geological Survey Miscellaneous Investigations Series Map I-844-K, 1 sheet.

Parker, J.T.C., 1993, Channel change on the Santa Cruz River, Pima County, Arizona: U. S. Geological Survey, Open-File Report 93-41, 65 p.

Pashley, E., F., Jr., 1966, Structure and stratigraphy of the central, northern, and eastern parts of the Tucson basin, Arizona: Tucson, University of Arizona, Ph. D. dissertation, 273 p.

Pima Association of Governments, 1983, Cortaro Area Pollution Source Assessment: Cortaro Area Study Final Report and Recommendations, 177 p., 6 plates

Pool, D.R., 1999, Aquifer-storage changes in the lower Canada del Oro sub-basin, Pima County, Arizona, 1996 - 1998: U.S. Geological Survey, Water-Resources Investigations Report 99-4067, 3 sheets.

Pool, D.R., 1986, Aquifer geology of alluvial basins of Arizona, in Anderson, T.W., and Johnson, I.A., eds., Regional Aquifer Systems of the United States, Southwestern Alluvial Basins of Arizona: American Water Resources Association Monograph Series 7, p. 25-35.

_____, D.R. and Schmidt, W., 1997, Measurement of ground-water storage change and specific yield using the temporal-gravity method near Rillito Creek, Tucson, Arizona: U.S. Geological Survey, Water-Resources Investigations Report 97-4125, 30 p.

Schladweiler, J.C., 2001, The Evolutionary Development of the Sanitary Sewage System for the Greater Tucson Metropolitan Area, Historian: Arizona Water & Pollution Control Association, online: www.sewerhistory.org/chrono_pc/

Schwalen, H.C. and Shaw, R.J., 1957, Ground water supplies of the Santa Cruz Valley of Southern Arizona Between Rillito Station and the international boundary: University of Arizona, Agricultural Experiment Station Bulletin 288, 119 p.

_____, H.C., 1942, Rainfall and runoff in the upper Santa Cruz River drainage: University of Arizona, Agricultural Experiment Station Bulletin 64, 244 p.

Smith, G.E.P., 1910, Groundwater supply and irrigation in the Rillito Valley: University of Arizona, Agricultural Experiment Station Technical Bulletin 95, 50 p.

Travers, B.C. and Mock, P.A., 1984, Groundwater modeling study of the upper Santa Cruz basin and Avra Valley in Pima and Santa Cruz Counties, southeastern Arizona: Arizona Department of Water Resources, Hydrology Division, Unnumbered Modeling Report, 2 v.

Turner, S.F. and others, 1943, Groundwater resources of the Santa Cruz basin, Arizona: U.S. Geologic Survey open-file report, unnumbered, 15 p.

Turner, S.F. 1947, Further investigations of the ground-water resources of the Santa Cruz basin, Arizona: U.S. Geological Survey open-file report, unnumbered, 49 p.

Webb, R.H. and Betancourt, J.L., 1990, Climatic Variability and flood frequency of the Santa Cruz River, Pima County Arizona: U.S. Geologic Survey Water-Supply Paper 2379, 40 p.

White, N.D. Matlock, W.G., and Schwalen, H.C., 1966, An appraisal of the ground-water resources of Avra and Altar Valleys, Pima County Arizona: Arizona State Land Department Water-Resources Report 25, 66 p.

Appendix A

Model Water Budgets

MODFLOW Steady-State Cumulative Water Budget

Length Units are Feet and Time Units are Days

Volumetric Budget For Entire Model At End Of Time Step 1 In Stress Period 1

Cumulative Volumes	L**3	Rates For This Time Step	L**3/T
In:		**In:**	
Storage =	0.0000	Storage =	0.0000
Constant Head =	1051273920.0000	Constant Head =	2880202.5000
Wells =	868700.0000	Wells =	2380.0000
Et =	0.0000	Et =	0.0000
Recharge =	3217810430.0000	Recharge =	8815919.0000
Total In =	4269953020.0000	Total In =	11698502.0000
Out:		**Out:**	
Storage =	0.0000	Storage =	0.0000
Constant Head =	923071232.0000	Constant Head =	2528962.2500
Wells =	2600322300.0000	Wells =	7124171.0000
Et =	747920448.0000	Et =	2049097.1200
Recharge =	0.0000	Recharge =	0.0000
Total Out =	4271313920.0000	Total Out =	11702230.0000
In - Out =	-1360932.0000	In - Out =	-3728.8750
Percent Discrepancy =	-0.03	Percent Discrepancy =	-0.03

Time Summary At End Of Time Step 1 In Stress Period 1

	Seconds	Minutes	Hours	Days	Years
Time Step Length	3.15360e+07	5.25600e+05	8760.0	365.00	0.99932
Stress Period Time	3.15360e+07	5.25600e+05	8760.0	365.00	0.99932
Total Time	3.15360e+07	5.25600e+05	8760.0	365.00	0.99932

Transient Cumulative Water Budget

VOLUMETRIC BUDGET FOR ENTIRE MODEL AT END OF TIME STEP 12 IN STRESS PERIOD 59

CUMULATIVE VOLUMES	L**3	RATES FOR THIS TIME STEP	L**3/T
IN:		IN:	
STORAGE =	353418183000.0000	STORAGE =	15622753.0000
CONSTANT HEAD =	49958543400.0000	CONSTANT HEAD =	3247487.2500
WELLS =	26405941200.0000	WELLS =	1226196.0000
ET =	0.0000	ET =	0.0000
RECHARGE =	387099001000.0000	RECHARGE =	20874556.0000
TOTAL IN =	816881664000.0000	TOTAL IN =	40970992.0000
OUT:		OUT:	
STORAGE =	59605643300.0000	STORAGE =	4476675.0000
CONSTANT HEAD =	42476949500.0000	CONSTANT HEAD =	1343789.6200
WELLS =	693147075000.0000	WELLS =	34801904.0000
ET =	21629380600.0000	ET =	347152.5940
RECHARGE =	0.0000	RECHARGE =	0.0000
TOTAL OUT =	816859054000.0000	TOTAL OUT =	40969520.0000
IN - OUT =	22620160.0000	IN - OUT =	1471.0312
PERCENT DISCREPANCY =	0.00	PERCENT DISCREPANCY =	0.00

TIME SUMMARY AT END OF TIME STEP 12 IN STRESS PERIOD 59

	SECONDS	MINUTES	HOURS	DAYS	YEARS
TIME STEP LENGTH	2.62800E+06	43800.	730.00	30.417	8.32763E-02
STRESS PERIOD TIME	3.15360E+07	5.25600E+05	8760.0	365.00	0.99932
TOTAL TIME	1.86062E+09	3.10103E+07	5.16839E+05	21535.	58.960

Appendix B

Model Residuals

Head Observation Weights

Assigning weights to observed head data used to calibrate the Tucson groundwater flow model is based on the method suggested by Hill (1998). In Guideline 6 (page 45), Hill suggests using the variance of the measurement error of the observed heads (water level elevations) as the basis for assigning weighting values. The observed water level elevations used in the Tucson model calibration come from the ADWR GroundWater Site Inventory (GWSI) database and are determined by subtracting a depth to water measurement from a well site elevation. Since most well site elevations in the GWSI are determined from U.S. Geological Survey (USGS) contour maps, the USGS vertical accuracy standards for contour maps can be used to estimate the variance of measurement error for well site elevation and, by extension, measurement errors for GWSI water level elevations.

The USGS accuracy standard states that 90 percent of sampled points on contour maps must be within plus or minus one-half of the maps contour interval (U.S. Geological Survey, 1980). The USGS accuracy standard is used when assigning the altitude accuracy of well sites in the GWSI and is one-half the contour interval of the map used to determine the site elevation. The altitude accuracy standard establishes a 90 percent confidence interval that well site elevations are plus or minus one-half a maps contour interval, or the assigned altitude accuracy in the GWSI. Assuming a normal distribution, a 90 percent confidence interval is constructed by adding plus or minus 1.65 times the standard deviation of the measurement error. The 1.65 can be looked up in any table that lists cumulative probabilities for the standardized normal distribution.

Substituting the altitude accuracy from the GWSI for the USGS accuracy standard in the formula from Hill (p.46,) for calculating the estimated standard deviation of the measurement error yields the following formula:

SD = GWSI Altitude Accuracy/1.65

where: SD = estimated standard deviation

An example using an altitude accuracy of 10 feet (map contour interval = 20 feet) is presented below and yields an estimated standard deviation for the well site measurement error of ±6.06 feet, which is also the measurement error for a GWSI water level from the site.

SD = 10 feet/1.65
SD = 6.06 feet

The MODFLOW-2000 Head Observation option will either accept an assigned weighting factor or will calculate a weighting factor for each observation head using the standard deviation of the measurement error (Harbaugh and others, 2000; Hill and others, 2000). The weighting factors presented in Table 1 were calculated by MODFLOW-2000 for each observation water level using site altitude accuracy data from the GWSI database to estimate the standard deviation of the measurement error as described above.

In Table B-1 altitude accuracies of one foot or less have had their elevations determined by land surveys. These well sites have very small altitude accuracies and, therefore, corresponding small elevation measurement errors. As a result, the estimated standard deviations are less than one and the weights, as calculated by MODFLOW-2000, are greater than one. To keep head weighting factors less than or equal to 1, these altitude accuracy values were assigned weighting factors between 0.909 and 1.0; with 1.0 being assigned to wells with the smallest elevation measurement errors (smallest altitude accuracy values).

Table B-1. Weighting factors for observed water levels as determined from site altitude accuracy values in the GWSI database.

GWSI Altitude Accuracy (Ft)	Estimated Standard Deviation	Assigned Weighting Factor
0.1	0.06	1.0
0.2	0.12	0.990
0.5	0.30	0.952
1.0	0.61	0.909
2.0	1.21	0.825
2.5	1.52	0.660
5.0	3.03	0.330
10.0	6.06	0.165
15.0	9.09	0.110
20.0	12.12	0.083
25.0	15.15	0.066
40.0	24.24	0.041
50.0	30.30	0.033

References:

Harbaugh, A.W., Banta, E.R., Hill, M.C., and McDonald, M.G., 2000, MODFLOW-2000, The U.S. Geological Survey Modular Ground-Water Model – User guide to modularization concepts and the groundwater flow process: U.S. Geological Survey, Water-Resources Investigations Report 00-92, 121 p.

Hill, M.C., 1998, Methods and guidelines for effective model calibration: U.S. Geological Survey, Water-Resources Investigations Report 98-4005, 90 p.

Hill, M.C., Banta, E.R., Harbaugh, A.W., and Anderman, E.R., 2000, MODFLOW-2000, The U.S. Geological Survey Modular Ground-Water Model – User guide to the observation, sensitivity, and parameter-estimation processes and three post-processing programs, U.S. Geological Survey, Water-Resources Investigations Report 00-184, 210 p.

U.S. Geological Survey, 1980, Accuracy specifications for topographic mapping, in Technical Instructions of the National Mapping Division: Reston, Virginia, Chapter 1B4, p. 1-13.

Table B-2. 1940 weighted residuals.

Cadastral Location	Weighted Residual (Ft)	Cadastral Location	Weighted Residual (Ft)
D-10-09 36DDD1	5.9	D-13-13 24DAB1	2.8
D-10-09 36DDD2	1.6	D-13-13 28ADD	0.4
D-11-10 17ADD	6.7	D-13-14 26DCD	-1.7
D-11-10 22ADD	-1.3	D-13-15 33CBB	-0.5
D-11-10 32DAA1	3	D-14-13 02CCD	1.2
D-11-10 32DAD	4	D-14-13 03BAC	-0.7
D-11-10 36DDB1	0.7	D-14-13 26ACA	-4.4
D-11-11 16CDD1	-9.6	D-14-13 26DBB	-1
D-11-11 26BDC	-1.2	D-14-13 34ADC	-0.2
D-11-11 30AAA	4.6	D-14-13 34DDC	-0.2
D-11-11 34ADD1	-2.7	D-14-13 35CAB	2.2
D-12-10 03DAA	2.3	D-14-13 35CAC1	-0.3
D-12-10 09BBB	2.7	D-14-13 35CDB	-2
D-12-10 12CB	-2.3	D-14-13 35CDC1	-2.2
D-12-10 20DD	-0.1	D-14-13 36CC	-4.3
D-12-10 26BBA	0	D-14-14 07AAA	2.3
D-12-11 01ACD	-0.1	D-14-14 08BAA	-14.7
D-12-11 08CBA	4.4	D-14-15 03DBD	-1.6
D-12-11 18DDD	2	D-14-15 05ADA	-7.8
D-12-11 29AAD	3	D-14-15 07DCB	0.5
D-12-11 33BB	-15.1	D-14-16 06CBB1	1.4
D-12-12 06BAD	-2.3	D-15-13 02CCA	-0.8
D-13-10 10BB	-6.2	D-15-13 11CBA	0.5
D-14-10 25CAA	7.4	D-15-13 15DDC	13.3
D-15-10 33CAC	5	D-15-13 22ADC1	-2.2
D-15-10 33DA	1.3	D-15-13 22DCC2	-0.6
D-15-10 34CAC	-4.7	D-15-13 26AAC	-7.5
D-15-11 09DAB	1.7	D-15-13 26BCB	-6.4
D-12-12 05CCC1	-1.8	D-15-13 27DDD1	-10.6
D-12-12 14ADA	-2.1	D-15-14 31CCC	0.2
D-12-12 16BAD	0.7	D-16-13 35AAA1	0.8
D-12-12 21BBD	3.1	D-16-13 35DAA	0.4
D-12-12 21CAA	2.8	D-16-13 36BB	1.8
D-12-12 27CDD	1.4	D-16-13 36CB	2.1
D-12-12 33AAA	2.1	D-16-13S01BBD	-0.5
D-12-12 35BBD	1	D-16-13S02BBA2	1.3
D-12-13 18AAD1	-11.7	D-16-13S02BDC	10.2
D-12-13 22BBB	1	D-16-14 07ABB	-0.8
D-12-13 31CDA	2.6	D-16-14 07BAD	1.4
D-12-13 32BDA	2.1	D-16-14 19AA	0.4
D-12-13 32CBC	20.2	D-16-14 20CBC1	1.3
D-13-12 01DAC	3.9	D-16-14 30CCD1	2.9
D-13-13 06BBB	6.3	D-16-14 31ACD	0.5
D-13-13 07DDC	0.3	D-16-14 31CDA1	0.7
D-13-13 08CCC1	1.1	D-16-14 32BAA	0.8
D-13-13 17DAD	0.8	D-16-14 32CA	0.9
D-13-13 23BDD1	-0.5	D-17-13 12DB	3.3

Table B-2. 1940 Weighted Residuals

Cadastral Location	Weighted Residual (Ft)
D-17-13 13BAD	1.1
D-17-13 13BD	0.3
D-17-13 25ABC	0.1
D-17-13 25CDD	1.5
D-17-13 25DDD	1.2
D-17-14 06CCC	5.7
D-17-14 07CDC	5.1
D-17-14 18CAB	1.8
D-17-14 31BDB	2.9
D-18-13 01BC	9.8
D-18-13 01BCC	1
D-18-13 01CBD	0.8
D-18-13 01CDD	1.1
D-18-13 02AA	-0.3
D-18-13 13BAC	1.1
D-18-13 14CDA	0.9
D-18-13 24BBB1UNSURV	0.5
D-18-13 26AAD	0.2
D-18-13 34ABC	-16.1
D-18-13 34AC UNSURV	1
D-19-13 03ADC1	-0.4
D-19-13 03BBA	0.6
D-19-13 16BDA	-3
D-19-13 21CAC	-0.9

Table B-3. 1960 weighted Residuals.

Cadastral Location	Weighted Residual (Ft)	Cadastral Location	Weighted Residual (Ft)
D-10-09 36DDD4	14	D-13-12 02AAB2	0.7
D-10-10 05DAD	18.4	D-13-12 02DAA	21.6
D-10-10 08AAA	2.2	D-13-12 02DAB	4.6
D-10-10 20DCC	7.9	D-13-12 02DDC	1.9
D-10-10 34CAB	10.5	D-13-12 12AAB	4.8
D-10-10 34CBB	6.3	D-13-12 12CAA	6.3
D-10-10 34DCD	-0.9	D-13-13 06AAA2	5.6
D-11-10 04DDD	0.1	D-13-13 06DAA1	33.1
D-11-10 10DDD	14.6	D-13-13 07CAA	9.7
D-11-10 14DAB	4.7	D-13-13 08BAA	35.5
D-11-10 15CDD	18	D-13-13 08CDD1	11.6
D-11-10 20DCC	6.9	D-13-13 09CDD1	39.8
D-11-10 20DDD	7.6	D-13-13 11BBC	28.3
D-11-10 26ADD	22.8	D-13-13 13BBA	2.1
D-11-10 27CDC1	7.9	D-13-13 13DDB	-0.2
D-11-10 32DAD	7.5	D-13-13 15BCD	20.8
D-11-11 11DCD	11.6	D-13-13 15CCD1	43.3
D-11-11 17DDD	5.3	D-13-13 16AAA	31.5
D-11-11 21AAA2	9.8	D-13-13 16CCD	8.1
D-11-11 32AAD	4.8	D-13-13 16DDA	31.2
D-11-11 32ADD	3.7	D-13-13 17DAD	7.2
D-11-11 33DAA	24	D-13-13 18ABB	30.6
D-11-12 34DDC	-0.9	D-13-13 20BBA2	42.3
D-11-14 32CCC1	4.2	D-13-13 21BAA	41.8
D-12-10 09DDD	-9.4	D-13-13 21DCC	44.4
D-12-10 11BCD	16.2	D-13-13 22BAD2	33.9
D-12-10 12CCD1	4.1	D-13-13 22BBD	41.2
D-12-10 21DDC	-22.7	D-13-13 22DAC1	37.2
D-12-10 27BBB	-36	D-13-13 25AAD	23.3
D-12-11 09DBB	10.5	D-13-13 26BAD1	38.6
D-12-11 16DAD	33.7	D-13-13 26BBB	41.9
D-12-12 07CBC	43	D-13-13 26BDD	37.7
D-12-12 08ACC	-5.8	D-13-13 26CDA	38.6
D-12-12 13DBB	-14.8	D-13-13 28AAC	44.5
D-12-12 14ADA	-1.7	D-13-13 28ADC	44.5
D-12-12 16BAD	0	D-13-13 28ADD	7
D-12-12 22ADC	1.2	D-13-13 33ABB	34.7
D-12-12 33AAA	0.5	D-13-13 33DAC	38.1
D-12-13 28DCA	1.6	D-13-13 34AAD	33.5
D-12-13 32AAA	4.4	D-13-13 34DCB	26.7
D-12-14 05CCD	-0.7	D-13-13 35BAA1	34.1
D-12-14 07CAA	2.3	D-13-13 35BCA	40.6
D-13-10 08ADA	-48.5	D-13-13 36DDC	19.6
D-13-11 31CCC1	-2	D-13-14 18CBC	0

Table B-3. 1960 Weighted Residuals

Cadastral Location	Weighted Residual (Ft)	Cadastral Location	Weighted Residual (Ft)
D-13-14 19BBB1	29.6	D-14-13 25DAA1	-3.8
D-13-14 19CAC	3.2	D-14-13 25DAA2	-3.6
D-13-14 20CBA1	9.3	D-14-13 26ACA	-6.8
D-13-14 20CBA2	10.1	D-14-13 26DBB	-5.7
D-13-14 20CBB	4.2	D-14-13 34ADC	-2.7
D-13-14 20CCB	2.9	D-14-13 34DDC	-1.2
D-13-14 21DCD	8.1	D-14-13 34DDD	-1.1
D-13-14 29BDB	3.7	D-14-13 35ADC	-1.7
D-13-14 29DDC2	6.3	D-14-13 35CAA	-2.7
D-13-14 30BBD	7.4	D-14-13 35CAB	-0.6
D-13-14 30CCC1	3.2	D-14-13 35CAC1	-2.2
D-13-14 30DBB1	17	D-14-13 35CCC	-2.2
D-13-14 31ACA	7	D-14-13 35CDB	-4.2
D-13-14 31DBA1	7.6	D-14-13 36ACA1	-9.7
D-13-14 32BAB1	1.7	D-14-13 36BAD	-9.6
D-13-14 32BDA	2	D-14-13 36CAC	-0.8
D-13-14 32DBA1	3	D-14-13 36DCD	0.6
D-13-14 32DCA1	3.7	D-14-14 01DDA1	0.5
D-13-14 33CBD	2.7	D-14-14 02ACD1	0.7
D-13-14 33CDC	4.4	D-14-14 02BDB	1.3
D-13-14 34ADA1	1.4	D-14-14 02DCA1	3.1
D-13-14 34CAD2	3.8	D-14-14 03ADC	0.5
D-13-14 35BAC1	-1.9	D-14-14 03CBC	-0.6
D-13-14 35BAD	-0.4	D-14-14 04AAD1	0.5
D-13-14 35BBA	0	D-14-14 05ADB1	1.8
D-13-14 36CBD	4.5	D-14-14 05DAC1	2.2
D-13-14 36CCD	7.3	D-14-14 05DCB	1.9
D-13-15 19CDD	4	D-14-14 07AAA	5.5
D-13-15 22CAD1	13.8	D-14-14 07DDA1	-9.2
D-13-15 22CDC	22.8	D-14-14 08ADA	0.6
D-13-15 25CAD	-1.8	D-14-14 08BAA	12.8
D-13-15 27BBA	19.8	D-14-14 08BAB	-26.5
D-13-15 27DDC	8.1	D-14-14 09AAC1	3
D-13-15 28ABD	1.7	D-14-14 09BCD1	0.9
D-13-15 30DDC	-0.3	D-14-14 10ACC1	-0.7
D-14-11 05CCD	0	D-14-14 10ACD	-1.7
D-14-11 08CCC	5.5	D-14-14 10DCB1	-0.3
D-14-11 27AAD	-8.9	D-14-14 10DCB2	-3.3
D-14-11 29DDD	-3.6	D-14-14 11AAC1	2.3
D-14-13 01DAB1	5.1	D-14-14 11BAC1	0.7
D-14-13 03CAC	32.8	D-14-14 11CCB1	-1.4
D-14-13 11DBB	5.2	D-14-14 11DBD1	-1.9
D-14-13 13CBC	-3.2	D-14-14 12AAC1	1
D-14-13 23BDA	-5.2	D-14-14 13ACD	3.6
D-14-13 24DAA	-0.1	D-14-14 13DCD	3.2

Table B-3. 1960 Weighted Residuals.

Cadastral Location	Weighted Residual (Ft)	Cadastral Location	Weighted Residual (Ft)
D-14-14 14ACC1	-3.7	D-15-11 11ADD	14.7
D-14-14 14CAA	-1	D-15-11 11DDD	22.5
D-14-14 14CAC	-3.8	D-15-13 01BCB	-6.3
D-14-14 15BCD1	-0.7	D-15-13 02ACA1	-1.9
D-14-14 15CDB2	-2.4	D-15-13 02CAA	-2.4
D-14-14 15DCA	-2.2	D-15-13 02CCA	0.3
D-14-14 16CBB1	-0.9	D-15-13 02DAB	-6.9
D-14-14 17ACC1	4.2	D-15-13 03DAB	0.2
D-14-14 17CAC	-0.9	D-15-13 10ABD	-1.7
D-14-14 17DBD	-0.8	D-15-13 10DAC	1.7
D-14-14 17DDB	-0.6	D-15-13 11ADB	-2.4
D-14-14 18ADB1	1.6	D-15-13 11CBA	12.5
D-14-14 19BDD2	-3.4	D-15-13 11DDB1	-20.6
D-14-14 20ACA	-2	D-15-13 11DDB2	14
D-14-14 20CBB	0.5	D-15-13 13ABC1	-6.4
D-14-14 21BCC	-5.5	D-15-13 14ACA	-1.7
D-14-14 21CAA	0.5	D-15-13 14CCD	15.5
D-14-14 22ADB1	-2.9	D-15-13 15BDC	9
D-14-14 22CBA1	-0.6	D-15-13 15CCD2	2.3
D-14-14 23AAB	-1.4	D-15-13 15DCC	4.7
D-14-14 24ABD	4	D-15-13 21ABA2	-0.3
D-14-14 24BAA	1.3	D-15-13 21BAD2	-5.8
D-14-14 24BDB	2.3	D-15-13 23CCB2	15.8
D-14-14 24CAA1	3.7	D-15-13 25CDC	-5
D-14-14 24CDD	3.4	D-15-13 26BCC	8.2
D-14-14 24DDD	17.8	D-15-13 27AAC	-11.7
D-14-14 28DAB	-0.7	D-15-13 27ABB1	-5.3
D-14-14 29AAA	-2.2	D-15-13 34ABD	-4.9
D-14-14 30BBD	-7.6	D-15-14 17DCB1	-5.1
D-14-15 01DAC	2.2	D-15-14 18CB	-4
D-14-15 03BBC	-0.9	D-15-14 18CBD	-38.4
D-14-15 07ADC	11.1	D-15-14 19CCC	-27.7
D-14-15 07BDB	2.3	D-15-14 19DBB	-10.1
D-14-15 07DBD	11.5	D-15-14 30ADA	-6
D-14-15 08CBD	17.2	D-15-14 31BBB	-5.8
D-14-15 16BDA	14.3	D-15-14 34BBC	-16.5
D-14-15 18AAC	5.1	D-15-15 25DBC1	3.1
D-14-15 18BAC1	3.7	D-15-16 19ACA	1.8
D-14-15 18CBA	3.4	D-16-10 10DDD	-32.8
D-14-15 18DBA	4.2	D-16-11 08CCC	66.2
D-14-15 21CAD	2.9	D-16-13 34AAB2	0.9
D-14-15 26AAB	2.5	D-16-13 35ADC	-0.4
D-14-15 29CBB	10.8	D-16-13 35BAB	-3.6
D-14-15 32BBB	-0.9	D-16-13 35BBB	8.1
D-15-10 35AAA	-26.2	D-16-13 36AAB	-0.7

Table B-3. 1960 Weighted Residuals

Cadastral Location	Weighted Residual (Ft)
D-16-13 36ACA	0
D-16-13S02BBA2	-12
D-16-13S02BDC	-4.4
D-16-14 07BAB	-1.9
D-16-14 07CCD	-1.3
D-16-14 17BCC	-1
D-16-14 17DAD	-6.3
D-16-14 18BDC	0.1
D-16-14 19ACD	0.3
D-16-14 19BBA1	0.3
D-16-14 19BCB	-0.4
D-16-14 19CBC	0.8
D-16-14 19CCD	4.6
D-16-14 20ACB	1.5
D-16-14 20ADA	0.9
D-16-14 20BBB	0.8
D-16-14 20CCC	5.4
D-16-14 25CBA	1.7
D-16-14 29ADA	0.9
D-16-14 29BCC	-0.8
D-16-14 30ACC	1.6
D-16-14 30CBB	5.8
D-16-14N06DCC	-2.1
D-16-16 09DCD1	7.4
D-17-13 01CAB	-2.3
D-17-13 01CDC	0.1
D-17-14 05ABA	4.6
D-17-14 07CCC	0.7
D-17-14 28DDA	-6.4
D-17-14 29CCA	1.2
D-17-15E07CDB1	-1.2
D-18-13 01CBD	0.9
D-18-13 01CDA	0.9
D-18-13 10AAD	2.1
D-18-13 10ADC	-4
D-18-13 10DCC	5.1
D-18-13 14BDB	2.3
D-18-13 24BBB2 UNSURV	2.9
D-18-13 26BA UNSURV	1.6
D-18-13 26CCD UNSURV	2.3
D-18-13 27ADC1UNSURV	2.4
D-18-13 36BCC	0.7
D-18-14 08BDB	0.5
D-19-13 05ACA1	3.9

Table B-4. 1983 Weighted Residuals

Cadastral Location	Weighted Residual (Ft)
D-09-10 29CDA PZ1	12
D-09-10 29CDA PZ2	-8.8
D-10-10 01BBB PZ1	-6.8
D-10-10 01BBB PZ2	-7.8
D-10-10 01BBB PZ3	-5.1
D-10-10 04BBB PZ1	-1.5
D-10-10 04BBB PZ2	-8.7
D-10-10 05DBA	-20.2
D-10-10 20DCC	-27.7
D-10-11 19BDB PZ1	0.4
D-10-11 19BDB PZ2	1.5
D-10-13 12DDA	4.1
D-10-14 06DCA	4.9
D-10-14 17ABB	3.3
D-10-14 19AAA	3.2
D-10-14 29DCA	21.6
D-11-10 15AAA	-3.7
D-11-10 22DDD2	-3.8
D-11-10 27CDC1	0.3
D-11-10 27DAA	4.1
D-11-11 09ACD PZ1	5
D-11-11 09ACD PZ2	5
D-11-11 23BBB PZ1	10.1
D-11-11 23BBB PZ2	10.4
D-11-12 31BCC PZ1	11.9
D-11-12 34DDC	1.4
D-11-14 04CCA	1.4
D-11-14 09BBD	2.2
D-11-14 21BBA	3.8
D-11-14 28ABD1	0.2
D-12-10 04DCC	-0.5
D-12-10 09DCD	-2.1
D-12-10 09DDD	-15.6
D-12-10 12CCD2	-5.5
D-12-10 12CCD3	-8.8
D-12-10 31DCD	-11.2
D-12-10 33CDC1	-14.1
D-12-10 33CDC2	-3.5
D-12-11E30CDD	-17.4
D-12-11E30DDD1	-17.5
D-12-11E30DDD2	-52.6
D-12-12 11DBD	0.8
D-12-12 12ABB	-2.6
D-12-12 13DBB	8.1
D-12-12 14BAC	7.3
D-12-12 14DDD	3.3
D-12-12 21AAA	6.8
D-12-12 21BDD	13.5
D-12-12 22ADC	39.5
D-12-12 27CBB	11.2
D-12-12 34BAA	13.3
D-12-12 36ADD	7.1
D-12-12 36BAB2	5.4
D-12-12 36CDC2	5.4
D-12-13 04CBD	7.2
D-12-13 07CBB	4
D-12-13 07DDD	3.3
D-12-13 08CAD	6.4
D-12-13 12DAA	5.9
D-12-13 13BCB	8.9
D-12-13 13CDD	5.3
D-12-13 13DAC	11.6
D-12-13 16BAD	8.5
D-12-13 17AAA	6.8
D-12-13 18BCC	1.6
D-12-13 20DAD	-40.6
D-12-13 22BBB	9.6
D-12-13 23CCC2	11.9
D-12-13 23DCA	6.9
D-12-13 24CBD1	11.1
D-12-13 24CBD2	5.8
D-12-13 25BCD	3.2
D-12-13 26CDB	2.9
D-12-13 26DAD	5.4
D-12-13 31BAA	7.1
D-12-13 31CCD	11.7
D-12-13 32BCD	9.2
D-12-13 35BAB	1.7
D-12-13 35DCD	7.7
D-12-13 36BCC	2.8
D-12-14 05ACC	-2.8
D-12-14 05CCD	-4.4
D-13-10 06DDC	-16.1
D-13-11 30CCC	14.9
D-13-11 31CCC1	18.5
D-13-11 31CDD1	12.5
D-13-12 02AAB2	4.6
D-13-12 12ABA	9

Table B-4. 1983 Weighted Residuals

Cadastral Location	Weighted Residual (Ft)	Cadastral Location	Weighted Residual (Ft)
D-13-12 12CAA	8.1	D-13-14 34ABB	17
D-13-13 01BBB	3.8	D-13-14 34ACB2	13.8
D-13-13 06DDD	5.2	D-13-14 34CAD2	18.6
D-13-13 08BAA	38.6	D-13-14 34DCC3	5.7
D-13-13 08DCB	6.7	D-13-14 35ADD	3.7
D-13-13 12ACB	5.4	D-13-14 35BAD	-8.4
D-13-13 13BBA	2.6	D-13-14 35CCA	6.4
D-13-13 14ABA	45.9	D-13-14 36CBD	25.3
D-13-13 14ABD	46.7	D-13-14 36CCD	28.9
D-13-13 14DDC2	5.4	D-13-15 22CAD1	-1
D-13-13 15DAA	7	D-13-15 22CDC	15.6
D-13-13 15DAC	3.8	D-13-15 27DDC	16.7
D-13-13 16AAA	39.3	D-13-15 28AAA	1.4
D-13-13 16DDA	43.3	D-13-15 30AAD	-1.2
D-13-13 17AAA	7.7	D-13-15 30DBD	-20.3
D-13-13 17ABC	6.7	D-13-15 30DDC	-0.8
D-13-13 19CDC	5.8	D-13-15 31ADA2	-2.6
D-13-13 20BBD	46.1	D-13-15 31CBB	30.9
D-13-13 23DBC	45.6	D-13-15 33CBB	-0.9
D-13-13 24DBD2	3	D-13-15 34AAC	1
D-13-13 25ABB	20.2	D-13-15 34CDB1	-3
D-13-13 25CDC	5.7	D-13-15 34CDB2	-4
D-13-13 26CAD	30.2	D-14-10 11AAA	6.4
D-13-13 28ADC	40.2	D-14-11 05CCD	15.9
D-13-13 28CCB	50	D-14-11 06CCD	23.6
D-13-13 33ABB	38.2	D-14-11 06DCC	18.3
D-13-13 33DAC	36.1	D-14-11 07BAD	16.7
D-13-13 35ADB	34.3	D-14-11 08CCC	14.2
D-13-13 35CCA	36.3	D-14-11 22CBB	4.3
D-13-13 36BBA	6.1	D-14-11 27AAD	5.6
D-13-13 36DDC	27.8	D-14-11 27BCC	3.8
D-13-14 18CBC	-3.3	D-14-11 29DDD	8.3
D-13-14 20CCD	-4	D-14-11 33CAA	1.4
D-13-14 27BAC2	-10.5	D-14-11 33CCD	12.6
D-13-14 27BAC3	-13.6	D-14-11 33DCD	16.7
D-13-14 28DDB	3.6	D-14-11 34AAD	1.7
D-13-14 29CBB	-2.1	D-14-11 34BBC1	12.8
D-13-14 30CCC1	3.9	D-14-11 34BBC2	3.5
D-13-14 30CCC2	9.4	D-14-11 34CCC	15.6
D-13-14 31CAC2	24.8	D-14-13 03CAC	31.8
D-13-14 32DCA1	11.6	D-14-13 03DCB1	10.2
D-13-14 32DCA2	1.9	D-14-13 11BAD	7.7
D-13-14 33ADD2	3.5	D-14-13 11DBB	3.1
D-13-14 33CBD	15.1	D-14-13 12DBD	4.8
D-13-14 33CDC	14.8	D-14-13 13CBC	-1.6

Table B-4. 1983 Weighted Residuals

Cadastral Location	Weighted Residual (Ft)	Cadastral Location	Weighted Residual (Ft)
D-14-13 23ACA	-4.3	D-14-14 19BDD1	1.2
D-14-13 23ACC	-1.4	D-14-14 19BDD1	1.2
D-14-13 24DAA	-1.2	D-14-14 19BDD2	-0.1
D-14-13 25CBD	-0.2	D-14-14 20ACA	2
D-14-13 26DBB	0	D-14-14 20BAB	1.7
D-14-13 35CAB	4.1	D-14-14 20CBB	1.3
D-14-13 35CAC1	7.4	D-14-14 20DBA	-0.3
D-14-13 35CDB	5.3	D-14-14 21BCC	1.1
D-14-13 36ACA1	-37.9	D-14-14 21CAA	1.7
D-14-13 36ACA2	-11.9	D-14-14 22ADB2	0.6
D-14-13 36BAD	-3.5	D-14-14 22CBA1	0
D-14-13 36CAC	1.5	D-14-14 22CBA2	-0.1
D-14-13 36DCD	-2.6	D-14-14 22DBC	-1
D-14-14 02BBB	3.5	D-14-14 24BAA	4.7
D-14-14 02BDB	8.2	D-14-14 24CAA1	7.6
D-14-14 03ADC	6.7	D-14-14 24CDD	4.8
D-14-14 03CBC	3.2	D-14-14 24DDD	19
D-14-14 03DBD2	12.8	D-14-14 28DAB	-0.5
D-14-14 04AAD1	5.3	D-14-14 29AAA	1.9
D-14-14 04AAD2	5.3	D-14-14 30BBD	-11.9
D-14-14 04CDB	3.8	D-14-14 30BBD	-11.9
D-14-14 04DAC2	1.2	D-14-14 32CDB	-15.2
D-14-14 05ADB1	3.4	D-14-14 35AAA	3.3
D-14-14 05ADB2	4.6	D-14-15 02DDA1	-11.4
D-14-14 07AAA	7.3	D-14-15 03DDC	-12.2
D-14-14 08ADA	7	D-14-15 04BAA1	-6.3
D-14-14 08BAA	9.5	D-14-15 04CCD	-18.1
D-14-14 08BAB	-26.7	D-14-15 04DAD	-6.2
D-14-14 09AAC2	12.4	D-14-15 06BBB	7.2
D-14-14 09ABC	2.3	D-14-15 07ADC	47.4
D-14-14 10ACD	9.3	D-14-15 07BBA3	11.8
D-14-14 10BCC	7.2	D-14-15 08CBD	56.8
D-14-14 10DCB2	7.8	D-14-15 09BDD	-19.4
D-14-14 10DCB3	3	D-14-15 09DCC1	92.6
D-14-14 11CCB2	2.5	D-14-15 10BDD	-5.2
D-14-14 14CAA	3.6	D-14-15 10CCC	-18
D-14-14 14CAC	6.5	D-14-15 14ACB1	6.4
D-14-14 15BCD2	1.4	D-14-15 15AAD	-0.6
D-14-14 15CDB2	0.7	D-14-15 15BAC	-19
D-14-14 15DCA	0.2	D-14-15 15CBB	-3.8
D-14-14 17ACC2	2.9	D-14-15 15DAD	1.5
D-14-14 17CAC	0.1	D-14-15 16CDB	30.7
D-14-14 17DBD	-0.6	D-14-15 17CAA	61.1
D-14-14 18ADB1	1.8	D-14-15 17CCD	45
D-14-14 18ADB2	2.3	D-14-15 18AAC	15.8

Table B-4. 1983 Weighted Residuals

Cadastral Location	Weighted Residual (Ft)	Cadastral Location	Weighted Residual (Ft)
D-14-15 18BAC2	12.5	D-15-14 03DAD	7
D-14-15 18CBA	11.9	D-15-14 04CAB1	-15.2
D-14-15 18CDA2	16.3	D-15-14 04CAB2	-16.9
D-14-15 18DBA	7.7	D-15-14 06CAA	-14.6
D-14-15 18DDD	41.5	D-15-14 06DBB2	-14.3
D-14-15 19ABD	-5.4	D-15-14 06DCB2	7.3
D-14-15 20BBC	-18.2	D-15-14 07CAB2	-13.1
D-14-15 21ADB	16.7	D-15-14 07CBC	-23.6
D-14-15 21DAD	3.8	D-15-14 08DDD	-31.2
D-14-15 26CBC	4.8	D-15-14 10DAC	-16.3
D-14-15 28CBA	-0.3	D-15-14 10DCD1	-29.2
D-14-15 28CCC	2.8	D-15-14 10DCD2	-29.3
D-14-15 28DDD	-0.6	D-15-14 13BBA	-19.7
D-14-15 29CBB	6.7	D-15-14 13BCC	-21.7
D-14-16 05DBD3	-0.9	D-15-14 13CBC	-22.1
D-14-16 07CCC	14.2	D-15-14 17AAD2	-15.2
D-15-10 33CBC2	-0.8	D-15-14 17ADD1	-12.7
D-15-10 35AAA	-34	D-15-14 17ADD2	-12.4
D-15-11 09AAA	5.3	D-15-14 18ABB	-12.1
D-15-11 11ADD	25	D-15-14 18BBB	12.6
D-15-11 11BBB	2.4	D-15-14 18CBD	-74.2
D-15-11 12CCC	10.2	D-15-14 19BAD	-16.3
D-15-11 20AAA	3.1	D-15-14 19CCC	-44.1
D-15-11 22CCC	-1.3	D-15-14 19DBB	-18.3
D-15-13 01ACC	-78.2	D-15-14 25BAA	-10.3
D-15-13 01BCB	12.8	D-15-14 27CBB	-2
D-15-13 02BBA1	4.1	D-15-14 27CBC	-6.5
D-15-13 11ADC	-5.6	D-15-14 29BAA	-8.5
D-15-13 11CBA	48.8	D-15-14 29BBB	-16.6
D-15-13 11DDB1	-58.6	D-15-14 29BDD	-5.5
D-15-13 12DBA	-17.2	D-15-14 30CBC	-9.4
D-15-13 13AAB	-8.9	D-15-14 31BCB	-9.7
D-15-13 13ABC1	-16.2	D-15-14 31CBB	-7.6
D-15-13 13ABC2	1.5	D-15-14 34BBC	-29.9
D-15-13 13CBA	0.8	D-15-15 04BBA	1.6
D-15-13 13CCC	-1.9	D-15-15 05BAB	4
D-15-13 13DCB	-47.3	D-15-15 06BBB	1.9
D-15-13 14BCC1	-2.3	D-15-15 15CAA	13
D-15-13 15CAC	72.1	D-15-15 16CBB PZ1	-4.9
D-15-13 21BAD2	-7.8	D-15-15 16CBB PZ2	-1.6
D-15-13 23AAD2	13.5	D-15-15 16CBB PZ3	20.2
D-15-13 23CCB2	49.5	D-15-15 18DCA	-3.8
D-15-13 27AAC	1.8	D-15-15 19BCA	-12.9
D-15-13 27ABB2	9.9	D-15-15 25DBC1	4.3
D-15-14 01DBA	0.1	D-15-15 25DBC2	4.3

Table B-4. 1983 Weighted Residuals

Cadastral Location	Weighted Residual (Ft)	Cadastral Location	Weighted Residual (Ft)
D-15-15 29DAC	3.1	D-16-15 05CBC PZ3	-9.8
D-15-15 30AAA	-2.3	D-16-15 09BBB	-2.4
D-15-15 36CDC	8.1	D-16-15 18ABD	-1.3
D-16-11 09ACD	6.6	D-16-15 27CCC	4.3
D-16-13 26AAA	6.5	D-16-16 09DCD1	8.4
D-16-13 26CAA	-1.5	D-17-13 01ABB	9.1
D-16-13 28ADD	13.3	D-17-13 24DAC	-2.3
D-16-13 34AAB2	-1.3	D-17-13 25BAB	0.5
D-16-13 35BAB	-1.3	D-17-13 25BCC	1.7
D-16-13 35BBB	-32.7	D-17-13 25CCD	3
D-16-13S02BBA2	9.7	D-17-13 25DCD	7.1
D-16-13S02BDC	10	D-17-13 26CAD	3.2
D-16-14 07CCD	-2.1	D-17-13 35DCB	5.2
D-16-14 07DCB2	-1.9	D-17-14 01BAA	-2.2
D-16-14 17BCC	-2.6	D-17-14 02BAA	-17.4
D-16-14 17DAD	-6.5	D-17-14 04ACA	-4.9
D-16-14 18BDC	-4.2	D-17-14 04BCB	-4.4
D-16-14 19ACD	-3.8	D-17-14 05CDA1	-1.3
D-16-14 19BBA1	0.1	D-17-14 05CDA2	-1.1
D-16-14 19BCB	-1.4	D-17-14 06ACD	-1.2
D-16-14 19CBC	-1.7	D-17-14 06BCB	-3
D-16-14 19CCD	-5.8	D-17-14 07ADB	-5.5
D-16-14 20ADA	-3.2	D-17-14 07ADD	-5.2
D-16-14 20CCC	5.1	D-17-14 07CCC	-2.7
D-16-14 21CCB	0.9	D-17-14 07DCD	-3.1
D-16-14 21DCD	4.5	D-17-14 08BDD2	-1.6
D-16-14 25AAA	-5.9	D-17-14 18DAD	-0.5
D-16-14 25BBB	-3.7	D-17-14 19CDD	-3.9
D-16-14 25CCD	-9.9	D-17-14 19DBD	-1.4
D-16-14 25DDD2	-5.8	D-17-14 21ACD	0.6
D-16-14 26CCC	-6.9	D-17-14 30ACA	2.3
D-16-14 28CCB	-5	D-17-14 30DBD	-0.3
D-16-14 29ADA	0.9	D-17-15 02DCD	2.5
D-16-14 29BDC	-2	D-18-13 01AAB	7.1
D-16-14 30CDC	-5.4	D-18-13 01CBC	14
D-16-14 30DCC	-6.4	D-18-13 01CDA	2.5
D-16-14 33ACC	-2.9	D-18-13 10AAC	7
D-16-14N04CDD	-8.9	D-18-13 10DCA	19
D-16-14N06CCD	-4.1	D-18-13 10DCD	10
D-16-14S05CAC	0.4	D-18-13 12CDB UNSURV	9.8
D-16-14S06CBA	5.1	D-18-13 12DCA1UNSURV	3.3
D-16-14S06CCD	-0.4	D-18-13 12DCA2UNSURV	3.3
D-16-15 01DBC	7.7	D-18-13 13AAC UNSURV	3.3
D-16-15 05CBC PZ1	2.7	D-18-13 13ABC UNSURV	1.7
D-16-15 05CBC PZ2	-4.9	D-18-13 13BAC	3.2

Table B-4. 1983 Weighted Residuals.

Cadastral Location	Weighted Residual (Ft)
D-18-13 13CBA UNSURV	7.3
D-18-13 14ADC UNSURV	3.9
D-18-13 16BBB	0.4
D-18-13 16CBB	5.1
D-18-13 21BBB1	2
D-18-13 21BCC1	-0.3
D-18-13 23BAD UNSURV	5.7
D-18-13 24BBB1UNSURV	4.4
D-18-13 24BCB1UNSURV	-0.1
D-18-13 24BCB2UNSURV	9
D-18-13 26AAD	4.5
D-18-13 26BA UNSURV	3.3
D-18-13 26BBD UNSURV	4.3
D-18-13 26CCD UNSURV	2
D-18-13 26DBA UNSURV	2.4
D-18-13 27ADA2UNSURV	5.3
D-18-13 27ADC1UNSURV	2.6
D-18-13 28BBB2	-11.4
D-18-13 29DCC1	-1.4
D-18-13 29DDC	-26.1
D-18-13 34AC UNSURV	2.6
D-18-13 35CBB2UNSURV	-3.1
D-18-13 36BCC	1.1
D-19-13 03ACC	25.6
D-19-13 03ADC2UNSURV	1.1
D-19-13 05ACA2	1
D-19-13 16BAD	7.6
D-19-13 17DDD	14.9
D-19-13 20CDA UNSURV	19.2
D-19-13 20DBC	-1.1
D-19-13 21BAA	15.3
D-19-13 21CBA	-0.6
D-19-13 29BCC	11.9
D-19-13 29BCC	10.5
D-19-13 29CBA	-2.8

Table B-5. 1999 Weighted Residuals

Cadastral Location	Weighted Residual (ft)
D-09-10 29CDA PZ1	2.9
D-09-10 29CDA PZ2	-14.6
D-10-10 05DBA	-23.3
D-10-10 09BBB	-9.2
D-10-10 20ACC	-13.5
D-10-10 20DCC	-24.2
D-10-10 21BCC	-8.3
D-10-10 34CAB2	-47.8
D-10-10 35CBC	-36.9
D-10-11 17CAB2	-1.4
D-10-11 19BDB PZ1	-4.8
D-10-11 19BDB PZ2	-4.8
D-10-13 12DDA	3.2
D-10-14 06DCA	3.2
D-10-14 17ABB	2.7
D-10-14 19AAA	2.7
D-10-14 19AAC	2.7
D-10-14 29DCA	9.8
D-11-10 10DDD	-24.8
D-11-10 12ADD	-2.7
D-11-10 13AAA2	-2
D-11-10 14BAA	-1.8
D-11-10 15AAA	-5
D-11-10 20DDD	-0.4
D-11-10 22DDD2	-14.5
D-11-10 27CDC1	-8.7
D-11-10 27DAA	-6.5
D-11-11 09ACD PZ1	2.3
D-11-11 09ACD PZ2	1
D-11-11 16CDD2	-3.7
D-11-11 17DDD	-7.4
D-11-11 21AAA2	-3.7
D-11-11 21ACD	-5.6
D-11-11 22DCC	-3
D-11-11 22DCD	-2.4
D-11-11 27ACC	-2.4
D-11-11 28ACC2	-4.3
D-11-11 28DDD2	-3.3
D-11-11 34ADD2	1.5
D-11-11 35DDD	-11.8
D-11-11E07DDD	-23.5
D-11-11W31DAD	-25.2
D-11-12 31DDD1	-29.6
D-11-12 31DDD2	-8.9
D-11-13 34DCB	9
D-11-14 04ABC	13.3
D-11-14 04CCA	0.1
D-12-10 04ACD	5.4

Cadastral Location	Weighted Residual (ft)
D-12-10 04DCC	-3.1
D-12-10 09DCD	-4
D-12-10 09DDD	-20.7
D-12-10 12CCD2	-7.4
D-12-10 12CCD3	-15.7
D-12-10 14DCC	-26
D-12-10 30AAB1	-0.7
D-12-10 31BDB	0.3
D-12-10 31DCD	-5.2
D-12-10 33CDC1	-9.9
D-12-10 33CDC2	-2.1
D-12-10 34CCA	-7.8
D-12-11 01DDA PZ1	12.8
D-12-11 01DDA PZ2	-32.5
D-12-11 09DBB	-3.2
D-12-11 12DAD	45.7
D-12-11 15ACA	-46.6
D-12-11 16DAD	-17.4
D-12-11 17ADD	-28.8
D-12-11E19DDD	-14.2
D-12-11E30CDD	-14.3
D-12-11E30DCD1	-22
D-12-11E30DDD1	-13.9
D-12-11E30DDD2	-42
D-12-12 05DCD	-0.4
D-12-12 05DDD	-7.7
D-12-12 06DAA2	-2.3
D-12-12 08DBA	3.3
D-12-12 12ABB	0.5
D-12-12 14DDD	4.4
D-12-12 16BBA1	6.3
D-12-12 21ADB	7.7
D-12-12 21BDD	14.7
D-12-12 21CAD2	7.9
D-12-12 21DCD	7.8
D-12-12 22ADC	38.1
D-12-12 22DAC2	6
D-12-12 25CAC1	10.1
D-12-12 25CAC2	9.6
D-12-12 25CCC	11.5
D-12-12 26BCA	5.2
D-12-12 26DBD	32.3
D-12-12 35ADD2	4.7
D-12-12 36ADD	5.8
D-12-12 36BAB2	5.8
D-12-12 36CDC2	4.2
D-12-13 07DDD	5.5
D-12-13 08CAD	9

Table B-5. 1999 Weighted Residuals.

Cadastral Location	Weighted Residual (ft)	Cadastral Location	Weighted Residual (ft)
D-12-13 12DAA	4	D-13-13 14ABD	31.1
D-12-13 17BCD	6.8	D-13-13 14CAD	17.5
D-12-13 18BCC	3.5	D-13-13 14DDC2	4.2
D-12-13 23CCC2	9.3	D-13-13 15DAA	5.5
D-12-13 24CBD1	9	D-13-13 15DAC	3.5
D-12-13 24CBD2	4.8	D-13-13 16AAA	31.7
D-12-13 25BCD	2.3	D-13-13 16BDB	6.4
D-12-13 26DAD	3.1	D-13-13 16CCD	5.9
D-12-13 27DBB	4	D-13-13 16DDA	20.3
D-12-13 29BCA	6.2	D-13-13 17AAA	7
D-12-13 31BAA	3.1	D-13-13 17ABC	6
D-12-13 31CCD	9.2	D-13-13 17BAD	5.5
D-12-13 31DCD2	9	D-13-13 17BDD2	11.8
D-12-13 32AAA	6.3	D-13-13 19ADA	5.9
D-12-13 32BCD	6.8	D-13-13 19CDC	4.5
D-12-13 36BCC	1.7	D-13-13 20DDC2	42.4
D-13-10 06DDC	-7.8	D-13-13 21BAA	34.1
D-13-10 14BCD	-2.8	D-13-13 21BAA	34.1
D-13-10 16DCD	0.8	D-13-13 22ABD	36
D-13-10 21ACA1	3.7	D-13-13 23BBA	35.6
D-13-10 21ACA2	3.8	D-13-13 23BBA	35.6
D-13-10 24ABB	0.6	D-13-13 23BBD	31.4
D-13-10 24DCC	12.1	D-13-13 23BDD2	31.1
D-13-10 25ACD	18.8	D-13-13 23DBC	35.4
D-13-10 25BDC2	4.5	D-13-13 24DBD2	4
D-13-10 25DCC	20.6	D-13-13 25ABB	12.3
D-13-11 17BCB PZ1	0.1	D-13-13 26BAD2	33.8
D-13-11 17BCB PZ2	1.4	D-13-13 26CDD	26.5
D-13-11 18DDC1	3.8	D-13-13 26DAC1	29.6
D-13-11 20DCC	4.7	D-13-13 28ADC	34.4
D-13-11 30CCC	17.9	D-13-13 28CCB	42.7
D-13-11 31CCC1	21.5	D-13-13 33ABB	31.2
D-13-11 31CDD1	7.6	D-13-13 34BBA1	29
D-13-12 02AAB2	8.4	D-13-13 34BDC	19.7
D-13-12 03DDD	-2.5	D-13-13 35ABD	26
D-13-12 12AAB	5.1	D-13-13 35ADB	14.6
D-13-12 12ABA	9	D-13-13 35ADB	14.6
D-13-12 12CAA	7.6	D-13-13 35CCD	8.2
D-13-12 14DCB	0.1	D-13-13 36DDC	10.9
D-13-13 06DDD	3.7	D-13-14 19BBB1	-8.7
D-13-13 08BAA	29.4	D-13-14 19DDA1	-4
D-13-13 08DCB	5.7	D-13-14 19DDB2	-4.4
D-13-13 09CAD	6.8	D-13-14 19DDD	-1
D-13-13 09DAD	6.8	D-13-14 20CCC	-3.3
D-13-13 12ACB	4.6	D-13-14 20CCD	-0.8
D-13-13 13BBA	1.5	D-13-14 20CDD2	-1.5
D-13-13 13CDC	3.7	D-13-14 25CCA	-10.2
D-13-13 14ABA	30.9	D-13-14 27BAC2	-14.1

Table B-5. 1999 Weighted Residuals

Cadastral Location	Weighted Residual (ft)	Cadastral Location	Weighted Residual (ft)
D-13-14 27BAC3	-16.7	D-14-13 24DAA	-6.5
D-13-14 27DDC3	-6.1	D-14-13 25CBD	-5.5
D-13-14 28DAD2	-2.4	D-14-13 25DAA1	-10.2
D-13-14 29ABB	-0.2	D-14-13 26DBB	-14.6
D-13-14 29CBB	-1.4	D-14-13 35ADA	-42
D-13-14 30BBD	2.9	D-14-13 35CAC1	-2.5
D-13-14 30CAA1	3.3	D-14-13 35CDC1	-2.9
D-13-14 30CAA1	3.3	D-14-13 35DDA	-6.8
D-13-14 30DBB1	13.7	D-14-13 35DDB1	-6.8
D-13-14 30DBB2	5.5	D-14-13 35DDB2	-6.3
D-13-14 31BDC2	21.9	D-14-13 36BAD	-76.8
D-13-14 31DBA3	3.6	D-14-13 36CAC	-4.1
D-13-14 32BAB2	15	D-14-13 36CCB	-7.1
D-13-14 32BBA	2.6	D-14-14 02ACD2	11.3
D-13-14 32DBA2	6.3	D-14-14 05DAC2	2.2
D-13-14 32DCA2	2	D-14-14 07AAA	-0.4
D-13-14 33ADD2	4.6	D-14-14 07BAA	9.5
D-13-14 33CBD	9	D-14-14 07DDA2	-3.9
D-13-14 34AAD	-7.2	D-14-14 08BAA	-3.8
D-13-14 36BCC	1.1	D-14-14 08BAB	-32.6
D-13-14 36CBD	39.9	D-14-14 09AAC2	0.4
D-13-14 36CCD	40.6	D-14-14 09ABC	-13.5
D-13-14 36CDB	5.8	D-14-14 10AAB	-1.6
D-13-15 22CAD1	7.4	D-14-14 10BCC2	-7.6
D-13-15 22CDC	15.6	D-14-14 11DBD2	-9.4
D-13-15 27DDC	1.6	D-14-14 12BDC1	4.5
D-13-15 30AAD	-0.5	D-14-14 12BDC2	12.5
D-13-15 31ADA2	-5.4	D-14-14 14CAC	-13.4
D-13-15 31DDC	43.8	D-14-14 15DAB	-2.2
D-13-15 33BDC1	-2.1	D-14-14 16CCC PZ1	-2.9
D-13-15 33CDB	-3.7	D-14-14 16CCC PZ2	-1.2
D-13-15 34CDB1	-1.9	D-14-14 16CCC PZ4	-5.5
D-13-15 35DDD	-2.1	D-14-14 17ACC2	-4.4
D-14-10 11AAA	10.2	D-14-14 17CAC	-6.7
D-14-10 12ABA	10	D-14-14 17DBD	-6.9
D-14-11 06CCD	27.2	D-14-14 19BDD2	-8.5
D-14-11 06DCC	20.9	D-14-14 20ACA	-31.1
D-14-11 07BAD	21.9	D-14-14 20BAB	-4.3
D-14-11 08CCC	17.8	D-14-14 20CBB	-6.2
D-14-11 22CBB	7.2	D-14-14 21BCC	-16.3
D-14-11 27AAD	15.4	D-14-14 22CBA2	-6.4
D-14-11 27CDA	4.4	D-14-14 24CAA1	-0.2
D-14-11 29DDD	21.9	D-14-14 24DDD	-7
D-14-11 33CAA	2.3	D-14-14 28DAB	-6.2
D-14-11 33CCD	30.2	D-14-14 29AAA	-23.5
D-14-13 03CAC	14.9	D-14-14 29ACB2	-0.4
D-14-13 11BAD	6.2	D-14-14 30ABD	-41.5
D-14-13 12DBD	-4.9	D-14-14 36AAD	-6.8

Table B-5. 1999 Weighted Residuals

Cadastral Location	Weighted Residual (ft)	Cadastral Location	Weighted Residual (ft)
D-14-14 36DDB	0.1	D-15-10 35AAA	-47.5
D-14-15 01CDA	-3.7	D-15-11 05CDD	2.7
D-14-15 01DCC	3.1	D-15-11 09AAA	10.3
D-14-15 04DAD	-35.4	D-15-11 11BBB	4.4
D-14-15 04DDD	-46.9	D-15-11 12CCC	12.6
D-14-15 05ABA	-34.9	D-15-11 15CCC	1.1
D-14-15 05DBA	15.4	D-15-11 20AAA	3.4
D-14-15 07BBA3	12.6	D-15-11 22CCC	-1.5
D-14-15 07DBD	35.9	D-15-11 22DDD	-3.5
D-14-15 08CBD	38.1	D-15-11 30BAC	-5
D-14-15 09ADA	-65.1	D-15-13 01DCC1	-16.2
D-14-15 09BDD	-61.3	D-15-13 02AAA1	-5.4
D-14-15 09DCC2	-9.5	D-15-13 02AAA2	-5.4
D-14-15 10CCC	-65.6	D-15-13 02ACA2	-1.9
D-14-15 15AAD	-28.5	D-15-13 02BBA1	-0.7
D-14-15 15BAC	-125.8	D-15-13 11AAD1	4.8
D-14-15 15BDC	-28.3	D-15-13 11ADC	-16
D-14-15 15CBB	-32.2	D-15-13 11CBA	38.7
D-14-15 15DAD	-25.5	D-15-13 12ACC1	9.8
D-14-15 16BBC	11.5	D-15-13 13ABB2	42.1
D-14-15 16BDA	43.5	D-15-13 13DBD1	22.4
D-14-15 16CDB	-19.1	D-15-13 21CAD	-3.4
D-14-15 17BAC	13.3	D-15-13 35BCD	0.4
D-14-15 17CAA	43.1	D-15-14 01DDB	1.4
D-14-15 17CCD	44.8	D-15-14 03DAD	11.1
D-14-15 18AAC	13.1	D-15-14 04CAB2	-21.5
D-14-15 18BAC2	10.2	D-15-14 07CBC	-35.9
D-14-15 18CDA2	13.6	D-15-14 07CCD1	6.9
D-14-15 20BBC	16.4	D-15-14 08DDD	-40.6
D-14-15 21ADB	-24.1	D-15-14 09BBB2	-43.9
D-14-15 21CBD	-7.7	D-15-14 13BBA	-26.7
D-14-15 21DAD	-8.6	D-15-14 13BCC	-28.2
D-14-15 22ABC	-47	D-15-14 13CBC	-28.1
D-14-15 23CBC	-4.6	D-15-14 17BAC	-41.6
D-14-15 23CCA	-14.4	D-15-14 17BDC	-41.3
D-14-15 26CBC	1.5	D-15-14 18CBC3	16.8
D-14-15 28CBA	-31.9	D-15-14 19BBB	-30
D-14-15 28CCC	-6	D-15-14 25BAA	-16.1
D-14-15 28DDD	-8.9	D-15-14 27CBC	-11.6
D-14-15 29CBB	-18.3	D-15-14 31BBB	-24.7
D-14-15 35BDB	1.3	D-15-14 31BCB	-25.9
D-14-16 04CCA2	0.4	D-15-14 31CBB	-21.5
D-14-16 05DBD3	-2.4	D-15-14 34BBC	-64.6
D-14-16 07CCC	-13.5	D-15-15 04BBA	-2.8
D-14-16 07CDC	-21.5	D-15-15 05BAB	-1.6
D-15-10 33BCC	-3.2	D-15-15 06BDC	3.5
D-15-10 33CBC2	-2	D-15-15 15CAA	1.7
D-15-10 33DBC1	-7.1	D-15-15 16CBB PZ1	-8.9

Table B-5. 1999 Weighted Residuals

Cadastral Location	Weighted Residual (ft)	Cadastral Location	Weighted Residual (ft)
D-15-15 16CBB PZ2	-8.3	D-16-14 31AAD	-5.9
D-15-15 16CBB PZ3	20.1	D-16-14 32ABC	-9.5
D-15-15 17ACB	-10.9	D-16-14 32BDD2	-6.6
D-15-15 19BCA	-18.6	D-16-14 32CDA	-11.4
D-15-15 21DCD	-0.3	D-16-14N04CDD	-20.6
D-15-15 24BBD	2.1	D-16-14N06CCD	-54.8
D-15-15 25DBC2	2.3	D-16-14N06DCC	-16.5
D-15-15 36CDC	8.7	D-16-14S05CAC	-7
D-15-16 29ADD	17.9	D-16-14S06CBA	-10.1
D-16-10 04BDA	-5.1	D-16-14S06CCD	-6.3
D-16-10 12ADB	14.7	D-16-15 01DBC	5.4
D-16-10 13ACA	12.9	D-16-15 05CBC PZ2	-7.5
D-16-11 08BDB	8.5	D-16-15 05CBC PZ3	-15.4
D-16-11 09ACD	8.4	D-16-15 09BBB	-5.9
D-16-13 34AAB2	-1.8	D-16-15 14ACB	-0.6
D-16-13 35BAB	-12.1	D-16-16 08AAB1	4.1
D-16-13 35BBB	-45.8	D-16-16 09DCD2	7.4
D-16-13 36ACC	9.6	D-16-16 16ABA	8.4
D-16-13 36DDD	2.7	D-17-13 01ABB	11.9
D-16-13S02BBA2	-12.3	D-17-13 01ACC2	1.5
D-16-13S02BDC	-10.6	D-17-13 01BAC	-0.6
D-16-14 07BAB	-18.1	D-17-13 01CDD	1
D-16-14 07BBA	-5.6	D-17-13 11DAD	-0.7
D-16-14 07CCD	-23.9	D-17-13 11DDB	-1
D-16-14 17BCC	-16.4	D-17-13 12ACD	-11.2
D-16-14 17DAD	-42.8	D-17-13 12CBC	-1.2
D-16-14 19ACD	-13.4	D-17-13 13ABB	-1.6
D-16-14 19BBA1	-11.8	D-17-13 22AAA	1.5
D-16-14 19BCB	-14.1	D-17-13 24DAC	-26.4
D-16-14 19CBC	-12.8	D-17-13 25BCC	-21.9
D-16-14 19CCD	-35.4	D-17-13 25CCD	-3.4
D-16-14 20ACB	-14.9	D-17-13 26CAD	-5.2
D-16-14 20ADA	-14.6	D-17-14 01BAA	-3.1
D-16-14 20CCC	-16.2	D-17-14 04ACA	-8.2
D-16-14 21CCB	-14.1	D-17-14 04BCB	-9.4
D-16-14 21DBB	-3.2	D-17-14 05CDA2	-3.7
D-16-14 21DCD	-8.4	D-17-14 06AAB	-5.1
D-16-14 25AAA	-12.3	D-17-14 06ACD	-4.7
D-16-14 25BBB	-6.5	D-17-14 07ADB	-7.5
D-16-14 25CCD	-14.3	D-17-14 07DCD	-6.7
D-16-14 25DDD2	-6	D-17-14 18DAD	-4.6
D-16-14 26CCC	-5.2	D-17-14 19DBD	-7.1
D-16-14 28CCB	-14.4	D-17-14 21ACD	-1
D-16-14 29ADA	-7.2	D-17-14 30ACA	-11.4
D-16-14 29BCC	-14.6	D-17-14 31BAC	-26
D-16-14 29BDC	-10.6	D-17-15 02DCD	1.6
D-16-14 30CCC	-20.4	D-18-13 01AAB	2.7
D-16-14 30DCC	-12.9	D-18-13 01ADC	-7.3

Table B-5. 1999 Weighted Residuals

Cadastral Location	Weighted Residual (ft)
D-18-13 01CDA	-0.9
D-18-13 01CDD	-4.3
D-18-13 02DAA	-3
D-18-13 02DCA2	2.2
D-18-13 10DCD	-2
D-18-13 12DCA2UNSURV	-4.7
D-18-13 13ABC UNSURV	-6.1
D-18-13 13CBA UNSURV	-8.7
D-18-13 14BDB2	-4.8
D-18-13 15ACC2	-2.9
D-18-13 16BBB	-6.8
D-18-13 21AAA	-4.7
D-18-13 23BAD UNSURV	-3
D-18-13 26CCD UNSURV	-5.1
D-18-13 26DBA UNSURV	-4.2
D-18-13 27ADA2UNSURV	-2.8
D-18-13 31AAA	-5
D-18-13 34DBC UNSURV	1.4
D-18-13 35CBB2UNSURV	-8.9
D-18-14 06DBA	-1.6
D-19-13 03ADC2UNSURV	-1.7
D-19-13 05ACA1	-2.8
D-19-13 05ACA2	-1.1
D-19-13 05DBD	-25.2
D-19-13 08BBB	-5
D-19-13 17ACA	-8.6
D-19-13 29BCC	-7.1

Appendix C

Hydrographs

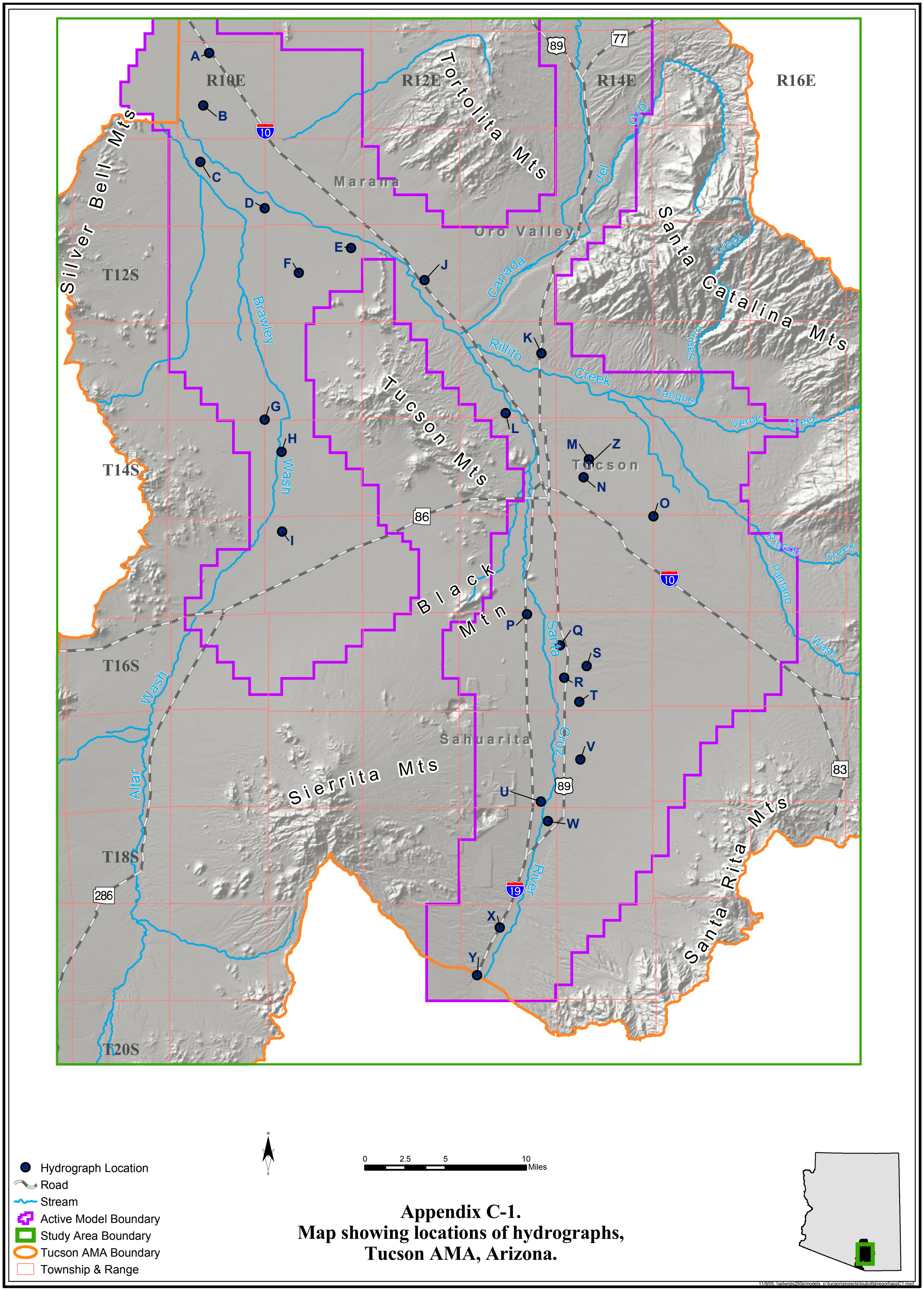

Appendix C-1.
Map showing locations of hydrographs,
Tucson AMA, Arizona.

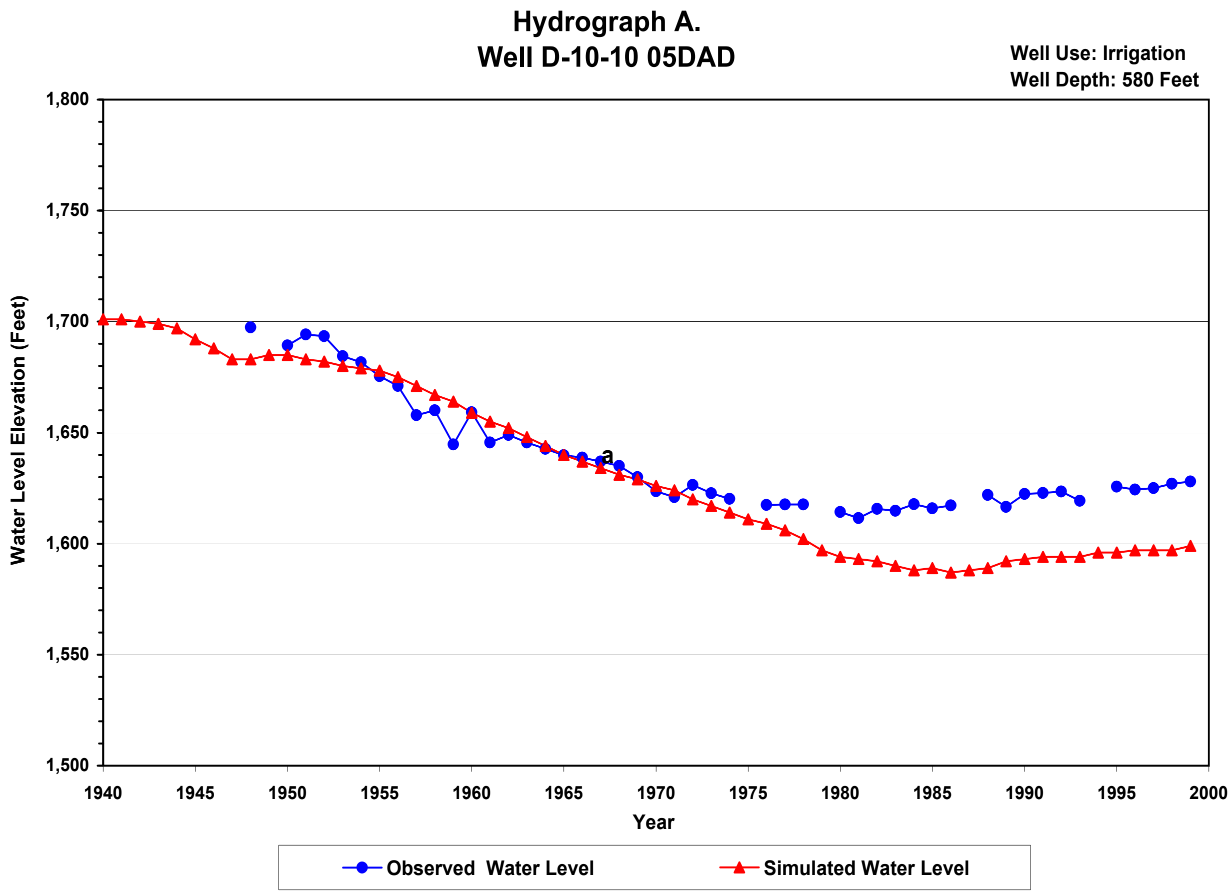
Hydrograph A.
Well D-10-10 05DAD
Well Use: Irrigation
Well Depth: 580 Feet
1,800
1,750
1,700
1,650
1,600
1,550
1,500
Water Level Elevation (Feet)
1940
1945
1950
1955
1960
1965
1970
1975
1980
1985
1990
1995
2000
Year
Observed Water Level
Simulated Water Level

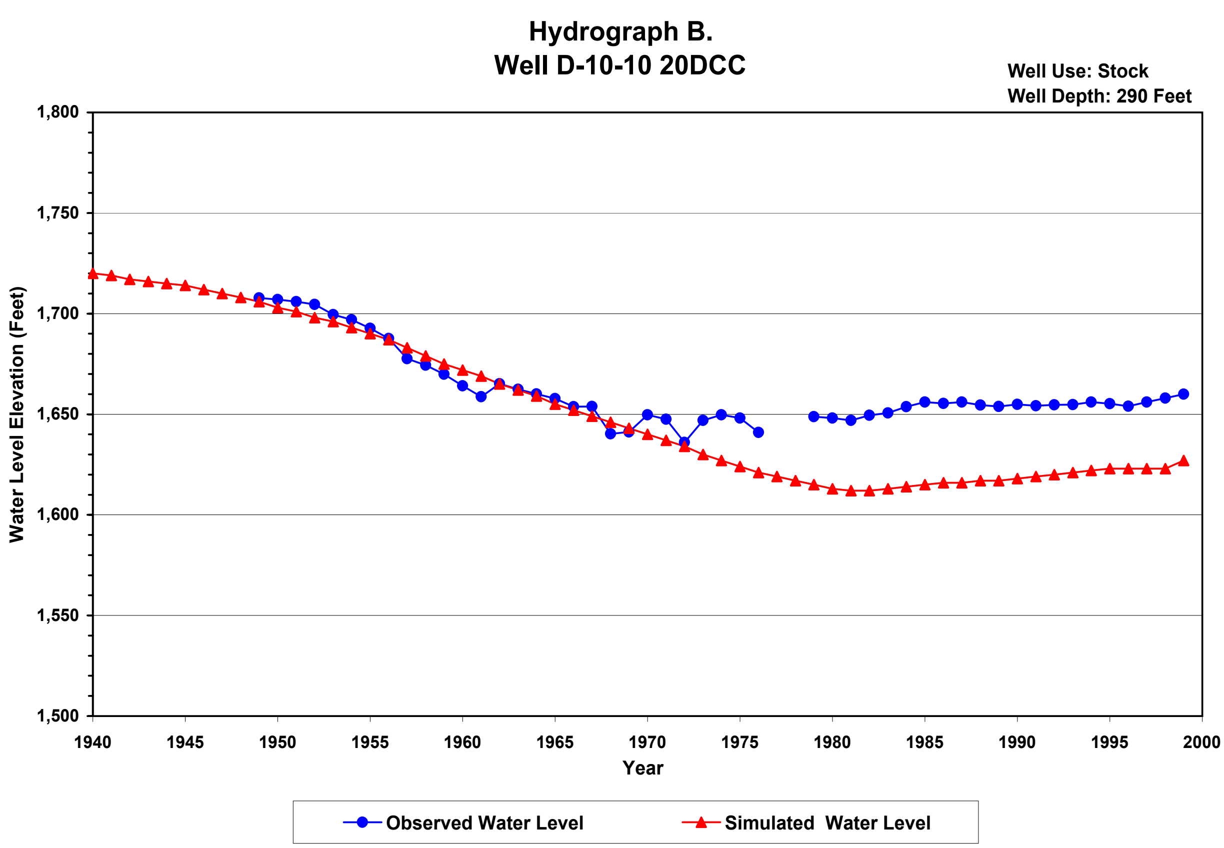
Hydrograph B.
Well D-10-10 20DCC
Well Use: Stock
Well Depth: 290 Feet
1,800
1,750
1,700
1,650
1,600
1,550
1,500
Water Level Elevation (Feet)
1940
1945
1950
1955
1960
1965
1970
1975
1980
1985
1990
1995
2000
Year
Observed Water Level
Simulated Water Level

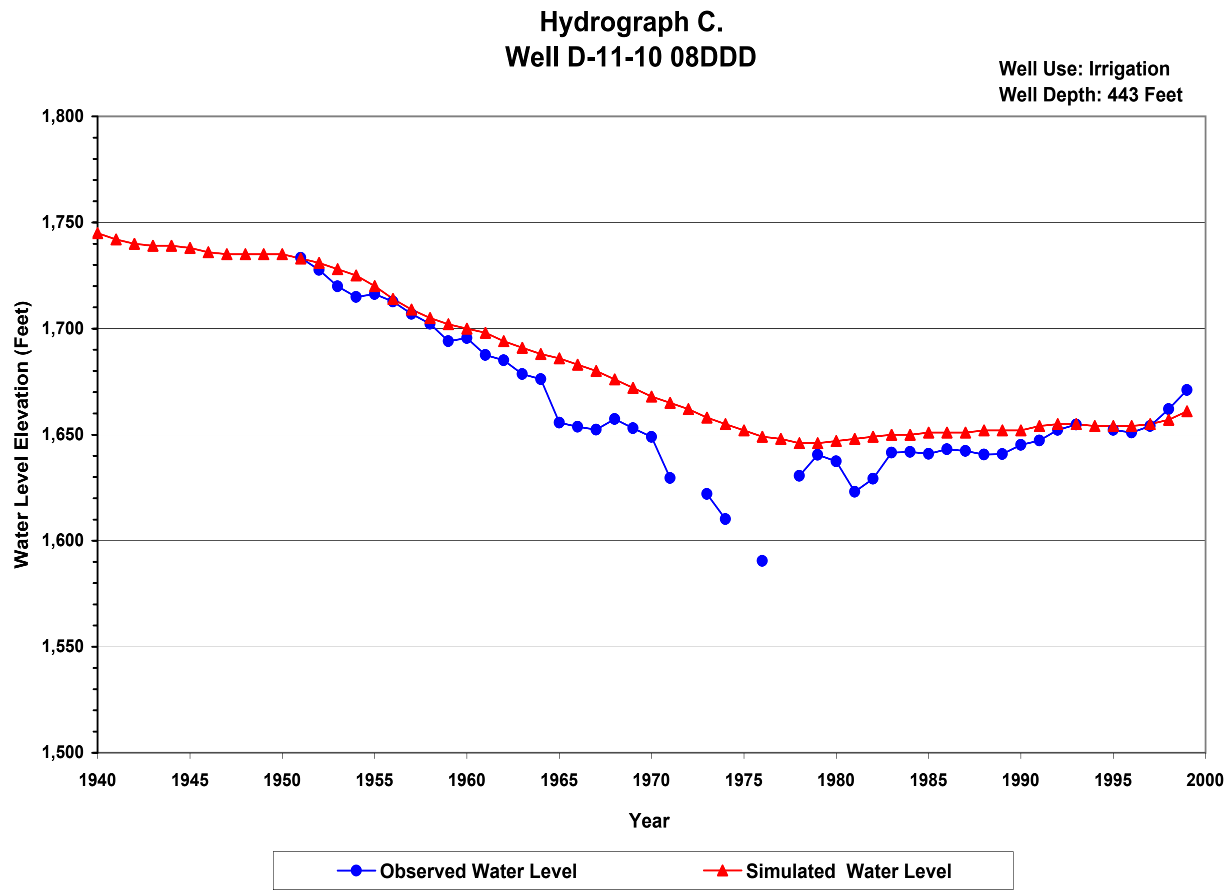

Hydrograph C.
Well D-11-10 08DDD
Well Use: Irrigation
Well Depth: 443 Feet
Water Level Elevation (Feet)
1,800
1,750
1,700
1,650
1,600
1,550
1,500
1940
1945
1950
1955
1960
1965
1970
1975
1980
1985
1990
1995
2000
Year
Observed Water Level
Simulated Water Level

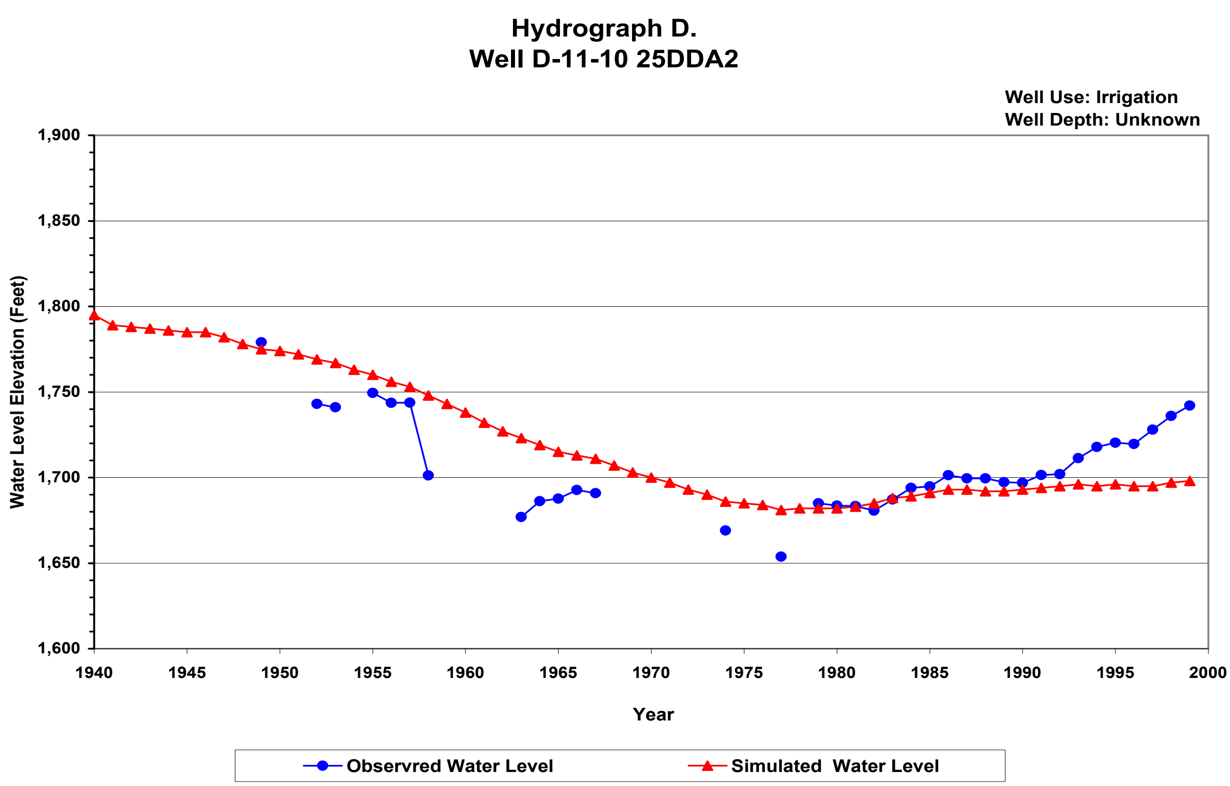

Hydrograph D.
Well D-11-10 25DDA2
Well Use: Irrigation
Well Depth: Unknown
Water Level Elevation (Feet)
1,900
1,850
1,800
1,750
1,700
1,650
1,600
1940
1945
1950
1955
1960
1965
1970
1975
1980
1985
1990
1995
2000
Year
Observervd Water Level
Simulated Water Level

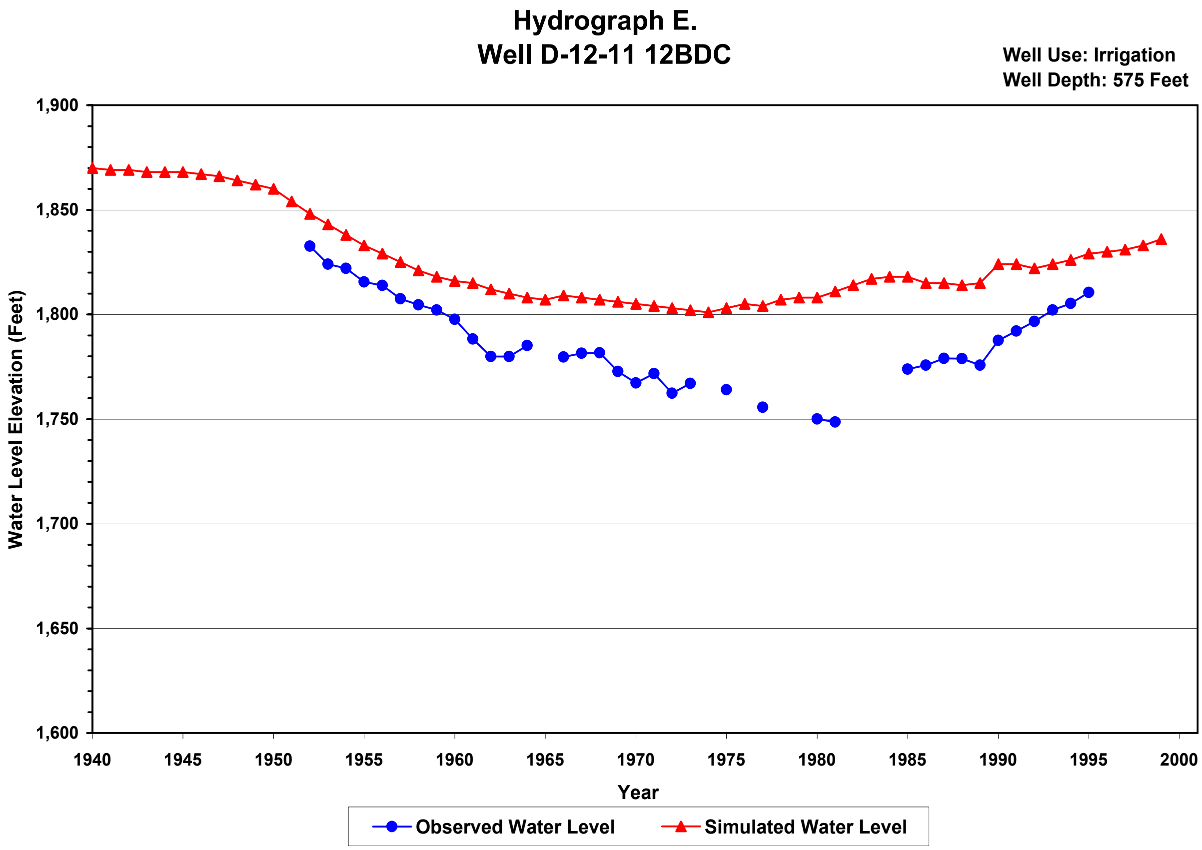
Hydrograph E.
Well D-12-11 12BDC
Well Use: Irrigation
Well Depth: 575 Feet
1,900
1,850
1,800
1,750
1,700
1,650
1,600
Water Level Elevation (Feet)
1940
1945
1950
1955
1960
1965
1970
1975
1980
1985
1990
1995
2000
Year
Observed Water Level
Simulated Water Level

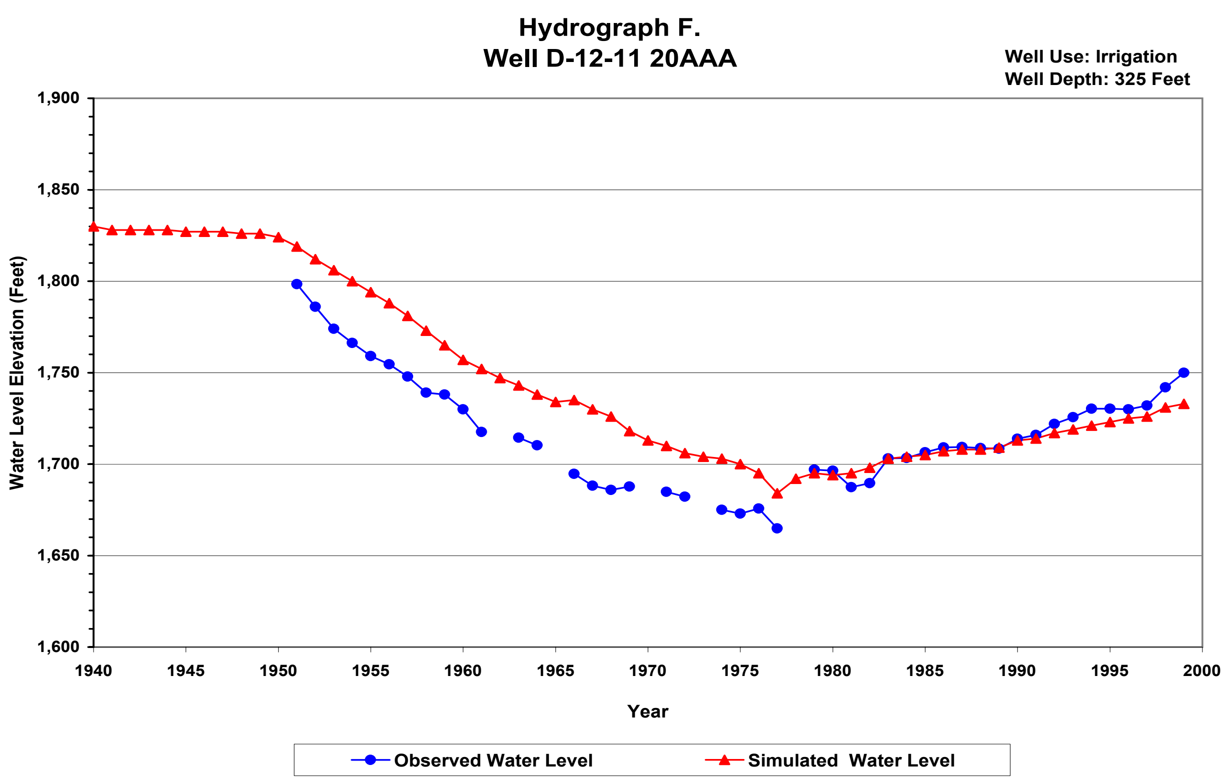
Hydrograph F.
Well D-12-11 20AAA
Well Use: Irrigation
Well Depth: 325 Feet
1,900
1,850
1,800
1,750
1,700
1,650
1,600
Water Level Elevation (Feet)
1940
1945
1950
1955
1960
1965
1970
1975
1980
1985
1990
1995
2000
Year
Observed Water Level
Simulated Water Level

Hydrograph G.
Well D-13-11 31CCC1

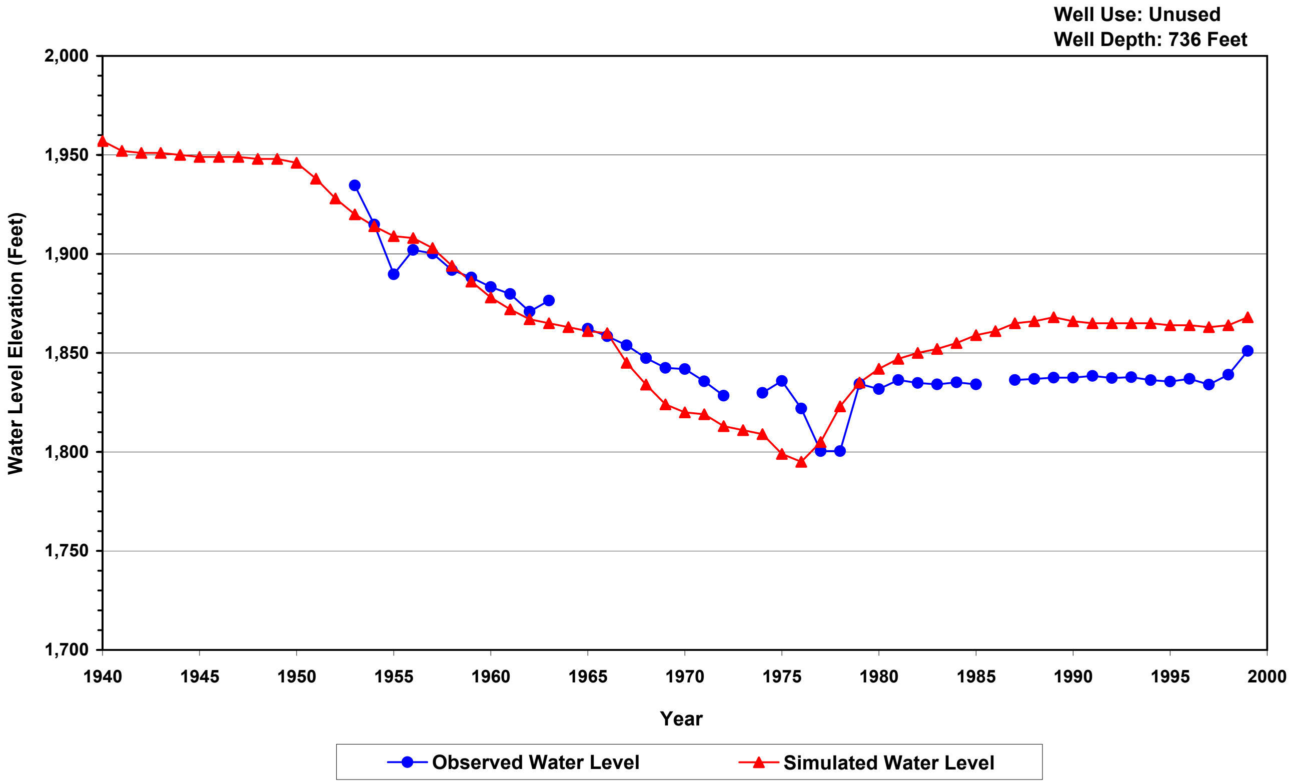

Hydrograph H.
Well D-14-11 08CCC

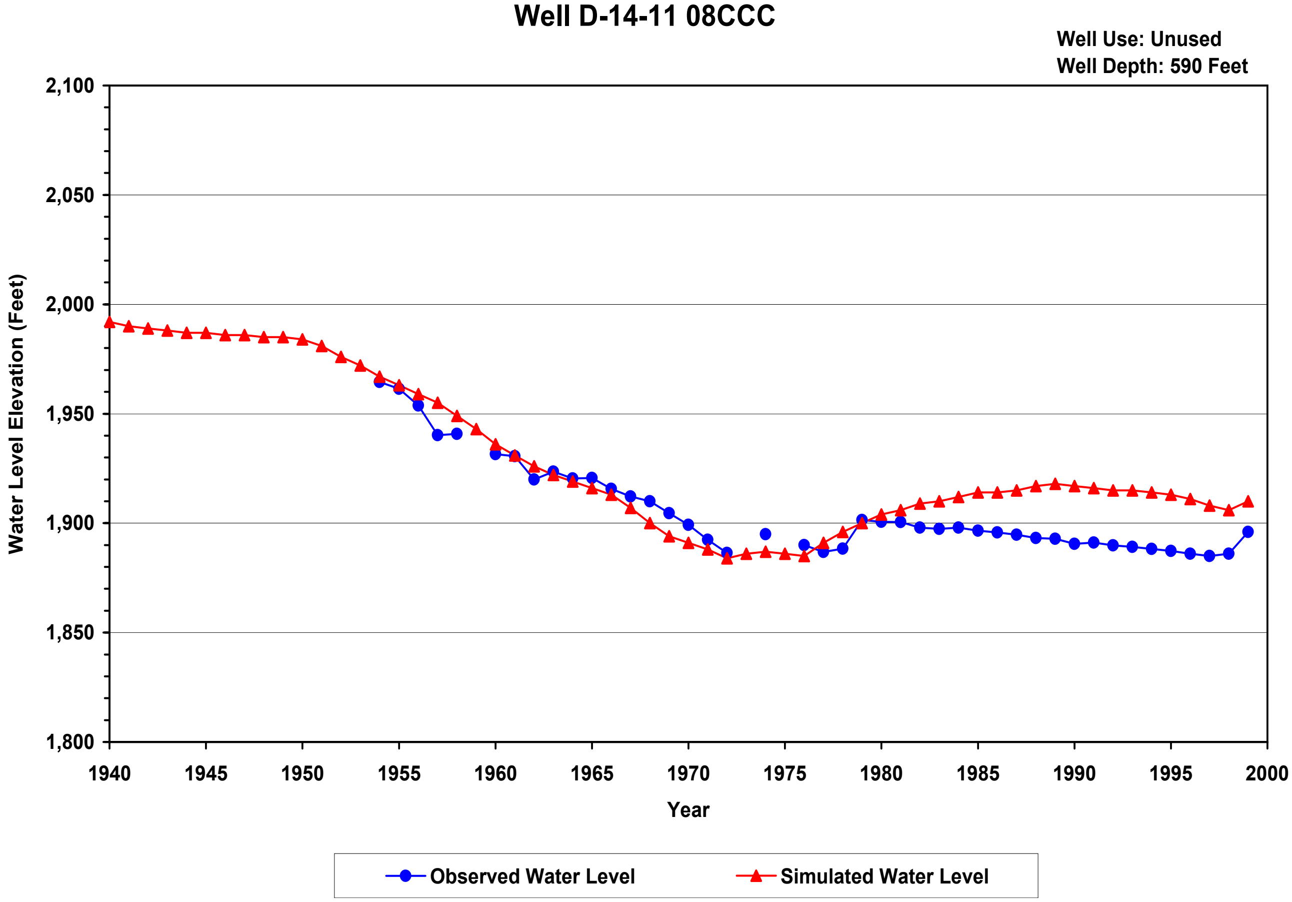

Hydrograph I.
Well D-15-11 05CCD

Well Use: Domestic
Well Depth: 712 Feet

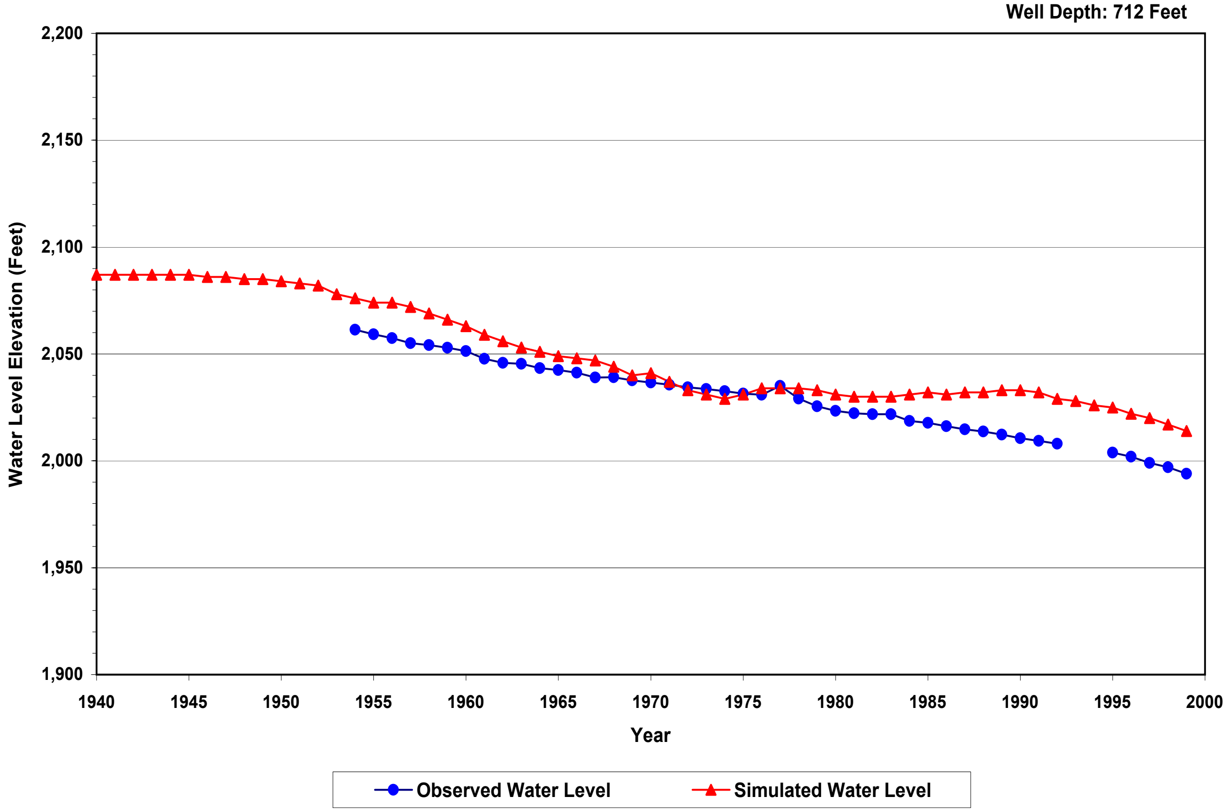

Hydrograph J.
Well D-12-12 22ADC

Well Use: Unused
Well Depth: 315 Feet

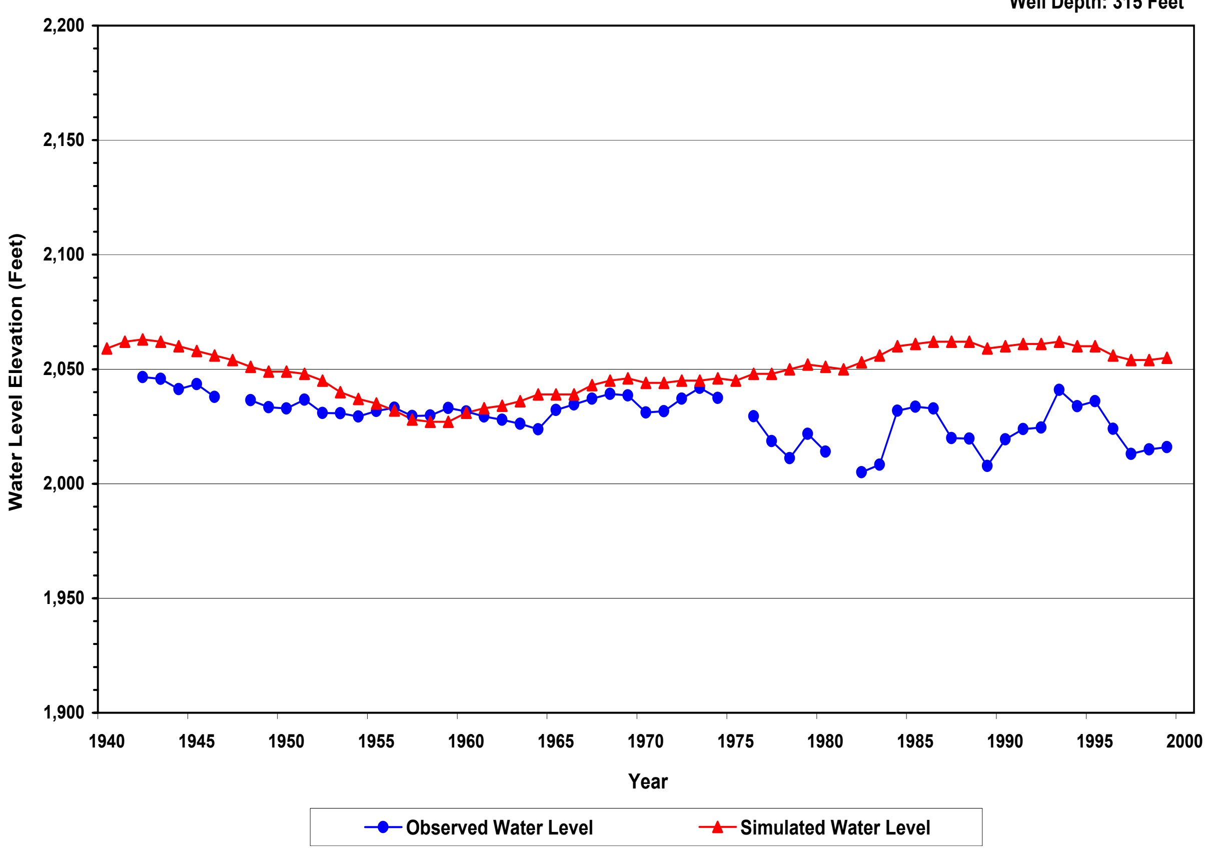

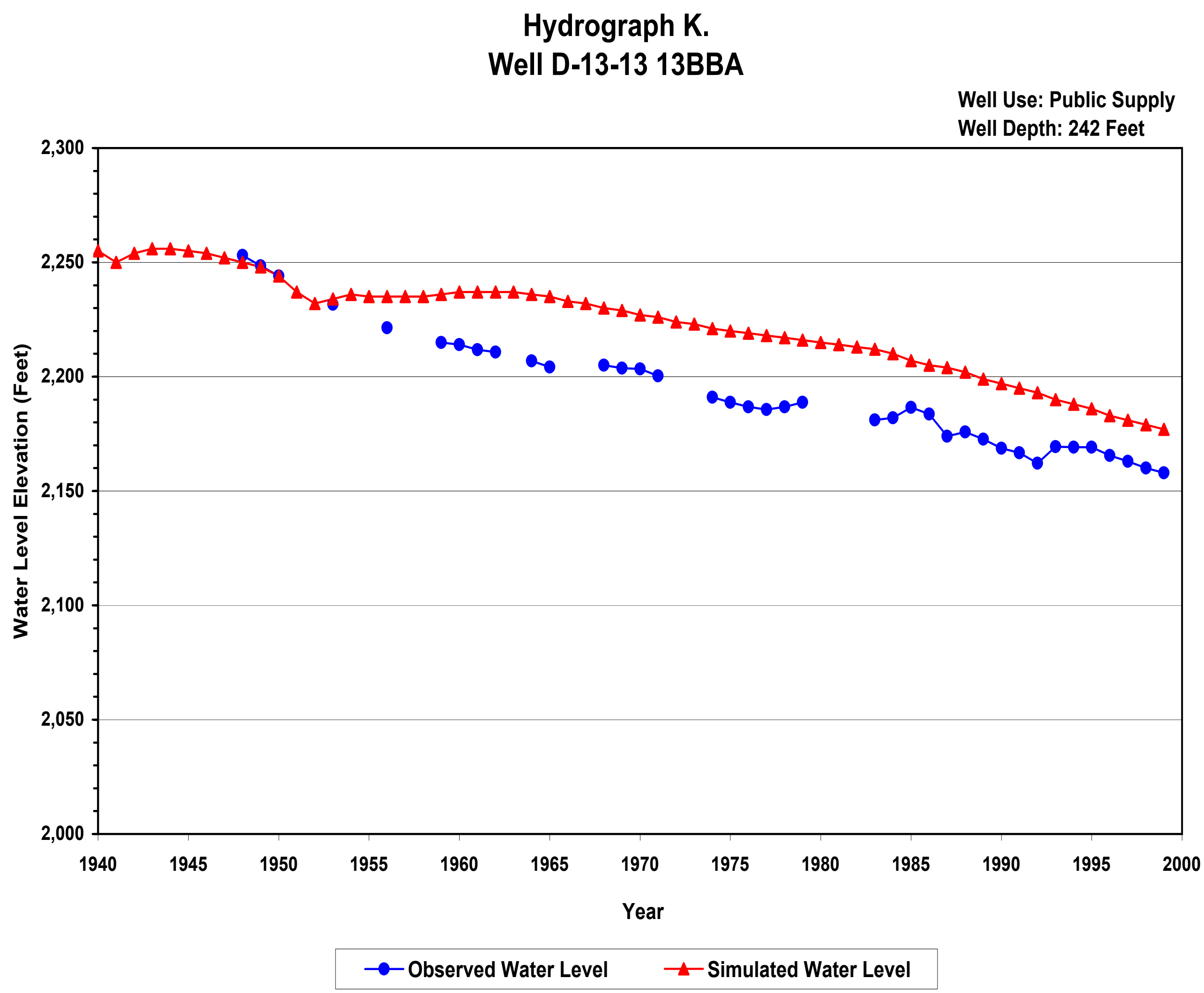
Hydrograph K.
Well D-13-13 13BBA
Well Use: Public Supply
Well Depth: 242 Feet
2,300
2,250
2,200
2,150
2,100
2,050
2,000
Water Level Elevation (Feet)
1940
1945
1950
1955
1960
1965
1970
1975
1980
1985
1990
1995
2000
Year
Observed Water Level
Simulated Water Level

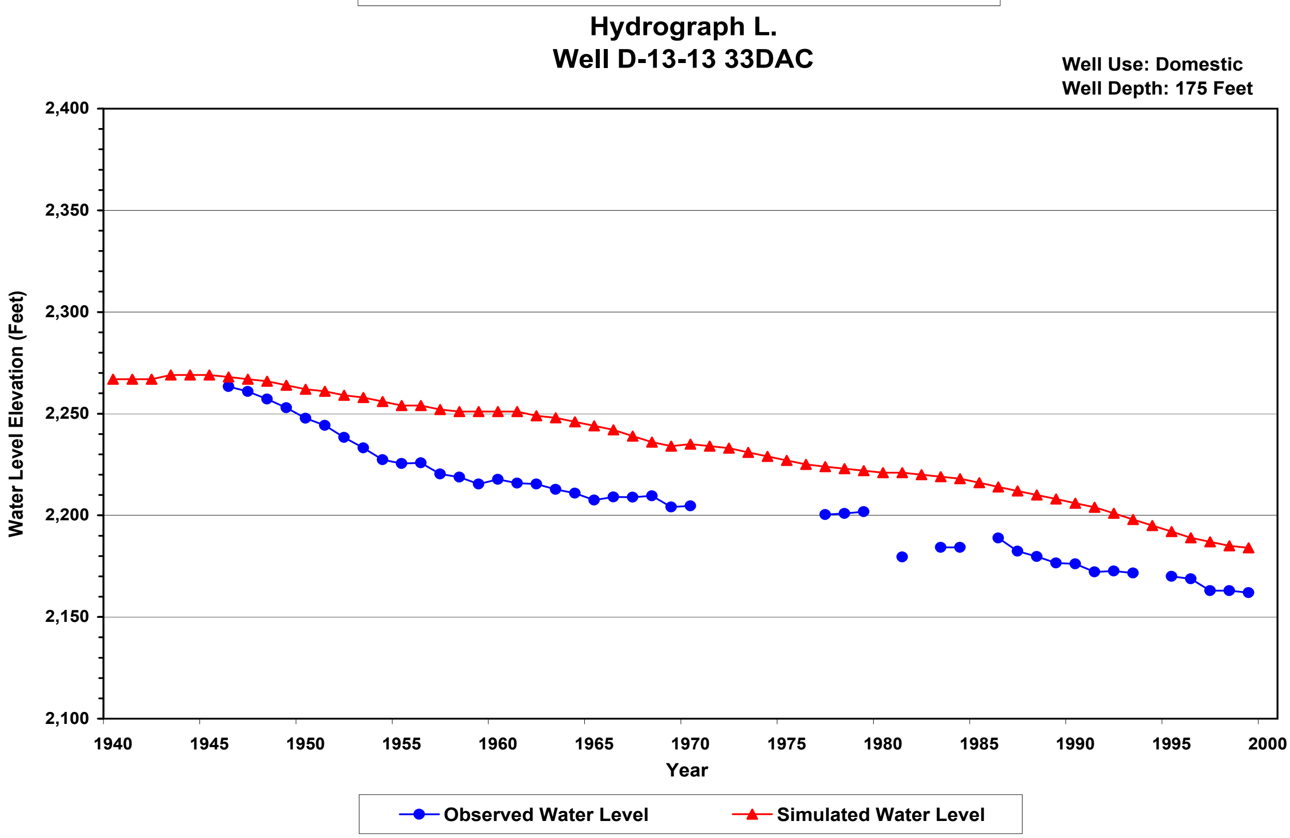
Hydrograph L.
Well D-13-13 33DAC
Well Use: Domestic
Well Depth: 175 Feet
2,400
2,350
2,300
2,250
2,200
2,150
2,100
Water Level Elevation (Feet)
1940
1945
1950
1955
1960
1965
1970
1975
1980
1985
1990
1995
2000
Year
Observed Water Level
Simulated Water Level

Hydrograph M.
Well D-14-14 16CBB1 & 2

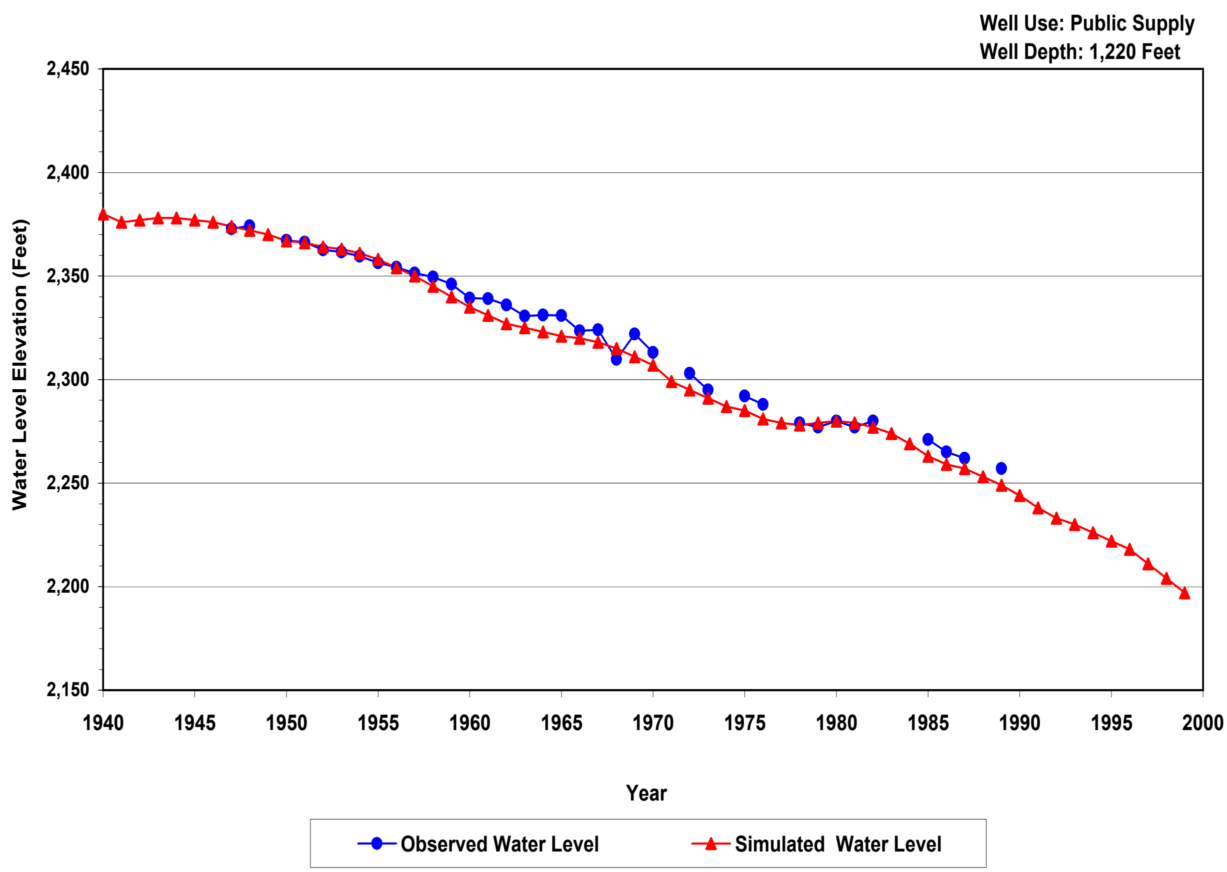

Hydrograph N.
Well D-14-14 20DBD

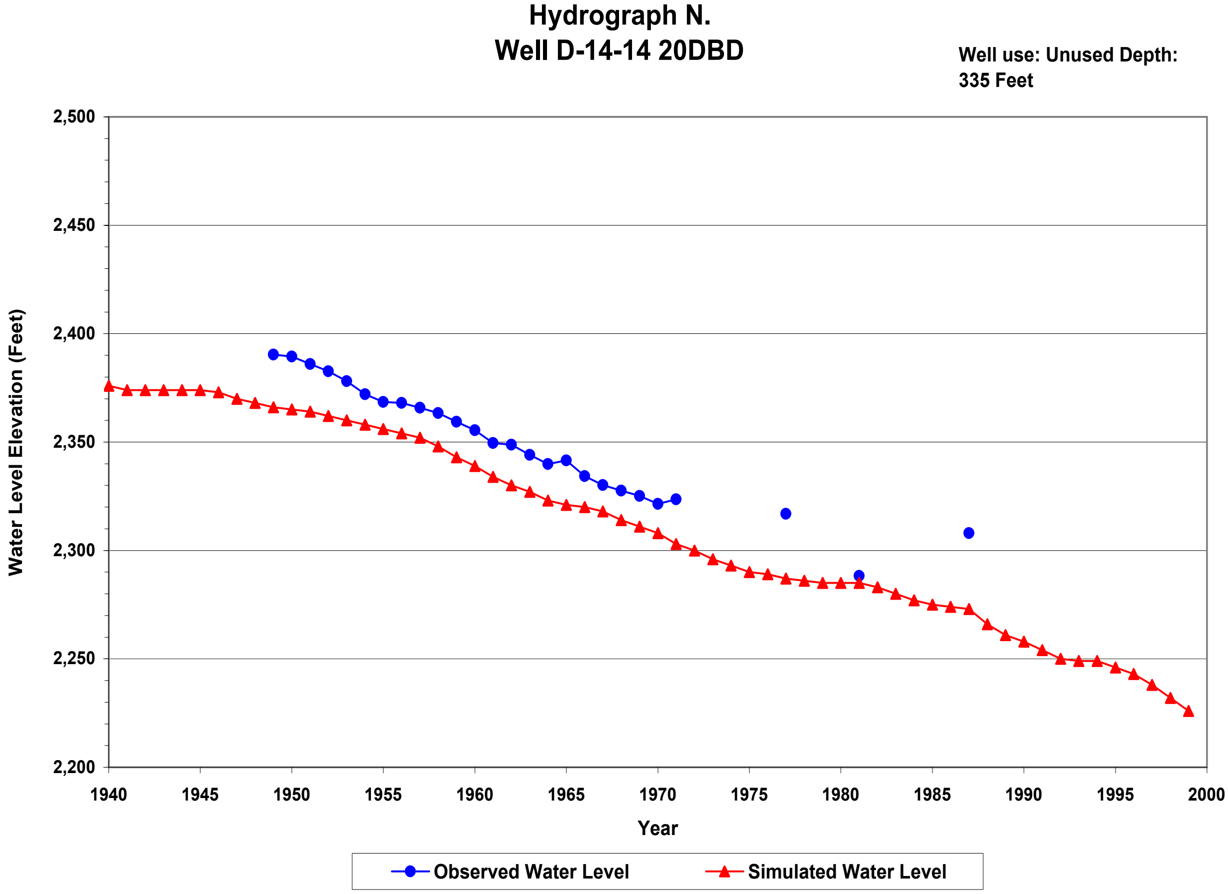

Hydrograph O.
Well D-15-15 06BBB

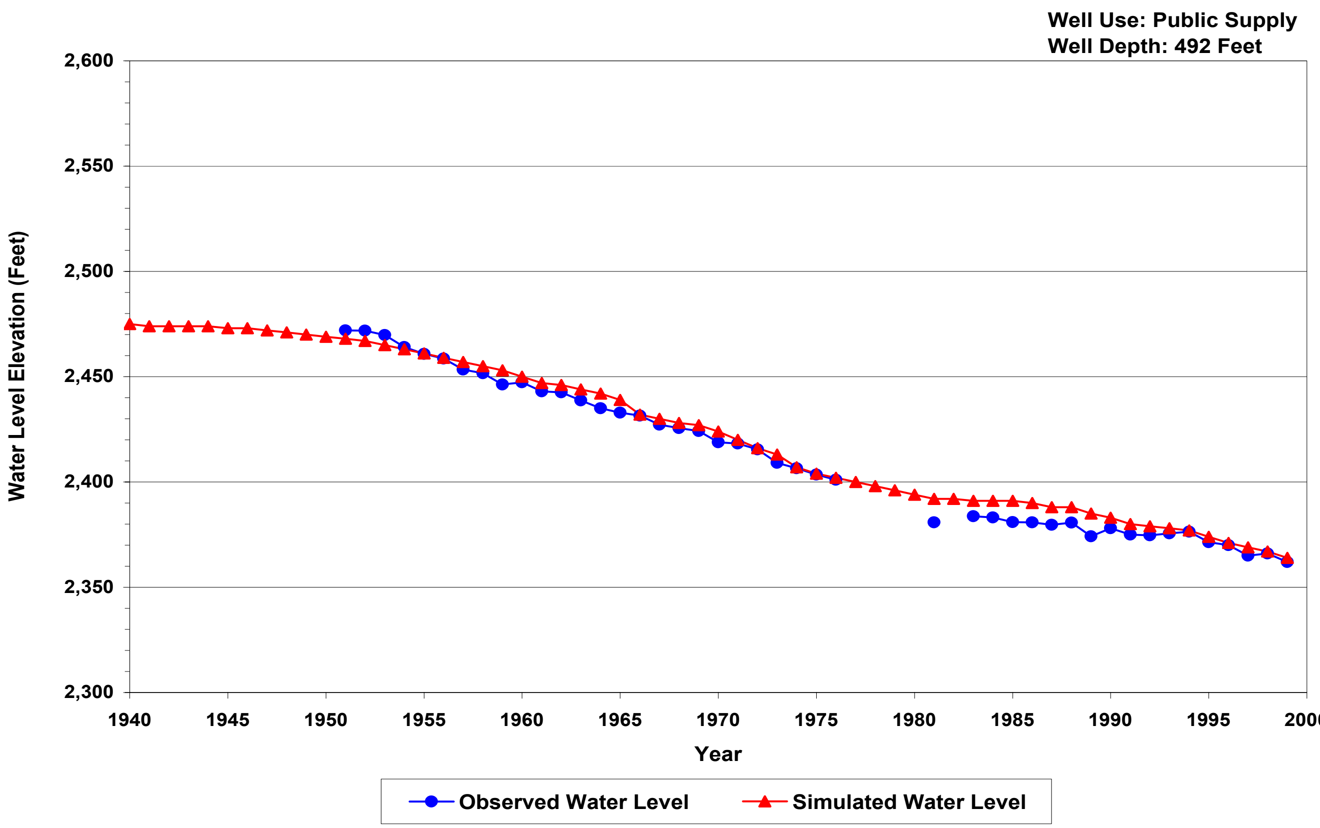

Hydrograph P.
Well D-16-13 S02BBA2

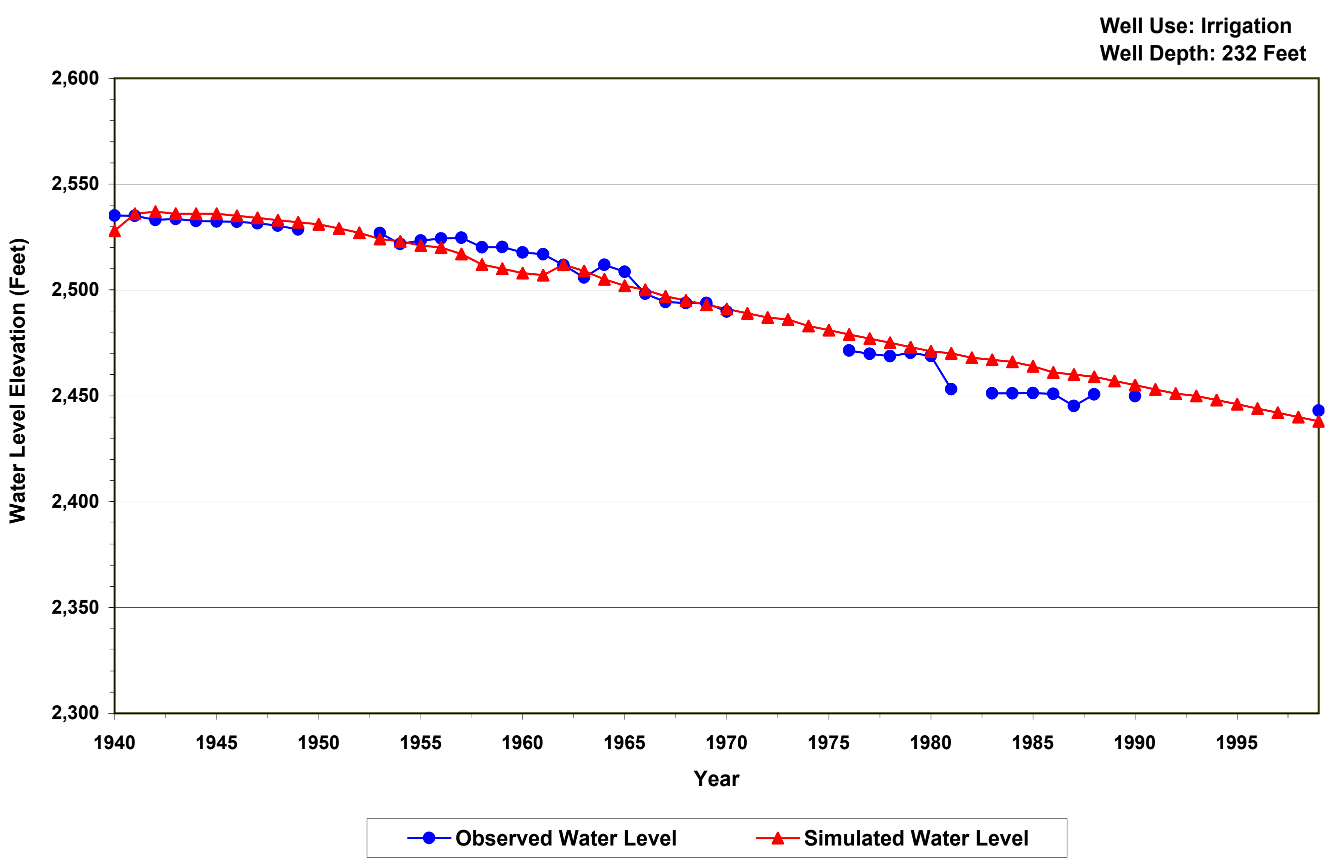

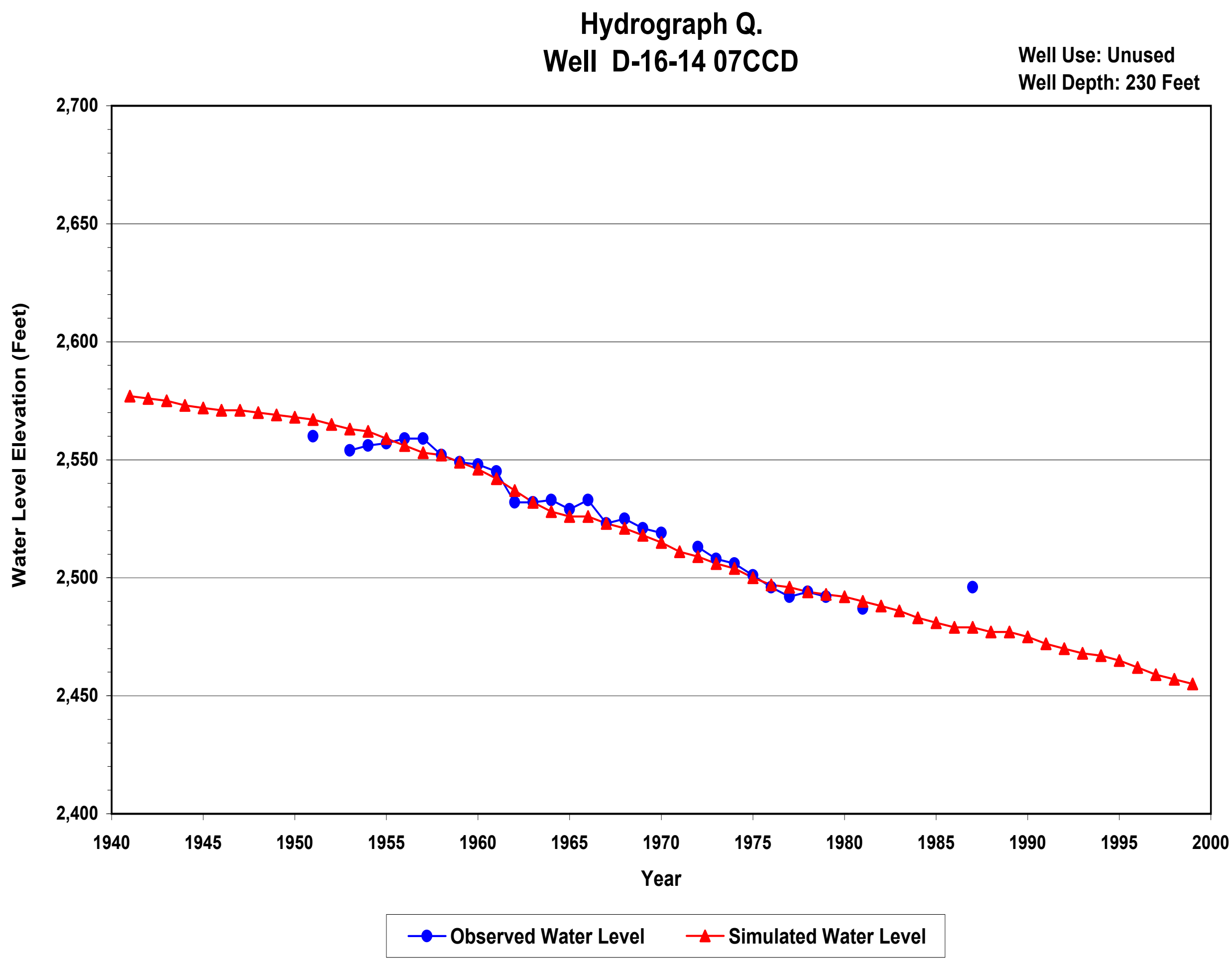
Hydrograph Q.
Well D-16-14 07CCD
Well Use: Unused
Well Depth: 230 Feet
Water Level Elevation (Feet)
2,700
2,650
2,600
2,550
2,500
2,450
2,400
1940
1945
1950
1955
1960
1965
1970
1975
1980
1985
1990
1995
2000
Year
Observed Water Level
Simulated Water Level

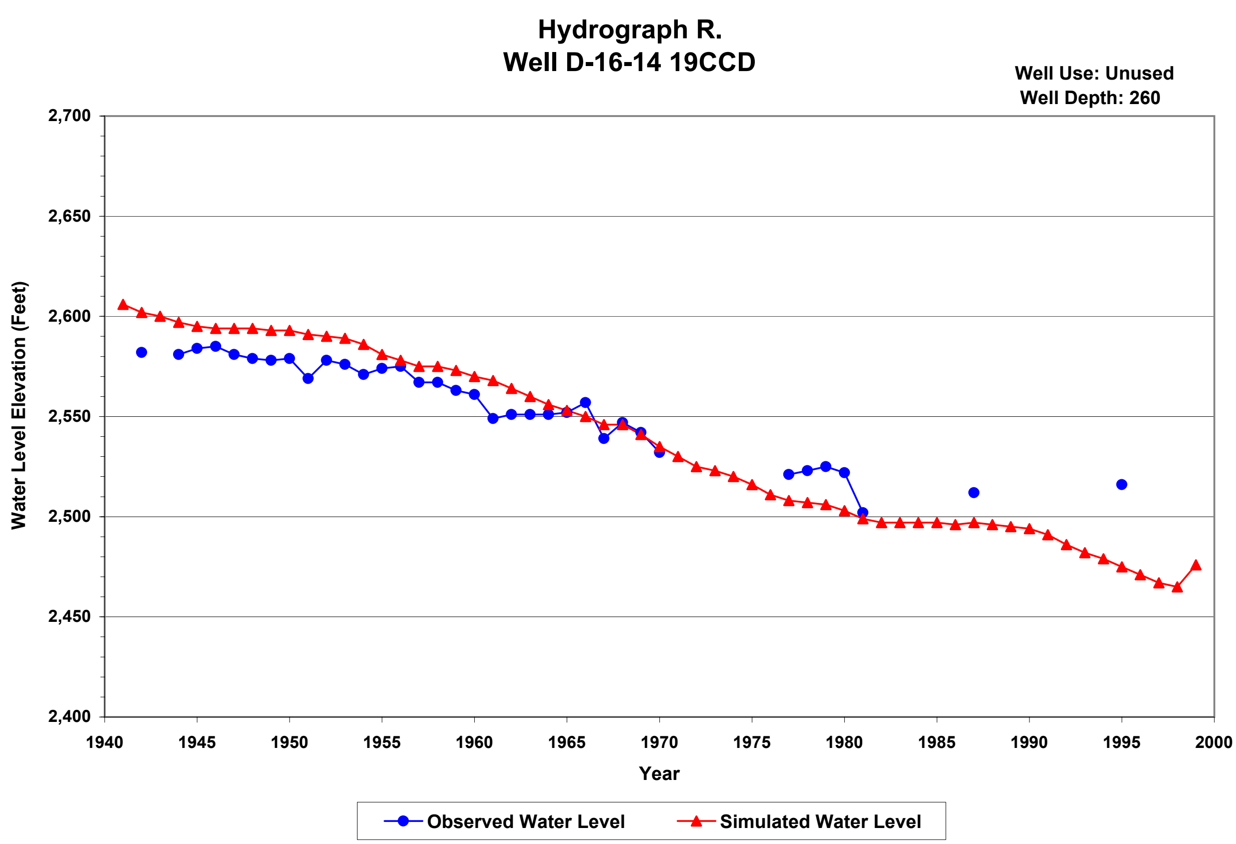
Hydrograph R.
Well D-16-14 19CCD
Well Use: Unused
Well Depth: 260
Water Level Elevation (Feet)
2,700
2,650
2,600
2,550
2,500
2,450
2,400
1940
1945
1950
1955
1960
1965
1970
1975
1980
1985
1990
1995
2000
Year
Observed Water Level
Simulated Water Level

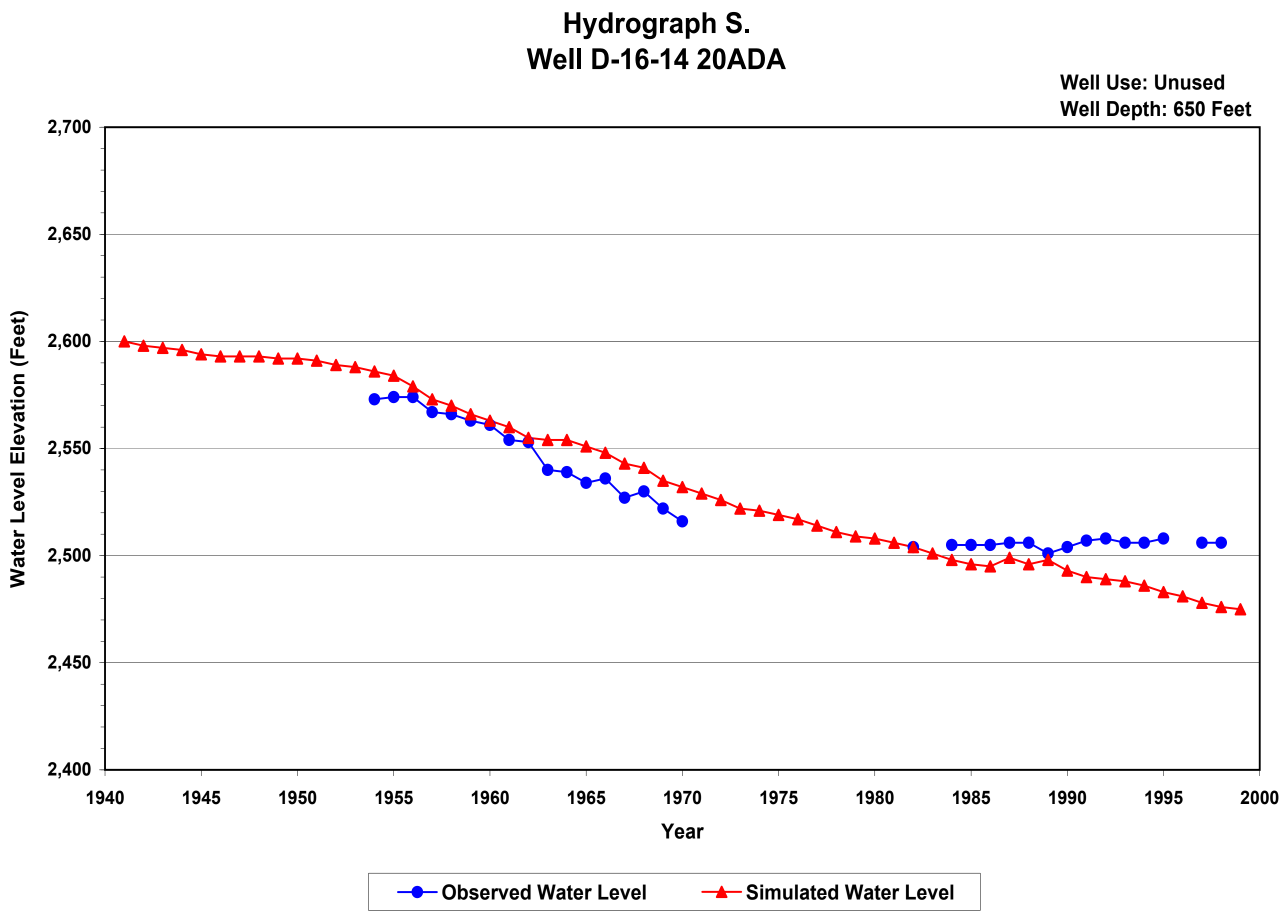
Hydrograph S.
Well D-16-14 20ADA
Well Use: Unused
Well Depth: 650 Feet
Water Level Elevation (Feet)
2,700
2,650
2,600
2,550
2,500
2,450
2,400
1940
1945
1950
1955
1960
1965
1970
1975
1980
1985
1990
1995
2000
Year
Observed Water Level
Simulated Water Level

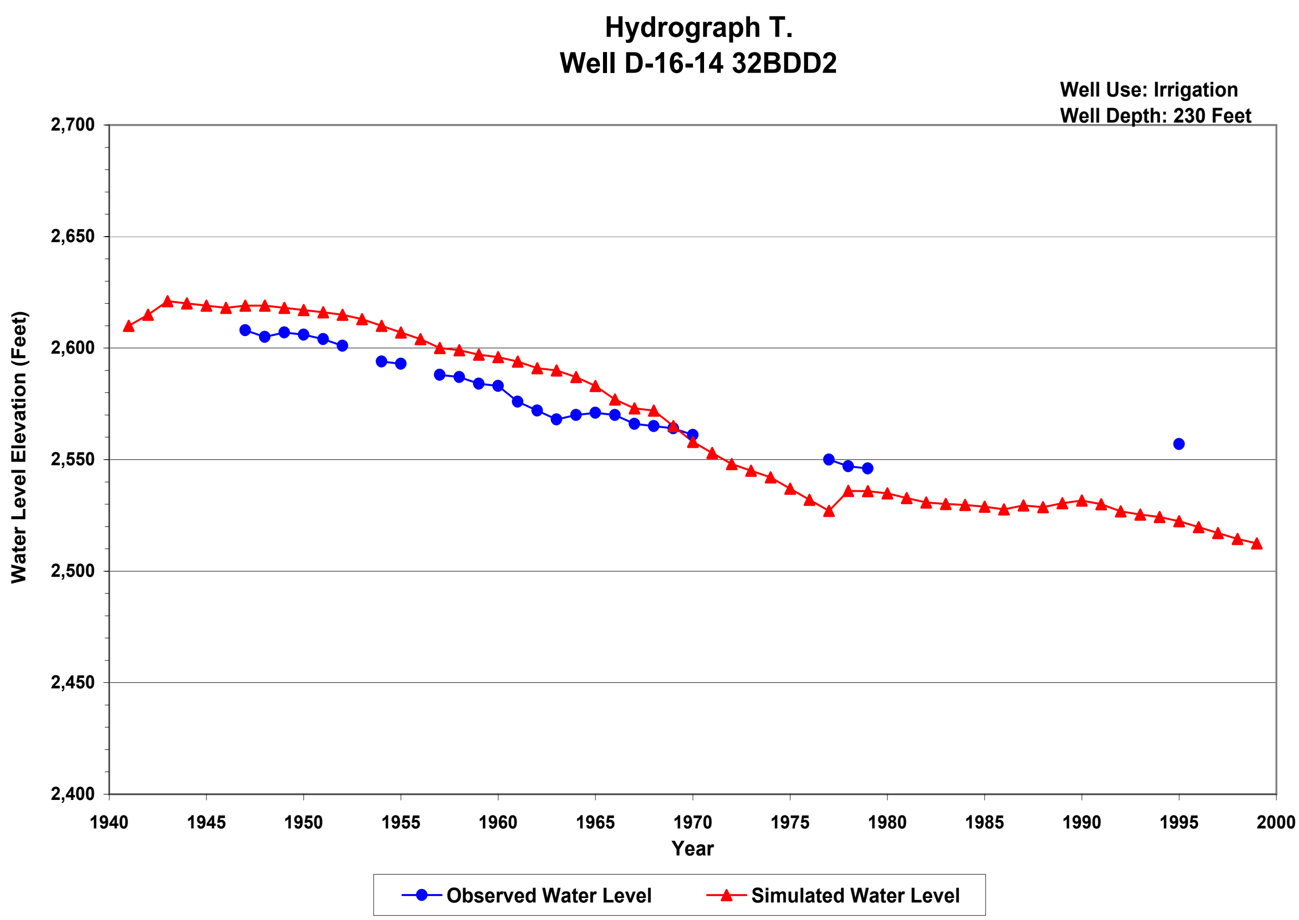
Hydrograph T.
Well D-16-14 32BDD2
Well Use: Irrigation
Well Depth: 230 Feet
Water Level Elevation (Feet)
2,700
2,650
2,600
2,550
2,500
2,450
2,400
1940
1945
1950
1955
1960
1965
1970
1975
1980
1985
1990
1995
2000
Year
Observed Water Level
Simulated Water Level

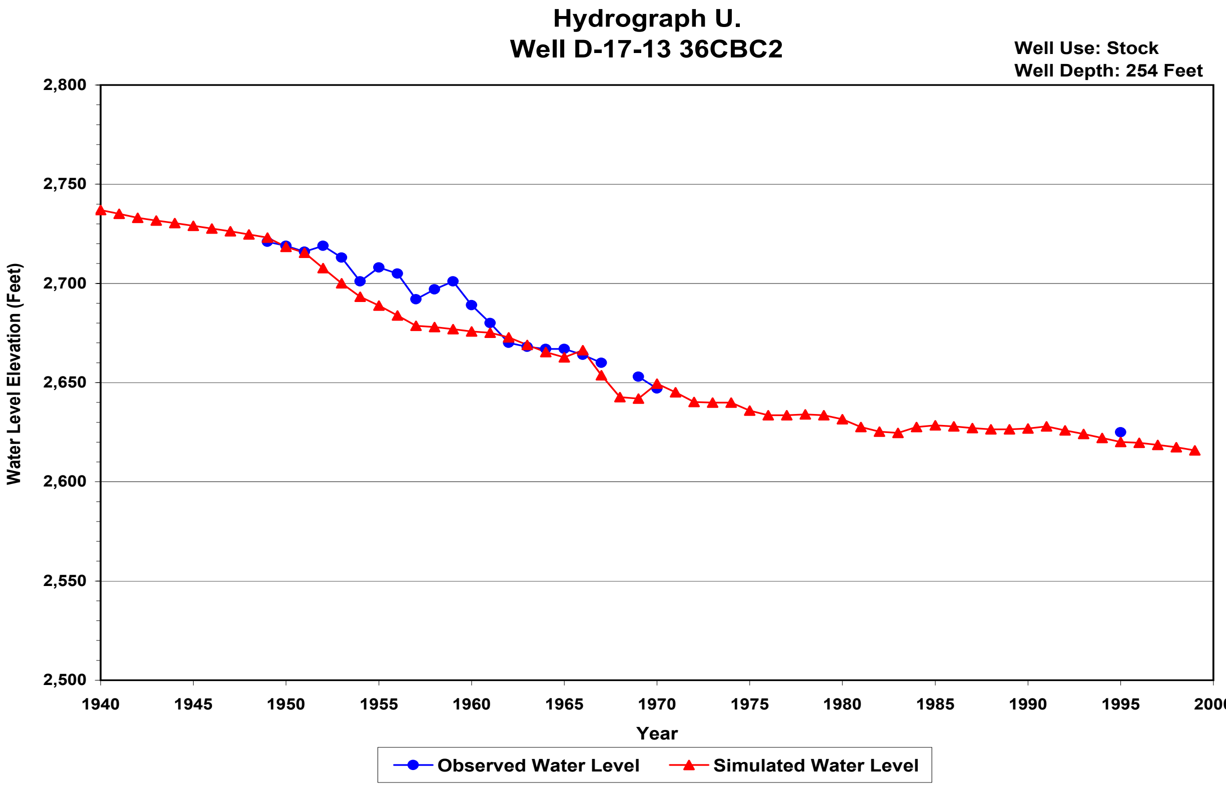
Hydrograph U.
Well D-17-13 36CBC2
Well Use: Stock
Well Depth: 254 Feet
Water Level Elevation (Feet)
2,800
2,750
2,700
2,650
2,600
2,550
2,500
1940
1945
1950
1955
1960
1965
1970
1975
1980
1985
1990
1995
2000
Year
Observed Water Level
Simulated Water Level

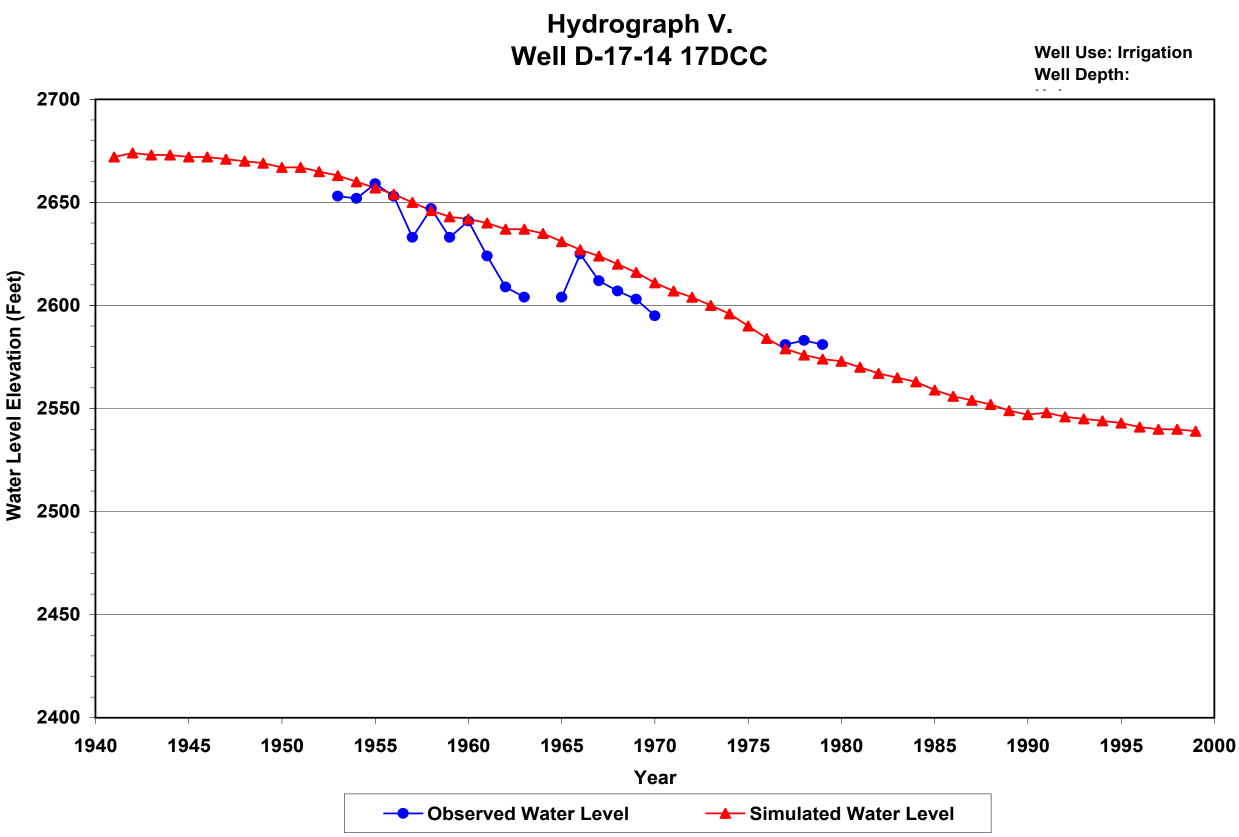
Hydrograph V.
Well D-17-14 17DCC
Well Use: Irrigation
Well Depth:
Water Level Elevation (Feet)
2700
2650
2600
2550
2500
2450
2400
1940
1945
1950
1955
1960
1965
1970
1975
1980
1985
1990
1995
2000
Year
Observed Water Level
Simulated Water Level

Hydrograph W.
Well D-18-13 01CDA

Well Use: Unused
Well Depth: 253 Feet

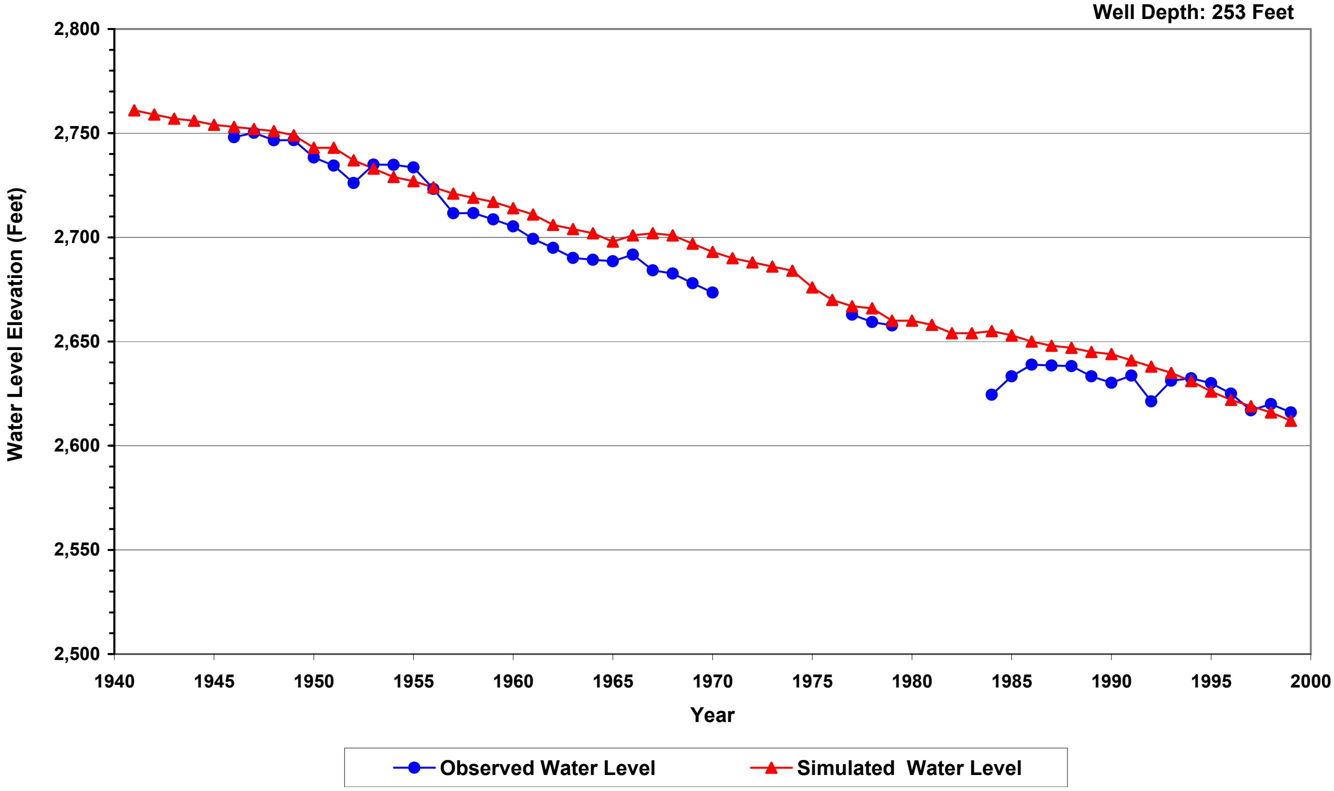

Hydrograph X.
Well D-19-13 09CAA

Well Use: Irrigation
Well Depth: Unknown

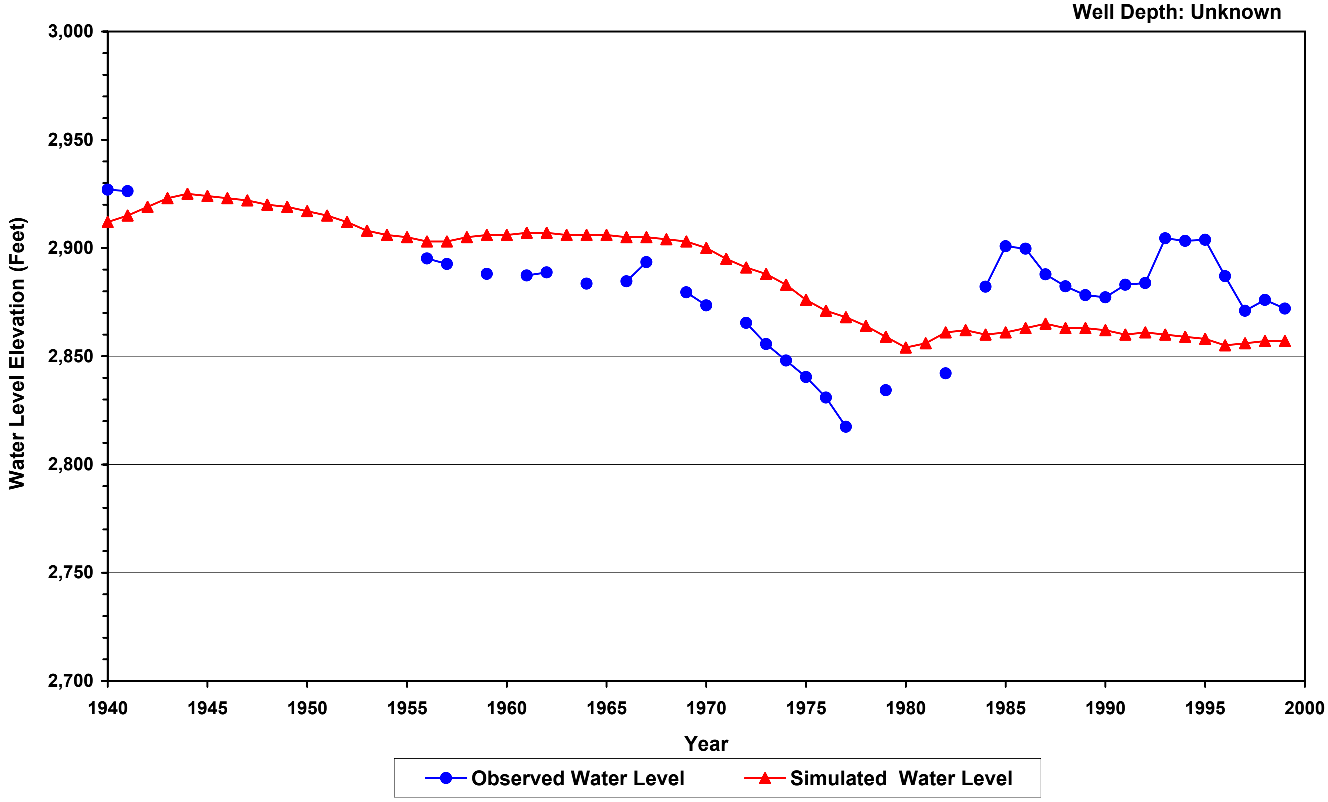

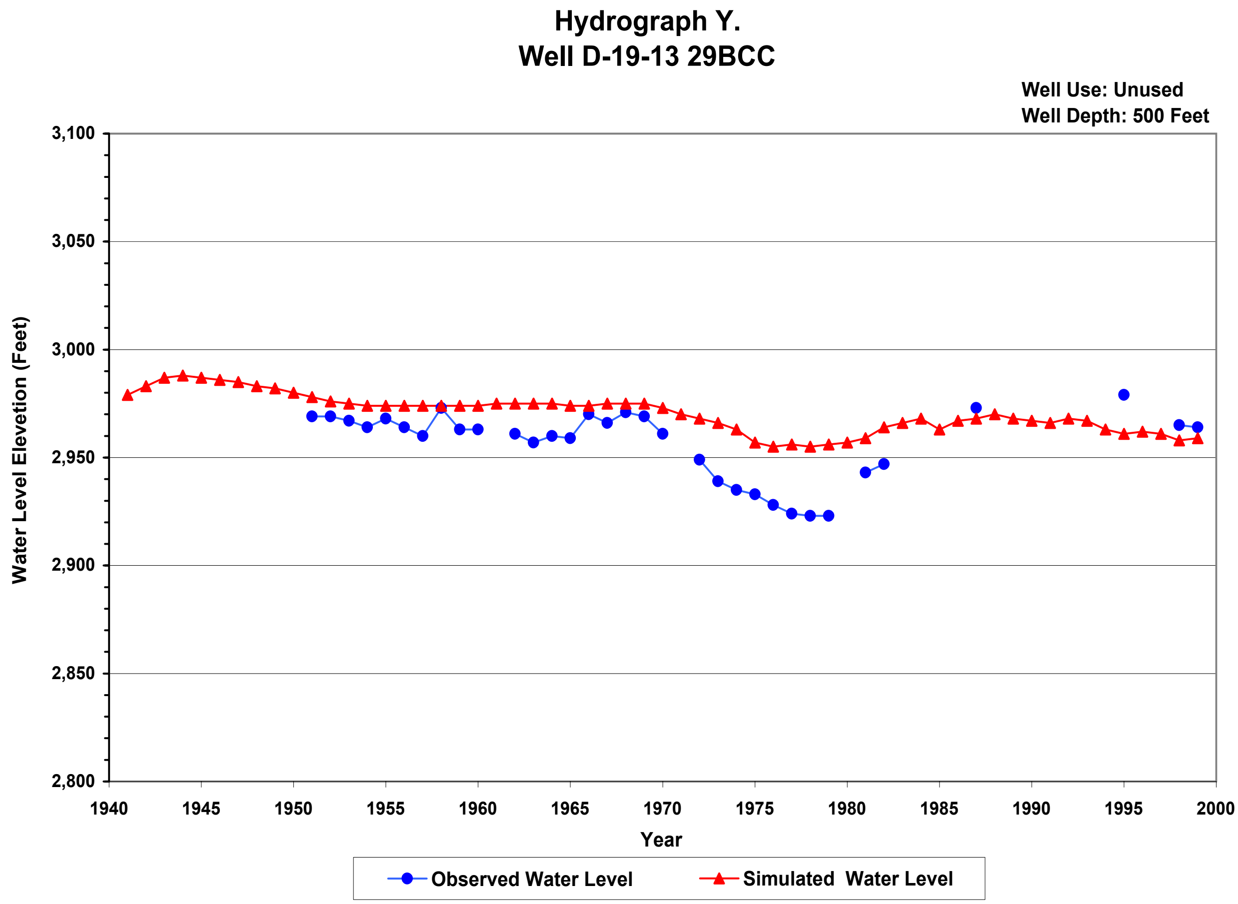
Hydrograph Y.
Well D-19-13 29BCC
Well Use: Unused
Well Depth: 500 Feet
Water Level Elevation (Feet)
3,100
3,050
3,000
2,950
2,900
2,850
2,800
1940
1945
1950
1955
1960
1965
1970
1975
1980
1985
1990
1995
2000
Year
Observed Water Level
Simulated Water Level

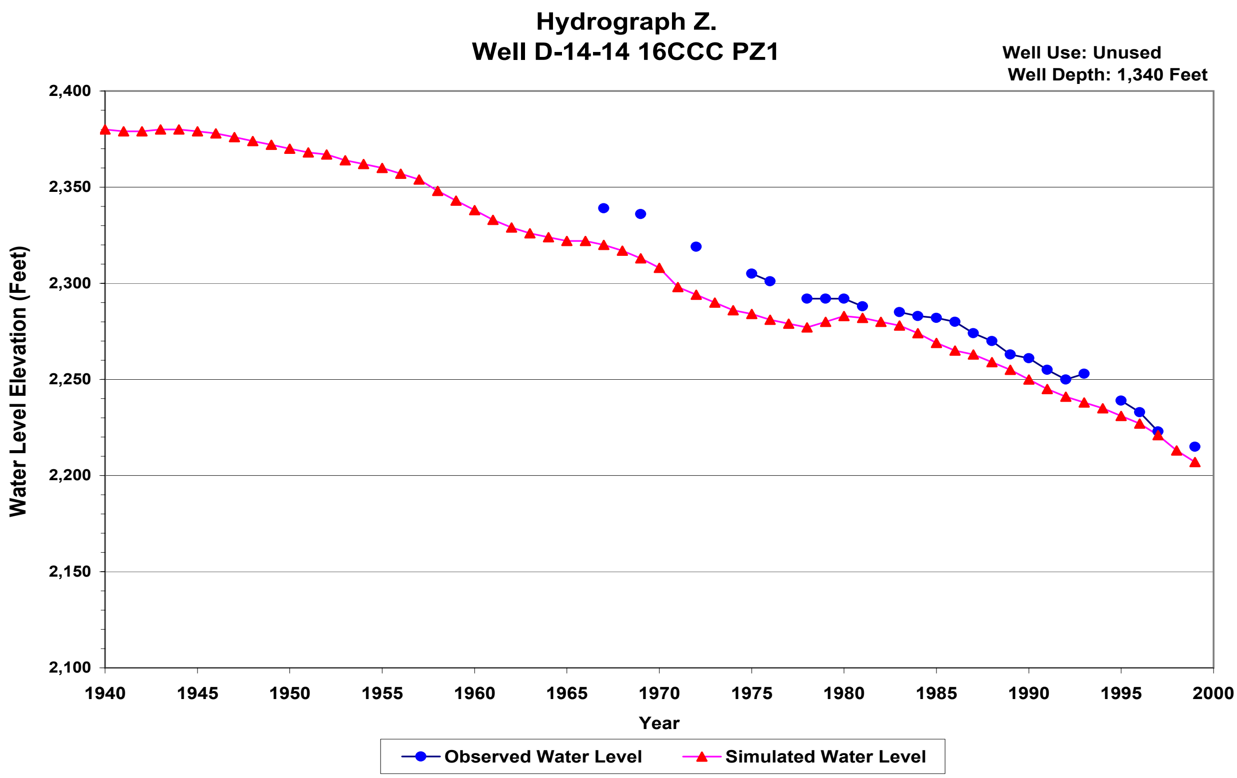
Hydrograph Z.
Well D-14-14 16CCC PZ1
Well Use: Unused
Well Depth: 1,340 Feet
Water Level Elevation (Feet)
2,400
2,350
2,300
2,250
2,200
2,150
2,100
1940
1945
1950
1955
1960
1965
1970
1975
1980
1985
1990
1995
2000
Year
Observed Water Level
Simulated Water Level